

	magnetic moment μ , interacting with a distribution of electromagnetic fields		
$\hat{H}_{U,\alpha}$	Hamiltonian of a charged particle in the presence of the attractive potential U , and of a magnetic string carrying the flux $\alpha=qF/2\pi\hbar c$	d_0	dimension of region of enclosed electric flux
$H_\nu^{(1)}$	Hankel function of the first kind	d_e	width of electron source
$\hat{H}_{\tilde{U},\alpha}^{(\Gamma_0)}$	Hamiltonian of a particle interacting with a shielded tube of magnetic flux	e	absolute value of electron charge
\hat{H}_0	unperturbed Hamiltonian	f	gauge function
\mathcal{I}	current flowing through a solenoid	g	Earth's gravitational acceleration
\mathcal{I}_0	moment of inertia of a rotating cylinder	\hbar	Planck's constant divided by 2π
$\hat{\mathcal{J}}$	operator of total kinetic angular momentum of a particle with spin $\frac{1}{2}$	i	imaginary unit
J_ν	Bessel function of order ν	\mathbf{j}	probability current
J	Josephson current	$\mathbf{j}^{(\alpha)}$	probability current for the scattering of a plane wave by an infinite magnetic string
J_0	maximum Josephson current	k	wave number
\mathcal{J}	supercurrent	m	canonical angular momentum divided by \hbar , assumes integer values
K	quantum-mechanical propagator for a charged particle interacting with a distribution of electromagnetic potentials φ, \mathbf{A}	\mathbf{p}	classical canonical momentum
$K_{R_0}^{(F)}$	propagator for a charged plane rotator in the presence of an enclosed magnetic flux F	$\hat{\mathbf{p}}$	operator of canonical momentum
K_n	n th component of the density of kinetic momentum of the state of a charged particle	q	electric charge of a particle
$\hat{\mathcal{L}}$	canonical angular momentum operator	r_0	radius of the flux region in the case of a cylindrical distribution of magnetic field
L_0	length of a magnetic string	r_f	radius of the biprism fiber
M	mass of charged particle	\mathbf{v}	kinematical field; velocity
N_0	number of turns of a solenoid	$\Delta\Phi_E$	electric phase shift
N	an integer number	$\Delta\Phi_B$	magnetic phase shift
R	nonintegrable phase factor	Δ	distance between consecutive fringes
R_0	radius of plane rotator	$\Delta\Phi_t$	phase shift for a toroidal distribution of magnetic flux
R_{PQ}	distance between the points P and Q in Sec. III; nonintegrable phase factor for a path connecting the points P and Q in Sec. IV	$\Delta\mathcal{E}$	energy shift produced by a variable magnetic flux
\tilde{S}	classical action, in general nonstationary	ΔT_c	change in the critical temperature produced by a flux F
S_Γ	classical action on stationary path Γ	$\hat{\Lambda}_\alpha$	operator of kinetic angular momentum
\mathcal{S}	source of charged particles	Φ	phase of the wave function
$\mathcal{S}_1, \mathcal{S}_2$	virtual images of \mathcal{S}	Φ_α	flux-dependent phase shift
U	attractive potential	Ψ	solution of Schrödinger equation including potentials φ, \mathbf{A}
\tilde{U}	repulsive potential	Ψ_δ	wave function of a packet of width δ
U_f	potential of the biprism fiber	$\tilde{\Psi}$	wave function representing the two-slit scattering of charged particles
U_0	inner potential of an element	$\Psi_{R_0}^{(F)}$	eigenstates of charged plane rotator in the presence of the enclosed flux F
V	electrostatic potential	Ψ_+, Ψ_-	components of the wave function of a particle of spin $\frac{1}{2}$
\hat{V}	potential-dependent perturbation	$\Psi_{\delta,\alpha}$	wave function for the scattering of a wave packet of width δ by an infinite magnetic string
\hat{W}	power operator	$\Psi_{D_0,\alpha}$	wave function for scattering by two parallel strings
$Y_{\lambda m}^{(\alpha)}$	eigenstate of the kinetic angular momentum operator $\hat{\Lambda}_\alpha^2$	$\Psi_{\rho_0,\alpha}$	wave function for scattering by circular magnetic string
Y_ν	Neumann function	$\Psi_{\varphi,\mathbf{A}}$	solution of Schrödinger equation including potentials φ, \mathbf{A}
a_0	separation between the virtual sources	Ω	closed loop
b_0	distance from particle source to biprism fiber	α	parameter proportional to the magnetic flux, $\alpha=qF/2\pi\hbar c$
c	velocity of light	$[\alpha]$	integer part of α
c_0	distance from particle source to the observing plane	γ	angle of deflection by biprism fiber
		δ	width of probability distribution of a wave packet

δ_t	phase difference between coherent components
δ_E	displacement of interference pattern produced by a uniform electric field
δ_B	displacement of interference pattern produced by a uniform magnetic field
λ	wavelength of incident particle; eigenvalue of Λ_α
$\lambda(r, z)$	kinetic angular momentum of a cylindrical wave packet
λ_p	London penetration depth
ρ^2	probability density
ρ_0	radius of circular magnetic string
$\hat{\sigma}$	Pauli matrices
τ_0	temporal dimension of region of enclosed flux
φ	scalar potential
φ_g	gravitational potential
ψ_α	wave function for the scattering of a plane wave by an infinite magnetic string
$\psi_{r_0\alpha}$	wave function for the scattering of a plane wave by a tube of flux of radius r_0
$\psi_{\tilde{R}_0, \alpha}$	wave function for scattering by a magnetic string, shielded by a cylinder of radius \tilde{R}_0
ψ_1, ψ_2	amplitudes for finding an electron pair on the two sides of a Josephson junction
ψ	effective wave function in a superconductor
ψ_n	wave function of a neutron beam

INTRODUCTION

The concept of electromagnetic field was introduced by Faraday and Maxwell to localize the description of the interaction of electrically charged particles. While the classical Lorentz forces depend on the electric and magnetic strengths acting directly on the charged particles, the quantum-mechanical Schrödinger equation for a charged particle involves the scalar and vector electromagnetic potentials. Since the potentials can be determined only up to the derivatives of a scalar function of space and time, the relation between the fields and potentials is not unique. However, as a change in the gauge of the potentials results in the multiplication of the wave function by a phase factor, it has been assumed that the existence of observable electromagnetic effects, in both classical and quantum mechanics, requires the direct action of the field strengths on the charged particles.

Although in classical physics the state of the electromagnetic continuum can be specified by the electric and magnetic strengths, it turns out that knowledge of the local field strengths is not sufficient for the consistent description of certain electromagnetic processes affecting the quantum-mechanical state of charged particles. One such process is the two-slit scattering of electrons in the presence of a magnetic flux confined to the region between the slits. Despite the fact that in this experiment the region of space accessible to the incident electrons is free of forces, the phases of the component waves of the

incident state are shifted oppositely on the two sides of the flux region, which generally produces observable fringe shifts in the interference pattern.

A characteristic property of the aforementioned quantum-mechanical processes is that the observable shifts in the interference patterns depend on the amount of electromagnetic flux enclosed between the interference paths. The fact that the physical effects of a distribution of magnetic field on the quantum interference of electrons are determined by the amount of enclosed magnetic flux was noted by Franz (1939). Further, Ehrenberg and Siday (1949), in a report on the refractive index in electron optics, predicted the existence of observable quantum interference phenomena associated with stationary magnetic fluxes. The full significance of the problem however, only became apparent after the detailed description of the quantum effects of the fluxes by Aharonov and Bohm (1959). Aharonov and Bohm considered quantum effects of both magnetic and electric fluxes, pointed out that the theoretical predictions were within the scope of existing experimental techniques, and most importantly emphasized the remarkable conceptual implications of the existence of these processes.

After a considerable debate in the literature concerning the physical significance of the Aharonov-Bohm effect, the currently accepted interpretation was proposed by Wu and Yang (1975) in terms of the concept of a nonintegrable phase factor. Thus owing to the action of the electromagnetic flux different physical situations in a region may have the same field strengths, while because of gauge arbitrariness different potentials in a region may describe the same situation. Wu and Yang (1975) stated that the consistent description of the interaction between a particle of charge q and the electromagnetic continuum requires the specification of a certain phase factor R , depending on path integrals of the scalar potential φ and of the vector potential \mathbf{A} ,

$$R = \exp \left[\frac{iq}{\hbar c} \int (c\varphi dt - \mathbf{A} d\mathbf{r}) \right],$$

so that the electromagnetism is the gauge-invariant manifestation of the nonintegrable phase factor R . While changes in the energy and kinetic momentum of a charged particle depend on the field strengths acting on the particle, it has recently been shown that the nonintegrable phase factor R is measured by changes in the parity of the state of the incident charged particles, due to their interaction with the electromagnetic continuum.

This paper is a review of the problem of the quantum effects of the electromagnetic fluxes. In Sec. I we describe the quantum effects of the fluxes in the quasi-classical approximation and discuss their relation with basic quantum-mechanical principles. In Sec. II we study the influence of modeling assumptions on the theoretically predicted effects of enclosed fluxes. In Sec. III we analyze the experiments demonstrating the reality of the quantum effects of electromagnetic and gravitational fluxes. Finally in Sec. IV we discuss the physical significance of these quantum effects, comparing the current in-

terpretation based on the concept of the nonintegrable phase factor with alternative approaches.

Among the previous papers considering the Aharonov-Bohm effect we mention the works of Merzbacher (1962), Erlichson (1970), Greenberger and Overhauser (1979), and Peshkin (1981b).

I. GENERAL PROPERTIES

A. Path-integral formalism in the quasiclassical approximation

The quantum effects of electromagnetic fluxes are a class of interactions having the remarkable property of persisting even for an arbitrarily small overlap between the region of space accessible to the incident charged particles and the distribution of field strengths. In general the enclosed fluxes modify the amplitude of propagation from one point of the space to the other by a phase factor, and therefore are qualitatively different from the momentum effects of distributions of field strengths acting directly on the charged particles.

The effects of enclosed fluxes often appear as observable changes in quantum interference patterns, although the fluxes may also affect the energy spectrum and kinetic momentum eigenvalues of the particles. Most of the relevant properties of the quantum effects of the fluxes can be discussed in terms of the two-slit interference experiment with charged particles. A convenient frame for the analysis of the two-slit scattering of charged particles is provided by the path-integral formalism of Feynman (1948). According to Feynman's rule, the quantum-mechanical propagator $K(\mathbf{r}, t; \mathbf{r}', t')$, which gives the amplitude for the particles to travel from the point \mathbf{r}', t' to the point \mathbf{r}, t , is proportional to the exponential of the classical action multiplied by i/\hbar , summed over all paths connecting the points \mathbf{r}', t' and \mathbf{r}, t . The utility of the path-integral formalism is then that in the quasiclassical approximation the dominant contribution to the propagator arises solely from the stationary paths connecting the incidence and observing regions.

In this section we analyze the formation of the quantum interference patterns with the aid of the path-integral formalism applied in the quasiclassical approximation. The evolution of the state Ψ of a particle of charge q and mass M , interacting with an electromagnetic field of sca-

lar potential φ and vector potential \mathbf{A} , is described by the Schrödinger equation

$$i\hbar \frac{\partial \Psi}{\partial t} = \hat{H} \Psi, \quad (1.1)$$

where the Hamiltonian operator \hat{H} has the expression

$$\hat{H} = \frac{1}{2M} \left[-i\hbar \nabla - \frac{q}{c} \mathbf{A} \right]^2 + q\varphi. \quad (1.2)$$

The fact that the evolution of the state Ψ can be described with the aid of a propagator is a consequence of the principle of superposition. Indeed, the state of the particle at the time t is determined by its expansion coefficients a_n over a complete set of eigenfunctions Ψ_n of Eq. (1.1),

$$\Psi(\mathbf{r}, t) = \sum_n a_n \Psi_n(\mathbf{r}, t), \quad (1.3)$$

$$i\hbar \frac{\partial \Psi_n}{\partial t} = \hat{H} \Psi_n. \quad (1.4)$$

Since the time-independent coefficients a_n are given by

$$a_n = \int \Psi_n^*(\mathbf{r}', t') \Psi(\mathbf{r}', t') d\mathbf{r}', \quad (1.5)$$

the expression of Ψ , Eq. (1.3), can be written as

$$\Psi(\mathbf{r}, t) = \int K(\mathbf{r}, t; \mathbf{r}', t') \Psi(\mathbf{r}', t') d\mathbf{r}', \quad (1.6)$$

where the propagator is

$$K(\mathbf{r}, t; \mathbf{r}', t') = \sum_n \Psi_n^*(\mathbf{r}', t') \Psi_n(\mathbf{r}, t). \quad (1.7)$$

Although the propagator K , Eq. (1.7), describes in principle all the properties of the interaction of the charged particle with the electromagnetic field, the actual determination of the eigenfunctions, Eq. (1.4), and the summation appearing in Eq. (1.7) can be carried out only for a limited number of situations. An equivalent expression for the propagator K can, however, be obtained with the aid of a technique known as the path-integral formalism (Feynman, 1948; Feynman and Hibbs, 1965). This equivalent formulation of nonrelativistic quantum mechanics is essentially made possible by the fact that the differential form of the Schrödinger equation

$$\Psi(\mathbf{r}, \tau + \Delta\tau) = \Psi(\mathbf{r}, \tau) - \frac{i}{\hbar} \hat{H} \Psi(\mathbf{r}, \tau) \Delta\tau \quad (1.8)$$

can be transformed into the integral representation

$$\Psi(\mathbf{r}, \tau + \Delta\tau) = \left[\frac{M}{2\pi i \hbar \Delta\tau} \right]^{3/2} \int \exp \left\{ \frac{i}{\hbar} \left[\frac{M(\mathbf{r} - \mathbf{r}')^2}{2\Delta\tau} + \frac{q}{c} \mathbf{A} \left[\frac{\mathbf{r} + \mathbf{r}'}{2}, \tau \right] (\mathbf{r} - \mathbf{r}') - q\varphi(\mathbf{r}', \tau) \Delta\tau \right] \right\} \Psi(\mathbf{r}', \tau) d\mathbf{r}', \quad (1.9)$$

where quadratic or higher-order terms in $\Delta\tau$ are neglected. In the limit of vanishing $\Delta\tau$, the kernel $M(\mathbf{r} - \mathbf{r}')^2/2\hbar\Delta\tau$ becomes very large unless \mathbf{r}' is near to \mathbf{r} , so that the result of the integration with respect to \mathbf{r}' depends only upon the value of the wave function and of its derivatives at \mathbf{r} [Eq. (1.8)]. The application of Eq. (1.9) at successive instants of time t_1, \dots, t_{N-1}, t then yields the wave function at the time t as

$$\Psi(\mathbf{r}, t) = \left[\frac{M}{2\pi i \hbar} \right]^{3N/2} \frac{1}{(t - t_{N-1})^{3/2} \dots (t_1 - t')^{3/2}} \int \exp \left[\frac{i}{\hbar} \tilde{S} \right] \Psi(\mathbf{r}', t') d\mathbf{r}_{N-1} \dots d\mathbf{r}_1 d\mathbf{r}', \quad (1.10)$$

where

$$\tilde{S} = \sum_{i=1}^N \left[\frac{1}{2M} \left(\frac{\mathbf{r}_i - \mathbf{r}_{i-1}}{t_i - t_{i-1}} \right)^2 + \frac{q}{c} \mathbf{A} \left(\frac{\mathbf{r}_i + \mathbf{r}_{i-1}}{2}, t_{i-1} \right) \frac{\mathbf{r}_i - \mathbf{r}_{i-1}}{t_i - t_{i-1}} - q\varphi(\mathbf{r}_{i-1}, t_{i-1}) \right] (t_i - t_{i-1}), \tag{1.11}$$

\mathbf{r}_0, t_0 being identical to \mathbf{r}', t' and \mathbf{r}_N, t_N to \mathbf{r}, t . For infinitesimal intervals $t_i - t_{i-1}$ the quantity \tilde{S} becomes the classical action for the path determined by the points (\mathbf{r}', t') , $(\mathbf{r}_1, t_1), \dots, (\mathbf{r}_{N-1}, t_{N-1}), (\mathbf{r}, t)$,

$$\tilde{S} = \int_{\mathbf{r}(\tau)} \left[\frac{1}{2} M \mathbf{v}^2 + \frac{q}{c} \mathbf{A} \mathbf{v} - q\varphi \right] d\tau, \tag{1.12}$$

where \mathbf{v} is the velocity of the particle on the path $\mathbf{r}(\tau)$ under consideration. If we now sum all the contributions in the exponential appearing in Eq. (1.10), the integration over the variables $d\mathbf{r}_{N-1} \cdots d\mathbf{r}_1$ becomes an integration over all paths connecting the end points \mathbf{r}', t' and \mathbf{r}, t . Several such paths are shown in Fig. 1. By comparing Eqs. (1.10) and (1.6), we see that the propagator is proportional to $\exp(i\tilde{S}/\hbar)$ integrated over all paths connecting the points \mathbf{r}', t' and \mathbf{r}, t (Feynman's rule),

$$K(\mathbf{r}, t; \mathbf{r}', t') = \text{const} \times \int_{\mathbf{r}', t'}^{\mathbf{r}, t} \exp(i\tilde{S}/\hbar) \mathcal{D}\mathbf{r}(\tau). \tag{1.13}$$

The symbol $\mathcal{D}\mathbf{r}(\tau)$ denotes the path integration, which was explicitly written in Eq. (1.10) as a multiple integration over the volume elements $d\mathbf{r}_{N-1} \cdots d\mathbf{r}_1$. Here $K(\mathbf{r}, t; \mathbf{r}', t')$ represents the amplitude for the particle to propagate from the point \mathbf{r}', t' to the point \mathbf{r}, t .

Let us use the path-integral technique to obtain the wave function of a charged particle interacting with a distribution of electric and magnetic fields. We represent the particle by a wave packet rather than a plane wave, because localizing the incident particle will enable us to make a clear distinction between the conventional effects of the field strengths and the effects of the enclosed elec-

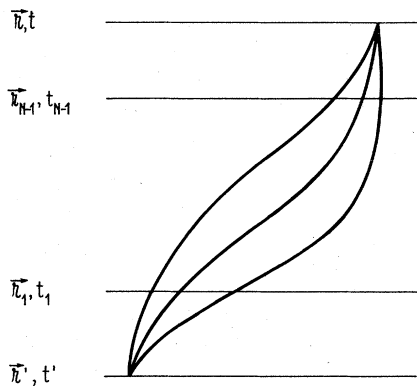


FIG. 1. Nonstationary paths connecting the points \mathbf{r}', t' and \mathbf{r}, t , which appear in the expression for the quantum-mechanical propagator of a particle in the path-integral formalism. According to Feynman's rule, the propagator $K(\mathbf{r}, t; \mathbf{r}', t')$ is proportional to the sum of $\exp(iS/\hbar)$ over all the paths connecting the points \mathbf{r}, t and \mathbf{r}', t' , where S is the classical action.

tromagnetic fluxes. The dominant contribution to the amplitude $K(\mathbf{r}, t; \mathbf{r}', t')$ arises from those paths for which the action in Eq. (1.13) is stationary. If we represent the incident particle by a wave packet centered on a certain point \mathbf{r}_0 at the time t_0 , the propagator in the vicinity of \mathbf{r}_0 can be approximated as

$$K(\mathbf{r}, t; \mathbf{r}', t_0) = \text{const} \times \sum_{\Gamma} \exp \left[\frac{i}{\hbar} S_{\Gamma}(\mathbf{r}, t; \mathbf{r}_0, t_0) + \frac{i}{\hbar} (\nabla_{\mathbf{r}_0} S)(\mathbf{r}' - \mathbf{r}_0) \right], \tag{1.14}$$

where Γ designates the stationary paths connecting the points \mathbf{r}_0, t_0 and \mathbf{r}, t . Assuming that the distribution of canonical momentum $\mathcal{A}(\mathbf{p})$ of the incident wave packet is

$$\Psi(\mathbf{r}', t_0) = \int \mathcal{A}(\mathbf{p}) e^{(i/\hbar)\mathbf{p}(\mathbf{r}' - \mathbf{r}_0)} d\mathbf{p},$$

then Eqs. (1.6) and (1.14) show that the amplitude $\tilde{\Psi}(\mathbf{r}, t)$ for the particle to arrive at \mathbf{r}, t is

$$\tilde{\Psi}(\mathbf{r}, t) = \text{const} \times \sum_{\Gamma} \mathcal{A}(\mathbf{p}_{\Gamma}^{(0)}) e^{(i/\hbar)S_{\Gamma}(\mathbf{r}, t; \mathbf{r}_0, t_0)}, \tag{1.15}$$

where $\mathbf{p}_{\Gamma}^{(0)} = -\nabla_{\mathbf{r}_0} S_{\Gamma}(\mathbf{r}, t; \mathbf{r}_0, t_0)$ represents the canonical momentum at \mathbf{r}_0, t_0 for the stationary path Γ under consideration. Expanding once more the stationary action in Eq. (1.15) around a certain point Q in the observing region yields

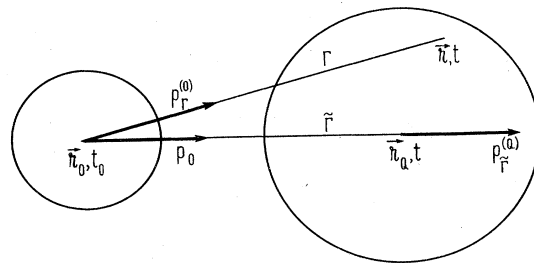


FIG. 2. Propagation of a free wave packet of incident momentum \mathbf{p}_0 , described with the aid of the path-integral formalism in the stationary approximation. The stationary paths $\Gamma, \tilde{\Gamma}$ are straight lines connecting the point \mathbf{r}_0, t_0 to the points \mathbf{r}, t and \mathbf{r}_Q, t , respectively, while $\mathbf{p}_{\Gamma}^{(0)}$ and $\mathbf{p}_{\tilde{\Gamma}}^{(0)}$ are the moments on the paths Γ and $\tilde{\Gamma}$, respectively.

$$\tilde{\Psi}(\mathbf{r}, t) = \text{const} \times \sum_{\Gamma} \mathcal{A}(\mathbf{p}_{\Gamma}^{(0)}) \exp \left[\frac{i}{\hbar} \mathbf{p}_{\Gamma}^{(Q)}(\mathbf{r} - \mathbf{r}_Q) + \frac{i}{\hbar} S_{\Gamma}(\mathbf{r}_Q, t; \mathbf{r}_0, t_0) \right], \quad (1.16)$$

where $\mathbf{p}_{\Gamma}^{(Q)} = \nabla_{\mathbf{r}_Q} S_{\Gamma}(\mathbf{r}_Q, t; \mathbf{r}_0, t_0)$ is the canonical momentum at Q along the path $\tilde{\Gamma}$ connecting \mathbf{r}_0, t_0 to \mathbf{r}_Q, t . Equations (1.15) and (1.16) provide a quasiclassical description of the evolution of the incident wave packet, and are the basis of the analysis in this section of the two-slit scattering of charged particles. Thus according to Eq. (1.16), the calculation of the wave function in the vicinity of Q at time t requires the determination of the stationary paths $\Gamma, \tilde{\Gamma}$ connecting the initial position \mathbf{r}_0, t_0 of the center of the packet to the points \mathbf{r}, t and \mathbf{r}_Q, t , respectively, and the evaluation of the momenta $\mathbf{p}_{\Gamma}^{(0)}$ and $\mathbf{p}_{\tilde{\Gamma}}^{(Q)}$ along these paths. Then the form of the envelope of the interference pattern can be obtained by inserting the dependence of $\mathbf{p}_{\Gamma}^{(0)}$ upon \mathbf{r} and t into the expression of the momentum distribution \mathcal{A} of the incident state, while the phases of the imaginary exponentials in Eq. (1.16) determine the position of the interference fringes.

As an example of application of Eq. (1.16) we consider a Gaussian wave packet moving freely with an average momentum \mathbf{p}_0 and having the momentum distribution

$$\mathcal{A}_{\delta}(\mathbf{p}) = \exp \left[-\frac{\delta^2}{2\hbar^2} (\mathbf{p} - \mathbf{p}_0)^2 \right]. \quad (1.17)$$

Assuming that the center of the wave packet at the time $t_0 = 0$ has been situated at $\mathbf{r}_0 = 0$, we determine according to Eq. (1.16) the probability distribution at the time t in the vicinity of the point

$$\mathbf{r}_Q = \frac{\mathbf{p}_0}{M} t, \quad (1.18)$$

$$\tilde{\Psi}_{\delta}(\mathbf{r}, t) = \frac{1}{\pi^{3/4} \delta^{3/2} (1 + i\hbar t/M\delta^2)^{3/2}} \exp \left[-\frac{(\mathbf{r} - \mathbf{r}_Q)^2}{2(\delta^2 + i\hbar t/M)} + \frac{i\mathbf{p}_0 \mathbf{r}}{\hbar} - \frac{i\mathbf{p}_0^2 t}{2\hbar M} \right]. \quad (1.22)$$

Since the real part of the term $1/(\delta^2 + i\hbar t/M)$ is equal to $\delta^2 M^2 / \hbar^2 t^2$ in the limit when $\delta^2 \ll \hbar t/M$, we see that apart from a diffraction term proportional to $i(\mathbf{r} - \mathbf{r}_Q)^2$ Eq. (1.16) leads to a proper description of the propagation of the wave packet.

B. Two-slit scattering of charged particles

In general, quantum interference patterns are produced as a result of scattering from various obstacles or field distributions, in the path of the incident particles. Of particular interest is the scattering by two parallel slits, which give rise to two coherent waves arriving in the observing region along paths that are slightly inclined with respect to one another, thereby producing a pattern of equally spaced fringes. In this section we discuss the effects of distributions of uniform electric and magnetic

fields upon the two-slit scattering of charged particles. The effects thus determined of the uniform fields will later serve as reference in a comparison with the quantum effects of enclosed electromagnetic fluxes.

Two-slit interference experiments with charged particles generally employ the electrostatic biprism of Möllenstedt and Düker (1956). The biprism consists of a thin metallized fiber set at a convenient potential with respect to a pair of grounded plates, as shown in Fig. 3.

The electric field of the fiber bends the coherent beams passing by the two sides of the fiber and superposes them in the observing region. As will be discussed in Sec. III.A, the paths of the particles emerging from the source \mathcal{S} are deflected by an angle $\pm\gamma$ which depends on the potential of the metallized fiber, but is independent of the incidence direction. Thus, if the average momentum of the incident particle is p_0 , the effect of the biprism is to produce two virtual sources \mathcal{S}_1 and \mathcal{S}_2 situated for

$$\mathbf{p}_{\tilde{\Gamma}}^{(Q)} = \mathbf{p}_0, \quad (1.19)$$

$$S_{\tilde{\Gamma}}(\mathbf{r}_Q, t; 0, 0) = \frac{M\mathbf{r}_Q^2}{2t}, \quad (1.20)$$

while the momentum $\mathbf{p}_{\Gamma}^{(0)}$ is given by

$$\mathbf{p}_{\Gamma}^{(0)} = M \frac{\mathbf{r}}{t}. \quad (1.21)$$

Then according to Eq. (1.16) the wave function of the packet can be expressed as

$$\tilde{\Psi}_{\delta}(\mathbf{r}, t) = \text{const} \times \exp \left[-\frac{\delta^2 M^2}{2\hbar^2 t^2} (\mathbf{r} - \mathbf{r}_Q)^2 + \frac{i}{\hbar} \mathbf{p}_0 \mathbf{r} - \frac{i\mathbf{p}_0^2 t}{2\hbar M} \right]. \quad (1.22)$$

For comparison, the exact normalized wave function of a wave packet having the momentum distribution specified in Eq. (1.17) is given by

fields upon the two-slit scattering of charged particles. The effects thus determined of the uniform fields will later serve as reference in a comparison with the quantum effects of enclosed electromagnetic fluxes.

Two-slit interference experiments with charged particles generally employ the electrostatic biprism of Möllenstedt and Düker (1956). The biprism consists of a thin metallized fiber set at a convenient potential with respect to a pair of grounded plates, as shown in Fig. 3. The electric field of the fiber bends the coherent beams passing by the two sides of the fiber and superposes them in the observing region. As will be discussed in Sec. III.A, the paths of the particles emerging from the source \mathcal{S} are deflected by an angle $\pm\gamma$ which depends on the potential of the metallized fiber, but is independent of the incidence direction. Thus, if the average momentum of the incident particle is p_0 , the effect of the biprism is to produce two virtual sources \mathcal{S}_1 and \mathcal{S}_2 situated for

small angles γ at the same distance from the observing plane as the source \mathcal{S} , and having the y component of the momentum distribution shifted by $\pm p_0\gamma$. Since every point in the illuminated part of the observing region is connected by two stationary paths Γ_1 and Γ_2 to the virtu-

al sources \mathcal{S}_1 and \mathcal{S}_2 , the wave function $\tilde{\Psi}(\mathbf{r},t)$ in the vicinity of a certain point Q in the observing region is obtained according to Eq. (1.16) by the superposition of the amplitudes of arrival along the stationary paths Γ_1 and Γ_2 shown in Fig. 3,

$$\tilde{\Psi}(\mathbf{r},t) = \text{const} \times \left[\mathcal{A}(\mathbf{p}_1^{(\mathcal{S}_1)}) \exp \left[\frac{i}{\hbar} \mathbf{p}_1^{(Q)}(\mathbf{r} - \mathbf{r}_Q) + \frac{i}{\hbar} S_1(\mathbf{r}_Q, t; \mathbf{r}_{\mathcal{S}_1}, t_0) \right] + \mathcal{A}(\mathbf{p}_2^{(\mathcal{S}_2)}) \exp \left[\frac{i}{\hbar} \mathbf{p}_2^{(Q)}(\mathbf{r} - \mathbf{r}_Q) + \frac{i}{\hbar} S_2(\mathbf{r}_Q, t; \mathbf{r}_{\mathcal{S}_2}, t_0) \right] \right], \quad (1.24)$$

where $\mathbf{p}_1^{(\mathcal{S}_1)}$ and $\mathbf{p}_2^{(\mathcal{S}_2)}$ are the initial momenta for the stationary paths Γ_1, Γ_2 connecting the point \mathbf{r}, t in the observing region to the virtual sources \mathcal{S}_1 and \mathcal{S}_2 , $\mathbf{p}_1^{(Q)}$ and $\mathbf{p}_2^{(Q)}$ are the arrival momenta at Q for the paths $\tilde{\Gamma}_1$ and $\tilde{\Gamma}_2$, and S_1 and S_2 are the classical actions along the latter paths.

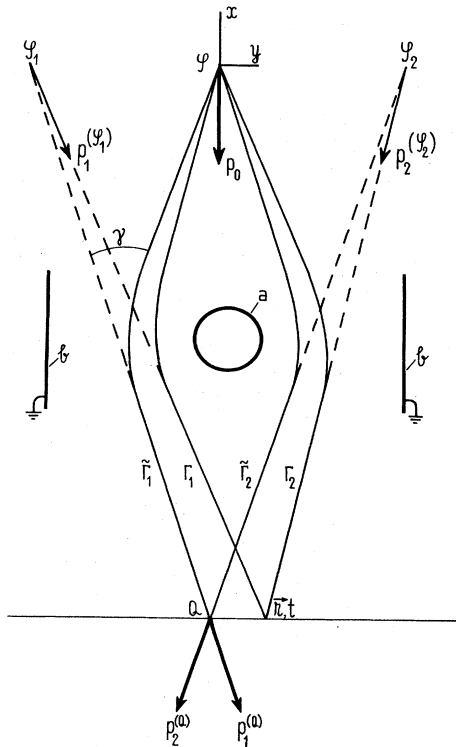


FIG. 3. Two-slit interference experiment with charged particles, based on the electrostatic biprism of Möllenstedt and Düker (1956). The electric field of the metallized fiber a , which is set at a convenient potential with respect to the grounded plates b , bends the paths of the particles emerging from the source \mathcal{S} by the angle γ , and thus gives rise to the virtual images $\mathcal{S}_1, \mathcal{S}_2$ of the source \mathcal{S} . The interference pattern in the vicinity of a certain point Q in the observing region is obtained as the superposition of the amplitudes of arrival of the particle at the point \mathbf{r}, t along the stationary paths Γ_1, Γ_2 .

Let us first apply Eq. (1.24) to the description of the two-slit interference in the absence of an electromagnetic field. We shall assume that the distribution of incident momentum appearing in Eq. (1.24) is given by Eq. (1.17), with the average incident momentum having only the x component $-p_0$, where $p_0 > 0$. Then, as discussed at the end of the preceding section, the interference pattern is produced by the superposition of the Gaussian wave packets arriving in the observing region from the directions of the virtual sources \mathcal{S}_1 and \mathcal{S}_2 , the probability distribution in each packet being cut at the corresponding limit of the geometrical shadow of the fiber. If the integration over \mathbf{r}' , in Eq. (1.6), leading from Eq. (1.14) to Eqs. (1.15) and (1.16) and further to Eq. (1.24), is performed relative to the center of the wave packet, then the momentum distribution \mathcal{A}_δ is real, and consequently it does not affect the relative phases of the two terms appearing in Eq. (1.24). Moreover, since the stationary paths connecting the observing region to the virtual sources \mathcal{S}_1 and \mathcal{S}_2 are straight lines, we have

$$p_{1x}^{(Q)} = \frac{M(x_Q - x_1)}{t - t_0}, \quad p_{1y}^{(Q)} = \frac{M(y_Q - y_1)}{t - t_0},$$

$$S_1(\mathbf{r}_Q, t; \mathbf{r}_1, t_0) = \frac{M(\mathbf{r}_Q - \mathbf{r}_1)^2}{2(t - t_0)},$$

where x_1, y_1 designate the position of the virtual source \mathcal{S}_1 . Then the phase of the first term in Eq. (1.24) becomes

$$\frac{M}{\hbar(t - t_0)} \left[(x_Q - x_1)x + (y_Q - y_1)y - \frac{x_Q^2 + y_Q^2}{2} + \frac{x_1^2 + y_1^2}{2} \right],$$

and the second term in Eq. (1.24) is analogous. If the biprism is symmetric, so that $x_1 = x_2, y_1 = -y_2$, the difference between the phases of the exponential terms in Eq. (1.24) becomes $M(y_2 - y_1)y / \hbar(t - t_0)$. Assuming that the particle is observed at the time $t - t_0 = M(x_Q - x_{\mathcal{S}}) / (-p_0)$, we obtain the well-known result that the interference pattern consists of a system of equally spaced

fringes separated by the distance $\lambda_0(x_Q - x_{\mathcal{S}})/(y_2 - y_1)$, the central fringe being bright, where $\lambda_0 = 2\pi\hbar/p_0$.

Now let us consider the effects of applied electric and magnetic fields on the two-slit scattering of charged particles. According to Eq. (1.24), the interference pattern can be analyzed by studying the paths connecting the points in the observing region to the virtual sources \mathcal{S}_1 and \mathcal{S}_2 . Thus we shall first consider the paths connecting the sources \mathcal{S}_1 or \mathcal{S}_2 to a certain point P in the observing region in the absence of the fields; then we shall determine the paths emerging with the same initial momentum from the virtual sources to arrive in the presence of the applied fields at a shifted position Q in the observing region; and finally we shall analyze the field-dependent probability distribution in the vicinity of the point Q by comparing it with the unperturbed distribution around the point P .

First we shall apply this program to the analysis of effects on the two-slit scattering of a uniform electric field E , which is perpendicular to the average momentum p_0 of the incident particle, as shown in Fig. 4. Since in the electric case the motion parallel to the incidence direction is uniform, all the paths emerging at the time t_0 from the virtual sources \mathcal{S}_1 or \mathcal{S}_2 to arrive at the time t in the observing region will intersect the region of electric field at the same instants t', t'' , which are independent of the electric field. Let us consider the path emerging at the time t_0 from the source \mathcal{S}_1 , to arrive at the time t at a certain point \tilde{x}, \tilde{y} in the observing plane. In the absence of the

electric field, the path connecting \mathcal{S}_1 to \tilde{x}, \tilde{y} is a straight line described parametrically by

$$x = x_1 - \frac{p_0}{M}(\tau - t_0), \tag{1.25a}$$

$$y = y_1 + \frac{\tilde{y} - y_1}{t - t_0}(\tau - t_0), \tag{1.25b}$$

where $t_0 \leq \tau \leq t$. Assuming that the interference pattern is observed at the time $t - t_0 = M(\tilde{x} - x_1)/(-p_0)$, the path emerging from \mathcal{S}_1 at the time t_0 with the same initial velocity components $[-p_0/M, (\tilde{y} - y_1)/(t - t_0)]$ admits in the presence of the electric field the parametric representation

$$x_E = x_1 - \frac{p_0}{M}(\tau - t_0), \quad t_0 \leq \tau \leq t, \tag{1.26a}$$

$$y_E = y_1 + \frac{\tilde{y} - y_1}{t - t_0}(\tau - t_0), \quad t_0 \leq \tau \leq t', \tag{1.26b}$$

$$y_E = y_1 + \frac{\tilde{y} - y_1}{t - t_0}(\tau - t_0) + \frac{1}{2} \frac{qE}{M}(\tau - t')^2, \quad t' \leq \tau \leq t'', \tag{1.26c}$$

$$y_E = y_1 + \frac{\tilde{y} - y_1}{t - t_0}(\tau - t_0) + \frac{1}{2} \frac{qE}{M}(t'' - t')^2 + \frac{qE}{M}(t'' - t')(\tau - t''), \quad t'' \leq \tau \leq t. \tag{1.26d}$$

Equations (1.26) describe a uniform motion between t_0 and t' , an accelerated motion between t' and t'' , and a uniform motion with a different velocity between t'' and t_0 . By comparing Eqs. (1.26d) and (1.25b) we see that the electric field has shifted the position of the arrival Q in the observing plane by an amount Δ_E given by

$$\Delta_E = \frac{1}{2} \frac{qE}{M}(t'' - t')^2 + \frac{qE}{M}(t'' - t')(t - t''). \tag{1.27}$$

This means that the amplitude $\mathcal{A}_s(-p_0/M, (\tilde{y} - y_1)/(t - t_0))$, which in the absence of the electric field contributed to the wave function at \tilde{x}, \tilde{y} , will now be measured at the shifted position $\tilde{x}, \tilde{y} + \Delta_E$. However, as can be appreciated from Eq. (1.27), the shift Δ_E depends neither on the initial position y_1 , nor on the initial y component of the velocity, so that all the paths emerging at the time t_0 from the virtual sources \mathcal{S}_1 or \mathcal{S}_2 and arriving in the observing plane at the time t will be shifted by the same distance Δ_E . Consequently, the envelope of the interference pattern will be displaced in the observing plane by the distance Δ_E .

Now the position of the interference extremes depends on the phases of the exponentials appearing in Eq. (1.24). Since the momenta $p_{1y}^{(Q)}$ and $p_{2y}^{(Q)}$ are both increased by $qE(t'' - t')$, while the displacement in the observing plane is normal to the x direction, the terms in Eq. (1.24) which are proportional to $p_1^{(Q)}$ and $p_2^{(Q)}$ do not affect the relative phase difference. Let us further determine the action S_E for the stationary path connecting the points \mathcal{S}_1 and Q in

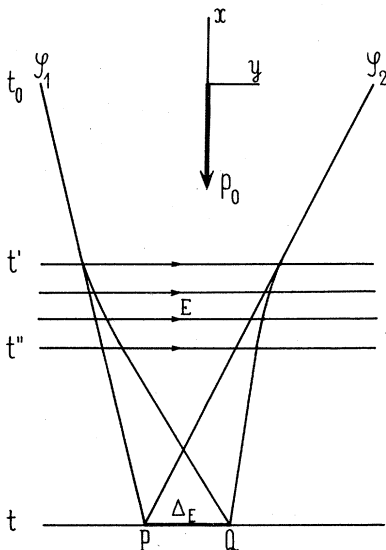


FIG. 4. Effect of an applied electric field E on the two-slit scattering of charged particles. The electric field bends the paths connecting the virtual sources \mathcal{S}_1 and \mathcal{S}_2 to the observing plane in such a way that the interference pattern is shifted as a whole by a certain distance Δ_E , leaving unaffected the position of the interference fringes relative to the envelope. The deflection shown in the drawing corresponds to a positive charge of the particle.

the presence of the field E , and compare it with the action for the unperturbed path \mathcal{S}_1P . Setting $\mathbf{A}=0$ and substituting the potentials $\varphi=0$ for $t_0 < \tau < t'$, $t'' < \tau < t$ and $\varphi = -Ey$ for $t' < \tau < t''$ in the expression of the action, Eq. (1.12), we obtain the action corresponding to the path, Eqs. (1.26), as

$$S_E(Q, t; \mathcal{S}_1, t_0) = S_0(P, t; \mathcal{S}_1, t_0) + qEy_P(t'' - t') + \frac{q^2 E^2}{6M} (t'' - t')^2 (3t - 2t' - t''), \quad (1.28)$$

where

$$S_0(P, t; \mathcal{S}_1, t_0) = \frac{M[(x_P - x_1)^2 + (y_P - y_1)^2]}{2(t - t_0)} \quad (1.29)$$

is the action for the path \mathcal{S}_1P in the absence of the electric field. As expected, the action in the presence of the electric field, Eq. (1.28), is obtained from the field-free action by adding certain terms depending on E . These terms, however, are independent of the position y_1 of the source point \mathcal{S}_1 , so that the change in the action $S_E(Q, t; \mathcal{S}_2, t_0)$ will be identical to the change in $S_E(Q, t; \mathcal{S}_1, t_0)$. Referring once more to Eq. (1.24), this means that the phase difference between the coherent waves arriving at Q in the presence of the electric field is equal to the phase difference between the coherent waves arriving at P in the absence of the field. We arrive thus at the conclusion that the position of the interference fringes relative to the envelope of the pattern is not affected by the applied electric field, i.e., the electric field shifts the interference pattern as a whole.

We turn now from the effects of an electric field to the effects of a uniform magnetic field B applied in the positive direction of the z axis, as shown in Fig. 5. Let us consider an unperturbed trajectory emerging at the time t_0 from the virtual source \mathcal{S}_1 , to arrive at the time t at the point \tilde{x}, \tilde{y} in the observing region. We shall assume that this path intersects the region of magnetic field at the times t' and t'' , and shall determine the trajectory of the particle in the presence of the applied field B by adding a correction to the unperturbed path. The x and y components of the velocity of the particle in the presence of the magnetic field are given by

$$v_x = \frac{\tilde{x} - x_1}{t - t_0}, \quad t_0 < \tau < t' \quad (1.30a)$$

$$v_y = \frac{\tilde{y} - y_1}{t - t_0}, \quad t_0 < \tau < t' \quad (1.30b)$$

$$v_x = \frac{\tilde{x} - x_1}{t - t_0} + \frac{qB(\tilde{y} - y_1)}{Mc(t - t_0)} (\tau - t'), \quad t' < \tau < t'' \quad (1.30c)$$

$$v_y = \frac{\tilde{y} - y_1}{t - t_0} - \frac{qB(\tilde{x} - x_1)}{Mc(t - t_0)} (\tau - t'), \quad t' < \tau < t'' \quad (1.30d)$$

$$v_x = \frac{\tilde{x} - x_1}{t - t_0} + \frac{qB(\tilde{y} - y_1)}{Mc(t - t_0)} (t'' - t'), \quad t'' < \tau < t_0 \quad (1.30e)$$

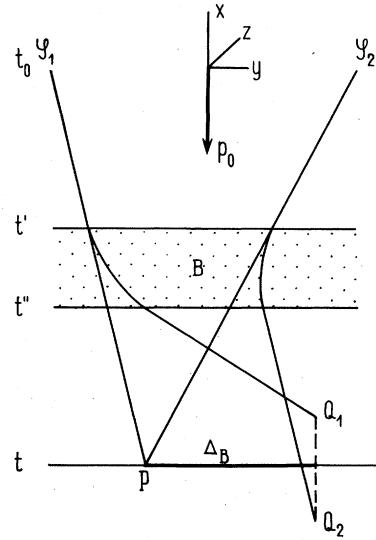


FIG. 5. Effect of an applied magnetic field B on the two-slit scattering of charged particles. The magnetic field bends the paths connecting the virtual sources \mathcal{S}_1 and \mathcal{S}_2 to the observing plane in such a way that the interference pattern is shifted as a whole by a certain distance Δ_B , leaving unaffected the position of the interference fringes relative to the envelope of the pattern. The deflection shown in the drawing corresponds to a magnetic field oriented along the $+z$ axis, and a positive charge of the particle.

$$v_y = \frac{\tilde{y} - y_1}{t - t_0} - \frac{qB(\tilde{x} - x_1)}{Mc(t - t_0)} (t'' - t'), \quad t'' < \tau < t_0 \quad (1.30f)$$

where quadratic terms in B have been neglected. By integrating Eqs. (1.30) with respect to the time, we find that the extremity of the path in the presence of the magnetic field is the point with coordinates

$$x_B^{(1)} = \tilde{x} + \frac{qB(\tilde{y} - y_1)(t'' - t')(2t - t' - t'')}{2Mc(t - t_0)}, \quad (1.31a)$$

$$y_B^{(1)} = \tilde{y} - \frac{qB(\tilde{x} - x_1)(t'' - t')(2t - t' - t'')}{2Mc(t - t_0)}. \quad (1.31b)$$

According to Eqs. (1.31), the point $x_B^{(1)}, y_B^{(1)}$ is obtained from the point x, y by a rotation of small angle

$$\alpha = \frac{qB(t'' - t')(2t - t' - t'')}{2Mc(t - t_0)}$$

about the point \mathcal{S}_1 . It can be shown analogously that the path emerging from the virtual source \mathcal{S}_2 , to arrive in the absence of the magnetic field at the point x, y of the observing plane, will be shifted by the magnetic field, so that its extremity is the point with coordinates

$$x_B^{(2)} = \tilde{x} - \frac{qB(\tilde{y} - y_1)(t'' - t')(2t - t' - t'')}{2Mc(t - t_0)}, \quad (1.32a)$$

$$y_B^{(2)} = \tilde{y} - \frac{qB(\tilde{x} - x_1)(t'' - t')(2t - t' - t'')}{2Mc(t - t_0)}. \quad (1.32b)$$

Since both paths are displaced in the y direction by the same distance,

$$\Delta_B = \frac{qB(\bar{x} - x_1)(t'' - t')(2t - t' - t'')}{2Mc(t - t_0)}, \quad (1.33)$$

it follows that the applied magnetic field shifts the envelope of the interference pattern by Δ_B .

As previously, the position of the interference fringes

depends on the phases of the exponential terms appearing in Eq. (1.24). If P is a certain point in the observing plane, we shall denote by Q_1 the point obtained from P by a rotation of angle ν about \mathcal{S}_1 , and by Q_2 the point obtained from P by a rotation of angle ν about \mathcal{S}_2 , as shown in Fig. 5. In this problem it is convenient to expand the stationary action appearing in the expression of the total wave function, Eq. (1.15), about different points Q_1, Q_2 , so that an equivalent form of Eq. (1.24) is

$$\begin{aligned} \tilde{\Psi}(\mathbf{r}, t) = \text{const} \times & \left[\mathcal{A}(\mathcal{S}_1^{(Q_1)}) \exp \left[\frac{i}{\hbar} \mathbf{p}_1^{(Q_1)}(\mathbf{r} - \mathbf{r}_{Q_1}) + \frac{i}{\hbar} S_1(\mathbf{r}_{Q_1}, t; \mathbf{r}_{\mathcal{S}_1}, t_0) \right] \right. \\ & \left. + \mathcal{A}(\mathcal{S}_2^{(Q_2)}) \exp \left[\frac{i}{\hbar} \mathbf{p}_2^{(Q_2)}(\mathbf{r} - \mathbf{r}_{Q_2}) + \frac{i}{\hbar} S_2(\mathbf{r}_{Q_2}, t; \mathbf{r}_{\mathcal{S}_2}, t_0) \right] \right], \end{aligned}$$

where $\mathbf{p}_1^{(Q_1)}$ is the momentum at Q_1 on the stationary path connecting \mathcal{S}_1 and Q_1 , and $\mathbf{p}_2^{(Q_2)}$ the momentum at Q_2 on the stationary path $\mathcal{S}_2 Q_2$. Since the y components of the momenta are increased by the amount $qp_0 B(t'' - t')/Mc$, while the y coordinates of the points Q_1 and Q_2 are equal, the terms in the expression of $\tilde{\Psi}$ which are proportional to $p_{1y}^{(Q_1)}$ and $p_{2y}^{(Q_2)}$ do not affect the relative phase of the coherent components. However, the different locations of the points Q_1 and Q_2 along the x direction result in a phase difference between the components 2 and 1 of

$$-\frac{qp_0 B(y_2 - y_1)(t'' - t')(2t - t' - t'')}{2Mc(t - t_0)}.$$

Now the actions S_1 and S_2 are computed from Eq. (1.12), for $\varphi=0$. Since the magnitude of \mathbf{v} is conserved by the magnetic field, the kinetic energy in the Lagrange function yields no change in the value of the action. The contribution to the phase difference of the remaining term $q\mathbf{A}\mathbf{v}/c$, which is given by

$$\frac{q}{\hbar c} \left[\int_{\mathcal{S}_2}^{Q_2} \mathbf{A} d\mathbf{r} - \int_{\mathcal{S}_1}^{Q_1} \mathbf{A} d\mathbf{r} \right],$$

is equal to

$$\frac{qB}{\hbar c} \frac{p_0(t'' - t')}{M} \frac{t - (t' + t'')/2}{t - t_0} (y_2 - y_1),$$

the plus sign being due to the fact that the sense of the integration in the x, y plane coincides with the sense of B . Therefore the field-dependent contributions to the phase cancel each other, and the position of the fringes relative to the envelope remains unchanged, up to quadratic terms in B . Thus the applied magnetic field displaces the interference pattern as a whole.

C. Quantum effects of electromagnetic fluxes

In principle, the properties of the electromagnetic field can be determined from the changes in the state of test charged particles interacting with the field. Since the changes in the kinematical state of a charged particle of velocity \mathbf{v} depend on the Lorentz force $q(\mathbf{E} + \mathbf{v} \times \mathbf{B}/c)$, the electromagnetic continuum is described in classical physics by the local values of the electric and magnetic field strengths \mathbf{E} and \mathbf{B} . The field strengths are often expressed in terms of the scalar and vector potentials φ, \mathbf{A} as

$$\mathbf{E} = -\nabla\varphi - \frac{1}{c} \frac{\partial \mathbf{A}}{\partial t}, \quad (1.34a)$$

$$\mathbf{B} = \nabla \times \mathbf{A}. \quad (1.34b)$$

The distribution of electromagnetic potentials is not uniquely determined by the distribution of field strengths, as a change in the gauge of the potentials

$$\varphi' = \varphi - \frac{1}{c} \frac{\partial f}{\partial t}, \quad (1.35a)$$

$$\mathbf{A}' = \mathbf{A} + \nabla f, \quad (1.35b)$$

leaves the field strengths unaffected, for an arbitrary gauge function f of space and time. Therefore, in classical electromagnetism, the potentials are considered as mathematical entities, without physical significance.

The evolution of the quantum-mechanical state of a charged particle is governed by Eqs. (1.1) and (1.2), which include as field variables the scalar and vector potentials φ, \mathbf{A} . Therefore it is conceivable that the physical significance of the potentials should eventually become apparent at the quantum-mechanical level of description of the interaction between the charged particles and the electromagnetic field. However, it can be shown by a direct calculation that the change in the gauge of the potentials specified in Eqs. (1.35) implies a phase transformation of the wave function,

$$\Psi' = \Psi e^{(iq/\hbar c)f}, \quad (1.36)$$

so that the gauge arbitrariness is not removed, even at the quantum-mechanical level of description of the interaction.

If such effects specific to the quantum nature of the interaction exist, they must depend on the electromagnetic flux, rather than on the local value of the potentials. This circumstance, already mentioned by Franz (1939), was independently discussed by Ehrenberg and Siday (1949), who predicted the existence of observable quantum interference phenomena associated with stationary magnetic fluxes. The full importance of the problem became clear after the detailed description of the quantum effects of the electromagnetic fluxes by Aharonov and Bohm (1959). The action of the enclosed fluxes on the quantum interference of charged particles, known as the Aharonov-Bohm effect, produces a shift of the interference fringes relative to the envelope of the pattern, while leaving the envelope unchanged. Since the observable fringe shifts persist even if the overlap between the incident particles and the distribution of electromagnetic flux is rendered arbitrarily small, the existence of the Aharonov-Bohm effect demonstrates that a knowledge of the field strengths in a certain region of the space is not sufficient to characterize completely the state of the electromagnetic continuum in that region.

As mentioned previously, the path-integral formalism is particularly suitable for quasiclassical analysis of the processes of quantum interference, for it reduces the quantum-mechanical problem to the computation of the classical action along the appropriate stationary paths. An examination of Eq. (1.16) for the observing region of the two-slit scattering wave function, and of the action, Eq. (1.12), shows that there are two distinct ways in which the applied electromagnetic fields act upon the charged particles to produce changes in the interference patterns. Both the location of the stationary paths appearing in Eq. (1.16), and the part of the action arising from the integral along these paths of the kinetic energy depend on the local strengths of the electric and magnetic fields. The shifts of the envelope of the interference pattern discussed in the preceding section are characteristic for this type of action of the field strengths. The other contribution arises from the remaining part of the action $\int (q \mathbf{A} \cdot \mathbf{v}/c - q\varphi) dt$, and it produces a fringe shift depending on the amount of electromagnetic flux enclosed between the stationary paths. The remarkable thing is that the aforementioned contributions are independent, in the sense that the amount of electromagnetic flux enclosed by a certain loop is not predetermined by the value of the field strengths at points on the loop. In particular, there are distributions of nonzero electromagnetic fluxes, which yield, however, vanishing field strengths in the vicinity of the unperturbed stationary paths. Such distributions leave the envelope of the interference pattern unchanged, while producing observable shifts of the fringes relative to the envelope.

Regions of space filled with nonzero electromagnetic

fields, which are complementary to regions of vanishing fields, occur rather frequently in physics, as, for example, shielded boxes or guided waves. Two simple configurations of special interest for our problem are the electric field distribution of a plane-parallel capacitor and the magnetic field distributions of an infinitely long solenoid. Although the field strengths are vanishing in the region exterior to the capacitor or the solenoid, the distribution of electromagnetic potentials within those regions are not negligible and, as will be discussed further, they lead in fact to observable electromagnetic effects.

Let us consider a one-dimensional, time-dependent quantum interference experiment in which the initial wave function of a charged particle is split into two coherent wave packets and then recombined to produce an interference pattern, as shown in Fig. 6(a). Moreover, an electric field E is applied after the separation of the packets, over a region of length d_0 situated between the packets, the field being removed after a time τ_0 before the recombination of the coherent packets. The electric field can be produced, for example, by a plane-parallel capacitor having two small holes in the plates, for the passage of the wave packets, as represented in Fig. 6(a). According to Eqs. (1.16), the presence of the applied electric field does not affect the envelope of the interference pattern, because the stationary paths connecting the points near the centers of the probability distribution at the initial and the final times lie entirely in field-free regions of space. Now although the scalar potential φ is constant in each of the two field-free regions exterior to the capacitor, there is a potential difference Ed_0 across the capacitor. This means that after the application of the electric field, the two coherent wave packets are immersed in regions of different scalar potentials. According to Eqs. (1.16) and (1.12), this means that the difference of the phases of the

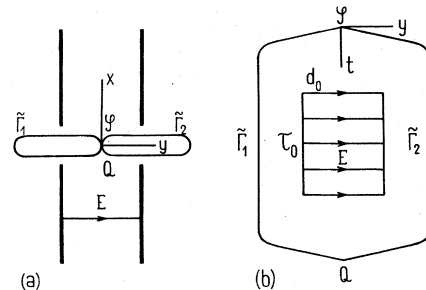


FIG. 6. Experiment demonstrating the quantum effects of electric fluxes. The initial wave function of a charged particle is split into two coherent wave packets, which are subsequently recombined to produce an interference pattern. The electric field E is applied after the separation of the wave packets, over a region of length d_0 situated between the packets, the field being removed after a time interval τ_0 before recombination. The envelope of the pattern is unchanged, but the fringes are shifted relative to the envelope of the pattern by a distance depending on the amount of electric flux $E d_0 \tau_0$ enclosed between the stationary paths $\tilde{\Gamma}_1$ and $\tilde{\Gamma}_2$. (a) Projection of the stationary paths in the x, y plane. (b) Projection of the stationary paths in the y, t plane.

wave packets 2 and 1, whose superposition produces the interference pattern, is modified by

$$\Delta\Phi_E = -\frac{1}{\hbar} \oint q\varphi dt, \tag{1.37}$$

where the integration is performed along the stationary paths $\tilde{\Gamma}_1, \tilde{\Gamma}_2$ connecting the source point \mathcal{S} to the observing point \mathcal{Q} , as shown in Fig. 6(b). Since the vector potential is zero in this problem, the integral, Eq. (1.37), represents the electric flux enclosed between the stationary paths,

$$-\oint \varphi dt = \int E dy dt, \tag{1.38}$$

so that

$$\Delta\Phi_E = \frac{qE\tau_0 d_0}{\hbar}. \tag{1.39}$$

Thus the electric field, although not acting directly on the charged particles, produces a shift of the fringes relative to the envelope of the interference pattern, which is a periodic function of the amount of enclosed electric flux.

A similar effect for magnetic flux can be demonstrated with the aid of an infinitely long solenoid of radius r_0 placed in the shadow of the fiber a of the electrostatic biprism a, b placed in the shadow of the fiber of the electrostatic biprism, as shown in Fig. 7. In this case, too, the magnetic field does not affect the stationary paths connecting the points in the incidence region to the points in the observing region. However, since the circulation of the vector

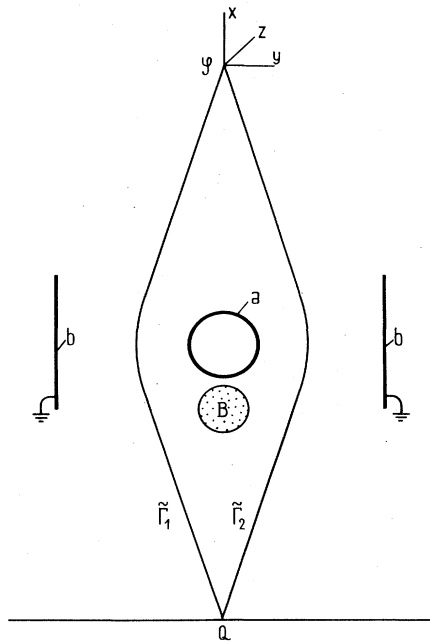


FIG. 7. Experiment demonstrating the quantum effects of magnetic fluxes. The magnetic field B of an infinitely long solenoid of radius r_0 , placed in the shadow of the fiber a of the electrostatic biprism a, b , leaves the envelope of the interference pattern unchanged, but shifts the position of the fringes relative to the envelope of the pattern by a distance depending on the magnetic flux $\pi r_0^2 B$ enclosed between the stationary paths $\tilde{\Gamma}_1, \tilde{\Gamma}_2$.

potential on a loop around the solenoid is equal to the magnetic flux enclosed by that loop, the vector potential has, roughly speaking, opposite orientations on the two sides of the flux region. Then according to Eqs. (1.16) and (1.12), there will be a change in the relative phase of the wave packets arriving in the observing region along different paths, given by

$$\Delta\Phi_B = \frac{q}{\hbar c} \oint \mathbf{A} \mathbf{v} dt. \tag{1.40}$$

Since $\mathbf{v} dt$ is just the differential path element $d\mathbf{r}$, we have

$$\oint \mathbf{A} \mathbf{v} dt = \int B dx dy, \tag{1.41}$$

where the integrations are performed, respectively, along the contour formed by the two stationary paths $\tilde{\Gamma}_1, \tilde{\Gamma}_2$ shown in Fig. 7, and on the surface delimited by that contour. Thus

$$\Delta\Phi_B = \frac{\pi q r_0^2 B}{\hbar c}, \tag{1.42}$$

so that the magnetic field, although not acting directly on the incident particle, produces a shift of the fringes relative to the envelope of the pattern, which is a periodic function of the amount of enclosed magnetic flux.

It is interesting to compare the effects of uniform electric or magnetic fields, like those considered in the preceding section, with the quantum effects of enclosed electric or magnetic fluxes. We have seen in Sec. I.B that uniform electric or magnetic fields displace an interference pattern as a whole, and moreover, if the slits are symmetric with respect to the incidence direction, the central fringe is bright in the absence as well as in the presence of the fields, as represented in Figs. 8(a) and 8(b). On the other hand, the enclosed fluxes leave the envelope of the interference pattern unchanged, but shift the position of the fringes relative to the envelope of the pattern by a distance depending periodically on the amount of enclosed electromagnetic flux. In particular, whenever the amount of enclosed electric flux $\int E dy dt$ is an integer multiple of $2\pi\hbar/q$, or the enclosed magnetic flux $\int B dx dy$ an integer multiple of $2\pi\hbar c/q$, there are no observable changes in the interference pattern, while for half-integer multiples of $2\pi\hbar/q$ or $2\pi\hbar c/q$, respectively, the positions of the light and dark fringes are interchanged, the central fringe becoming dark, as shown in Fig. 8(c). The distinction between the effects of uniform and enclosed fields has been particularly emphasized by Boyer (1973b), and more recently by Greenberger and Overhauser (1979).

According to Wigner (1959), the Aharonov-Bohm effect must be observable if conventional quantum theory is right, and if such effects are found to be absent under conditions where they are predicted, that would necessitate a break from existing quantum theory. The reality of the Aharonov-Bohm effect is now firmly established, and several textbooks have already mentioned the effect (Feynman, Leighton, and Sands, 1965; Tomonaga, 1966; Sakurai, 1967; Baym, 1969). The importance of the problem is due to the fact that the quantum effects of the

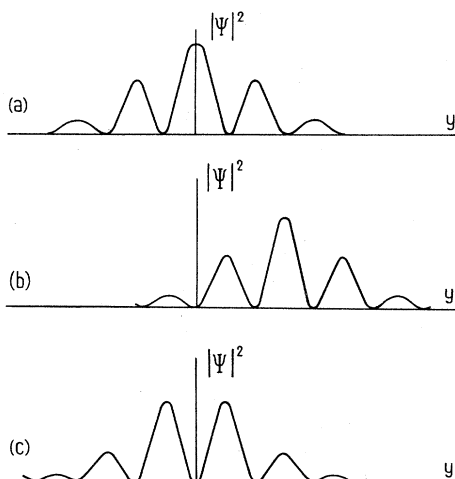


FIG. 8. Effects of various applied electromagnetic fields on the probability distribution in the observing region, for two-slit scattering of charged particles. (a) Unperturbed interference pattern. (b) Pattern displaced as a whole by a uniform electric or magnetic field. (c) Fringe shift produced by an enclosed electric flux of $\pi\hbar/q$ or by an enclosed magnetic flux of $\pi\hbar c/q$. In this case the position of the light and dark fringes are interchanged with respect to the unperturbed pattern, while the envelope remains unchanged.

fluxes demonstrate the limitations of the concept of local field strength in quantum mechanics. Thus, in the period preceding the discovery of the Aharonov-Bohm effect, a region of space free of field strengths was considered electromagnetically empty, even if multiconnected. Now we see that the result of certain quantum interference experiments in field-free, multiconnected spaces is not always the same, and in order to account for this fact we have to invoke the presence of electromagnetic potentials acting on the charged particles, or to accept the possibility of a nonlocal action of the distributions of inaccessible field strengths, or to formally ascribe the results to changes in the boundary conditions applied to the frontier of the accessible multiconnected region. Whatever should be the explanation, it remains true that a knowledge of the field strengths acting directly on the charged particles does not provide a complete description of the state of the electromagnetic continuum in the multiconnected region accessible to the incident particles. More information is needed beyond knowledge of the local field strengths to specify the state of the electromagnetic continuum in a restricted region of space; this is the point demonstrated by the Aharonov-Bohm effect.

D. Bohr's complementarity principle

The work of Aharonov and Bohm attracted considerable attention to the problem of the quantum effects of the fluxes. Apparently the first reaction to the work of Aharonov and Bohm was that it was wrong. However, an indirect confirmation of the reality of the Aharonov-

Bohm effect was soon reported by Furry and Ramsey (1960), who pointed out that the existence of an action of the electromagnetic fluxes of the type described by Aharonov and Bohm is fully consistent with the principle of complementarity. This principle, formulated by Bohr (1928), states that quantum-mechanical systems may be characterized by two different kinds of description, whose applicability is mutually exclusive (for a historical review see Jammer, 1966). The wave and particle descriptions of a particle are said to be complementary; an experiment that demonstrates the particle-like nature of electrons will not also show their wavelike nature, and vice versa. In the case of two-slit scattering, if we determine which slit the particle went through along its particle-like path from the source to the observing region, then according to the principle of complementarity the process of measurement of the path must exert an action on the incident particle that is sufficient to destroy the wavelike interference pattern. We shall discuss in this section a series of two-slit scattering experiments in which the electric and magnetic fields play the role of the perturbing action inherent in any measuring process. Thus we shall see that the existence of effects of this type is not only consistent with, but also required by, the principle of complementarity.

As suggested by Furry and Ramsey (1960), the slit through which the incident particle passed as it traveled from the source to the observing region can be determined in principle by placing a charged test body between the two slits, and by observing the direction of the momentum change produced during the passage of the scattered particle. In order that the particle should not be subject to any field produced by the test body, a condition necessary for the electric Aharonov-Bohm effect, the region beyond the slits is electrostatically shielded by two metal pipes \mathcal{P}' and \mathcal{P}'' , as shown in Fig. 9. Moreover, the test body of charge q_0 is held fixed halfway between two condenser plates attached to the pipes until the incident particle is inside the pipes and will be brought back to that position before the particle emerges from the pipes, the test body moving freely only for a time interval τ_0 when the particle is certain to be inside the shielding pipes. Following Furry and Ramsey, we first determine for the arrangement described above the magnitude of the momentum change produced by the passage of the incident particle through one of the slits, and hence obtain the uncertainty in the position of the test body that is consistent with the measuring of the momentum change. Then we relate the uncertainty in the position of the test body to the uncertainty in the potential difference between the two pipes, and find out that the resulting potential uncertainty is just that required to destroy the interference pattern by an electric Aharonov-Bohm effect.

The magnitude of the electric field acting on the test body can be determined from the potential difference between the two pipes. The potential difference V produced by the presence of the incident charged particle in one or the other of the tubes is

$$V = \pm \frac{q}{2\mathcal{C}_0}, \quad (1.43)$$

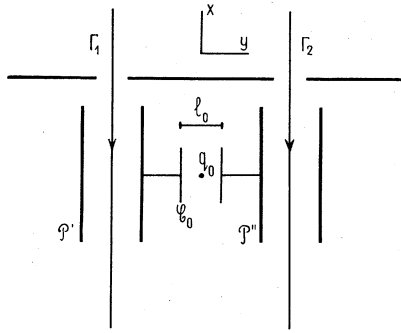


FIG. 9. Complementarity of the wavelike and particle-like properties of matter in two-slit scattering of charged particles, according to Furry and Ramsey (1960). The slit through which the incident particle passed can be determined from the direction of the momentum change of a test body of charge q_0 placed between the plates of a condenser \mathcal{C}_0 attached to the two metal pipes \mathcal{P}' and \mathcal{P}'' . However, the possibility of measuring this momentum change entails an uncertainty in the position of the test body, and consequently an uncertainty in the potential difference between the shielding pipes \mathcal{P}' and \mathcal{P}'' . The uncertainty in the potential difference is then sufficient to destroy the wavelike interference pattern by an electric Aharonov-Bohm effect, while there is no field acting along the stationary paths connecting the regions of incidence and observation.

where \mathcal{C}_0 is the total capacity of the condenser and attached pipes. This result can be obtained with the aid of Green's electrostatic reciprocity theorem, stating that in a system of conductors for which the potentials are V_i when the charges are q_i and V'_i when the charges are q'_i , these quantities fulfill the relation

$$\sum q_i V'_i = \sum q'_i V_i, \quad (1.44)$$

the zero of the potential being at infinity (see, for example, Panofsky and Phillips, 1962). If Eq. (1.44) is applied to the case of two conductors carrying the charges Q and $-Q$, respectively, it yields

$$(V'_1 - V'_2) - (V_1 - V_2) = \frac{qV_1}{Q}, \quad (1.45)$$

with the notations of Fig. 10. However the charge Q can be expressed as $\mathcal{C}_0(V_1 - V_2)$, where \mathcal{C}_0 is the capacity of the system of two conductors, so that the right-hand side of Eq. (1.45) becomes $qV_1/\mathcal{C}_0(V_1 - V_2)$. Now if the two conductors are the shielding pipes \mathcal{P}' and \mathcal{P}'' shown in Fig. 9, we have $V_1 = -V_2$, because of their symmetry. If we let the charge Q become vanishingly small, the potentials V_1 and V_2 go to zero, and in this limit the ratio $qV_1/(V_1 - V_2)$ becomes $q/2\mathcal{C}_0$, which is the result, Eq. (1.43).

Assuming that the plates of the condenser attached to the pipes are separated by the distance l_0 , the magnitude of the electric field acting on the test body is, according to Eq. (1.43),

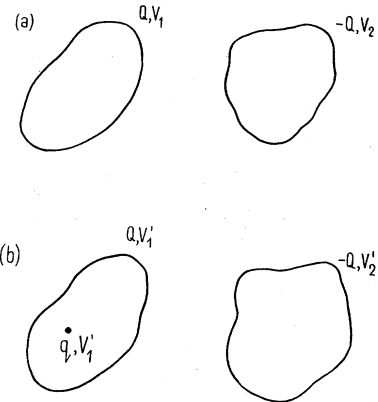


FIG. 10. Evaluation of the potential difference between two conducting bodies, induced by a charge q placed inside one of the conductors. According to Green's electrostatic reciprocity theorem, the charges and the potentials in situations (a) and (b) fulfill the relation $(V'_1 - V'_2) - (V_1 - V_2) = qV_1/Q$.

$$E = \frac{q}{2l_0\mathcal{C}_0}. \quad (1.46)$$

The force on the test body is q_0E , and it produces a change in the momentum of $q_0E\tau_0$. If this momentum is to be measured, the uncertainty in the initial momentum of the test particle must be smaller than $q_0E\tau_0$. This can be arranged provided that the uncertainty Δy in the position of the test particle is larger than $\hbar/2q_0E\tau_0$,

$$\Delta y > \frac{\hbar}{2q_0E\tau_0}. \quad (1.47)$$

If the condition (1.47) is fulfilled, we can determine which slit the particle went through. In this case, according to the complementarity principle, the measuring process must exert a certain action on the incident particle, which would destroy the coherence of the interfering beams. As previously mentioned, such a perturbation cannot be the result of a direct action of the field strengths. The only remaining possibility is that the perturbation be due to the electric flux enclosed between the two pipes, which is just the effect predicted by Aharonov and Bohm. In order to see that this is indeed the case, we recall, following Furry and Ramsey, that the displacement by y of the test body from its central position produces a potential difference

$$\tilde{V} = \frac{q_0}{\mathcal{C}_0} \frac{y - l_0/2}{l_0}, \quad (1.48)$$

as can be shown by applying Green's reciprocity theorem to the plane-parallel geometry. Then, due to the uncertainty in the position y of the test body, there will be an uncertainty $\Delta\tilde{V}$ in the potential, which according to Eq. (1.47) is

$$\Delta\tilde{V} > \frac{\hbar}{q\tau_0}. \quad (1.49)$$

However, as discussed in Sec. I.C, the uncertainty $\Delta\tilde{V}$ induces, by an electric Aharonov-Bohm effect, an uncertainty $\Delta\Phi_E$ in the phase difference,

$$\Delta\Phi_E = q\tau_0\Delta\tilde{V}/\hbar > 1, \tag{1.50}$$

so that, as required by the principle of complementarity, the interference pattern is indeed wiped out by the measuring process used to identify which slit the particle went through.

A different way of tracing the path of the charged particle from the source to the observing region was suggested by Furry and Ramsey (1960), who described a conceptual experiment in which a search coil of N_0 turns is placed beyond the slits and connected to the condenser plates \mathcal{C}_0 , as shown in Fig. 11. The passage of the charged particle along one or the other of the stationary paths induces, by Lenz's law, a current in the search coil, and the measurement of the charge accumulated on the condenser as a result of the flow of this current will then reveal which slit the particle went through. In this experiment, too, the regions including the stationary paths are shielded, so that the incident particle will not be subject to any field produced by the coil. As the shielding conductors do not play a direct role in the measuring process, they have not been represented in Fig. 11. Following Furry and Ramsey, we determine for the arrangement described above the current induced in the search coil by the changing magnetic flux of the incident particle, and hence the charge accumulated on the plates of the condenser as a result of the flow of that current. We find that the uncertainties of the charge on the condenser and of the magnetic flux in the coil are complementary; the

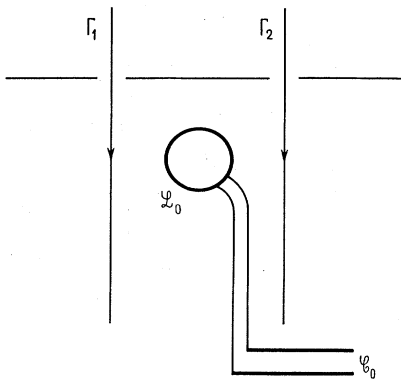


FIG. 11. Another example of complementarity of the wavelike and particle-like properties of matter in two-slit scattering of charged particles, according to Furry and Ramsey (1960). The slit through which the incident particle passed is determined in this experiment by measuring the charge deposited on the plates of the capacitor \mathcal{C}_0 by the currents induced in the search coil \mathcal{L}_0 during passage of the incident particle. However, the uncertainties in the charge on the capacitor plates and the flux in the search coil are complementary; the flux uncertainty that is consistent with measurement of the path of the particle through the slits is sufficient to destroy the interference pattern by a magnetic Aharonov-Bohm effect.

uncertainty in the flux consistent with measurement of the charge variation produced by the passage of the incident particle is just that required to destroy the wavelike interference pattern by a magnetic Aharonov-Bohm effect.

If we assume that the resistance of the search coil is zero, then the current induced in the coil is that required to prevent any change of the magnetic flux. Since a current \mathcal{I} flowing through an N_0 -turn search coil of radius r_0 and length L_0 gives rise to a total magnetic flux

$$F(\mathcal{I}) = \frac{4\pi^2 r_0^2 N_0^2 \mathcal{I}}{L_0 c},$$

it follows that the current $\Delta\mathcal{I}$ induced in the coil by the changing magnetic flux F_q of an incident particle of charge q is given by

$$\Delta\mathcal{I} = \frac{cF_q L_0}{4\pi^2 r_0^2 N_0^2}. \tag{1.51}$$

Then the charge ΔQ accumulated on the plates of the condenser \mathcal{C}_0 after the passage of the particle becomes

$$\Delta Q = \frac{cL_0}{4\pi^2 r_0^2 N_0^2} \int F_q dt. \tag{1.52}$$

Now let us determine the magnetic flux F_q produced by a particle of velocity v_0 moving along a straight line in the x direction, in a search coil whose axis is at a distance d from the path of the particle, as shown in Fig. 12. In order to obtain F_q we shall compute the flux through a single turn, as the z component of the magnetic field at the center of the turn multiplied by its area, and then shall integrate all the contributions along the axis of the coil. For a particular position x of the incident particle the total magnetic flux is thus

$$F_q = \frac{2\pi r^2 q v_0 d N_0}{c(x^2 + d^2)L_0}, \tag{1.53}$$

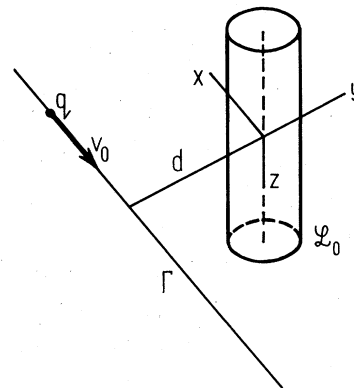


FIG. 12. Variables in the calculation of the magnetic flux F_q produced by a particle of charge q and velocity v_0 through a search coil \mathcal{L}_0 whose axis is at a distance d from the path of the particle.

and a further integration with respect to $dt = dx/v_0$ yields, according to Eq. (1.52), the charge ΔQ accumulated on the plates of the condenser,

$$\Delta Q = \frac{q}{2N_0}. \quad (1.54)$$

Let us now look more closely at the measuring device in Fig. 11, formed by the search coil and the attached condenser. From a classical viewpoint, this system is described by the Lagrange function

$$L(Q, \mathcal{F}) = \frac{1}{2} \mathcal{L}_0 \mathcal{F}^2 - \frac{1}{2\mathcal{C}_0} Q^2, \quad (1.55)$$

where \mathcal{L}_0 is the inductance of the coil. The canonical momentum $\mathcal{L}_0 \mathcal{F}$ corresponding to the Lagrange function, Eq. (1.55), is equal to $N_0 F_1 / c$, where F_1 is the flux through a single turn of the coil, so that the Hamiltonian of the problem is

$$H(Q, N_0 F_1 / c) = \frac{N_0^2 F_1^2}{2\mathcal{L}_0 c^2} + \frac{Q^2}{2\mathcal{C}_0}. \quad (1.56)$$

According to the quantum-mechanical rules, the quantization of the system is obtained by replacing the canonical momentum $N_0 F_1 / c$ in Eq. (1.56) by the operator $-i\hbar \partial / \partial Q$ (Marcuse, 1970). Hence the uncertainties of the charge on the condenser plates and of the flux in the search coil are correlated by

$$\Delta Q \Delta \left[\frac{N_0 F_1}{c} \right] > \frac{\hbar}{2}. \quad (1.57)$$

If the charge $\Delta Q = q/2N_0$ appearing in Eq. (1.54) is to be measured, then the uncertainty in the single-turn magnetic flux F_1 must necessarily exceed

$$\Delta F_1 > \frac{\hbar c}{q}. \quad (1.58)$$

If the condition (1.58) is fulfilled, then we *can* determine which slit the particle went through along its path from the incidence region to the observing plane. In this case, according to the complementarity principle, the measuring device must exert a certain action on the incident particle, which destroys the coherence of the interfering components. Since this perturbation cannot be due to the field strengths because of the shielding, it necessarily follows that the perturbation is the result of an action of the fluxes associated with the search coil and eventually the attached condenser. The perturbing action is indeed provided by the magnetic Aharonov-Bohm effect due to the flux enclosed in the search coil. As discussed in Sec. I.C, the uncertainty ΔF_1 in the magnetic flux produces an uncertainty in the relative phase $\Delta \Phi_B$ of the coherent components, given by

$$\Delta \Phi_B = \frac{q \Delta F_1}{\hbar c} > 1. \quad (1.59)$$

Therefore, as required by the principle of complementarity, the interference pattern is indeed wiped out by the

measuring process used to identify which slit the particle went through.

It must be stressed that the lower limits for uncertainties in the values of the electric and magnetic fluxes, Eqs. (1.49) and (1.58), exist only to the extent we insist upon determining the path of the incident particle through the two slits. On the other hand, in conventional two-slit scattering experiments, where such a constraint does not apply, the electric and magnetic fluxes can be defined with arbitrary accuracy, thereby producing well-determined observable effects in the interference patterns.

E. Ehrenfest's adiabatic principle

Enclosed electromagnetic fluxes not only affect the quantum interference patterns, but can also produce changes in the energy and kinetic momentum *eigenvalues* of bound-state systems. Since the effects of electric fluxes involve time-dependent perturbations and therefore non-stationary states, the eigenvalue shifts appear as effects of enclosed magnetic fluxes. In this section we analyze the effects on a charged plane rotator of the magnetic flux enclosed by an infinitely-long solenoid, and show that the flux-dependent shifts of the energy and kinetic angular momentum eigenvalues are consistent with Ehrenfest's adiabatic principle (Peshkin, Talmi, and Tassie, 1961; Weisskopf, 1961; Noerdlinger, 1962; Peshkin, 1981a, 1981b; Kobe, 1982; Frolov and Skarzhinsky, 1983). Moreover, we demonstrate that the combined effect of quantization of the canonical angular momentum in integer multiples of \hbar and the flux dependence of the energy eigenvalues is to produce a flux-dependent phase shift proportional to the angle of rotation of the charged particle about the magnetic flux (Gerry and Singh, 1979; Lewis, 1983; Guillod and Huguenin, 1984).

The charged plane rotator is a mechanical system in which the motion of a particle of charge q and mass M is restricted to the circumference of a circle of radius R_0 . We assume, further, that a magnetic flux can be applied along the axis of rotation with the aid of a long solenoid, so that the strength of the magnetic field is zero in the region of the circumference of rotation, as shown in Fig. 13. We shall analyze the stationary states of the plane rotator in the presence of the magnetic flux from the viewpoint of the old quantum theory, an approach which is important because it allows us to determine the energy and momentum eigenvalues without reference to the corresponding wave functions. According to Bohr (1913), dynamical equilibrium in the stationary states is governed by the laws of classical mechanics, and the different stationary states are determined for circular orbits by the condition that the canonical angular momentum be equal to an integer multiple of \hbar . In the case of the plane rotator, the paths are restricted to the circumference of radius R_0 , and the allowed classical motions are characterized by a constant angular velocity. Then the canonical angular momentum $m\hbar$ is

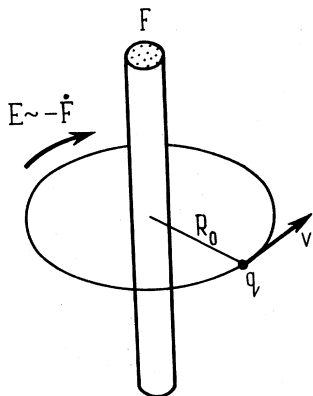


FIG. 13. Plane rotator of radius R_0 in the presence of the magnetic flux F of an infinitely long solenoid. The canonical angular momentum of the stationary states of this system is quantized in integer multiples of \hbar , whereas the energy and the kinetical angular momentum eigenvalues depend on the amount of enclosed flux, in accordance with Ehrenfest's adiabatic principle.

$$m\hbar = \left[Mv + \frac{q}{c} A_\theta \right] R_0, \tag{1.60}$$

where v is the velocity of the particle and A_θ the azimuthal component of the vector potential. The expression of A_θ in a gauge with symmetry of rotation is

$$A_\theta = \frac{F}{2\pi R_0}, \tag{1.61}$$

where F is the enclosed magnetic flux. If the canonical angular momentum is quantized in integer multiples of \hbar , the kinetic angular momentum of the stationary orbits assumes, according to Eqs. (1.60) and (1.61), the values

$$MvR_0 = \left[m - \frac{qF}{2\pi\hbar c} \right] \hbar, \tag{1.62}$$

and the energy corresponding to these orbits is given by

$$E_{R_0 m}^{(F)} = \frac{\hbar^2}{2MR_0^2} \left[m - \frac{qF}{2\pi\hbar c} \right]^2, \quad m=0, \pm 1, \dots \tag{1.63}$$

It is apparent from Eq. (1.63) that the observable difference between the energies of two stationary orbits depends on the amount of enclosed magnetic flux,

$$E_{R_0 m'}^{(F)} - E_{R_0 m''}^{(F)} = \frac{\hbar^2}{2MR_0^2} \left[m'^2 - m''^2 - \frac{qF}{\pi\hbar c} (m' - m'') \right]. \tag{1.64}$$

As pointed out by Peshkin (1981a,1981b), this bound-state Aharonov-Bohm effect is an example of quantum action of enclosed fluxes where there is no overlap between the charged particles and the distribution of field strengths.

The energy levels from Eq. (1.63) are represented in Fig. 14 as functions of the magnetic flux F . The energy levels are periodic and even functions of the flux F , as stated by Byers and Yang (1961).

The fact that the canonical angular momentum can assume only values which are integer multiples of \hbar is an instance of the Sommerfeld quantization conditions. According to Sommerfeld (1916), the stationary states of a certain periodic system are determined by the condition that the integral of the canonical momentum \tilde{p} over a period of the generalized coordinate \tilde{q} be a non-negative integer multiple \tilde{N} of the quantum of action $2\pi\hbar$,

$$\oint \tilde{p} d\tilde{q} = 2\pi\hbar\tilde{N}. \tag{1.65}$$

In the case of the plane rotator, the coordinate \tilde{q} appearing in Eq. (1.65) is the angle of rotation, while the conjugate momentum \tilde{p} becomes the canonical angular momentum $m\hbar$. Now if the parameters defining the system under consideration are slowly varied, it can be shown that the integral, Eq. (1.65), is constant up to exponentially small terms (see, for example, Landau and Lifschitz, 1960). Then if the conditions (1.65) are used to determine the stationary states of the system, it follows that allowed orbits are transformed during an adiabatic change into allowed quantum orbits (Ehrenfest, 1916). Thus Ehrenfest's adiabatic principle enables us to determine the stationary states of deformed systems which are adiabatically related to undeformed systems with known quantum conditions (Jammer, 1966).

Let us assume that the known quantum system is the plane rotator in the absence of magnetic flux, the flux being subsequently increased adiabatically from zero to a certain value F . In the absence of magnetic flux the canonical and kinetical momenta are identical, and both are quantized in integer multiples of \hbar , so that the energy levels have the form

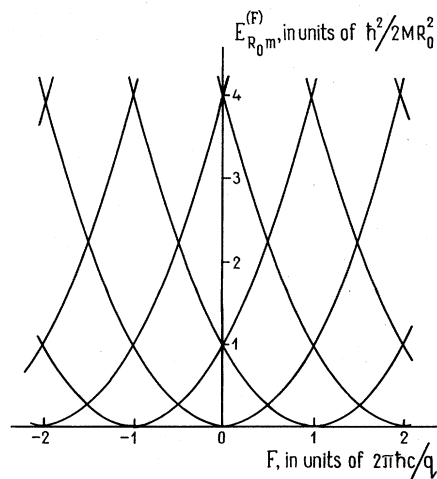


FIG. 14. Energy levels $E_{R_0 m}^{(F)}$ of a plane rotator of radius R_0 as a function of the enclosed magnetic flux F . The energy terms are periodic and even functions of the flux F .

$$E_{R_0 m}^{(0)} = \frac{\hbar^2 m^2}{2MR_0^2}, \quad m=0, \pm 1, \dots \quad (1.66)$$

If the magnetic flux is now slowly raised from zero to its final value F , the changing flux will produce an electromotive force acting on the rotator to modify its kinetic angular momentum, as indicated in Fig. 13. Since the rate of change of the kinetic angular momentum is proportional to the rate of change of the magnetic flux, we have

$$d(MvR_0) = -\frac{q}{2\pi c} dF. \quad (1.67)$$

Taking into account the expression of the vector potential, Eq. (1.61), it follows that the canonical angular momentum $(Mv + qA_\theta/c)R_0$ is conserved during the adiabatic raising of the flux. As in the absence of flux the angular momentum was quantized in integer multiples of \hbar , we conclude that it is the *canonical* angular momentum which remains quantized in integers for arbitrary values of the flux. Analogously, the change in the energy of the rotator is given by

$$dE_{R_0 m}^{(F)} = -\frac{q}{2\pi c MR_0^2} \left[m\hbar - \frac{qF}{2\pi c} \right] dF, \quad (1.68)$$

which, when integrated with respect to F with the initial condition, Eq. (1.66), yields the previous expression of the energy levels, Eq. (1.63). As pointed out by Weisskopf (1961), if the particle is in the orbit then it is no surprise that it changes its state when the flux is switched on. The remarkable thing is that the stationary states are the same even if the particle enters the orbit *after* switching on the flux, and thus the particle notices the presence of a magnetic field in which it does not move.

In order to see that the flux dependence of the energy levels gives rise to an Aharonov-Bohm phase shift, let us consider now the wave-function description of the charged plane rotator. From the quantization of the canonical angular momentum and from the expression of the energy eigenvalues, Eq. (1.63), we infer that the normalized eigenstates of the rotator are

$$\Psi_{R_0 m}^{(F)}(\theta, t) = \frac{1}{(2\pi)^{1/2}} \exp \left[im\theta - \frac{i\hbar \left[m - \frac{qF}{2\pi\hbar c} \right]^2}{2MR_0^2} t \right], \quad (1.69)$$

where θ is the angular position of the particle. We can evaluate the effects of the magnetic flux on the rotating particle by considering the propagator of the problem, which according to Eq. (1.7) is given by

$$K_{R_0}^{(F)}(\theta, t; \theta', 0) = \frac{1}{2\pi} \sum_{m=-\infty}^{\infty} \exp \left[im(\theta - \theta') - \frac{i\hbar \left[m - \frac{qF}{2\pi\hbar c} \right]^2}{2MR_0^2} t \right]. \quad (1.70)$$

The series given by Eq. (1.70) can be summed with the aid of the Poisson sum formula

$$\sum_{m=-\infty}^{\infty} a_m = \sum_{n=-\infty}^{\infty} \mathcal{F}(2\pi n), \quad (1.71)$$

where \mathcal{F} is the Fourier transform of a_m ,

$$\mathcal{F}(\zeta) = \int_{-\infty}^{\infty} a_m e^{-im\zeta} dm, \quad (1.72)$$

and where the variable m in Eq. (1.72) is formally considered to be continuous (Morse and Feshbach, 1953, p. 483). Applying the sum formula, Eq. (1.71), to the series, Eq. (1.70), we obtain the expression of the propagator in the form

$$K_{R_0}^{(F)}(\theta, t; \theta', 0) = \left[\frac{MR_0^2}{2\pi i \hbar t} \right]^{1/2} \sum_{n=-\infty}^{\infty} \exp \left[\frac{iMR_0^2}{2\hbar t} (\theta - \theta' - 2\pi n)^2 + \frac{iqF}{2\pi\hbar c} (\theta - \theta' - 2\pi n) \right]. \quad (1.73)$$

This expression has also been derived by Gerry and Singh (1979) with the aid of the path-integral technique. The general term in Eq. (1.73) represents the amplitude of a particle starting from the point θ' at the time $t=0$, and arriving at the point θ at the time t , after n rotations around the magnetic flux, in a sense given by the sign of n . According to Eq. (1.73), the amplitude for the particle to be at the point θ is the sum of the amplitudes of arrival at θ after an arbitrary number of rotations around the magnetic flux. In the presence of enclosed magnetic flux, the phases of these contributions are shifted by

$qF(\theta - \theta' - 2\pi n)/2\pi\hbar c$, a quantity proportional to the product of the magnetic flux and the angle swept out by the path of the particle.

Let us use the propagator, Eq. (1.73), to determine the evolution of a wave packet having an average angular velocity ω at the time $t=0$,

$$\Psi_{R_0, \delta}^{(F)} \sim \exp \left[-\frac{(\theta' - \theta_0)^2}{2\delta^2} + i \left[\frac{MR_0^2 \omega}{\hbar} + \frac{qF}{2\pi\hbar c} \right] \theta' \right]. \quad (1.74)$$

The dominant contribution to the wave function at the time t , Eq. (1.6), arises from that term n in the expression of the propagator, Eq. (1.73), for which the argument of the exponential function is stationary when integrated over θ' ,

$$\theta - \theta_0 - 2\pi n - \omega t = 0, \quad \theta' \simeq \theta_0. \quad (1.75)$$

Thus the flux-dependent part of the propagator becomes in this approximation $\exp(iqF\omega t/2\pi\hbar c)$, which means that the phase at the center of the moving packet is progressively shifted by an amount proportional to the enclosed magnetic flux.

F. Invariance of the quantum effects of the fluxes

While a knowledge of the field strengths acting directly on a charged particle is not sufficient to describe the quantum effects of electromagnetic fluxes, the specification of the distribution of electromagnetic potentials overdetermines the electromagnetic field. We shall demonstrate in this section that the quantum interference effects described by Ehrenberg and Siday, and Aharonov and Bohm, depend in fact on the amount of enclosed electromagnetic flux. Moreover, we shall discuss the gauge invariance of these quantum effects, as well as their relativistic invariance.

Let us consider a distribution of field strengths completely contained in a certain space-time region, while in a complementary region the field strengths are zero. From the relations between the field strengths and the potentials, Eqs. (1.34), it follows that in the region where the field strengths are zero, the potentials can be obtained by differentiation of a certain function g of space and time,

$$\varphi = -\frac{1}{c} \frac{\partial g}{\partial t}, \quad (1.76a)$$

$$\mathbf{A} = \nabla g. \quad (1.76b)$$

The function g is in general multivalued in the field-free region, where it is defined by Eqs. (1.76); its value increases by

$$F = \oint_{\Omega} (c\varphi dt - \mathbf{A} dr) \quad (1.77)$$

for each additional rotation, along a loop Ω , around the region. The sign of F depends on the sense of rotation. The circulation of the electromagnetic potentials, Eq. (1.77), can be expressed with the aid of the four-dimensional Stokes's theorem as an integral over a surface Σ spanning the loop Ω ,

$$F = \int_{\Sigma} (E_x c dt dx + E_y c dt dy + E_z c dt dz + B_x dy dz + B_y dx dz + B_z dx dy). \quad (1.78)$$

The quantity in Eq. (1.78) represents the four-dimensional electromagnetic flux through the surface Σ . It can be shown that as a result of Maxwell's equations $\nabla \times \mathbf{E} = -\partial \mathbf{B}/c\partial t$ and $\text{div} \mathbf{B} = 0$, the electromagnetic flux

F , Eq. (1.78), evaluated on a closed surface in four-dimensional space, is zero, so that the choice of the surface Σ spanning the closed loop Ω is indifferent. We have already encountered the notions of flux of the electric field, Eq. (1.38), and flux of the magnetic field, Eq. (1.41), in the discussion of the electric and magnetic Aharonov-Bohm effects. It must be stressed that the notion of electric flux as it appears in Eq. (1.78) is different from the conventional, three-dimensional flux of the electric field, which is related to Coulomb's law.

If we consider again the expression of the potentials, Eqs. (1.76), we see that we could eliminate the potentials φ, \mathbf{A} from the field-free region by a gauge transformation, Eqs. (1.35), generated by the function $f = -g$. After this transformation the Schrödinger equation becomes formally identical to the equation for a free particle. However, the boundary conditions to be imposed on the new wave function are different from the conventional requirements of continuity and single valuedness, because the exponential appearing in the transformation, Eq. (1.36), is not in general single valued. All the properties that previously were derived from the Schrödinger equation, including the potentials, will be obtained in the new gauge from the boundary condition that the solution of the free-particle Schrödinger equation be multiplied by $\exp(iqF/\hbar c)$ after encircling once the region of the enclosed flux F . Thus the quantity that correctly describes the electromagnetic effects in quantum mechanics is the nonintegrable phase factor $\exp(iqF/\hbar c)$ (Byers and Yang, 1961; Wu and Yang, 1975).

The mechanism by which the boundary conditions provide a description of the quantum effects of the fluxes can be demonstrated in the problem of the charged plane rotator, discussed in the preceding section. The Schrödinger equation including the vector potential, Eq. (1.61), is

$$\frac{\hbar^2}{2MR_0^2} \left[-i \frac{\partial}{\partial \theta} - \frac{qF}{2\pi\hbar c} \right]^2 \psi_{R_0}^{(F)} = E_{R_0}^{(F)} \psi_{R_0}^{(F)}, \quad (1.79)$$

where the eigenstates $\psi_{R_0}^{(F)}$ are obtained as continuous, single-valued solutions of the equation. By a gauge transformation, Eq. (1.35), generated by the function $f = -F\theta/2\pi$, the Schrödinger equation becomes simply

$$-\frac{\hbar^2}{2MR_0^2} \frac{\partial^2 \psi_{R_0}^{(F)'}}{\partial \theta^2} = E_{R_0}^{(F)} \psi_{R_0}^{(F)'}, \quad (1.80a)$$

where the new boundary condition on the wave function $\psi_{R_0}^{(F)'}$ is that

$$\psi_{R_0}^{(F)' }(\theta + 2\pi) = e^{-iqF/\hbar c} \psi_{R_0}^{(F)' }(\theta). \quad (1.80b)$$

The solutions of Eq. (1.80a) have the form $\psi_{R_0}^{(F)' } \sim \exp(i\lambda\theta)$, and the condition, (1.80b) yields $\lambda = m - qF/2\pi\hbar c$, where m is an integer. Then the energy eigenvalues are

$$E_{R_0}^{(F)m} = \frac{\hbar^2}{2MR_0^2} \left[m - \frac{qF}{2\pi\hbar c} \right]^2,$$

in agreement with the previous result, Eq. (1.63), obtained by conventional analysis of the problem.

The criterion that restricted the transformations of the potentials to the form of Eqs. (1.35), was that the field strengths remain unchanged under the transformation. Now a gauge transformation generated by a multivalued gauge function f , which preserves, however, the single valuedness of the potentials, changes the amount of electromagnetic flux enclosed by a certain loop, because the singularities of the function f are equivalent to distributions of electromagnetic flux threading the loop. Therefore, the gauge transformations that leave the distribution of field strengths invariant throughout the space correspond in general to single-valued functions f . Multivalued gauge transformations may, however, conserve the distribution of field strengths in certain regions of the space, as happened, for example, with the transformation discussed at the beginning of this section. As pointed out by Kretschmar (1965a), the elimination of the potentials must be accompanied by a corresponding change in the boundary conditions for the wave functions, such that the flux appearing explicitly in the Schrödinger equation and the flux hidden in the boundary conditions should always add up to the actual electromagnetic flux. By this means the quantum effects of the fluxes are obtainable even when the potentials are formally eliminated from the region accessible to the charge particles. The important conclusion of this analysis is that the observable effects of the enclosed electromagnetic fluxes depend on the nonintegrable phase factor $\exp(iqF/\hbar c)$. Consequently these quantum effects are periodic functions of the amount of enclosed flux, and are invariant to *regular* gauge transformations.

The quantum effects of electromagnetic flux are also invariant to Lorentz transformations. Thus the distinction made in Sec. I.C between electric and magnetic Aharonov-Bohm effects is to a certain extent arbitrary, for the electric and magnetic fields themselves depend on the choice of the system of reference (Lenz, 1962). To see this, let us suppose that we observe the magnetic Aharonov-Bohm effect in a system of reference where the center of mass of the incident wave packet is at rest. In that system, the solenoid has a velocity $-v_0$, equal and opposite to the velocity v_0 of the incident particle in the laboratory system. If in the laboratory system the axial magnetic field of the solenoid were B and the electric field were zero, the moving solenoid would enclose the same magnetic field B and also a transverse electric field $E = Bv_0/c$, where second-order terms in v_0/c are neglected. The paths of the coherent wave packets and the position of a cross section through the solenoid are shown in Fig. 15, as they are seen in the two systems of reference described above. In the laboratory system there is a contribution to the flux arising from the magnetic field, which is given by $\pi r_0^2 B$, where r_0 is the radius of the solenoid, as can be appreciated from Fig. 15(a). In the system of reference of the solenoid, the stationary paths now lie in the y', t' plane, so that only the electric field contributes to the flux. This contribution is given by the

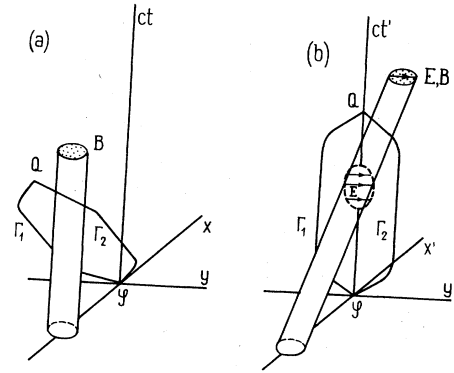


FIG. 15. Relativity of the quantum effects of electromagnetic fluxes. (a) The quantum effects of a flux enclosed in a solenoid appear in the laboratory system as due to the magnetic component. (b) In a system of reference where the center of mass of the incident particle is at rest, the same quantum effects appear as due to the flux of the electric field enclosed within the moving solenoid. The cylinders represent the position of the cross section of the solenoid in the x, y plane at successive instants of time.

electric field $E = v_0 B/c$ multiplied by the area of the elliptic projection of the region of enclosed fields in the y', t' plane, so that the enclosed flux is also equal to $\pi r_0^2 B$. The point is that what appears to be an effect of the electric flux can be equally regarded as an effect of the magnetic flux. The concept providing an invariant description of the Aharonov-Bohm effect is thus the electromagnetic flux, Eq. (1.77) or (1.78).

G. Conservation of the physical quantities

Ehrenfest (1927) demonstrated that the time derivatives of the average position, momentum, energy, and angular momentum of a particle are given by averages of the operators corresponding, respectively, to the classical velocity, force, power, and torque. The conservation of energy and momentum in connection with the Aharonov-Bohm effect has been discussed more recently by Boyer (1973a, 1973b). We show in this section that the changes in the average values of the aforementioned quantities depend on the product of the field strengths times the probability density, whence we conclude that the average position, momentum, energy, and angular momentum of a charged particle are not affected by distributions of enclosed fluxes.

In order to describe the flow of a certain mechanical quantity described by the operator \hat{V} , we shall consider the density of \hat{V} corresponding to a certain state Ψ ,

$$\frac{1}{2}(\Psi^* \hat{V} \Psi + \Psi \hat{V}^* \Psi^*) = \text{Re}(\Psi^* \hat{V} \Psi). \quad (1.81)$$

According to Eq. (1.1), the time derivative of the first term in the expression of the density of \hat{V} is given by

$$\begin{aligned} \frac{\partial}{\partial t}(\Psi^* \hat{V} \Psi) \\ = \Psi^* \frac{\partial \hat{V}}{\partial t} \Psi + \frac{i}{\hbar} [(\hat{H} \Psi)^* \hat{V} \Psi - \Psi^* \hat{V} \hat{H} \Psi] . \end{aligned} \quad (1.82)$$

Since the terms appearing in Eq. (1.82) are not averaged over the entire space, we cannot use the Hermitian property of \hat{H} to simplify the terms; instead we must employ the transposition relation

$$\frac{\partial}{\partial t}(\Psi^* \hat{V} \Psi) + \frac{1}{2M} \operatorname{div} \left[\Psi^* \left[\hat{\mathbf{p}} - \frac{q}{c} \mathbf{A} \right] \hat{V} \Psi + (\hat{V} \Psi) \left[\hat{\mathbf{p}} - \frac{q}{c} \mathbf{A} \right]^* \Psi^* \right] = \Psi^* \left[\frac{\partial \hat{V}}{\partial t} + \frac{i}{\hbar} (\hat{H} \hat{V} - \hat{V} \hat{H}) \right] \Psi , \quad (1.84)$$

the physical content being provided according to Eq. (1.81) by the real parts of the terms. The terms on the left-hand side of Eq. (1.84) describe the rate of accumulation of \hat{V} and the flux of \hat{V} into the local vicinity, while the term on the right-hand side represents the source of the quantity \hat{V} .

The equations describing the conservation of the physical quantities can be derived by substituting in Eq. (1.84) the quantum-mechanical operators corresponding to those quantities. The continuity equation for the probability density $\Psi \Psi^*$ is obtained from Eq. (1.84) for $\hat{V} = 1$,

$$\frac{\partial}{\partial t}(\Psi^* \Psi) + \operatorname{div} \mathbf{j} = 0 , \quad (1.85a)$$

where the probability current \mathbf{j} is

$$\mathbf{j} = \frac{1}{2M} \left[\Psi^* \left[\hat{\mathbf{p}} - \frac{q}{c} \mathbf{A} \right] \Psi + \Psi \left[\hat{\mathbf{p}} - \frac{q}{c} \mathbf{A} \right]^* \Psi^* \right] . \quad (1.85b)$$

The vector field \mathbf{j} appearing in Eq. (1.85b) may be interpreted as a probability current. To demonstrate this we substitute in Eq. (1.84) $\hat{V} = x$, $\hat{V} = y$, and $\hat{V} = z$. Thus we infer that the rate of change of the average position is given by

$$\frac{d}{dt} \langle \Psi | \mathbf{r} \Psi \rangle = \left\langle \Psi \left| \frac{1}{M} \left[\hat{\mathbf{p}} - \frac{q}{c} \mathbf{A} \right] \Psi \right. \right\rangle , \quad (1.86)$$

where the angular brackets denote the spatial average, so that the operator

$$\hat{\mathbf{v}} = \frac{1}{M} \left[-i\hbar \nabla - \frac{q}{c} \mathbf{A} \right] \quad (1.87)$$

corresponds to the velocity of the particle. If the state is stationary, then the continuity equation becomes simply $\operatorname{div} \mathbf{j} = 0$, so that the integral of the normal component of the probability current \mathbf{j} over a closed surface is zero for any stationary solution of the Schrödinger equation. In the quasiclassical approximation the wave function of the charged particle assumes the form $\Psi = \exp(iS/\hbar)$, where S is the classical action, and the probability current, Eq. (1.85b), becomes

$$\begin{aligned} (\hat{H} \Psi)^* X - \Psi^* \hat{H} X = \frac{i\hbar}{2M} \operatorname{div} \left[\Psi^* \left[\hat{\mathbf{p}} - \frac{q}{c} \mathbf{A} \right] X \right. \\ \left. + X \left[\hat{\mathbf{p}} - \frac{q}{c} \mathbf{A} \right]^* \Psi^* \right] , \end{aligned} \quad (1.83)$$

where X and Ψ are two arbitrary functions, and $\hat{\mathbf{p}} = -i\hbar \nabla$ is the operator for the canonical momentum. Substituting $X = \hat{V} \Psi$ in Eq. (1.83) and then using Eq. (1.82) yields

$$\mathbf{j} = \frac{1}{M} \left[\nabla S - \frac{q}{c} \mathbf{A} \right] \Psi \Psi^* ,$$

i.e., the product of the probability density $\Psi \Psi^*$ and the classical velocity $(\nabla S - q \mathbf{A}/c)/M$.

The density of the kinematical momentum is the real part of $\Psi^* (\hat{\mathbf{p}} - q \mathbf{A}/c) \Psi$, and has the same expression as the probability current, Eq. (1.85b). Unlike the density of the canonical momentum $\hat{\mathbf{p}} = -i\hbar \nabla$, the density of the kinematical momentum is invariant to gauge changes of the vector potential \mathbf{A} , Eq. (1.35b), when they are accompanied by a phase transformation of the wave function, Eq. (1.36),

$$\Psi'^* \left[-i\hbar \nabla - \frac{q}{c} \mathbf{A}' \right] \Psi' = \Psi^* \left[-i\hbar \nabla - \frac{q}{c} \mathbf{A} \right] \Psi . \quad (1.88)$$

The equations describing the conservation of the kinematical momentum, which are obtained from Eq. (1.84) by making successively the substitutions $\hat{V} = \hat{p}_x - q A_x/c$, $\hat{V} = \hat{p}_y - q A_y/c$, $\hat{V} = \hat{p}_z - q A_z/c$, have the form

$$\frac{\partial}{\partial t} K_n + \frac{\partial}{\partial x_k} \Gamma_{kn} = \Psi^* F_n \Psi , \quad (1.89)$$

where

$$K_n = \Psi^* \left[\hat{p}_n - \frac{q}{c} A_n \right] \Psi , \quad (1.90a)$$

$$\begin{aligned} \Gamma_{kn} = \frac{1}{2M} \left\{ \Psi^* \left[\hat{p}_k - \frac{q}{c} A_k \right] \left[\hat{p}_n - \frac{q}{c} A_n \right] \Psi \right. \\ \left. + \left[\hat{p}_n - \frac{q}{c} A_n \right] \Psi \left[\hat{p}_k - \frac{q}{c} A_k \right]^* \Psi^* \right\} , \end{aligned} \quad (1.90b)$$

$$\hat{F}_n = q \left[-\frac{\partial \phi}{\partial x_n} - \frac{1}{c} \frac{\partial A_n}{\partial t} \right] + \frac{q}{2Mc} \left[\left[\hat{p}_k - \frac{q}{c} A_k \right] \left[\frac{\partial A_k}{\partial x_n} - \frac{\partial A_n}{\partial x_k} \right] + \left[\frac{\partial A_k}{\partial x_n} - \frac{\partial A_n}{\partial x_k} \right] \left[\hat{p}_k - \frac{q}{c} A_k \right] \right], \quad (1.90c)$$

and where the indices k, n range over the spatial coordinates x, y, z , repeated indices being summed. The real part of the vector components K_n , Eq. (1.89a), represents the density of the kinematical momentum, the real part of the generally asymmetric tensor Γ_{kn} , Eq. (1.90b), represents the current of the momentum density as the n th component of the momentum flowing in the direction k , while the quantities \hat{F}_n , Eq. (1.90c), are the components of the operator for the force exerted by the field strengths on the charged particle. Then the conservation equation (1.89) shows that the average momentum of a charged particle can be modified only by a direct action of the field strengths. If the distribution of field strengths is surrounded by finite barriers which render the probability of the presence of the particle in the region of the fields very small while keeping the wave function nonsingular, then by taking the average of Eq. (1.89) we see that the total kinetic momentum is not changed by distributions of enclosed electromagnetic fields.

A similar treatment of the kinetic energy density can be obtained from the operator $\hat{V} = (\hat{p} - q\mathbf{A}/c)^2/2M$, and yields the time variation of the energy as

$$\frac{\partial \mathcal{E}}{\partial t} + \text{div} \Gamma_{\mathcal{E}} = \Psi^* \hat{W} \Psi, \quad (1.91)$$

where

$$\mathcal{E} = \frac{1}{2M} \Psi^* \left[\hat{p} - \frac{q}{c} \mathbf{A} \right]^2 \Psi, \quad (1.92a)$$

$$\Gamma_{\mathcal{E}} = \frac{1}{4M^2} \left[\Psi^* \left[\hat{p} - \frac{q}{c} \mathbf{A} \right] \left[\hat{p} - \frac{q}{c} \mathbf{A} \right]^2 \Psi + \left[\hat{p} - \frac{q}{c} \mathbf{A} \right]^2 \left[\hat{p} - \frac{q}{c} \mathbf{A} \right]^* \Psi^* \right], \quad (1.92b)$$

$$\hat{W} = \frac{q}{2M} \left[\left[\hat{p} - \frac{q}{c} \mathbf{A} \right] \left[-\nabla \phi - \frac{1}{c} \frac{\partial \mathbf{A}}{\partial t} \right] + \left[-\nabla \phi - \frac{1}{c} \frac{\partial \mathbf{A}}{\partial t} \right] \left[\hat{p} - \frac{q}{c} \mathbf{A} \right] \right]. \quad (1.92c)$$

In this case the scalar \mathcal{E} , Eq. (1.92a), represents the kinetic energy density, the vector $\Gamma_{\mathcal{E}}$, Eq. (1.92b), represents the current of energy density, and the quantity \hat{W} , Eq. (1.92c), is the operator for the power transferred from the field to the particle. Equation (1.91) shows that the average energy of the particle can be changed only by the

direct action of an electric field, and not by an enclosed electromagnetic field. It must be stressed that all the conservation equations discussed in this section are valid only if the wave function Ψ is a solution of the time-dependent Schrödinger equation (1.1).

The fact that inaccessible electromagnetic fluxes do not affect the average value of the kinetic momentum is apparently contradicted by some results reported by Kobe (1979), and later by Bocchieri and Loinger (1982), concerning the two-slit scattering of charged particles. Kobe analyzes the diffraction pattern produced by two Gaussian slits, by assuming that the motion is classical along the incidence direction and quantum mechanical in the transverse directions, and moreover assumes that the effect of the enclosed flux is to shift the relative phase of the waves passing through the two slits. These approximations reduce the problem of two-slit scattering to that of the one-dimensional quantum interference of two Gaussian wave packets, whose relative phase is modified by an amount proportional to the enclosed magnetic flux. Kobe (1979) points out that when the two wave packets arrive in the observing plane, the average kinetical momentum has a nonzero average value, although there is no force to act on the particle. According to Kobe, the conservation of the total momentum would be secured by a transfer of momentum to the material of the slits. However, the aforementioned flux dependence of the average kinetical momentum is in fact due to the approximations made in the analysis of the scattering problem, and the nonzero average momentum actually arises from the overlap of the Gaussian wave packets representing coherent components passing through the two slits. The same type of analysis would have yielded *no* flux-dependent momentum change if rectangular slits were used instead of Gaussian slits. To see this explicitly, let us consider the free-particle one-dimensional states $X_1 \exp(i\Phi_1)$ and $X_2 \exp(i\Phi_2)$, whose phases can be adjusted by the constants Φ_1 and Φ_2 , and which satisfy at the time $t=0$ the conditions

$$\int X_1^* y X_2 dy = 0, \quad (1.93a)$$

$$\int X_1^* \frac{\partial X_2}{\partial y} dy = 0. \quad (1.93b)$$

The conditions of Eqs. (1.93) are fulfilled if X_1 and X_2 assume nonzero values in disjoint regions of the space, as for example in the case of scattering by two rectangular slits. If the momentum representations of the wave functions X_1 and X_2 are

$$X_1(y, 0) = \int a_k^{(1)} e^{iky} dk, \quad (1.94a)$$

$$X_2(y, 0) = \int a_k^{(2)} e^{iky} dk, \quad (1.94b)$$

then the wave functions at the time t are

$$X_1(y, t) = \int a_k^{(1)} e^{iky - i\hbar k^2 t/2M} dk, \quad (1.95a)$$

$$X_2(y, t) = \int a_k^{(2)} e^{iky - i\hbar k^2 t/2M} dk. \quad (1.95b)$$

The average position and the average momentum for the state $\bar{X} = X_1 \exp(i\Phi_1) + X_2 \exp(i\Phi_2)$ at the time t are given by

$$\langle \tilde{X}(t) | y \tilde{X}(t) \rangle = \langle X_1(t) | y X_1(t) \rangle + \langle X_2(t) | y X_2(t) \rangle + 2\pi \int dk \left[e^{-i(\Phi_1 - \Phi_2)} a_k^{(1)*} \left[i \frac{\partial a_k^{(2)}}{\partial k} + \frac{\hbar k t}{M} a_k^{(2)} \right] + e^{i(\Phi_1 - \Phi_2)} a_k^{(1)} \left[i \frac{\partial a_k^{(2)}}{\partial k} + \frac{\hbar k t}{M} a_k^{(2)} \right]^* \right], \quad (1.96a)$$

$$\langle \tilde{X}(t) | \hat{p}_y X(t) \rangle = \langle X_1(t) | p_y X_1(t) \rangle + \langle X_2(t) | p_y X_2(t) \rangle + 2\pi \hbar \int k dk \left(e^{-i(\Phi_1 - \Phi_2)} a_k^{(1)*} a_k^{(2)} + e^{i(\Phi_1 - \Phi_2)} a_k^{(1)} a_k^{(2)*} \right). \quad (1.96b)$$

However, the conditions (1.93) in the momentum representation take the form

$$\int a_k^{(1)*} \frac{\partial a_k^{(2)}}{\partial k} dk = 0, \quad (1.97a)$$

$$\int k a_k^{(1)*} a_k^{(2)} dk = 0, \quad (1.97b)$$

which means that the interference terms in Eqs. (1.96) are equal to zero; thus, under the stated conditions, the average position and momentum are not affected by the choice of the relative phase between the interfering waves.

The remark that inaccessible fluxes might affect not only the phase, but also the momentum of a charged particle can in fact be traced back to the original work of Aharonov and Bohm (1959), this suggestion being later developed by Aharonov, Pendleton, and Peterson (1969). These authors consider an electron incident upon a grating consisting of enclosed magnetic fluxes, and from the fact that the phase difference between consecutive partial waves is shifted by an amount proportional to the enclosed flux, thus affecting the directions of constructive interference, they conclude that the grating would change the momentum of the incident electron. What really happens is that the magnetic flux shifts the position of the interference fringes relative to the envelope of the pattern, while the average kinetic momentum and the location of the envelope of the interference pattern are independent of the amount of enclosed flux. This can be demonstrated by extending the analysis developed in Eqs. (1.93)–(1.97) to an arbitrary number of rectangular slits. This same explanation applies, as well, to an assertion by von Westenholz (1973), that the entire interference pattern is shifted by an enclosed magnetic flux.

The fact that there is no deflection of the average kinetic momentum of an electron passing enclosed magnetic flux was emphasized by Boyer (1972a, 1973a, 1973b). Boyer (1972a, 1972b) also pointed out that the diffraction angle θ_F at which the phase difference due to the inequality of the path lengths compensates the phase shift produced by an enclosed magnetic flux F is given by $\theta_F = qF/acp_0$, where a is the separation between the slits and p_0 the incident momentum of the particle of charge q . Although the expression of the angle θ_F is independent of Planck's constant, Erlichson (1972) stressed that the flux-dependent angular shift still converges to zero in the classical limit, for the classical limit is obtained for vanishingly small values of the ratio λ_0/a , where $\lambda_0 = 2\pi\hbar/p_0$.

In order to analyze the conservation of angular momentum we must also consider the spin of the charged particle. We shall restrict our analysis to a particle of spin $\frac{1}{2}$,

so that the wave function becomes the two-component spinor Ψ_+, Ψ_- . The Hamiltonian of the particle of charge q and magnetic moment μ is

$$\hat{H}_{q,\mu} = \frac{1}{2M} \left[\hat{\mathbf{p}} - \frac{q}{c} \mathbf{A} \right]^2 + q\varphi - \mu \hat{\boldsymbol{\sigma}} \cdot \mathbf{B}, \quad (1.98)$$

where σ are the Pauli matrices

$$\hat{\sigma}_x = \begin{bmatrix} 0 & 1 \\ 1 & 0 \end{bmatrix}, \quad \hat{\sigma}_y = \begin{bmatrix} 0 & -i \\ i & 0 \end{bmatrix}, \quad \hat{\sigma}_z = \begin{bmatrix} 1 & 0 \\ 0 & -1 \end{bmatrix}. \quad (1.99)$$

The operator of the total kinetic angular momentum is

$$\hat{\mathbf{J}} = \mathbf{r} \times \left[\hat{\mathbf{p}} - \frac{q}{c} \mathbf{A} \right] + \frac{1}{2} \hbar \hat{\boldsymbol{\sigma}}, \quad (1.100)$$

and according to Eq. (1.84) the rate of change of the angular momentum operator $\hat{\mathbf{J}}$ is given by

$$\frac{d\hat{\mathbf{J}}}{dt} = \frac{1}{2} (\mathbf{r} \times \hat{\mathbf{F}} - \hat{\mathbf{F}} \times \mathbf{r}) + \mathbf{r} \times \nabla(\mu \hat{\boldsymbol{\sigma}} \cdot \mathbf{B}) + \mu \hat{\boldsymbol{\sigma}} \times \mathbf{B}, \quad (1.101)$$

where the divergence term was omitted. The operator $\hat{\mathbf{F}}$ represents the force exerted by the electromagnetic field via the electric charge q of the particle, and takes the form of Eq. (1.90c). While the operator $\mathbf{r} \times \hat{\mathbf{F}}$ is not Hermitian in the presence of a magnetic field, the symmetrized vector product $(\mathbf{r} \times \hat{\mathbf{F}} - \hat{\mathbf{F}} \times \mathbf{r})/2$ represents the operator for the torque on the particle due to the force $\hat{\mathbf{F}}$. The remaining terms in Eq. (1.96) depend on the magnetic moment μ of the particle, and as in the classical situation, they arise from the operator of the force $\nabla(\mu \hat{\boldsymbol{\sigma}} \cdot \mathbf{B})$ and from the torque exerted by the field \mathbf{B} acting on the magnetic moment μ of the particle. According to Eq. (1.101), the rate of change of the kinetic angular momentum $\hat{\mathbf{J}}$ is proportional to the intensities of the electric and magnetic field strengths; in particular, if the wave function of the particle is vanishing in the region of the field strengths, then the angular momentum of the particle will not be affected by the distribution of enclosed electromagnetic fields.

Since the part of the Hamiltonian (1.98) dependent on the magnetic moment μ of the particle is proportional to the strength \mathbf{B} of the magnetic field, we conclude that there are no effects of enclosed electromagnetic fluxes on the spin of the particle. However, Aharonov and Vardi (1979) have considered an arrangement by which an enclosed magnetic flux could apparently modify the average value of the spin of a particle. In this arrangement a beam of spin- $\frac{1}{2}$ particles polarized in the y direction is split and then recombined by using an interaction of the

form $\hat{H}_{int} = -\mu z \hat{\sigma}_z$ in the regions I and II shown in Fig. 16. Moreover, a magnetic flux F , oriented in the positive y direction, is enclosed between the stationary paths Γ_1 and Γ_2 shown in Fig. 16. The wave function of the incident particle is the spinor

$$\frac{1}{2^{1/2}} \begin{pmatrix} e^{-i\pi/4} \\ e^{i\pi/4} \end{pmatrix},$$

and since the enclosed flux F shifts the phase of the components passing on the two sides of the flux region by $\pm qF/2\hbar c$, the wave function of the final state is proportional to

$$\frac{1}{2^{1/2}} \left[\begin{pmatrix} e^{-i\pi/4} \\ 0 \end{pmatrix} e^{-iqF/2\hbar c} + \begin{pmatrix} 0 \\ e^{i\pi/4} \end{pmatrix} e^{iqF/2\hbar c} \right]. \quad (1.102)$$

Now the spinor

$$\frac{1}{2^{1/2}} \begin{pmatrix} e^{-i\pi/4 - iqF/2\hbar c} \\ e^{i\pi/4 + iqF/2\hbar c} \end{pmatrix}$$

is an eigenstate of the operator $\hat{\sigma}_y = \cos(qF/\hbar c)\hat{\sigma}_y - \sin(qF/\hbar c)\hat{\sigma}_x$, so that the particle emerges with the spin rotated about the z axis by an angle $qF/\hbar c$. Accord-

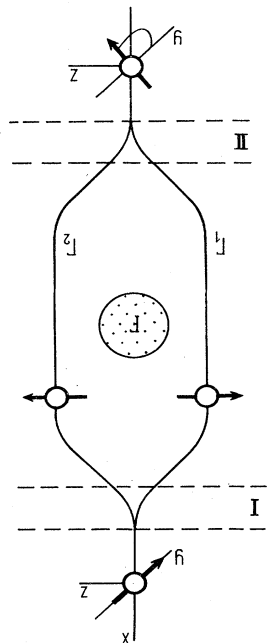


FIG. 16. Effect of an enclosed magnetic flux on the direction of the spin of an incident particle. The incident beam of spin- $\frac{1}{2}$ particles polarized in the y direction is split and then recombined by using an interaction of the form $\hat{H}_{int} = -\mu z \hat{\sigma}_z$ in regions I and II. Since the enclosed magnetic flux shifts the relative phase of the components passing by the two sides of the flux region by $qF/2\hbar c$, the particle emerges with the spin rotated by an angle $qF/\hbar c$ about the z axis. The transfer of kinetic angular momentum occurs, however, in regions I and II and is due to the torque exerted by the magnetic field acting in those regions.

ing to Aharonov and Vardi (1979), this experiment would demonstrate the existence of quantum effects of electromagnetic fluxes on internal degrees of freedom, other than the electric charge. However, the final state, Eq. (1.102), depends on the product of the magnetic flux times the charge of the particle, rather than on the magnetic moment μ . Moreover, the transfer of angular momentum to the particle occurs in the regions I and II shown in Fig. 16, and is due to the torque exerted by the magnetic field strengths acting in those regions. Thus the experiment described by Aharonov and Vardi actually shows that if two wave packets are superposed in the presence of an interaction of the form $-\mu z \hat{\sigma}_z$, the angular momentum of the final state depends on the initial relative phase of the wave packets, and does not demonstrate a direct action of the enclosed flux on the spin of the particle.

To see this in detail, let us consider the problem of a charged particle of spin $\frac{1}{2}$ interacting with a magnetic field $B = B'z$ oriented along the z axis, where B' is a constant. We shall assume that the state of the particle at the time $t=0$ can be represented by a Gaussian wave packet at rest, the spin being in the x, y plane and making an angle ν_0 with the y axis, as shown in Fig. 17. The wave function of the particle is the spinor

$$\frac{1}{2^{1/2}} \begin{pmatrix} \Psi_+(x, y, z, t) \\ \Psi_-(x, y, z, t) \end{pmatrix},$$

which gives the amplitudes Ψ_+ and Ψ_- for the particle with spin in the $+$ or $-$ direction, respectively. According to Eq. (1.98), the wave functions Ψ_+ and Ψ_- are solutions of the Schrödinger equations

$$-\frac{\hbar^2}{2M} \nabla^2 \Psi_+ - \mu z B' \Psi_+ = i\hbar \frac{\partial \Psi_+}{\partial t}, \quad (1.103a)$$

$$-\frac{\hbar^2}{2M} \nabla^2 \Psi_- + \mu z B' \Psi_- = i\hbar \frac{\partial \Psi_-}{\partial t}, \quad (1.103b)$$

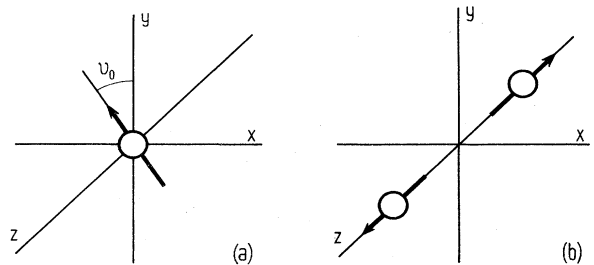


FIG. 17. Conservation of angular momentum in the quantum interference of particles with spin. (a) The initial Gaussian wave packet, with the spin in the x, y plane at an angle ν_0 with respect to the y axis. (b) An applied magnetic field of the form $B = B'z$, where B' is a constant, splits the packet into two coherent components having their spin orientation along the magnetic field, while the phases at the centers of these wave packets differ now by ν_0 . The change of angular momentum is due to the torque exerted by the applied field on the magnetic moment of the particle.

where the constant B' is the gradient of the magnetic field, and the charge of the particle is assumed to be $q=0$. The solutions of Eqs. (1.103) can be obtained by considering a transformation to an accelerated system of reference (Greenberger and Overhauser, 1979),

$$\Psi_+(x,y,z,t) = \Psi_+^{(0)} \left[x, y, z - \frac{1}{2} \frac{\mu B'}{M} t^2, t \right] \times \exp \left[\frac{i}{\hbar} \mu B' z t - \frac{i}{\hbar} \frac{\mu^2 B'^2 t^3}{6M} \right], \quad (1.104a)$$

$$\Psi_-(x,y,z,t) = \Psi_-^{(0)} \left[x, y, z + \frac{1}{2} \frac{\mu B'}{M} t^2, t \right] \times \exp \left[-\frac{i}{\hbar} \mu B' z t - \frac{i}{\hbar} \frac{\mu^2 B'^2 t^3}{6M} \right], \quad (1.104b)$$

where $\Psi_+^{(0)}$ and $\Psi_-^{(0)}$ are the free-particle normalized solutions

$$\begin{aligned} \left[\begin{array}{c} \Psi_+^{(0)} \\ \Psi_-^{(0)} \end{array} \right] &= \frac{1}{2^{1/2} \pi^{3/4} \delta^{3/2} (1 + i \hbar t / M \delta^2)^{3/2}} \\ &\times \exp \left[-\frac{x^2 + y^2 + z^2}{2\delta^2 (1 + i \hbar t / M \delta^2)} \right] \left[\begin{array}{c} e^{-i v_0 / 2 - i \pi / 4} \\ e^{i v_0 / 2 + i \pi / 4} \end{array} \right]. \end{aligned} \quad (1.105)$$

It is apparent from Eq. (1.104) that the components Ψ_+ and Ψ_- are moving with increasingly large momentum in the $+z$ and $-z$ directions. The spinor

$$\left[\begin{array}{c} e^{-i v_0 / 2 - i \pi / 4} \\ e^{i v_0 / 2 + i \pi / 4} \end{array} \right]$$

in Eq. (1.105) is an eigenstate of the operator $\hat{\sigma}_y = \cos v_0 \hat{\sigma}_y - \sin v_0 \hat{\sigma}_x$, so that it indeed describes a particle having its spin rotated by an angle v_0 with respect to the y axis. Now after a certain time t when the distance between the wave packets Ψ_+ and Ψ_- is large compared to their width δ , $\mu B' t^2 / M \gg \delta$, the packet arriving at the positive end of the z axis has the spin in the $+z$ direction, while the packet arriving at the negative end has the spin in the $-z$ direction, so that the total spin is now zero. The change in the kinetic angular momentum of the particle is due to the torque exerted by the applied field B . According to Eq. (1.101), the operator for the rate of change of the angular momentum is given in the present problem by

$$\frac{d}{dt} (\hat{J}_x + i \hat{J}_y) = -i \mu B' \hat{\sigma}_z (x + iy) - i \mu B' z (\hat{\sigma}_x + i \hat{\sigma}_y). \quad (1.106)$$

By taking the average of the operator, Eq. (1.106), with respect to the wave function, Eqs. (1.104), we find that the torque due to the applied magnetic field is given by

$$\begin{aligned} \frac{d}{dt} (J_x + i J_y) &= -\frac{\mu^2 B'^2 \delta^2 t}{\hbar} \left[1 + \frac{\hbar^2 t^2}{2M^2 \delta^4} \right] e^{i(v_0 + \pi/2)} \\ &\times \exp \left[-\frac{\mu^2 B'^2 \delta^2 t^2}{\hbar^2} - \frac{\mu^2 B'^2 t^4}{4M^2 \delta^2} \right]. \end{aligned} \quad (1.107)$$

Integrating the torque [Eq. (1.107)] with respect to the time yields the change in angular momentum produced by the applied magnetic field,

$$\Delta J_x = \frac{\hbar}{2} \sin v_0, \quad \Delta J_y = -\frac{\hbar}{2} \cos v_0. \quad (1.108)$$

The variation, Eq. (1.108), is indeed equal to the difference between the magnetic moment of the final state, which is zero, and the initial angular momentum $J_x^{(0)} = -(\hbar/2) \sin v_0$, $J_y^{(0)} = (\hbar/2) \cos v_0$. Conversely, the shift of the relative phase of the spinor components by $v_0/2$ [Eq. (1.105)] will be converted by the magnetic interaction $-\mu z \hat{\sigma}_z$ into a rotation of the spin of the particle in the recombined state. In the case of the arrangement discussed by Aharonov and Vardi (1979), the phase shift is produced by the enclosed flux, but the change in the direction of the spin takes place partly before, and partly after, the action of the flux on the *charge* of the particle. Therefore it does not seem appropriate to regard such processes as demonstrating a direct action of the electromagnetic flux on the spin of the incident particle.

H. Effects of the fluxes in the hydrodynamical formulation of quantum mechanics

Madelung (1926) has shown that the Schrödinger equation for the wave function of a charged particle interacting with a distribution of electromagnetic potentials can be replaced by a set of hydrodynamical-type equations for the probability density and current, which depend only on the electric and magnetic field *strengths*. The question arises, then, of how it is possible that distributions of enclosed electromagnetic fields should produce observable effects on the quantum interference patterns. We shall see in this section that the quantum effects of the fluxes arise in the hydrodynamical formulation of quantum mechanics as the result of the small, but nonzero penetration of the wave function in the region of the field strengths. Thus, unlike the classical situation where a knowledge of the field strengths in the vicinity of the particle path is sufficient for a description of the motion, a complete characterization of the quantum-mechanical motion requires specification of the field strengths even in regions where the probability of finding the particle is arbitrarily small.

The hydrodynamical form of the quantum-mechanical equations can be obtained by substituting in Eqs. (1.1) and (1.2) the wave function written in the form

$$\Psi = \rho e^{i\Phi}, \quad (1.109)$$

and then by separating the real and imaginary parts. The equation obtained by equating the real part to zero is

$$\hbar \frac{\partial \Phi}{\partial t} + \frac{1}{2M} \left[\hbar \nabla \Phi - \frac{q}{c} \mathbf{A} \right]^2 + q\varphi - \frac{\hbar^2}{2M} \frac{\Delta \rho}{\rho} = 0, \quad (1.110)$$

and that for the imaginary part is

$$\frac{\partial(\rho^2)}{\partial t} + \operatorname{div} \left[\frac{1}{M} \left[\hbar \nabla \Phi - \frac{q}{c} \mathbf{A} \right] \rho^2 \right] = 0. \quad (1.111)$$

In the classical limit, when the term $-\hbar^2 \Delta \rho / 2M\rho$ becomes negligible, Eq. (1.110) approaches the Hamilton-Jacobi equation for a particle interacting with the potentials φ, \mathbf{A} , while Eq. (1.111) is the continuity equation for the density ρ^2 and the current $\rho^2 \mathbf{v}$, where the velocity field \mathbf{v} is given by

$$\mathbf{v} = \frac{1}{M} \left[\hbar \nabla \Phi - \frac{q}{c} \mathbf{A} \right]. \quad (1.112)$$

Now the differentiation of Eq. (1.110) with respect to the spatial variables yields a form depending only on ρ and \mathbf{v} ,

$$M \left[\frac{\partial \mathbf{v}}{\partial t} + (\mathbf{v} \cdot \nabla) \mathbf{v} \right] = q \left[-\nabla \varphi - \frac{1}{c} \frac{\partial \mathbf{A}}{\partial t} \right] - M \mathbf{v} \times \operatorname{curl} \mathbf{v} + \frac{\hbar^2}{2M} \nabla \frac{\Delta \rho}{\rho}. \quad (1.113)$$

However, according to Eq. (1.112) we have

$$\operatorname{curl} \mathbf{v} = -\frac{q}{Mc} \mathbf{B}, \quad (1.114)$$

so that the hydrodynamical form of the quantum-mechanical equations is

$$M \left[\frac{\partial \mathbf{v}}{\partial t} + (\mathbf{v} \cdot \nabla) \mathbf{v} \right] = q \mathbf{E} + \frac{q}{c} \mathbf{v} \times \mathbf{B} + \frac{\hbar^2}{2M} \nabla \frac{\Delta \rho}{\rho}, \quad (1.115)$$

$$\frac{\partial(\rho^2)}{\partial t} + \operatorname{div}(\rho^2 \mathbf{v}) = 0, \quad (1.116)$$

where the variables ρ, \mathbf{v} are related to the wave function Ψ by

$$\rho^2 = \Psi \Psi^* \quad (1.117)$$

and

$$M \mathbf{v} = \frac{i\hbar}{2} \frac{\Psi \nabla \Psi^* - \Psi^* \nabla \Psi}{\Psi \Psi^*} - \frac{q}{c} \mathbf{A}. \quad (1.118)$$

Strocchi and Wightman (1974), in considering the problem of the quantum effects of the fluxes from the hydrodynamical viewpoint, have raised an interesting question of consistency. They remark that while Eqs. (1.114)–(1.116) are local equations involving the field strengths \mathbf{E} and \mathbf{B} , they still lead to the prediction of observable effects depending on distributions of inaccessible field strengths. Strocchi and Wightman (1974) attribute the quantum effects of the fluxes to the penetration of the wave function into the region of nonvanishing fields. Thus even if the wave function were kept out of the region of nonvanishing fields by infinitely large repulsive potentials, there would still be a reminiscence of the presence of the fluxes in the need to specify the tangential component of the velocity field \mathbf{v} at the boundary of the accessible region. The fact that the Aharonov-Bohm effect results from boundary conditions in the approximate topology of a complete separation between the region accessible to the particle and the distribution of field strengths was previously pointed out by Schulman (1971). The physical importance of the penetration of the incident particle in the region of the field strengths has also been emphasized by Wisnivesky and Aharonov (1967), Jánossy (1970), Menikoff and Sharp (1977), Casati and Guarneri (1979), and Costa de Beauregard and Vigoureaux (1982). The connection between the hydrodynamical formulation of quantum mechanics and the quantum effects of the fluxes was recently discussed by Takabayashi (1983) and Wódkiewicz (1984).

The possibility that the tail of the wave function of the particle might account for the finite observable effects of the fluxes on the quantum interference patterns is due to the fact that the velocity field \mathbf{v} , Eq. (1.118), and the quantum potential $-\hbar^2 \Delta \rho / 2M\rho$ appearing in Eq. (1.115) assume finite values, even in regions where the probability ρ^2 becomes very small. Specifically, if we consider a scalar quantity with dimensions of energy $M\mathbf{v}^2/2 - \hbar^2 \Delta \rho / 2M\rho$ and a momentum field $M\mathbf{v}$, it can be shown from Eqs. (1.110) and (1.112) that the integral of these quantities along a closed loop in four-dimensional space is related to the amount of electromagnetic flux through that loop,

$$\oint \left[\left(\frac{1}{2} M \mathbf{v}^2 - \frac{\hbar^2}{2M} \frac{\Delta \rho}{\rho} \right) dt - M \mathbf{v} d\mathbf{r} \right] = -\hbar \oint \left[\frac{\partial \Phi}{\partial t} dt + \frac{\partial \Phi}{\partial \mathbf{r}} d\mathbf{r} \right] - \frac{q}{c} \oint (c\varphi dt - \mathbf{A} d\mathbf{r}). \quad (1.119)$$

Since the wave function must be single valued, the phase increase $\Delta \Phi = \oint [(\partial \Phi / \partial t) dt + (\partial \Phi / \partial \mathbf{r}) d\mathbf{r}]$ must be an integer multiple N of 2π , so that we have

$$\oint \left[\left(\frac{1}{2} M \mathbf{v}^2 - \frac{\hbar^2}{2M} \frac{\Delta \rho}{\rho} \right) dt - M \mathbf{v} d\mathbf{r} \right] + \frac{q}{c} \oint (c\varphi dt - \mathbf{A} d\mathbf{r}) = -2\pi \hbar N, \quad N = 0, \pm 1, \dots \quad (1.120)$$

In particular, if the integration loop belongs to three-dimensional space, the condition (1.120) becomes

$$\oint \mathbf{M} \cdot d\mathbf{r} = 2\pi\hbar N - \frac{q}{c} \int \mathbf{B} \cdot d\mathbf{a},$$

a form reported by Jánossy (1970). The quantization condition, Eq. (1.120), is not affected by the presence of repulsive barriers surrounding the region of the field strengths, and although the probability ρ^2 of finding the particle in the region of the field strengths may become vanishingly small, the hydrodynamical formulation of quantum mechanics still yields the quantum effects of the fluxes. As can be appreciated from Eq. (1.120), these effects are periodic functions of the enclosed flux F , with the period $2\pi\hbar c/q$, where q is the charge of the particle. If the integration loop crosses a nodal line of the density ρ^2 , then the constant N in Eq. (1.120) may assume half-integer values, too. Such an example will be discussed in Sec. II.A.

In order to see in detail how the quantum effects of the fluxes arise in the hydrodynamical formulation of quantum mechanics, we shall consider the problem of an enclosed electric field acting on a charged particle. First, we solve the problem in the conventional, wave-function representation, and then evaluate the corresponding hydrodynamical variables. We assume that the initial state is a superposition of two Gaussian wave packets of width δ and momentum $\hbar k_0$,

$$X_\delta(y,0) = \frac{1}{2^{1/2}\pi^{1/4}\delta^{1/2}} \exp\left[-\frac{(y+y_0)^2}{2\delta^2} + ik_0y\right] + \frac{1}{2^{1/2}\pi^{1/4}\delta^{1/2}} \exp\left[-\frac{(y-y_0)^2}{2\delta^2} - ik_0y\right]. \quad (1.121)$$

At the time $t=0$ an electric field E is applied along the y axis in the region $-d_0/2 < y < d_0/2$, and then removed after a time interval τ_0 . The wave function of the particle during the period when the electric field is applied can be represented with a good approximation by

$$X_\delta^{(E)}(y,t) = \begin{cases} X_\delta(y,0)e^{-iqEt d_0/2\hbar}, & y < -\frac{d_0}{2} & (1.122a) \\ X_\delta(y,0)e^{iqEty/\hbar}, & -\frac{d_0}{2} < y < \frac{d_0}{2} & (1.122b) \\ X_\delta(y,0)e^{iqEt d_0/2\hbar}, & \frac{d_0}{2} < y & (1.122c) \end{cases}$$

where $0 < t < \tau_0$. Equation (1.122b) is an approximate form of the wave function [Eq. (1.104a)] for the quantum-mechanical motion under the influence of a constant acceleration. Since we are interested in values of the electric field such that $qE\tau_0 d_0 \sim \hbar$, the displacement of the probability distribution occurring between $-d_0/2$ and $d_0/2$, which is of the order of $qE\tau_0^2/2M \sim \hbar^2/2MqEd_0^2$, can be neglected for large values of E . Equations (1.122a) and (1.122c) describe the phase changes due to the scalar

potential in the field-free regions, which preserve the continuity of the wave function $X_\delta^{(E)}$ at $\pm d_0/2$. At the time $T = My_0/\hbar k_0$ both wave packets have their centers at $y=0$, and the wave function is

$$X_\delta^{(E)}(y,T) = \frac{2^{1/2}}{\pi^{1/4}\delta^{1/2}(1+iy_0/k_0\delta^2)^{1/2}} \times \exp\left[-\frac{y^2}{2\delta^2(1+iy_0/k_0\delta^2)}\right] \times \cos\left[k_0y - \frac{qE\tau_0 d_0}{2\hbar}\right], \quad (1.123)$$

where exponentially small terms of the order of $\exp(-y_0^2/2\delta^2)$ have been neglected. Now the probability density of the initial state is

$$\rho_\delta^2(y,0) = \frac{1}{2\pi^{1/2}\delta} e^{-(y+y_0)^2/\delta^2} + \frac{1}{2\pi^{1/2}\delta} e^{-(y-y_0)^2/\delta^2} + \frac{1}{\pi^{1/2}\delta} e^{-(y^2+y_0^2)/\delta^2} \cos(k_0y), \quad (1.124)$$

and the velocity field

$$v_\delta(y,0) = \frac{\hbar k_0}{M} \frac{e^{-2yy_0/\delta^2} - e^{2yy_0/\delta^2} - \frac{2y_0}{k_0\delta^2} \sin(2k_0y)}{e^{-2yy_0/\delta^2} + e^{2yy_0/\delta^2} + 2\cos(2k_0y)}. \quad (1.125)$$

According to Eqs. (1.122), the probability density at the time τ_0 is not effected by the electric field,

$$\rho_\delta^{(E)}(y,\tau_0)^2 \simeq \rho_\delta(y,0)^2, \quad (1.126)$$

while the velocity field at the time τ_0 is

$$v_\delta^{(E)}(y,\tau_0) = \begin{cases} v_\delta(y,0) + \frac{qE\tau_0}{M}, & |y| < \frac{d_0}{2} & (1.127a) \\ v_\delta(y,0), & |y| > \frac{d_0}{2} & (1.127b) \end{cases}$$

The final probability density at the time T is then

$$\rho_\delta^{(E)}(y,T)^2 = \frac{2}{\pi^{1/2}\delta(1+y_0^2/k_0^2\delta^4)^{1/2}} \times \exp\left[-\frac{y^2}{\delta^2(1+y_0^2/k_0^2\delta^4)}\right] \times \cos^2\left[k_0y - \frac{qE\tau_0 d_0}{2\hbar}\right]. \quad (1.128)$$

These hydrodynamical quantities have been represented in Fig. 18 for the values of the parameters $k_0 = \pi/\delta$, $y_0 = 3\delta$, $d_0 = 2\delta$, and for values of the enclosed electric flux of $E\tau_0 d_0 = 0, \pi\hbar/2q, \pi\hbar/q$. We see that the initial probability distribution $\rho_\delta(y,\tau_0)^2$ is practically unaffected by the

electric field, which acts on the exponentially small tail of the wave packets. However, although the probability $\rho_\delta(y, \tau_0)^2$ is very small in the region between the two packets, the initial velocity field $v_\delta^{(E)}(y, \tau_0)$ has finite values in that region. Moreover, the initial pattern of the velocity field at the time τ_0 depends markedly on the electric flux, in such a way that the area under the curve of $v_\delta^{(E)}$ vs y , comprised between the ordinates of two points, gives the phase difference between those points. After a certain time the differences in the pattern of the velocity field $v_\delta^{(E)}$ appear as flux-dependent changes in the probability distribution $\rho_\delta^{(E)}(y, T)^2$. In particular, the assertion by Jánossy (1974) that the penetration of the quantum states

in the region of the field strengths would not noticeably affect the motion of the incident particles appears to be unfounded.

If we consider again Eq. (1.110), we set that it is a Hamilton-Jacobi equation for a charged particle interacting with a vector potential \mathbf{A} and an effective potential energy $q\varphi - \hbar^2 \Delta \rho / 2M\rho$. If the wave function Ψ were known, for example by solving the Schrödinger equation for Ψ , then the action $\hbar\Phi$ could formally be used to define via Eq. (1.110) a set of classical trajectories for a particle

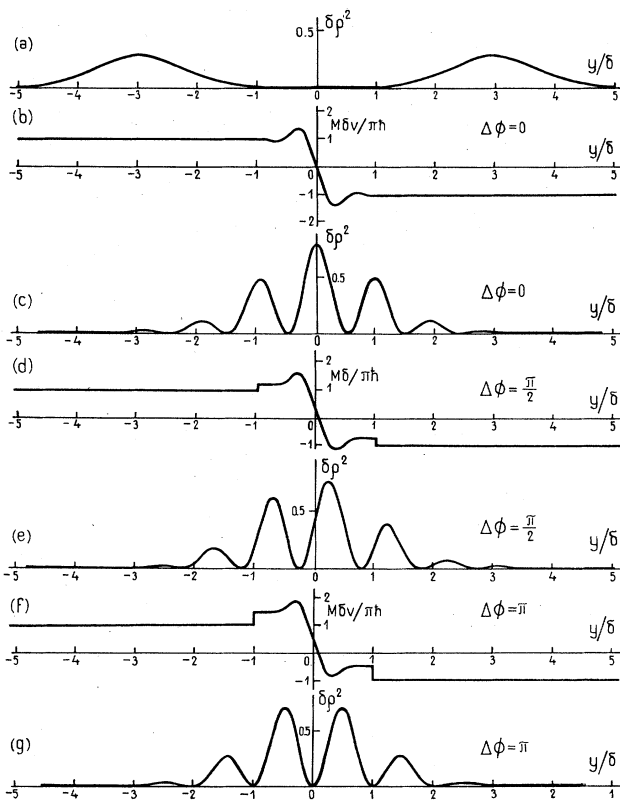
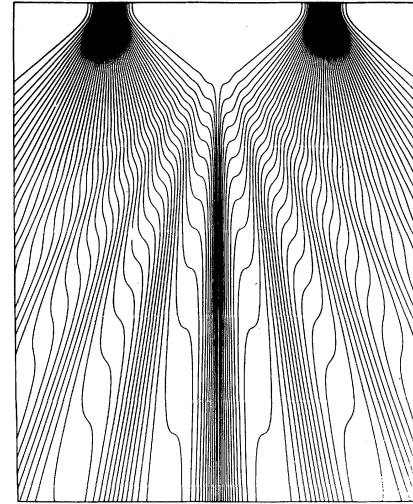
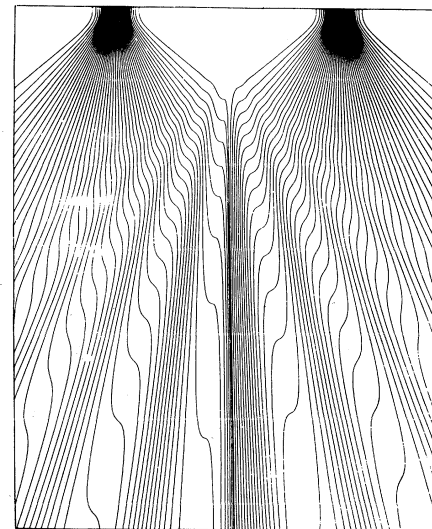


FIG. 18. Hydrodynamical representation of the quantum interference of two Gaussian wave packets. (a) The packets of width δ are initially centered at $y_0 = \pm 3\delta$, and have an incident momentum $Mv_0 = \mp \pi\hbar/\delta$. (b), (d), and (f) The relative phase of the wave packets is shifted by an electric field acting for a short period of time in the region of the tail of the packets, between $-\delta$ and δ . The enclosed electric field does not affect the probability distribution, but changes the velocity field v . (c), (e), and (g) Interference patterns observed after a time $y_0/v_0 = 3M\delta^2/\pi\hbar$, when both packets have their centers at $y_0 = 0$, corresponding to amounts of enclosed flux causing phase shifts of $0, \pi/2$, and π , respectively. The difference $\Delta\phi_E$ between the initial phases at the centers of the packets is π times the area under the curve of v vs y , comprised between the ordinates of the points $y_0 = \pm 3\delta$.



(a)



(b)

FIG. 19. Lines of the probability current for two-slit scattering of a particle of charge q : (a) in the absence of flux, as reported by Philippidis, Dewdney, and Hiley (1979); (b) in the presence of a magnetic flux $\pi\hbar c/2q$ enclosed between the two slits, as reported by Philippidis, Bohm, and Kaye (1982). The probability density is proportional to the number of lines per unit of length. The central light peak from (a) is displaced by the enclosed flux of (b) by a quarter of a fringe.

of charge q and mass M acted on by the force derived from the aforementioned effective energy and vector potential. The classical velocity of the particle at a certain point of its trajectory is given by $(\hbar\nabla\Phi - q\mathbf{A}/c)/M$, evaluated at that point. However, since the field \mathbf{v} has an identical expression [Eq. (1.112)], the ensemble of these classical trajectories yields the pattern of the probability current, Eq. (1.85b). Such a technique based on the quantum potential $-\hbar^2\Delta\rho/2M\rho$ was used by Philippidis, Dewdney, and Hiley (1979) in the case of two-split scattering of a free particle. Later, Philippidis, Bohm and Kaye (1982) applied the same technique to scattering by two slits in the presence of a line of magnetic flux placed between the slits. The patterns of the probability currents thus obtained are reproduced in Fig. 19. Because of the continuity equation the probability density is proportional to the number of lines per unit of length in the observing region. We see in Fig. 19(a) a central peak accompanied by smaller satellites. In Fig. 19(b) we see that the effect of an enclosed flux $F = \pi\hbar c/2q$ is to create an asymmetric pattern, similar to that shown in Fig. 18(e), which corresponded to the same phase difference of $\pi/2$.

II. ANALYTIC REPRESENTATIONS

A. Scattering of a plane wave by an infinite magnetic string

The observable effects of enclosed fluxes arise from phase shifts followed by the quantum interference of the components of the incident state passing by different sides of the flux region. In order to analyze the role of the field strengths in the Aharonov-Bohm effect, we shall consider in this section detailed solutions of the Schrödinger equation for several relevant configurations of incident states and field distributions. We shall see that the quantum effects of the fluxes exist even if the overlap between the incident particles and the field strengths is rendered arbitrarily small, thereby forcing us to reconsider the role of field strengths in the description of an electromagnetic interaction.

An important example of distribution of field strengths for which the Schrödinger equation can be solved explicitly is that of the magnetic flux of a long solenoid of small transverse cross section. In the limit when the cross section becomes vanishingly small while the magnetic flux enclosed in the solenoid is kept constant, such a configuration is known as a magnetic string. In this section we shall discuss the scattering by an infinitely long magnetic string of a beam of charged particles represented in the incidence region by a plane wave. As shown by Aharonov and Bohm (1959), the infinite magnetic string produces a shift in the phase of the plane wave, which is proportional to the amount of enclosed flux, and which gives rise to an emergent radial wave whose amplitude is a periodic function of the enclosed flux. The scattering contribution has not, however, the conventional form of a cylindrical wave in all asymptotic directions, but rather it is concentrated

in the vicinity of a half-plane Π parallel to the incidence direction and having its edge coincident with the magnetic string. This structure of the wave function in the vicinity of the half-plane Π is due to the quantum-mechanical scattering of the phase-shifted components of the incident state, which pass by the opposite sides of the string; thus the associated observable changes in the probability distribution are a manifestation of the quantum effects of the magnetic flux enclosed in the string.

Let us assume that we have an infinite magnetic string carrying the flux F and coinciding with the z axis, as shown in Fig. 20. The vector potential of the string can be represented by the components

$$A_\theta(r) = \frac{F}{2\pi r}, \quad A_r = 0, \quad A_z = 0, \quad (2.1)$$

where r and θ are the polar coordinates in the x,y plane. Since the vector potential is independent of z , we shall assume that the flux-dependent wave function is uniform in the z direction. The Schrödinger equation for a particle of charge q , mass M , and energy $\hbar^2 k^2/2M$, moving in the presence of the magnetic string, is

$$\frac{\partial^2\psi}{\partial r^2} + \frac{1}{r} \frac{\partial\psi}{\partial r} + \left[k^2 - \frac{1}{r^2} \left(-i \frac{\partial}{\partial\theta} - \alpha \right)^2 \right] \psi = 0, \quad (2.2)$$

where the parameter α is given by

$$\alpha = \frac{qF}{2\pi\hbar c}. \quad (2.3)$$

The single-valued eigenfunctions of Eq. (2.2) are

$$J_{|m-\alpha|}(kr)e^{im\theta}, \quad m = 0, \pm 1, \dots \quad (2.4)$$

and, as shown by Aharonov and Bohm (1959), the wave function for the scattering of a plane wave of momentum $\hbar k$, incident from the positive end of the x axis, has the form

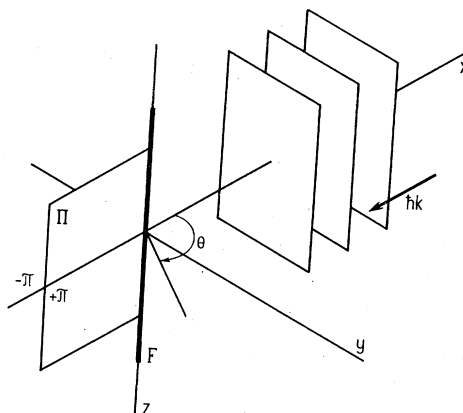


FIG. 20. Scattering of a plane wave by an infinite magnetic string carrying the flux F . The string produces a progressive shift in the phase of the incident wave, which is proportional to the amount of enclosed flux, and gives rise to a scattered wave whose amplitude is a periodic function of the magnetic flux. The amplitude of the scattered wave becomes very large in the vicinity of the half-plane Π , due to quantum diffusion of the phase-shifted components of the incident state, passing by opposite sides of the string.

$$\psi_\alpha(r, \theta) = \sum_{m=-\infty}^{\infty} \exp \left[-i \frac{\pi}{2} |m - \alpha| \right] J_{|m - \alpha|}(kr) e^{im\theta}, \tag{2.5}$$

where the origin of the angle θ coincides with the positive part of the x axis, and m is an integer. It is apparent from Eqs. (2.5) and (2.3) that the wave functions $\psi_{\alpha+N}$ and ψ_α , for scattering by strings carrying magnetic fluxes that differ by an integer multiple N of $2\pi\hbar c/q$, are connected by

$$\psi_{\alpha+N}(r, \theta) = e^{iN\theta} \psi_\alpha(r, \theta), \tag{2.6}$$

while the wave functions ψ_α and $\psi_{-\alpha}$, for scattering by strings carrying opposite fluxes, are related by

$$\psi_{-\alpha}(r, \theta) = \psi_\alpha(r, -\theta). \tag{2.7}$$

Taking into account the symmetry properties, Eqs. (2.6) and (2.7), we can restrict our analysis of the scattering to

$$\begin{aligned} \psi_\alpha = & \frac{1}{2} e^{-ikr \cos \theta} \int_0^\infty d\xi e^{i\xi \cos \theta} \{ e^{-i\pi\alpha/2} J_{\alpha-1}(\xi) + e^{i\theta+i\pi/2} J_\alpha(\xi) + e^{i\pi\alpha/2} [J_{1-\alpha}(\xi) + e^{i\theta-i\pi/2} J_{-\alpha}(\xi)] \} \\ & - \frac{1}{2} e^{-i\pi\alpha/2+i\pi/2} \sin(\pi\alpha) e^{-ikr \cos \theta} \int_{kr}^\infty d\xi e^{i\xi \cos \theta} [H_{1-\alpha}^{(1)}(\xi) + e^{i\theta-i\pi/2} H_{-\alpha}^{(1)}(\xi)], \end{aligned} \tag{2.8}$$

where the right-hand side of Eq. (2.8) is equal to the series in Eq. (2.5), for values of α within the range $0-1$. The first integral in Eq. (2.8) can be evaluated with the aid of the formula

$$\int_0^\infty e^{i\xi \cos \theta} J_\nu(\xi) d\xi = \frac{e^{i\nu(\pi/2 - |\theta|)}}{|\sin \theta|}, \tag{2.9}$$

where $0 < |\theta| < \pi$ and $-1 < \nu$ (Abramowitz and Stegun, 1965). If the range of the angle θ were different, then additional phase factors would have appeared on the right-hand side of Eq. (2.9), thus ensuring the periodicity of the integral with respect to θ . Repeated application of Eq. (2.9) yields the first integral in Eq. (2.8) as

$$\psi_\alpha^{(i)} = e^{-ikr \cos \theta + i\alpha\theta}. \tag{2.10}$$

We see that in a first approximation the effect of the enclosed magnetic flux is to shift the phase of the unperturbed incident wave $\exp(-ikr \cos \theta)$ by $\alpha\theta$. Since in the presence of the magnetic string the field of the probability current, Eq. (1.85b), corresponding to the wave function $\psi_\alpha^{(i)}$, consists of vectors of magnitude $\hbar k/M$ oriented in the $-x$ direction, the wave function $\psi_\alpha^{(i)}$ is referred to as the incident state of the problem. The second integral in Eq. (2.8) can be evaluated for $kr \gg 1$ by substituting the asymptotic expression of the Hankel functions,

$$H_\nu^{(1)}(\xi) = \left[\frac{2}{\pi\xi} \right]^{1/2} \exp \left[i \left[\xi - \frac{\pi}{2} \nu - \frac{\pi}{4} \right] \right], \quad \xi \gg 1 \tag{2.11}$$

which yields the scattered wave

values of the parameter α within the range $0-\frac{1}{2}$. The parameter in Eq. (2.3) is often defined as $\tilde{\alpha} = -qF/2\pi\hbar c$, which is convenient when the analysis is restricted to the scattering of a negatively charged electron. The wave functions corresponding to the two conventions can easily be transformed one into another with the aid of Eq. (2.7). From Eqs. (2.3) and (2.2) it also follows that the scattering of a particle of charge Zq by a string of flux F is similar to the scattering of a particle of charge q by a flux ZF , where Z can be positive or negative.

Now it is convenient to transform the series given by Eq. (2.5) into a closed form, which can be done by first considering separately the terms involving positive and negative values of m , then differentiating these sums with respect to kr and using recurrence relations for the Bessel functions to simplify the terms, and finally integrating the resulting first-order differential equations (Aharonov and Bohm, 1959; Kretzschmar, 1965b). The integral representation is

$$\begin{aligned} \psi_\alpha^{(s)} = & - \frac{2e^{-i\pi/4}}{\pi^{1/2}} \sin(\pi\alpha) e^{-ikr \cos \theta + i\theta/2} \\ & \times \int_{(2kr)^{1/2} \cos(\theta/2)}^\infty e^{i\xi^2} d\xi. \end{aligned} \tag{2.12}$$

In the region where $(2kr)^{1/2} \cos(\theta/2) \gg 1$, i.e., at large values of kr and not too close to the negative part of the x axis, the expression of the scattered wave, Eq. (2.12), can be further simplified by using the asymptotic form of the complex Fresnel integral. Then the wave function in the asymptotic region becomes

$$\psi_\alpha = e^{-ikr \cos \theta + i\alpha\theta} - \sin(\pi\alpha) \frac{e^{i\theta/2}}{\cos(\theta/2)} \frac{e^{ikr + i\pi/4}}{(2\pi kr)^{1/2}}, \tag{2.13}$$

which is valid for $(2kr)^{1/2} \cos(\theta/2) \gg 1$. Equation (2.13) was first obtained by Aharonov and Bohm (1959), and alternative derivations have since been reported by Kretzschmar (1965b), Corinaldesi and Rafeli (1978), and Berry *et al.* (1980). It is apparent from Eq. (2.13) that the magnetic string shifts the phase of the incident plane wave by $\alpha\theta$ and gives rise to a scattered wave whose amplitude becomes very large in the vicinity of the half-plane $|\theta| = \pi$.

In order to obtain ψ_α in the asymptotic region $kr \gg 1$, but in the vicinity of the half-plane Π where $(2kr)^{1/2} \cos(\theta/2) \ll 1$, we must use in Eq. (2.12) the expansion appropriate for this region,

$$\int_{(2kr)^{1/2} \cos(\theta/2)}^\infty e^{i\xi^2} d\xi = \frac{1}{2} \pi^{1/2} e^{i\pi/4} - (2kr)^{1/2} \cos(\theta/2). \tag{2.14}$$

Then the scattered-wave equation (2.12) becomes, in the region $kr \gg 1, \pi - |\theta| \ll (2/kr)^{1/2}$,

$$\begin{aligned} \psi_\alpha^{(s)} = & -\sin(\pi\alpha)e^{-ikr \cos\theta + i\theta/2} \\ & + \frac{2}{\pi^{1/2}}e^{-i\pi/4} \sin(\pi\alpha)e^{-ikr \cos\theta + i\theta/2} \\ & \times (2kr)^{1/2} \cos(\theta/2). \end{aligned} \quad (2.15)$$

We see from Eq. (2.15) that in the vicinity of the negative part of the x axis the scattered wave does not become vanishingly small, but rather converges for given kr and $|\theta| \rightarrow \pi$ to the finite limits $\pm i \sin(\pi\alpha) \exp(ikr)$, the sign being negative for θ near π and positive for θ near $-\pi$. However, the discontinuities in the incident wave [Eq. (2.10)], and the scattered wave [Eq. (2.15)], occurring at $|\theta| = \pi$, cancel each other, and the expression of the wave function in the region $kr \gg 1, \pi - |\theta| \ll (2/kr)^{1/2}$ becomes

$$\begin{aligned} \psi_\alpha = & \cos(\pi\alpha)e^{ikr} + \frac{2}{\pi^{1/2}}e^{-i\pi/4} \sin(\pi\alpha)e^{ikr + i\theta/2} \\ & \times (2kr)^{1/2} \cos(\theta/2), \end{aligned} \quad (2.16)$$

where terms of the order of $1/(kr)^{1/2}$ or smaller have been neglected. Thus when $|\theta| \rightarrow \pi$ the square of the wave function converges to $|\psi_\alpha|^2 \rightarrow \cos^2(\pi\alpha)$ (Berry *et al.*, 1980). As can be appreciated from Eq. (2.12), the crossover between the asymptotic behavior, Eq. (2.13), and the form of Eq. (2.16) occurs for $(2kr)^{1/2} \cos(\theta/2) \cong 1$, i.e., for the parabola $2kx = 1 - k^2y^2$. However, for α near $\frac{1}{2}$, the first term in Eq. (2.16) becomes very small, and the principal contribution to the wave function in the vicinity of the half-plane $|\theta| = \pi$ is given by the second term. Thus, when $\alpha \rightarrow \frac{1}{2}$, continuous change by $2\pi\alpha$ in the phase of the wave function occurs across the much narrower region $kx = -2(ky)^2/\pi^2(1-2\alpha)^2$. The wave function in the observing region is represented in Fig. 21 for several values of the parameter α .

For $\alpha=0$, the series equation (2.5) represents a free plane wave,

$$\psi_0 = e^{-ikr \cos\theta}, \quad (2.17)$$

and the pattern of the probability current consists of straight lines, as shown in Fig. 22(a).

For $0 \leq \alpha < \frac{1}{2}$, the wave function ψ_α , Eq. (2.5), can be approximated in the vicinity of the magnetic string, where $kr \ll 1$, by the expansion

$$\psi_\alpha(r, \theta) = \frac{e^{-i\pi\alpha/2}(kr)^\alpha}{2^\alpha \Gamma(1+\alpha)} + \frac{e^{-i\pi(1-\alpha)/2}(kr)^{1-\alpha}}{2^{1-\alpha} \Gamma(2-\alpha)} e^{i\theta} + \frac{e^{-(i\pi/2)(1+\alpha)}(kr)^{1+\alpha}}{2^{1+\alpha} \Gamma(2+\alpha)} e^{-i\theta} + \frac{e^{-(i\pi/2)(2-\alpha)}(kr)^{2-\alpha}}{2^{2-\alpha} \Gamma(3-\alpha)} e^{2i\theta}. \quad (2.18)$$

Thus for $\alpha \neq 0$ the wave function is vanishing on the string. The convergence of the series to zero at $kr=0$, Eq. (2.5), is not, however, uniform with respect to α , since for $\alpha=0$ the wave function has the value $\psi_0=1$ at the origin. The first terms in the expression of the polar components of the probability current, Eq. (1.85b), corresponding to the wave function ψ_α , are

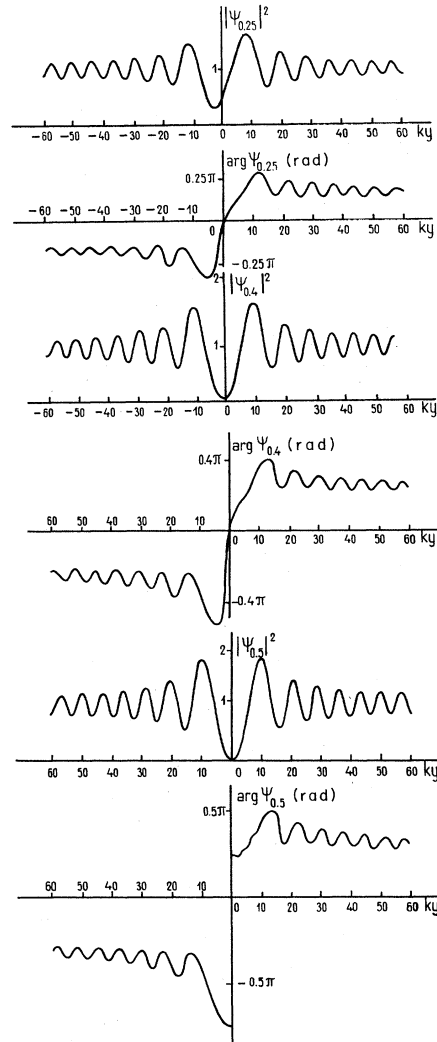


FIG. 21. Wave function ψ_α for the scattering of a plane wave by an infinite magnetic string of flux F , for several values of the parameter $\alpha = qF/2\pi\hbar c$, in the plane $kx = -20$ of the observing region. The square of the wave function at the center of the pattern in the observing plane is $|\psi_\alpha|^2 = \cos^2 \pi\alpha$, and it converges to 1 for large values of ky . The phase of ψ_α on the two wings of the observing plane oscillates around the values $\pm\alpha\theta$ for $0 \leq \alpha < \frac{1}{2}$ and varies continuously from negative to positive values. The phase of $\psi_{1/2}$ is discontinuous by π at $y=0$.

$$\frac{Mj_r^{(\alpha)}}{\hbar k} = -\frac{(\frac{1}{2}-\alpha)\cos(\theta+\pi\alpha)}{\Gamma(1+\alpha)\Gamma(2-\alpha)} - \frac{(kr)^{2\alpha}\cos\theta}{2^{1+2\alpha}\Gamma(1+\alpha)\Gamma(2+\alpha)} - \frac{(1-\alpha)kr\sin(2\theta+\pi\alpha)}{2\Gamma(1+\alpha)\Gamma(3-\alpha)} - \frac{\alpha kr\sin(2\theta+\pi\alpha)}{2\Gamma(2-\alpha)\Gamma(2+\alpha)} - \frac{(kr)^{2-2\alpha}\cos\theta}{2^{3-2\alpha}\Gamma(2-\alpha)\Gamma(3-\alpha)}, \tag{2.19a}$$

$$\frac{Mj_\theta^{(\alpha)}}{\hbar k} = \frac{(\frac{1}{2}-\alpha)\sin(\theta+\pi\alpha)}{\Gamma(1+\alpha)\Gamma(2-\alpha)} + \frac{(1-\alpha)(kr)^{1-2\alpha}}{2^{2-2\alpha}\Gamma^2(2-\alpha)} - \frac{\alpha(kr)^{2\alpha-1}}{2^{2\alpha}\Gamma^2(1+\alpha)} + \frac{(\frac{1}{2}+\alpha)(kr)^{2\alpha}\sin\theta}{2^{2\alpha}\Gamma(1+\alpha)\Gamma(2+\alpha)} - \frac{(1-\alpha)kr\cos(2\theta+\pi\alpha)}{2\Gamma(1+\alpha)\Gamma(3-\alpha)} - \frac{\alpha kr\cos(2\theta+\pi\alpha)}{2\Gamma(2+\alpha)\Gamma(2-\alpha)} + \frac{(\frac{3}{2}-\alpha)(kr)^{2-2\alpha}\sin\theta}{2^{2-2\alpha}\Gamma(2-\alpha)\Gamma(3-\alpha)}. \tag{2.19b}$$

Since the series expansion of the square modulus of the wave function, Eq. (2.5), is

$$\psi_\alpha\psi_\alpha^* = \frac{(kr)^{2\alpha}}{2^{2\alpha}\Gamma^2(1+\alpha)} + \frac{kr\sin(\theta+\pi\alpha)}{\Gamma(1+\alpha)\Gamma(2-\alpha)} + \frac{(kr)^{2-2\alpha}}{2^{2-2\alpha}\Gamma^2(2-\alpha)} + \dots, \tag{2.20}$$

the dominant term at very small values of kr in the expression of the azimuthal component of the velocity field $\mathbf{v}^{(\alpha)} = \mathbf{j}^{(\alpha)}/\psi_\alpha\psi_\alpha^*$ is

$$M\mathbf{v}_\theta^{(\alpha)} = -\frac{\hbar\alpha}{r}, \quad kr \ll 1. \tag{2.21}$$

Consequently the circulation of $M\mathbf{v}^{(\alpha)}$ around the string is equal to $-2\pi\hbar\alpha$. For values of α outside the interval $0-\frac{1}{2}$ it can be shown with the aid of Eqs. (2.6) and (2.7) that the circulation of the velocity field $M\mathbf{v}^{(\alpha)}$ is equal to $-2\pi\hbar$ multiplied by the difference between α and the nearest integer to that value of α . For half-integer values of α the circulation of $M\mathbf{v}^{(\alpha)}$ is equal to zero, as will be discussed later.

According to Eq. (1.118) the field $M\mathbf{v}^{(\alpha)}$ is the sum of a canonical contribution

$$i\hbar(\psi_\alpha\nabla\psi_\alpha^* - \psi_\alpha^*\nabla\psi_\alpha)/2\psi_\alpha\psi_\alpha^*$$

and the term $-q\mathbf{A}/c$. At extremely small values of kr the canonical contribution is of the order of $(kr)^{-2\alpha}$, while the vector potential is of the order of $1/kr$, so that the angular component of the velocity field is dominated in this region by the vector potential. However, the vector potential decreases faster than the angular canonical component with increasing kr , so that these quantities become equal at a certain point in the vicinity of the string. For values of the parameter α such that $0 < \alpha \ll \frac{1}{2}$, the components of the probability current vanish at the point

$$kr_0 = \alpha, \quad \theta_0 = \frac{\pi}{2} - \frac{\pi\alpha}{2}. \tag{2.22}$$

Then for values of kr of the order of kr_0 the probability current can be approximated by

$$\frac{Mj_r^{(\alpha)}}{\hbar k} = -\cos\left[\theta + \frac{\pi\alpha}{2}\right], \tag{2.23a}$$

$$\frac{Mj_\theta^{(\alpha)}}{\hbar k} = \sin\left[\theta + \frac{\pi\alpha}{2}\right] - \frac{\alpha}{kr}. \tag{2.23b}$$

The fact that $\mathbf{j}^{(\alpha)} = 0$ means that the lines of the probability current have a bifurcation point, which separates the incident probability flow from the current circulating at very small distances around the magnetic string. It can be shown by integrating Eqs. (2.23) that the lines of the probability current are given by

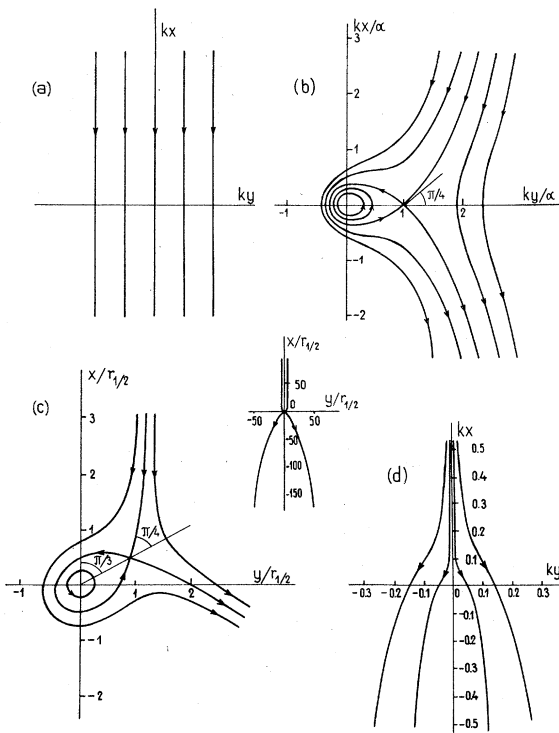


FIG. 22. Lines of the probability current $\mathbf{j}^{(\alpha)}$ for the scattering of a plane wave by an infinite magnetic string of flux F , for several values of the parameter $\alpha = qF/2\hbar c$. (a) For $\alpha=0$ the wave function is a free plane wave, and the probability flows along straight lines. (b) For very small positive values of α the pattern of the current has a bifurcation point at $kr_0 = \alpha$, $\theta_0 = \pi/2 - \pi\alpha/2$. (c) For values of α near $\frac{1}{2}$ the bifurcation point is situated at $kr_{1/2} = -[(1-2\alpha)/3^{1/2}]\ln[(1-2\alpha)/3^{1/2}]$, $\theta_{1/2} = \pi/3$. (d) For $\alpha = \frac{1}{2}$ the lines of the probability current are symmetric with respect to the x axis. The differences between (a) and (b), and between (c) and (d), are restricted to the regions kr of the order of kr_0 and $kr_{1/2}$, respectively.

$$\frac{kx'}{\alpha} = \pm \left[e^{2ky'/\alpha - 2a_0} - \left(\frac{ky'}{\alpha} \right)^2 \right]^{1/2}, \quad (2.24)$$

the bifurcation line corresponding to $a_0=1$, where $x' = x \cos(\pi\alpha/2) - y \sin(\pi\alpha/2)$ and $y' = x \sin(\pi\alpha/2) + y \cos(\pi\alpha/2)$. The bifurcation of the probability current in the case $0 < \alpha \ll \frac{1}{2}$ is shown in Fig. 22(b), as given by Eq. (2.24).

For values of α such that $0 < \frac{1}{2} - \alpha \ll \frac{1}{2}$ the condition $j^{(\alpha)} = 0$ yields the coordinates of the bifurcation point,

$$kr_{1/2} = -\frac{1-2\alpha}{3^{1/2}} \ln \frac{1-2\alpha}{3^{1/2}}, \quad \theta_{1/2} = \frac{\pi}{3}. \quad (2.25)$$

Then for values of kr of the order of $kr_{1/2}$ the probability current can be approximated by

$$\frac{M_{j_r}^{(\alpha)}}{\hbar k} = -\frac{4}{3\pi} kr \cos\theta - \frac{4}{3\pi} kr \cos 2\theta, \quad (2.26a)$$

$$\begin{aligned} \frac{M_{j_\theta}^{(\alpha)}}{\hbar k} &= \frac{2}{\pi} (1-2\alpha) \ln \frac{1-2\alpha}{3^{1/2}} + \frac{8}{3\pi} kr \sin\theta \\ &+ \frac{4}{3\pi} kr \sin 2\theta. \end{aligned} \quad (2.26b)$$

The lines of the probability current obtained by the integration of Eqs. (2.26) are given by

$$\frac{kr}{k\bar{r}_{1/2}} = \frac{3^{3/2} \pm [27 - 2 \cdot 3^{3/2} b_0 (2 \sin\theta + \sin 2\theta)]^{1/2}}{2(2 \sin\theta + \sin 2\theta)}, \quad (2.27)$$

the bifurcation line corresponding to the value of the parameter $b_0=1$. The pattern of the probability current in the case $0 < \frac{1}{2} - \alpha \ll \frac{1}{2}$, calculated according to Eq. (2.27), is represented in Fig. 22(c). It can be shown that as a consequence of the relation $\text{curl} j^{(\alpha)} = 0$, valid in the field-free region, the lines of the probability current emerging from the bifurcation point cross each other at right angles.

For $\alpha = \frac{1}{2}$ the wave function, Eq. (2.5), can be written in the form

$$\psi_{1/2} = \frac{2}{\pi^{1/2}} e^{-ikr \cos\theta + i\theta/2 - i\pi/4} \int_0^{(2kr)^{1/2} \cos(\theta/2)} e^{i\xi^2} d\xi. \quad (2.28)$$

The wave function $\psi_{1/2}$ has a nodal line at $|\theta| = \pi$, as can be appreciated from Fig. 23, and apart from the phase factor $\exp(i\theta/2)$ it is identical to the solution describing the scattering of a plane wave by a knife edge (Morse and Feshbach, 1953, pp. 1383–1387). For $|kx| \ll 1$, $|ky| \ll 1$, the components of the probability current are given by

$$j_x^{(1/2)} = -\frac{2}{3} + \frac{kx}{3(k^2x^2 + k^2y^2)^{1/2}}, \quad (2.29a)$$

$$j_y^{(1/2)} = \frac{ky}{3(k^2x^2 + k^2y^2)^{1/2}}. \quad (2.29b)$$

The lines of the probability current obtained by the integration of Eqs. (2.29) are given by

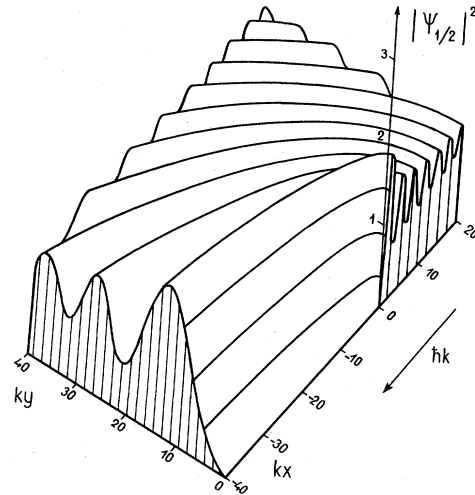


FIG. 23. Scattering of a plane wave by an infinite magnetic string carrying a flux $F = \pi\hbar c/q$. The string coincides with the z axis, and the kinetic momentum $\hbar k$ of the incident beam is oriented in the $-x$ direction. The probability distribution $|\psi_{1/2}|^2$, which is symmetric with respect to the direction of propagation, has a nodal line on the negative part of the x axis and approaches the value 1 in the region where $k[x + (x^2 + y^2)^{1/2}] \gg 1$.

$$kx = \frac{c_0}{2ky} - \frac{(ky)^3}{2c_0}, \quad (2.30)$$

where c_0 is a parameter. These lines are represented in Fig. 22(d). We see that for $\alpha = \frac{1}{2}$ the lines of the probability current are symmetric with respect to the x axis. Consequently the circulation around the string of the velocity field $M\mathbf{v}^{(1/2)}$ is equal to zero. This is due to the fact that the phase of $\psi_{1/2}$ is discontinuous by π at the nodal plane $|\theta| = \pi$, so that the contribution to the circulation of the kinematical field arising from the canonical part of $M\mathbf{v}^{(1/2)}$ is in this particular case different from zero, and thus can compensate for the contribution arising from the vector potential. More generally, the phase of a wave function on the two sides of a nodal line can differ by an integer multiple of π , and this is why the constant N in Eq. (1.120) may assume integer as well as half-integer values.

Now let us analyze the flow of the kinetic momentum for the scattering of a plane wave by an infinite magnetic string. As can be appreciated from Eq. (2.13), in the region of large kr and not too close to the plane $|\theta| = \pi$, the wave function ψ_α can be separated into two components representing, respectively, a pattern of constant probability current flowing in the incidence direction, and a radial flow of probability. If the incident wave is collimated by passing through a slit, then we can measure the flow of probability and momentum in the radial wave. The flow of the momentum density is described by the tensor Γ_{kn} , Eq. (1.90b), representing the n th component of the kinetic momentum passing through a unit area per

unit time, in the direction k . If we introduce in Eq. (1.90b), the scattering term appearing in Eq. (2.13), we obtain

$$\Gamma_{rr}^{(s)} = \frac{\hbar^2 k \sin^2(\pi\alpha)}{2\pi M r \cos^2(\theta/2)}, \quad kr \gg 1, \quad |\theta| < \pi, \quad (2.31)$$

the other components of the tensor $\Gamma^{(s)}$ being negligible in this region. Thus at large kr the momentum current per radian $r\Gamma_{rr}$ converges to a certain finite limit, which suggests that there is a certain amount of kinetic momentum exchanged between the incident wave and the magnetic string. In order to see this, let us consider the tensor $\Gamma^{(\alpha)}$ corresponding to the total wave, Eq. (2.5), in the vicinity of the magnetic string. The components $\Gamma_{rr}^{(\alpha)}, \Gamma_{r\theta}^{(\alpha)}$ describing the radial flow of momentum, obtained by substituting in Eq. (1.90b) the expression of ψ_α , are

$$\frac{2M\Gamma_{rr}^{(\alpha)}}{\hbar^2 k^2} = \frac{\alpha(kr)^{2\alpha-2}}{2^{2\alpha}\Gamma(1+\alpha)} + \frac{2\alpha(1-\alpha)(kr)^{-1}\sin(\theta+\pi\alpha)}{\Gamma(1+\alpha)\Gamma(2-\alpha)}, \quad (2.32a)$$

$$\frac{2M\Gamma_{r\theta}^{(\alpha)}}{\hbar^2 k^2} = \frac{2\alpha(1-\alpha)(kr)^{-1}\cos(\theta+\pi\alpha)}{\Gamma(1+\alpha)\Gamma(2-\alpha)}. \quad (2.32b)$$

However, we are interested in the radial flow of the components of the momentum along fixed directions, say x and y . These components, given by $\Gamma_{rx}^{(\alpha)} = \cos\theta\Gamma_{rr}^{(\alpha)} - \sin\theta\Gamma_{r\theta}^{(\alpha)}$, $\Gamma_{ry}^{(\alpha)} = \sin\theta\Gamma_{rr}^{(\alpha)} + \cos\theta\Gamma_{r\theta}^{(\alpha)}$, are

$$\frac{2M\Gamma_{rx}^{(\alpha)}}{\hbar^2 k^2} = \frac{\alpha(kr)^{2\alpha-2}\cos\theta}{2^{2\alpha}\Gamma(1+\alpha)} + \frac{2\alpha(1-\alpha)(kr)^{-1}\sin(\pi\alpha)}{\Gamma(1+\alpha)\Gamma(2-\alpha)}, \quad (2.33a)$$

$$\frac{2M\Gamma_{ry}^{(\alpha)}}{\hbar^2 k^2} = \frac{\alpha(kr)^{2\alpha-2}\sin\theta}{2^{2\alpha}\Gamma(1+\alpha)} + \frac{2\alpha(1-\alpha)(kr)^{-1}\cos(\pi\alpha)}{\Gamma(1+\alpha)\Gamma(2-\alpha)}, \quad (2.33b)$$

where $kr \ll 1$. Then the momentum current flowing out of a cylinder of very small radius r , centered on the string, is equal to

$$\int \Gamma_{rx}^{(\alpha)} r d\theta = \frac{2\sin^2(\pi\alpha)\hbar^2 k}{M}, \quad (2.34a)$$

$$\int \Gamma_{ry}^{(\alpha)} r d\theta = \frac{2\sin(\pi\alpha)\cos(\pi\alpha)\hbar^2 k}{M}. \quad (2.34b)$$

According to Eqs. (2.34), no momentum is exchanged between the incident wave and the string for $\alpha=0$. For $\alpha=\frac{1}{2}$, when the wave function is symmetric with respect to the y axis, there is a maximum flow of the x component of momentum, and no flow of the y component of momentum.

We have previously seen that for $kr \ll 1$ the lines of the probability current are circling around the magnetic string. The fact that the tensor $\Gamma^{(\alpha)}$ of the momentum flow is not equal to zero shows that in the vicinity of the magnetic string the wave function has large incoming and outgoing radial components which interfere to make up a radial standing wave. How it is possible that a flux distribution of vanishingly small radius should impart a finite

amount of momentum to the incident charged particles is a question that will be further discussed in Sec. II.E.

In the region near the x axis the wave function cannot be separated into incident and scattered components, and we can measure only the total wave, Eq. (2.5). The wave function in the observing region [Eq. (2.16)] is in fact just what we would expect to result from the interference of the half-waves passing by the opposite sides of the string. As shown by Morse and Feshbach (1953, p. 1385), the half-wave u_+ crossing the positive part of the y axis has, in the absence of the magnetic string, the form

$$u_+(r, \theta) = \frac{1}{\pi^{1/2}} e^{-ikr \cos\theta - i\pi/4} \int_{-\infty}^{\pm(2kr)^{1/2} \cos(\theta/2)} e^{i\xi^2} d\xi, \quad (2.35)$$

where the plus sign applies to $0 < \theta < \pi$ and the minus sign to $-\pi < \theta < 0$. The asymptotic behavior of u_+ in the region $kr \gg 1$, $|\theta| < \pi$ is

$$u_+ = \begin{cases} e^{-ikr \cos\theta} - \frac{e^{ikr + i\pi/4}}{(8\pi kr)^{1/2} \cos(\theta/2)}, & 0 < \theta < \pi \\ \frac{e^{ikr + i\pi/4}}{(8\pi kr)^{1/2} \cos(\theta/2)}, & -\pi < \theta < 0, \end{cases} \quad (2.36)$$

so that u_+ is indeed concentrated at positive angles θ . The half-wave u_- crossing the negative part of the y axis is related to u_+ by

$$u_-(r, \theta) = u_+(r, -\theta). \quad (2.37)$$

It is apparent from Eqs. (2.36) and (2.37) that in the absence of the string the waves diffusing from the incident components which pass by opposite sides of the string cancel each other, so that the sum of the two half-waves is simply the unperturbed incident state,

$$u_+(r, \theta) + u_-(r, \theta) = e^{-ikr \cos\theta}. \quad (2.38)$$

However, in the presence of the magnetic string the phase of the half-wave crossing the positive part of the y axis is shifted by $\pi\alpha$ in the vicinity of the plane $|\theta| = \pi$, while the phase of the half-wave crossing the negative part of the y axis is shifted by $-\pi\alpha$, so that the total wave function becomes

$$\tilde{\psi}_\alpha = e^{i\pi\alpha} u_+ + e^{-i\pi\alpha} u_-, \quad kr \gg 1, \quad \pi - |\theta| \ll \left[\frac{2}{kr} \right]^{1/2}. \quad (2.39)$$

An evaluation of the integrals appearing in Eqs. (2.35) and (2.37) with the aid of Eq. (2.14) does indeed yield an expression equivalent to the asymptotic form, Eq. (2.16). This shows that in the observing region the effects of the magnetic string arise from flux-dependent phase shifts followed by quantum interference.

When we have represented the enclosed flux by a magnetic string, we have implicitly assumed that the wavelength of the incident particles is large compared to the radius of the magnetic filament. Although this is hardly

the case in actual experiments, physical analogs of the scattering of a plane wave by an infinite magnetic string are encountered in the scattering of surface water waves by an irrotational vortex (Berry *et al.*, 1980), or in the behavior of an electron in a crystal that includes a screw dislocation (Kawamura, Zempo, and Irie, 1982).

B. Scattering of a wave packet by an infinite magnetic string

It is apparent from the analysis developed in the preceding section that the combined effect on an incident plane wave of the flux-dependent phase shifts and quantum diffusion is to produce a rather complicated pattern of probability and momentum. In particular, the scattering of a plane wave by an infinite magnetic string is characterized by a nonzero exchange of kinetic momentum between the incident plane wave and the string, reflected in Eq. (2.13) by the term proportional to $\exp(ikr)/(kr)^{1/2}$. This term is frequently interpreted as the amplitude of the scattering cross section of the incident particle by the magnetic string (Aharonov and Bohm, 1959; Peshkin, Talmi, and Tassie, 1961; Corinaldesi and Rafeli, 1978; Henneberger, 1980; Peshkin, 1981b). Since the space is free of forces except at the magnetic string, the presence of the incident particle in the region of the string is essential for such an exchange to occur. In order to distinguish between the phase effects and the momentum effects of enclosed fluxes, we shall consider in this section the scattering of a wave packet of finite extension by a string of magnetic flux. We shall see that the amplitude is an exponentially small function of the square of the ratio between the impact parameter and the width of the packet, so that the scattering amplitude becomes vanishingly small as the width of the packet goes to zero. This means that the exchange of kinetic momentum encountered at the scattering of a plane wave is a secondary effect preceded by the diffusion and interference of the phase-shifted components of the in-

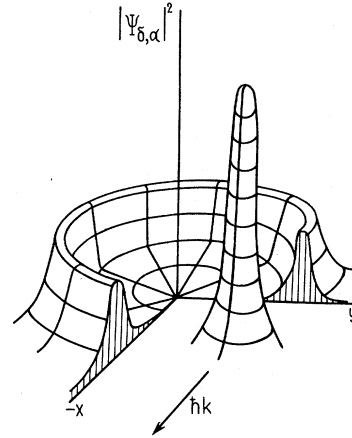


FIG. 24. Scattering of a wave packet of finite width by a magnetic string coinciding with the z axis. The effect of the magnetic string is to shift the phase at the center of the incident packet by an amount proportional to the enclosed flux. The amplitude of the radial scattered wave is an exponentially small function of the square of the ratio between the impact parameter and the width of the packet, and it becomes vanishingly small as the width of the packet goes to zero.

cident wave. In the same time, the phase at the center of the incident wave packet is progressively shifted by an amount proportional to the enclosed flux, a result that is consistent with the quasiclassical analysis of the problem. Thus the observable effects of enclosed fluxes arise from phase shifts followed by interference, and primarily involve no changes in the kinetic momentum of the incident particles.

We shall assume that the incident state is a wave packet of width δ , centered at time $t=0$ at the point \vec{r}_0, θ_0 , and traveling with momentum $\hbar k$ in the negative x direction, as shown in Fig. 24,

$$\Psi_{\delta,\alpha}(r',\theta',0) = \frac{1}{\pi^{1/2}\delta} \exp \left[i\alpha\theta' - ikr'\cos\theta' - \frac{(r'\cos\theta' - \tilde{r}_0\cos\tilde{\theta}_0)^2 + (r'\sin\theta' - \tilde{r}_0\sin\tilde{\theta}_0)^2}{2\delta^2} \right]. \tag{2.40}$$

We shall determine the time evolution of the wave packet in the presence of the magnetic string with the aid of the Green's-function technique, which yields the wave function at the time t in the form

$$\Psi_{\delta,\alpha}(r,\theta,t) = \int G_\alpha(r,\theta,t;r',\theta',0)\Psi_{\delta,\alpha}(r',\theta',0)r'dr'd\theta'. \tag{2.41}$$

In general, the Green's function is a sum of products of eigenfunctions over the complete set of states of the given problem. The eigenfunctions for a particle of charge q , mass M , and energy $\hbar^2k^2/2M$, interacting with a magnetic string carrying the flux $F = 2\pi\hbar c\alpha/q$, are

$$\frac{1}{(2\pi)^{1/2}} J_{|m-\alpha|}(kr) e^{im\theta - i\hbar k^2 t/2M}, \tag{2.42}$$

where the canonical momentum m is an integer. Consequently, as reported by Kretzschmar (1965b), the Green's function for the scattering by an infinite magnetic string is

$$G_\alpha(r,\theta,t;r',\theta',0) = \frac{1}{2\pi} \sum_{m=-\infty}^{\infty} \int k dk J_{|m-\alpha|}(kr) J_{|m-\alpha|}(kr') \times e^{-i\hbar k^2 t/2M + im(\theta-\theta')}. \tag{2.43}$$

An equivalent, but less tractable form of G_α was obtained by Gerry and Singh (1979) with the aid of the path-integral formalism. An integration over k in Eq. (2.43) can be carried out with the result

$$G_\alpha(r, \theta, t; r', \theta', 0) = -\frac{iM}{2\pi\hbar t} e^{(iM/2\hbar t)(r^2+r'^2)} \times \sum_{m=-\infty}^{\infty} e^{-(i\pi/2)|m-\alpha|} J_{|m-\alpha|} \left[\frac{Mrr'}{\hbar t} \right] \times e^{im(\theta-\theta')}. \tag{2.44}$$

By comparing the expression of G_α , Eq. (2.44), with the series, Eq. (2.5), we find that

$$G_\alpha(r, \theta, t; r', \theta', 0) = -\frac{iM}{2\pi\hbar t} e^{(iM/2\hbar t)(r^2+r'^2)} \psi_\alpha \left[\frac{Mrr'}{\hbar t}, \theta-\theta' \right]. \tag{2.45}$$

Thus we can use Eqs. (2.6) and (2.7) to infer that

$$G_{\alpha+N}(r, \theta, t; r', \theta', 0) = e^{iN(\theta-\theta')} G_\alpha(r, \theta, t; r', \theta', 0),$$

where N is an integer, and

$$G_{-\alpha}(r, \theta, t; r', \theta', 0) = G_\alpha(r, -\theta, t; r', -\theta', 0).$$

Moreover, we can use the asymptotic expression of ψ_α , Eq. (2.13), to obtain the asymptotic form of the Green's function for $Mrr'/\hbar t \gg 1$, $(2Mrr'/\hbar t)^{1/2} \cos(\theta-\theta')/2 \gg 1$ as

$$G_\alpha = -\frac{iM}{2\pi\hbar t} \exp\{(iM/2\hbar t)[r^2+r'^2-2rr'\cos(\theta-\theta')] + i\alpha(\theta-\theta')\} - \left[\frac{M}{\hbar t} \right]^{1/2} \frac{\sin(\pi\alpha)}{\cos[(\theta-\theta')/2]} \frac{\exp\{(iM/2\hbar t)(r^2+r'^2+2rr') - i\pi/4\}}{(8\pi^3 rr')^{1/2}}, \tag{2.46}$$

where $|\theta-\theta'| < \pi$ and $0 \leq \alpha < 1$ (Kretzschmar, 1965b). It is apparent from Eq. (2.46) that the first term of G_α is proportional to the free-particle Green's function,

$$G_0 = -\frac{iM}{2\pi\hbar t} e^{(iM/2\hbar t)(r-r')^2}, \tag{2.47}$$

so that we have approximately

$$G_\alpha \simeq G_0 e^{i\alpha(\theta-\theta')}, \quad |\theta-\theta'| < \pi. \tag{2.48}$$

On the other hand, for $Mrr'/\hbar t \gg 1$ and $\pi - |\theta-\theta'| \ll (2\hbar t/Mrr')^{1/2}$ we obtain from Eqs. (2.45) and (2.16) the Green's function

$$G_\alpha = -\frac{iM}{2\pi\hbar t} e^{(iM/2\hbar t)(r^2+r'^2+2rr')} \cos(\pi\alpha) - \frac{M}{\pi^{3/2}\hbar t} \sin(\pi\alpha) \exp\{(iM/2\hbar t)(r^2+r'^2+2rr') + i(\theta-\theta')/2 + i\pi/4\} \left[\frac{2Mrr'}{\hbar t} \right]^{1/2} \cos \left[\frac{\theta-\theta'}{2} \right], \tag{2.49}$$

where $0 \leq \alpha < 1$. Consequently, when $\pi - |\theta-\theta'| \ll (2\hbar t/Mrr')^{1/2}$ the Green's function is approximately

$$G_\alpha \simeq G_0 \cos(\pi\alpha), \tag{2.50}$$

and in particular $G_{1/2}$ has a nodal surface at $|\theta-\theta'| = \pi$.

Assuming now that the width δ and the impact parameter $d = \tilde{r}_0 \sin \tilde{\theta}_0$ of the incident packet are small compared to the distance \tilde{r}_0 , $\delta \ll \tilde{r}_0$, $d \ll \tilde{r}_0$, we shall expand the cosine functions appearing in Eqs. (2.40) and (2.46) in powers of θ_0 and θ' up to second-order terms. In this approximation the expression of the initial state becomes

$$\Psi_{\delta, \alpha}(r', \theta', 0) = \frac{1}{\pi^{1/2}\delta} \exp \left[i\alpha\theta' - ikr' \left[1 - \frac{\theta'^2}{2} \right] - \frac{r'^2 + \tilde{r}_0^2 - 2r'\tilde{r}_0 \left[1 - \frac{\theta'^2 - 2\theta'\tilde{\theta}_0 + \tilde{\theta}_0^2}{2} \right]}{2\delta^2} \right], \tag{2.51}$$

while the scattering term of the Green's function contains the factor

$$\frac{e^{i(\theta-\theta')/2}}{\cos[(\theta-\theta')/2]} \simeq \frac{e^{i(\theta-\theta')/2}}{\cos[(\theta-\tilde{\theta}_0)/2]}. \tag{2.52}$$

Since the major contribution to the integral in Eq. (2.41) arises from the region near the center of the wave packet represented in Eq. (2.51), the integrations over dr' and $d\theta'$ can be extended without noticeable error from $-\infty$ to ∞ . The result of the integration is then

$$\Psi_{\delta,\alpha}^{(s)} = -\frac{1}{\pi^{1/2}\delta} \left[1 + \frac{i\tilde{r}_0}{k\delta^2} \right]^{-1/2} \left[1 + \frac{i\hbar t}{M\delta^2} \right]^{-1/2} \sin(\pi\alpha) \frac{e^{i\theta/2}}{\cos[(\theta - \tilde{\theta}_0)/2]} \times \frac{e^{ikr+i\pi/4}}{(2\pi kr)^{1/2}} \exp \left[\varepsilon' - i(1-i\varepsilon'') \frac{\tilde{r}_0^2 \tilde{\theta}_0^2}{2\delta^2} - \frac{i\hbar k^2 t}{2M} - \frac{\left[r + \tilde{r}_0 - \frac{\hbar kt}{M} - \frac{\tilde{r}_0^2 \tilde{\theta}_0^2}{2} \right]^2}{2a^2 \left[1 + \frac{i\hbar t}{M\delta^2} \right]} \right], \tag{2.53}$$

where

$$\varepsilon' = \left(\frac{1}{2} - \alpha \right) \tilde{\theta}_0 \frac{\tilde{r}_0/k\delta^2}{1+i\tilde{r}_0/k\delta^2} - \frac{i(\frac{1}{2}-\alpha)^2}{2k\tilde{r}_0(1+i\tilde{r}_0/k\delta^2)}, \tag{2.54a}$$

and

$$\varepsilon'' = \frac{\hbar t}{M\delta^2 + i\hbar t} - \frac{r}{(k\delta^2 + i\tilde{r}_0)(1+i\hbar t/M\delta^2)}, \tag{2.54b}$$

and where we have neglected terms of higher order than quadratic in the angles $\tilde{\theta}_0, \theta'$. Now in order for the spreading of the wave packet to be negligible for path lengths of the order of \tilde{r}_0 it is necessary that $\tilde{r}_0/k\delta^2 \ll 1$. Assuming further that $k\tilde{r}_0 \gg 1$, the quantities defined in Eqs. (2.54) are negligible, $|\varepsilon'| \ll 1$, $|\varepsilon''| \ll 1$, and the expression of the scattered wave becomes

$$\Psi_{\delta,\alpha}^{(s)} = -\frac{1}{\pi^{1/2}\delta} \sin(\pi\alpha) e^{-\tilde{r}_0^2 \tilde{\theta}_0^2 / 2\delta^2} \frac{e^{i\theta/2}}{\cos(\theta/2)} \frac{e^{ikr+i\pi/4}}{(2\pi kr)^{1/2}} \times \exp \left[-\frac{i\hbar k^2 t}{2M} - \frac{\left[r + \tilde{r}_0 - \frac{\hbar kt}{M} - \frac{\tilde{r}_0^2 \tilde{\theta}_0^2}{2} \right]^2}{2\delta^2} \right]. \tag{2.55}$$

$$\Psi_{\delta,\alpha}^{(i)}(r, \theta, t) = \frac{1}{\pi^{1/2}\delta(1+i\hbar t/M\delta^2)} \exp \left[i\alpha\theta - ikr \cos\theta - \frac{i\hbar k^2 t}{2M} - \frac{\left[r \cos\theta - \tilde{r}_0 \cos\tilde{\theta}_0 + \frac{\hbar kt}{M} \right]^2 + (r \sin\theta - \tilde{r}_0 \sin\tilde{\theta}_0)^2}{2\delta^2(1+i\hbar t/M\delta^2)} \right]. \tag{2.56}$$

We see from Eq. (2.56) that the phase at the center of the incident wave packet is progressively shifted by an amount proportional to the enclosed flux, as predicted on the basis of the quasiclassical approximation. Thus the cross section for the scattering of a localized particle by an infinite magnetic string converges to zero, and the observable effects of enclosed fluxes arise in this case from phase shifts followed by quantum interference.

In the analysis of the quantum effects of the fluxes it is conventionally assumed that the charged particles interact with classical electromagnetic distributions. However, in principle, the quantum fluctuations of the electromagnetic field affect the particle, by producing uncertainties in the phase. The question arises then, to what extent are the quantum effects of the fluxes influenced by the zero-

point fluctuations of the electromagnetic field? Mitler (1961) has shown that, according to quantum field theory, the presence of the enclosed fluxes will be manifest by shifts of the interference fringes with respect to the no-flux case, and moreover this effect will be masked by the vacuum fluctuations to the same extent as the ordinary, no-flux interference pattern. It is consistent, then, to assume in our analysis that the electromagnetic potentials can be specified as given functions of position and time.

Since the first term in Eq. (2.46) is proportional to the Green's function of a free particle, the application of that part of G_α on the initial state, Eq. (2.40), yields the wave function at the time t of a free wave packet, multiplied by the factor $\exp(i\alpha\theta)$,

C. Quantization of angular momentum in the presence of a magnetic string

The quantization of angular momentum for systems possessing spherical symmetry can be regarded as a conse-

quence of the commutation relations between the angular momentum operators. If such a spherically symmetric system is intersected by an infinite magnetic string passing through the center, the symmetry of the newly formed system will be partly spherical and partly cylindrical. While the commutation relations between components of the angular momentum operators are not affected in the field-free region outside the magnetic string, these relations include additional flux-dependent terms when applied in the region of flux inside the magnetic string. We therefore expect that the space of the kinetic angular momentum eigenfunctions of a system in the presence of a magnetic string should be different from the conventional space of the spherical eigenfunctions.

In this section we shall determine the eigenstates of a charged particle bound by an attractive potential U in the vicinity of an infinite magnetic string, a problem considered by Kretzschmar (1965c). Assuming that the potential U is spherically symmetric, $U = U(\rho)$, the Hamiltonian of the particle of charge q and mass M , in the presence of a magnetic string placed along the z axis and carrying the flux F , is given in spherical coordinates by

$$\hat{H}_{U,\alpha} = -\frac{\hbar^2}{2M} \left[\frac{\partial^2}{\partial \rho^2} + \frac{2}{\rho} \frac{\partial}{\partial \rho} - \frac{1}{\rho^2} \hat{\Lambda}_\alpha^2 \right] + U(\rho), \quad (2.57)$$

where $\hat{\Lambda}_\alpha^2$ is the operator of the total kinetic angular momentum, given by

$$\hat{\Lambda}_\alpha^2 = -\frac{1}{\sin\theta} \frac{\partial}{\partial \theta} \left[\sin\theta \frac{\partial}{\partial \theta} \right] + \frac{1}{\sin^2\theta} \left[-i \frac{\partial}{\partial \varphi} - \alpha \right]^2. \quad (2.58)$$

In this section ρ represents the spherical distance, θ is the spherical polar angle, and φ is the azimuthal angle. The eigenfunctions of the Hamiltonian, Eq. (2.57), can be determined as products of radial and angular momentum eigenfunctions,

$$\hat{H}_{U,\alpha} \psi_{U,\alpha} = E_{U,\alpha} \psi_{U,\alpha}, \quad (2.59)$$

$$(1-x)^{-|m-\alpha|} \mathcal{F}[-\lambda - |m-\alpha|, \lambda+1 - |m-\alpha| | 1 - |m-\alpha| | (1-x)/2].$$

The eigenfunctions are those solutions of Eq. (2.63) which fulfill the boundary condition that $P_{\lambda,\alpha}$ vanish on the string, i.e., $P_{\lambda,\alpha} = 0$ at $x = \pm 1$. The solution

$$P_\lambda^{-|m-\alpha|}(x) = \frac{1}{\Gamma(1 + |m-\alpha|)} \left[\frac{1-x}{1+x} \right]^{|m-\alpha|/2} \mathcal{F} \left[-\lambda, \lambda+1 \left| |m-\alpha| + 1 \right| \frac{1-x}{2} \right] \quad (2.65)$$

is equal to zero at $x=1$, while the other independent solution is divergent at $x=1$ and therefore cannot be an eigenfunction. An equivalent expression of the function in Eq. (2.65) can be obtained by using the formula relating the hypergeometric solution about one singularity to the solution about the other singularity (Morse and Feshbach, 1953, p. 546),

$$P_\lambda^{-|m-\alpha|}(x) = \frac{\Gamma(|m-\alpha|)}{\Gamma(|m-\alpha| + \lambda + 1)\Gamma(|m-\alpha| - \lambda)} \left[\frac{1-x}{1+x} \right]^{|m-\alpha|/2} \mathcal{F} \left[-\lambda, \lambda+1 \left| 1 - |m-\alpha| \right| \frac{1+x}{2} \right] + \frac{\Gamma(-|m-\alpha|)}{\Gamma(-\lambda)\Gamma(\lambda+1)} \left[\frac{1-x^2}{4} \right]^{|m-\alpha|/2} \mathcal{F} \left[|m-\alpha| + \lambda + 1, |m-\alpha| - \lambda \left| |m-\alpha| + 1 \right| \frac{1+x}{2} \right]. \quad (2.66)$$

$$\psi_{U,\alpha} = \mathcal{R}_{U,\alpha} Y_{\lambda,m}^{(\alpha)}(\theta, \varphi). \quad (2.60)$$

Moreover, the eigenfunctions of the kinetic angular momentum operator

$$\hat{\Lambda}_\alpha^2 Y_{\lambda,m}^{(\alpha)} = \lambda(\lambda+1) Y_{\lambda,m}^{(\alpha)} \quad (2.61)$$

are also products of functions of θ and φ of the form

$$Y_{\lambda,m}^{(\alpha)} = P_{\lambda,\alpha}(\theta) e^{im\varphi}. \quad (2.62)$$

Since the parabola $\lambda(\lambda+1)$ is symmetric with respect to the value $\lambda = -\frac{1}{2}$, we choose to describe the eigenvalues defined in Eq. (2.61) by the branch $\lambda > -\frac{1}{2}$. The condition of single valuedness of the wave function renders the z projection of the canonical angular momentum m an integer. Then the θ -dependent part of $Y_{\lambda,m}^{(\alpha)}$ is a solution of the equation

$$\frac{1}{\sin\theta} \frac{\partial}{\partial \theta} \left[\sin\theta \frac{\partial P_{\lambda,\alpha}}{\partial \theta} \right] + \left[\lambda(\lambda+1) - \frac{(m-\alpha)^2}{\sin^2\theta} \right] P_{\lambda,\alpha} = 0. \quad (2.63)$$

The differential equation (2.63) can be transformed by a change of variables $x = \cos\theta$, and a change of function

$$P_{\lambda,\alpha} = \left[\frac{1-x}{1+x} \right]^{|m-\alpha|/2} u_{\lambda,\alpha},$$

into the form

$$(1-x^2) \frac{d^2 u_{\lambda,\alpha}}{dx^2} - 2(x + |m-\alpha|) \frac{du_{\lambda,\alpha}}{dx} + \lambda(\lambda+1) u_{\lambda,\alpha} = 0. \quad (2.64)$$

The independent solutions of Eq. (2.64) can be expressed as linear combinations of the hypergeometric functions

$$\mathcal{F}[-\lambda, \lambda+1 | |m-\alpha| + 1 | (1-x)/2]$$

and

It is apparent from Eq. (2.66) that $P_\lambda^{-|m-\alpha|}$ is divergent at $x = -1$, unless the coefficient of the first term vanishes. Since we have chosen to describe the eigenvalue $\lambda(\lambda+1)$ by the branch $\lambda > -\frac{1}{2}$, the aforementioned coefficient can be zero only at the poles of $\Gamma(|m-\alpha|-\lambda)$, so that the eigenvalues are given by

$$\lambda = |m-\alpha| + N, \quad N=0,1,2,\dots \quad (2.67)$$

We see that while the canonical angular momentum is unaffected by the string, the eigenvalues of the total kinetic angular momentum have an explicit dependence on the amount of enclosed magnetic flux. The eigenfunctions of the total kinetic angular momentum operator are thus

$$Y_{\lambda,m}^{(\alpha)} \sim P_\lambda^{-|m-\alpha|} (\cos\theta)e^{im\varphi}. \quad (2.68)$$

The ensemble of allowed values of λ and m is shown in Fig. 25. For noninteger α there are two intercalated ladders of eigenvalues λ , defined by $\lambda^+ = 1 - (\alpha - [\alpha])$, $2 - (\alpha - [\alpha])$, \dots , and $\lambda^- = \alpha - [\alpha]$, $1 + \alpha - [\alpha]$, \dots , where $[\alpha]$ denotes the integer part of α , $\alpha \leq [\alpha] < \alpha + 1$. The "positive" ladder is generated by those values of m for which $m - \alpha > 0$, while the "negative" ladder corresponds to the values $m - \alpha < 0$. The admissible values of m are $[\alpha] + 1, [\alpha] + 2, \dots, \lambda^+ + \alpha - 1, \lambda^+ + \alpha$ for eigenvalues λ^+ which belong to the "positive" ladder, and $\alpha - \lambda^-, \alpha - \lambda^- + 1, \dots, [\alpha] - 1, [\alpha]$ for eigenvalues λ^- which belong to the "negative" ladder. The parity of the eigenfunctions is $(-1)^{\lambda+\alpha}$ and $(-1)^{\lambda-\alpha}$ for the "posi-

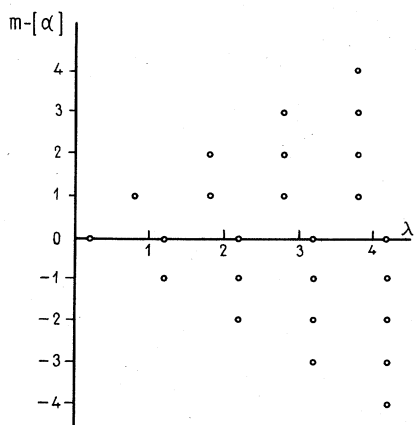


FIG. 25. Ensemble of the eigenvalues λ of the operator of the total kinetic angular momentum, and of the eigenvalues $m - [\alpha]$ of the z projection of the kinetic angular momentum, where $[\alpha]$ is the integer part of α . For noninteger α there are two intercalated ladders of eigenvalues λ , situated at $\lambda^+ = 1 - (\alpha - [\alpha]), 2 - (\alpha - [\alpha]), \dots$, and $\lambda^- = \alpha - [\alpha], 1 + \alpha - [\alpha], \dots$, respectively. The admissible values of m are $[\alpha] + 1, [\alpha] + 2, \dots, \lambda^+ + \alpha - 1, \lambda^+ + \alpha$ for eigenvalues λ^+ belonging to the first ladder, and $\alpha - \lambda^-, \alpha - \lambda^- + 1, \dots, [\alpha] - 1, [\alpha]$ for eigenvalues λ^- belonging to the second ladder.

tive" and "negative" ladders, respectively.

The pattern of kinetic angular momentum eigenvalues shown in Fig. 25 is different for noninteger α from that of conventional systems with true spherical symmetry. This is due to the fact that the commutation relations between operators of the kinetic angular momentum involve additional, flux-dependent terms when applied inside the magnetic string, as will be shown in Sec. II.E. In the region outside the magnetic string, the operators of the kinetic angular momentum are

$$\hat{\Lambda}_x = \hat{L}_x - \frac{\alpha \cos\theta \cos\varphi}{\sin\theta}, \quad (2.69a)$$

$$\hat{\Lambda}_y = \hat{L}_y - \frac{\alpha \cos\theta \sin\varphi}{\sin\theta}, \quad (2.69b)$$

$$\hat{\Lambda}_z = \hat{L}_z, \quad (2.69c)$$

where the operators of the canonical angular momentum are

$$\hat{L}_x = i \sin\varphi \frac{\partial}{\partial\theta} + \frac{i \cos\theta \cos\varphi}{\sin\theta} \frac{\partial}{\partial\varphi}, \quad (2.70a)$$

$$\hat{L}_y = -i \cos\varphi \frac{\partial}{\partial\theta} + \frac{i \cos\theta \sin\varphi}{\sin\theta} \frac{\partial}{\partial\varphi}, \quad (2.70b)$$

$$\hat{L}_z = -i \frac{\partial}{\partial\varphi}. \quad (2.70c)$$

Let us now determine the result of the operators $\hat{\Lambda}_+ = \hat{\Lambda}_x + i\hat{\Lambda}_y$ and $\hat{\Lambda}_- = \hat{\Lambda}_x - i\hat{\Lambda}_y$ on the eigenfunctions, Eq. (2.68). Kretzschmar (1965c) has shown that

$$\hat{\Lambda}_+ Y_{\lambda,m}^{(\alpha)}(\theta,\varphi) \sim (\lambda + \alpha - m)^{1/2} Y_{\lambda,m+1}^{(\alpha)}(\theta,\varphi), \quad m \neq [\alpha]. \quad (2.71)$$

This means that $\hat{\Lambda}_+$ acts as a raising operator, except at the upper ends of the vertical ladders with respect to m represented in Fig. 25. While $\hat{\Lambda}_+ Y_{\lambda^+, \lambda^+ + \alpha}^{(\alpha)}$ terminates the upper vertical ladder, it can be shown that the function $\hat{\Lambda}_+ Y_{\lambda^-, [\alpha]}$ is different from zero and has singularities at $\theta = 0$ and $\theta = \pi$, so that it cannot be a superposition of the eigenfunctions corresponding to the particular value of λ^- under consideration. As pointed out by Kretzschmar (1965c), the function $\hat{\Lambda}_+ Y_{\lambda^-, [\alpha]}^{(\alpha)}$ can, however, be expanded over a series of states involving all the values λ^+ of the complementary ladders. Analogously we have

$$\hat{\Lambda}_- Y_{\lambda,m}^{(\alpha)}(\theta,\varphi) \sim (\lambda - \alpha + m)^{1/2} Y_{\lambda,m-1}^{(\alpha)}(\theta,\varphi), \quad m \neq [\alpha] + 1, \quad (2.72)$$

which means that $\hat{\Lambda}_-$ acts as a lowering operator, except at the lower end of the vertical ladders for the canonical momentum m . While $\hat{\Lambda}_- Y_{\lambda^-, \alpha - \lambda^-} = 0$ terminates the lower vertical ladders, it can be shown that the function $\hat{\Lambda}_- Y_{\lambda^+, [\alpha] + 1}^{(\alpha)}$ is different from zero and has singularities at $\theta = 0$ and $\theta = \pi$, so that it is not a superposition of the eigenfunctions corresponding to the value of λ^+ under consideration. In fact, $\hat{\Lambda}_- Y_{\lambda^+, [\alpha] + 1}^{(\alpha)}$ is a superposition of

states involving all the values λ^- of the complementary ladders.

The Aharonov-Bohm effect of a magnetic string can be regarded as a consequence of quantization of the projection along the string of the canonical angular momentum in integer multiples of \hbar (Tassie and Peshkin, 1961; Kretzschmar, 1965a; Peshkin, 1981b). The vector potential of a magnetic string is singular on the string; consequently the space accessible to the particle is multiconnected, and the eventual use of multivalued functions cannot be excluded *a priori*. However, since an infinite magnetic string is the idealized limit of a physical distribution of magnetic moments, which preserves the single valuedness of the space, it still turns out that the wave functions must be single valued (Merzbacher, 1962). For example, an infinite magnetic string can be regarded as a string of finite length L_0 , in the limit when L_0 becomes very large. Assuming that the string of flux F is oriented along the z axis and has its middle point at the origin, the magnetic field in the region near the center of the string goes to zero as $1/L_0^2$, while the distribution of the return field extends up to distances of the order of $r \simeq L_0$ from the string, such that the total return flux $\int_0^\infty B_z(r,z)2\pi r dr = -F$ is equal in magnitude and opposite in sign to the flux inside the string. Let us assume that a cylindrical wave packet is approaching the magnetic string from the region of large r , so that the velocity field, Eq. (1.118), of this packet has in the asymptotic region $r \gg L_0$ a negative radial component of magnitude $\hbar k$ and a certain angular component $m_0 \hbar/r$, as shown in Fig. 26. As the cylindrical wave packet travels toward the string, each section of the packet will be acted on by a certain angular force due to the return magnetic field. The quasiclassical change in the kinetic angular momentum $\lambda(r,z)$ of a section of the cylindrical packet, situated at height z , due to the torque exerted by the return field is given by

$$\frac{d\lambda(r,z)}{dr} = \frac{q}{\hbar c} r B_z(r,z), \quad (2.73)$$

whence we obtain by integration

$$\lambda(r,z) - m_0 = \frac{q}{\hbar c} \int_r^\infty r B_z(r,z) dr. \quad (2.74)$$

Now the lines of the vector potential \mathbf{A}_{L_0} of the finite-length magnetic string are circles centered on the z axis, which are parallel to the x,y plane. Since at very large distances $r \gg L_0$ we have $A_{L_0,\theta} \sim 1/r^2$, we can express the vector potential with the aid of Stokes's theorem as

$$A_{L_0,\theta}(r,z) = -\frac{1}{r} \int_r^\infty B_z(r,z) r dr. \quad (2.75)$$

Then from Eqs. (2.74) and (2.75) it follows that

$$\lambda(r,z) + \frac{q}{\hbar c} r A_{L_0,\theta}(r,z) = m_0, \quad (2.76)$$

which means that the canonical angular momentum is a constant independent of the position r of the cylindrical packet, having the same value for any section z of the

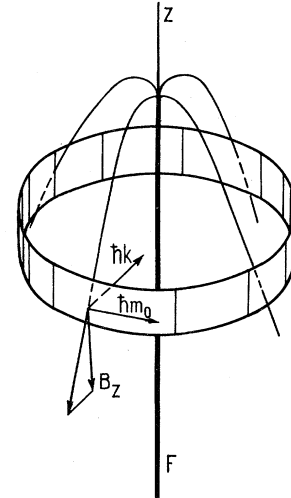


FIG. 26. Effect of the return magnetic field of a finite-length string on an incident cylindrical wave packet converging toward the string. The kinetic angular momentum m_0 of the section of the radial wave depends on the distance to the string and on the height of the section under consideration. However, the action of the return field is exactly compensated for by a corresponding variation of the vector potential of the string, a circumstance which renders the z component of the canonical angular momentum of the packet a constant of motion.

packet. Thus, while the kinetic angular momentum of a section of the radial packet depends on both the distance r to the magnetic string and the height z of the section under consideration, the action of the return field is exactly compensated by the corresponding variation of the vector potential, a circumstance which renders the canonical angular momentum, Eq. (2.76), a constant of motion. Since the state of the particle is not affected by the finite-length string at very large distances $r \gg L_0$, the canonical and kinetic angular momenta are identical in that region and assume values that are integer multiples of \hbar . However, the canonical angular momentum m being a constant, it follows that m is indeed an integer throughout the space.

From the quantization of the canonical angular momentum it follows that the eigenfunctions of a particle in the presence of the finite-length string are proportional to $\exp(im\theta)$, where m is an integer. Then in the adiabatic limit of large lengths L_0 , the eigenfunctions of a particle of kinetic energy $\hbar^2 k^2 / 2M$ are

$$\frac{1}{(2\pi)^{1/2}} J_{|s|}(kr) e^{im\theta - i\hbar k^2 t / 2M}, \quad m = 0, \pm 1, \dots, \quad (2.77)$$

where

$$s = m + \frac{q}{\hbar c} \int_r^\infty B_z(r,z) r dr. \quad (2.78)$$

When $L_0 \rightarrow \infty$ these eigenfunctions converge toward the eigenfunctions for the infinite magnetic string, Eq. (2.42).

D. Scattering of plane waves by closed magnetic strings

We have mentioned in the preceding section that the return field of a segment of magnetic string becomes vanishingly small as the length of the string becomes very large. However, it is not permissible to neglect the return magnetic field *a priori*, because although the magnitude of the field becomes very small for long strings, the spreading of the return field increases indefinitely. In order to show that the Aharonov-Bohm effect persists even if the return flux is taken into consideration, we shall analyze in this section scattering by a pair of infinite strings parallel to the *z* axis and carrying opposite fluxes, and, further, scattering by a circular magnetic string.

First let us consider a pair of parallel strings that intersect the plane *z*=0 at *x*=0, *y*=±*D*₀/2. We shall assume that in the absence of the magnetic strings the incident state is a wave packet of width *δ* and kinetic momentum *ħk* oriented in the *-x* direction, as shown in Fig. 27, the crest of the packet being situated at the time *t*=0 at *x*=*x*₀<0,

$$\Psi_{\delta}(x,y,t) = \frac{1}{\pi^{1/4}\delta^{1/2}} \frac{1}{(1+i\hbar t/M\delta^2)} \times \exp\left[-ikx - \frac{i\hbar k^2 t}{2M} - \frac{(x+\hbar kt/M-x_0)^2}{2\delta^2(1+i\hbar t/M\delta^2)}\right]. \tag{2.79}$$

In the presence of the magnetic strings the wave function in a certain plane *x*=*x*₀ situated behind the strings can be obtained from the unperturbed wave function Ψ_{δ} through multiplication by a phase factor which takes into account the magnetic fluxes enclosed in the two strings; the subsequent evolution of the state thus determined is that of a free wave packet. It can be shown that this ap-

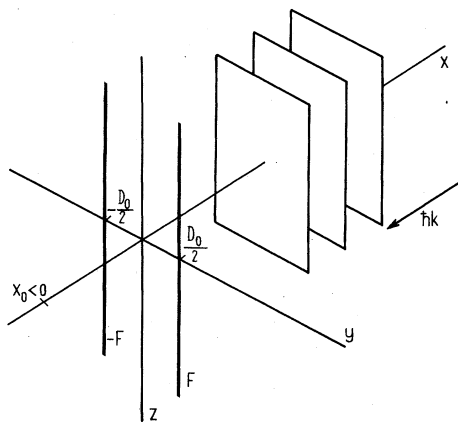


FIG. 27. Wave packet of width *δ* and kinetic momentum *ħk* oriented in the *-x* direction, incident on a pair of infinite strings parallel to the *z* axis and carrying opposite magnetic fluxes.

proach, which is similar to the techniques used in the computation of optical diffraction patterns, yields the correct wave function in the vicinity of the shadow of the two strings. As we have discussed in Sec. I.A, the quasi-classical flux-dependent shift of the phase of the wave function is equal to the path integral of the vector potential, $(q/\hbar c) \int \mathbf{A} \cdot d\mathbf{r}$, evaluated along the lines Γ of the probability current connecting the incidence region to the plane *x*=*x*₀. The vector potential of the two strings has the components

$$A_{D_0,x} = -\frac{F(y-D_0/2)}{2\pi[x^2+(y-D_0/2)^2]} + \frac{F(y+D_0/2)}{2\pi[x^2+(y+D_0/2)^2]}, \tag{2.80a}$$

$$A_{D_0,y} = \frac{Fx}{2\pi[x^2+(y-D_0/2)^2]} - \frac{Fx}{2\pi[x^2+(y+D_0/2)^2]}, \tag{2.80b}$$

the string at *y*=*D*₀/2 carrying the flux *F* and the string at *y*=-*D*₀/2 carrying the flux *-F*. It can be shown that the lines of the vector potential \mathbf{A}_{D_0} constitute the family of circles shown in Fig. 28, which are orthogonal to the circles of arbitrary radius passing through the points *x*=0, *y*=±*D*₀/2. Since the space is free of forces,

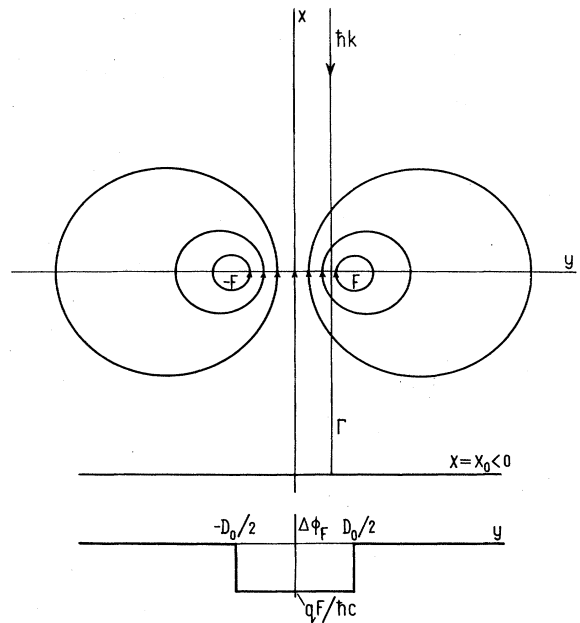


FIG. 28. Phase shift produced by a pair of parallel strings carrying opposite magnetic fluxes ±*F*. The phase shift is equal to the integral $(q/\hbar c) \int \mathbf{A} \cdot d\mathbf{r}$ evaluated along the lines of the probability current Γ connecting the incidence region to the plane *x*=*x*₀. The lines of the vector potential constitute a family of circles which are orthogonal to circles of arbitrary radius passing through the points *x*=0, *y*=±*D*₀/2.

the integration paths mentioned above are straight lines connecting the incidence region to the plane $x = x_0$. If the position of the plane $x = x_0$ is such that $-x_0 \gg D_0$, then the shift of the phase of the wave function, obtained by integration of the component $A_{D_0,x}$ with respect to x , Eq. (2.80), is equal to $-qF/\hbar c = -2\pi\alpha$ in the region $x = x_0$, $|y| < D_0/2$, and is zero in the complementary region $|y| > D_0/2$, as shown in the lower part of Fig. 28. Then in the presence of the two strings, the wave function in the plane $x = x_0$ has the form

$$\Psi_{D_0,\alpha}(x,y,0) = \frac{1}{\pi^{1/4}\delta^{1/2}} R_\alpha(y,0) \times \exp\left[-ikx - \frac{(x-x_0)^2}{2\delta^2}\right], \quad (2.81)$$

where

$$R_\alpha(y,0) = \begin{cases} e^{-2i\pi\alpha}, & |y| < D_0/2 \\ 1, & |y| > D_0/2. \end{cases} \quad (2.82a)$$

$$(2.82b)$$

The evolution of the state, Eqs. (2.81) and (2.82), in the region $x < x_0, t > 0$ is essentially that of a free wave packet. Since the free-particle propagator, Eq. (2.47), is the product of the propagators for the x and for the y directions, and since the state described by Eq. (2.81) is also a product of a function of x times the function $R_\alpha(y,0)$, the state at the time t can be obtained by considering separately the propagation in the x direction and the diffusion of R_α in the y direction. The component of the wave function at the time t is

$$R_\alpha(y,t) = \int G_0(y,t;y',0) R_\alpha(y',0) dy', \quad (2.83)$$

where

$$G_0 = \left[-\frac{iM}{2\pi\hbar t}\right]^{1/2} \exp\left[\frac{iM}{2\hbar t}(y-y')^2\right]. \quad (2.84)$$

It is convenient in the calculations to write $R_\alpha = 1 + T_\alpha$ so that the application of the Green's function to the constant term reproduces the unity constant, while the term T_α yields the scattering contribution. Thus the y component of the wave function in the vicinity of the negative part of the x axis is given by

$$R_\alpha(y,t) = 1 + \frac{2e^{-i\pi\alpha-3i\pi/4}}{\pi^{1/2}} \sin(\pi\alpha) \times \int_{(M/2\hbar t)^{1/2}(-D_0/2-y)}^{(M/2\hbar t)^{1/2}(D_0/2-y)} e^{i\xi^2} d\xi. \quad (2.85)$$

The motion of the particle in the x direction simply describes the propagation of the wave packet (in the $-x$ direction) whose crest at the time t is given by

$$x_c = x_0 - \frac{\hbar k}{M} t.$$

Since the process of diffusion in the y direction is in general slow compared to the propagation in the $-x$ direc-

tion, we can now neglect the constant x_0 in the above equation, so that the enclosed fluxes produce in the vicinity of each of the strings an Aharonov-Bohm effect independent of the presence of the other string,

$$R_\alpha = e^{-i\pi\alpha} \cos(\pi\alpha), \quad y = \pm D_0/2, \quad 0 < -x_c \ll kD_0^2. \quad (2.86)$$

However, as the wave packet is traveling along the $-x$ direction, the quantum diffusion along the y direction mixes contributions arising from the vicinity of both strings, and thus produces an interference pattern characterized by a surface spanning the strings and extending itself in the $-x$ direction up to distances of the order of kD_0^2 , as shown in Fig. 29.

After a long time t when $-x_c \gg kD_0^2$, the wave function, Eq. (2.84), has in the vicinity of the negative part of the x axis the asymptotic expression

$$R_\alpha(y,t) = 1 + \left[\frac{2}{\pi}\right]^{1/2} e^{-i\pi\alpha-3i\pi/4} \sin(\pi\alpha) \left[\frac{kD_0^2}{-x_c}\right]^{1/2}, \quad (2.87)$$

where $-x_c = \hbar kt/M$. We see from Eq. (2.87) that the effects of the pair of magnetic strings are still periodic with the amount of enclosed flux, but the scattering term has in this case the conventional form of a cylindrical outgoing wave in all asymptotic directions.

While the connection between the parallel strings carrying opposite fluxes is supposed to lie at infinity, a circular

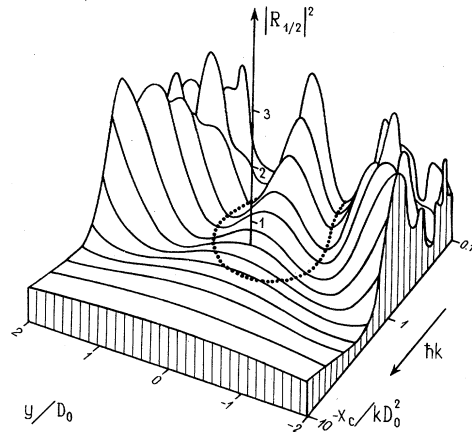
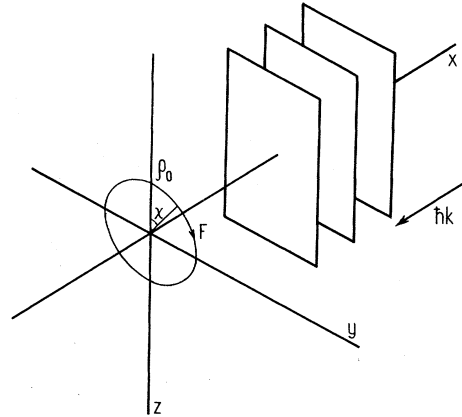


FIG. 29. Scattering of a particle of charge q and mass M by a pair of parallel strings carrying opposite fluxes of magnitude $F = \pi\hbar c/|q|$. The incident state was assumed to be a Gaussian wave packet propagating in the $-x$ direction and uniform along the y direction. The strings are parallel to the z axis and intersect the plane $z=0$ at $x = 0, y = \pm D_0/2$. The diagram represents the probability distribution $|R_{1/2}|^2$ on the crest $x_c = -\hbar kt/M$ of the packet, at successive positions. The flux enclosed by the magnetic strings affects the probability distribution mainly in the vicinity of a surface, shown in cross section by the dotted line, which spans the strings and extends in the $-x$ direction up to distances of the order of $-kD_0^2$.

magnetic string represents an example of an enclosed flux restricted to a finite region. Formulas describing the scattering of charged particles by a toroidal distribution of magnetic flux have been reported by Lyuboshits and Smorodinski (1978). We shall see that the effects of the enclosed flux are observable mainly in the vicinity of a rotation surface spanning the loop of flux, while the effects at large distances are attenuated by quantum diffusion. Let us assume that a circular magnetic string of radius ρ_0 and carrying the flux F is perpendicular to the direction of incidence of a wave packet of width δ along the x axis, and which is uniform in the y and z directions, as shown in Fig. 30. The incident wave packet is described by



$$\Psi_{\delta}(x,y,z,t) = \frac{1}{\pi^{1/4}\delta^{1/2}} \frac{1}{(1+i\hbar t/M\delta^2)^{1/2}} \times \exp \left[-ikx - \frac{i\hbar k^2 t}{2M} - \frac{(x-x_0+\hbar kt/M)^2}{2\delta^2(1+i\hbar t/M\delta^2)} \right], \quad (2.88)$$

FIG. 30. Scattering of a wave packet of kinetic momentum $\hbar k$, oriented in the $-x$ direction, by a circular magnetic string of radius ρ_0 lying in the y,z plane. The magnetic flux F enclosed by the circular string perturbs the probability distribution mainly in the vicinity of a rotation surface limited by the string and extending in the $-x$ direction up to distances of the order of $-k\rho_0^2$.

so that the crest of the wave packet is situated at the time $t=0$ in a certain plane $x=x_0 < 0$. As discussed previously, the quasiclassical flux-dependent phase shift of the wave function in the plane $x=x_0$ is equal to the path integral of the vector potential, $(q/\hbar c) \int \mathbf{A} \cdot d\mathbf{r}$, evaluated

on the straight lines connecting the incidence region with the plane $x=x_0$. The vector potential of the circular string can be determined by noting that the expression of the vector potential \mathbf{A} in terms of the magnetic field \mathbf{B} , together with the gauge relation $\text{div } \mathbf{A} = 0$,

$$\text{curl } \mathbf{A} = \mathbf{B}, \quad (2.89a)$$

$$\text{div } \mathbf{A} = 0, \quad (2.89b)$$

is analogous to the expression of the magnetic field \mathbf{B} in terms of the current distribution \mathbf{j} which generates the field, and the divergence relation $\text{div } \mathbf{B} = 0$,

$$\text{curl } \mathbf{B} = \frac{4\pi}{c} \mathbf{j}, \quad (2.90a)$$

$$\text{div } \mathbf{B} = 0. \quad (2.90b)$$

Then by analogy with Biot and Savart's law, the vector potential of a closed string Ω carrying the flux F is

$$\mathbf{A}(\mathbf{r}) = -\frac{F}{4\pi} \int_{\Omega} \frac{\mathbf{R} \times d\mathbf{s}}{R^3}, \quad (2.91)$$

where $d\mathbf{s}$ is a differential element on the loop Ω , and \mathbf{R} is the vector from $d\mathbf{s}$ to the point \mathbf{r} . Consequently, the distribution of vector potential of a circular magnetic string of radius ρ_0 is similar to the distribution of magnetic field of a current loop having the same radius. Then it can be shown that if $-x_0 \gg \rho_0$, the phase shift of the wave function is $-qF/\hbar c = -2\pi\alpha$ for those points in the $x=x_0$ plane whose distance ρ to the x axis is $\rho < \rho_0$, and is equal to zero for $\rho > \rho_0$. Thus in the presence of the circular magnetic string the wave function in the plane $x=x_0$ has the form

$$\Psi_{\rho_0,\alpha}(x,\rho,\chi,0) = \frac{1}{\pi^{1/4}\delta^{1/2}} [1 + W_{\alpha}(\rho,0)] \exp \left[-ikx - \frac{(x-x_0)^2}{2\delta^2} \right], \quad (2.92)$$

where

$$1 + W_\alpha(\rho, 0) = \begin{cases} e^{-2i\pi\alpha}, & \rho < \rho_0 \\ 1, & \rho > \rho_0. \end{cases} \tag{2.93a}$$

$$\tag{2.93b}$$

The variables ρ, χ appearing in Eq. (2.92) represent in this section the polar coordinates in the $x = x_0$ plane. As in the case of the pair of parallel strings, the total wave function at the time $t > 0$ in the observing region $x < x_0$ is the product of a one-dimensional wave function $\Psi_\delta(x, t)$, which describes propagation in the $-x$ direction, by a transverse wave function $\tilde{R}_\alpha(\rho, \chi, t)$ evolving from the initial state $1 + W_\alpha$,

$$\Psi_{\rho_0, \alpha}(x, \rho, \chi, t) = \Psi_\delta(x, t) \tilde{R}_\alpha(\rho, \chi, t). \tag{2.94}$$

The function $\Psi_\delta(x, t)$ is identical to that written in Eq. (2.88), while \tilde{R}_α is given by

$$\tilde{R}_\alpha(\rho, \chi, t) = -\frac{iM}{2\pi\hbar t} \int_0^\infty \rho' d\rho' \int_0^{2\pi} d\chi' [1 + W_\alpha(\rho', 0)] \exp\left[\frac{iM}{2\pi\hbar t} [\rho^2 + \rho'^2 - 2\rho\rho' \cos(\chi - \chi')]\right]. \tag{2.95}$$

Since the action of the free-particle Green's function on a constant term reproduces that term, the part of the integral corresponding to unity [appearing in the parenthesis on the right-hand side of Eq. (2.95)] is simply equal to 1. By substituting the expression of W_α , Eq. (2.93), and integrating with respect to χ' we obtain the wave function in the vicinity of the negative part of the x axis as

$$\Psi_{\rho_0, \alpha}(x, \rho, \chi, t) = \Psi_\delta(x, t) \left[1 - \frac{2M}{\hbar t} \sin(\pi\alpha) e^{-i\pi\alpha} \int_0^{\rho_0} e^{iM(\rho^2 + \rho'^2)/2\hbar t} J_0\left[\frac{M\rho\rho'}{\hbar t}\right] \rho' d\rho' \right]. \tag{2.96}$$

The integral in Eq. (2.96) describes the quantum diffusion of the probability from a cylinder of radius ρ_0 . If the center of the packet is in the vicinity of the magnetic loop, $-x_c \ll k\rho_0^2$, the integral can be evaluated with the aid of the formula (Abramowitz and Stegun, 1965, p. 486)

$$\int_0^\infty e^{ia^2\rho'^2} J_0(b\rho') \rho' d\rho' = \frac{i}{2a^2} e^{-ib^2/4a^2}. \tag{2.97}$$

Then the wave function on the surface of the cylinder $\rho = \rho_0$, bounded at $x = 0$ by the circular string, is given by

$$\Psi_{\rho_0, \alpha} = \Psi_\delta(x, t) e^{-i\pi\alpha} \cos(\pi\alpha), \quad \rho = \rho_0, \quad -k\rho_0^2 \ll x < 0. \tag{2.98}$$

The scattering term in Eq. (2.96) has a significant influence on the probability distribution up to distances of the order of $x_c \simeq -k\rho_0^2$, beyond which the quantum diffusion mixes contributions arising from various parts of the loop. Thus the circular magnetic string produces an Aharonov-Bohm effect in the vicinity of a rotation surface spanning the string, and extending itself in the negative x direction up to distances of the order of $-k\rho_0^2$. Beyond that region the wave function, Eq. (2.96), becomes

$$\Psi_{\rho_0, \alpha} = \Psi_\delta(x, t) \left[1 - \sin(\pi\alpha) e^{-i\pi\alpha} \frac{M\rho_0^2}{\hbar t} \right], \tag{2.99}$$

Since $-x_c = \hbar kt/M$, the scattering term in Eq. (2.99) represents the part of a spherical wave propagating in the vicinity of the $-x$ axis, with an amplitude proportional to the area of the loop; this amplitude depends periodically on the amount of enclosed magnetic flux.

E. Scattering of a plane wave by a tube of magnetic flux

We have seen in Sec. II.A that there is a certain exchange of kinetic momentum between an incident plane wave and a magnetic string. In order to understand the mechanism of this momentum transfer, we shall consider in this section the scattering of a plane wave by a magnetic flux F uniformly distributed inside a cylinder of radius r_0 , as shown in Fig. 31. We shall see that while at low intensities of the magnetic field $F/\pi r_0^2$ the action of the tube of flux on the incident particles is different from that of a magnetic string carrying the same flux, the scattering by the distributed flux approaches the scattering by a magnetic string when the radius r_0 becomes very small, $kr_0 \ll 1$.

Since an incident particle of momentum $\hbar k$ acquires a normal momentum component of the order of $4\hbar\alpha/r_0$ as it traverses the flux region, the angular deflection of the particle is of the order of $4\alpha/kr_0$. The dimensionless parameter α proportional to the flux, defined in Eq. (2.3), is not restricted in this section to the range $0 - \frac{1}{2}$, but may assume any value. If $\gamma_{r_0} = 4\alpha/kr_0 \ll 1$, we can obtain the wave function in the quasiclassical approximation,

$$\psi_{r_0, \alpha} = e^{(i/\hbar)S_\alpha}. \tag{2.100}$$

The reduced action S_α appearing in Eq. (2.100) is given by

$$S_\alpha = \int_\Gamma \left[M\mathbf{v} + \frac{q}{c} \mathbf{A} \right] ds, \tag{2.101}$$

where $M\mathbf{v}$ is the classical kinetic momentum on the stationary path Γ connecting the incidence region to the

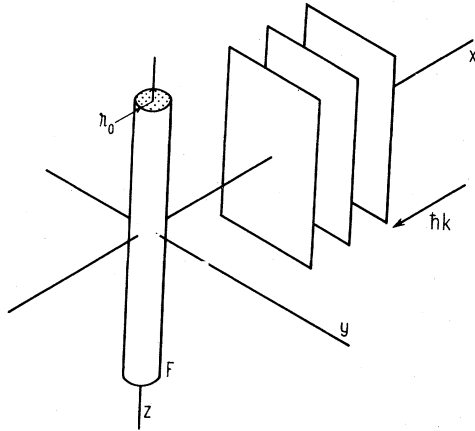


FIG. 31. Scattering by a magnetic flux F , uniformly distributed inside a cylinder of radius r_0 . While at low intensities of the magnetic field $F/\pi r_0^2$ the action of the tube of flux on the incident particles is different from that of a magnetic string carrying the same amount of flux, scattering by the distributed flux converges toward scattering by a magnetic string when the radius r_0 becomes very small, $kr_0 \ll 1$.

point where the wave function is to be determined. Since on the stationary path Γ we have $\mathbf{v}ds = v ds$, and moreover the magnitude of the classical velocity \mathbf{v} is conserved by the magnetic field, the contribution arising from the first term in the integral, Eq. (2.101), depends on the length of the path Γ . Now the lengths of the paths Γ and Γ_0 connecting a given point in the observing region to the points in the incidence region, in the presence and in the absence, respectively, of the magnetic flux, differ for small deflection angles $\gamma_{r_0} \ll 1$ by terms of the order of $\gamma_{r_0}^2$, so that as long as we are interested in first-order effects with respect to the magnetic flux we can perform the integration in Eq. (2.101) along the unperturbed path Γ_0 . This point, which was emphasized by Greenberger and Overhauser (1979), will be further discussed in Sec. III.G. Thus the wave function $\psi_{r_0,\alpha}$ has the form

$$\psi_{r_0,\alpha} = \psi_0 e^{i\Phi_\alpha}, \tag{2.102}$$

where $\psi_0 = \exp(-ikx)$ is the unperturbed incident wave, and

$$\Phi_\alpha = \frac{q}{\hbar c} \int_{\Gamma_0} \mathbf{A} ds. \tag{2.103}$$

The unperturbed path Γ_0 appearing in Eq. (2.103) is a straight line parallel to the x axis, as shown in Fig. 32. In order to determine Φ_α we note that in a gauge where the lines of the vector potential are circles around the center of the region of flux, the path Γ_0 connecting the point P in the incidence region to the point Q in the observing region can be completed without affecting the value of Φ_α by a line QO to the center O of the flux distribution, and further by a line OP' along the x axis, back to the incidence region. With these paths, the phase of the wave

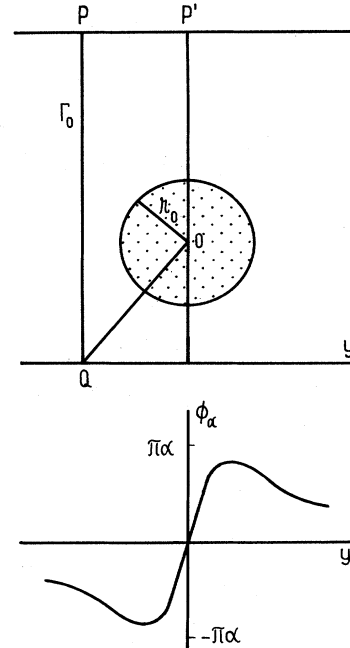


FIG. 32. Scattering by a magnetic flux $F = 2\pi\hbar c\alpha/q$, uniformly distributed inside a cylinder of radius r_0 , in the quasiclassical limit $4\alpha/kr_0 \ll 1$. The quasiclassical wave function is $\tilde{\psi}_{r_0,\alpha} = \exp(-ikx + i\Phi_\alpha)$, where the phase Φ_α is proportional to the amount of flux enclosed by the loop $PQOP'P$. If the line PQ does not intersect the region of flux, then $\Phi_\alpha = \alpha\theta$. On the other hand, if we displace the point Q from negative to positive values of the coordinates y in the observing plane, the phase varies continuously between $-\pi\alpha$ and $\pi\alpha$, having a zero on the half-plane $|\theta| = \pi$.

function at the point Q is proportional to the amount of magnetic flux enclosed by the path $PQOP'P$, and if the line PQ does not intersect the region of the flux, then

$$\Phi_\alpha = \alpha\theta, \quad -\pi < \theta < \pi. \tag{2.104}$$

The quasiclassical wave function representing the scattering by the tube of magnetic flux is thus

$$\psi_{r_0,\alpha} = e^{-ikx + i\alpha\theta}, \quad -\pi < \theta < \pi, \tag{2.105}$$

and except in the vicinity of the negative part of the x axis it approaches the wave function for the scattering by a string of flux, Eqs. (2.13) and (2.6). Now if we displace the point Q from a negative to a positive value of the coordinate y in the observing plane, the path PQ will intersect the region of magnetic flux beyond a certain position of Q , so that the phase Φ_α varies continuously between $-\pi\alpha$ and $\pi\alpha$, having a zero on the half-plane $|\theta| = \pi$, as shown in the lower part of Fig. 32. In order to appreciate the differences between scattering by a distribution of flux and scattering by a string of flux, let us consider the circulation of the kinematical field $M\mathbf{v}$ defined in Eq. (1.112). As discussed in Sec. II.A, the circulation of the $M\mathbf{v}$ around a magnetic string is a periodic

function of the amount of enclosed flux, given by $-2\pi\hbar$ multiplied by the difference between α and the nearest integer, the circulation being zero for half-integer values of α . This is due to the fact that, according to Eq. (2.6), the phase of the wave function representing scattering by a string is in general discontinuous at $|\theta| = \pi$ by an integer multiple of 2π , although the wave function itself is continuous. In the case of a tube of flux and in the weak-field limit $4\alpha/kr_0 \ll 1$, it is not only the wave function, but also the phase which varies continuously across the half-plane $|\theta| = \pi$, and therefore the corresponding circulation of $M\mathbf{v}$ is simply proportional to $-2\pi\hbar\alpha$. Thus in the weak-field limit the action of the distribution magnetic flux is different from that of a string carrying the same flux, the differences being, however, restricted mainly to the region near the negative part of the x axis.

If the radius of the tube of flux is so small that diffraction effects are dominant, then we must solve the corresponding Schrödinger equation. The vector potential of the cylindrical distribution of magnetic flux is given in polar coordinates r, θ in the plane $z=0$ by

$$A_r^{(r_0)} = 0, \tag{2.106a}$$

$$A_\theta^{(r_0)} = \begin{cases} \frac{Fr}{2\pi r_0^2}, & r < r_0 \\ \frac{F}{2\pi r}, & r > r_0 \end{cases} \tag{2.106b}$$

$$\tag{2.106c}$$

and the Schrödinger equation for a particle of incident energy $\hbar^2 k^2 / 2M$ is

$$\frac{\partial^2 \psi}{\partial r^2} + \frac{1}{r} \frac{\partial \psi}{\partial r} + \left[k^2 - \left[-i \frac{\partial}{\partial \theta} - \frac{q}{\hbar c} r A_\theta^{(r_0)} \right]^2 \right] \psi = 0. \tag{2.107}$$

$$A_m = - \frac{J_{|m-\alpha|}(kr_0) \chi_m^{(\alpha)'}(kr_0) - J'_{|m-\alpha|}(kr_0) \chi_m^{(\alpha)}(kr_0)}{H_{|m-\alpha|}^{(1)}(kr_0) \chi_m^{(\alpha)'}(kr_0) - H_{|m-\alpha|}^{(1)'}(kr_0) \chi_m^{(\alpha)}(kr_0)}, \tag{2.112a}$$

$$B_m = \frac{J_{|m-\alpha|}(kr_0) H_{|m-\alpha|}^{(1)'}(kr_0) - J'_{|m-\alpha|}(kr_0) H_{|m-\alpha|}^{(1)}(kr_0)}{\chi_m^{(\alpha)}(kr_0) H_{|m-\alpha|}^{(1)'}(kr_0) - \chi_m^{(\alpha)'}(kr_0) H_{|m-\alpha|}^{(1)}(kr_0)}, \tag{2.112b}$$

where the prime denotes the derivative. By comparing Eqs. (2.110) and (2.112) with the solution for scattering by a string of flux, Eqs. (2.4) and (2.5), we infer that the wave function for scattering by a tube of flux is

$$\psi_{r_0, \alpha} = \sum_{m=-\infty}^{\infty} e^{-i(\pi/2)|m-\alpha|} \psi_{r_0, m}^{(\alpha)}(r, \theta). \tag{2.113}$$

From Eqs. (2.110)–(2.112), the wave function $\psi_{r_0, \alpha}$ has the property that

$$\psi_{r_0, -\alpha}(r, \theta) = \psi_{r_0, \alpha}(r, -\theta), \tag{2.114}$$

and therefore we can restrict our analysis to positive values of α . Since

The eigenfunctions of Eq. (2.107) have the form

$$\psi_{r_0, m}^{(\alpha)}(r, \theta) = \chi_m^{(\alpha)}(r) e^{im\theta}, \quad m = 0, \pm 1, \dots, \tag{2.108}$$

where $\chi_m^{(\alpha)}$ is an eigenfunction of the equations

$$\frac{d^2 \chi_m^{(\alpha)}}{dr^2} + \frac{1}{r} \frac{d\chi_m^{(\alpha)}}{dr} + \left[k^2 - \left[\frac{m}{r} - \frac{\alpha r}{r_0^2} \right]^2 \right] \chi_m^{(\alpha)} = 0, \tag{2.109a}$$

$r < r_0,$

$$\frac{d^2 \chi_m^{(\alpha)}}{dr^2} + \frac{1}{r} \frac{d\chi_m^{(\alpha)}}{dr} + \left[k^2 - \frac{(m-\alpha)^2}{r^2} \right] \chi_m^{(\alpha)} = 0, \tag{2.109b}$$

$r > r_0.$

It can be shown by solving Eqs. (2.109) that the eigenfunctions $\psi_{r_0, m}^{(\alpha)}$ have the form

$$\psi_{r_0, m}^{(\alpha)} = \begin{cases} [J_{|m-\alpha|}(kr) + A_m H_{|m-\alpha|}^{(1)}(kr)] e^{im\theta}, & r > r_0 \\ B_m \chi_m^{(\alpha)}(kr) e^{im\theta}, & r < r_0 \end{cases} \tag{2.110a}$$

$$\tag{2.110b}$$

where

$$\chi_m^{(\alpha)}(kr) = (kr)^{|m|} e^{-ar^2/2r_0^2} \times \mathcal{F} \left[\frac{|m| + 1 - m}{2} - \frac{k^2 r_0^2}{4\alpha} \middle| |m| + 1 \right] \left[\frac{\alpha r^2}{r_0^2} \right]. \tag{2.111}$$

The function \mathcal{F} in Eq. (2.111) is the confluent hypergeometric function, as defined by Morse and Feshbach (1953). The coefficients A_m and B_m can be determined from the continuity conditions at $r=r_0$ of $\psi_{r_0, m}^{(\alpha)}$ and $\partial \psi_{r_0, m}^{(\alpha)} / \partial r$,

$$H_\nu^{(1)}(\xi) = \frac{i}{\sin(\pi\nu)} (e^{-i\pi\nu} J_\nu - J_{-\nu}), \tag{2.115}$$

while for $|z| \ll 1$

$$J_\nu(\xi) \simeq \frac{z^\nu}{2^\nu \Gamma(\nu+1)}, \tag{2.116}$$

Eqs. (2.112) imply that for $kr_0 \ll 1$ the coefficients A_m and B_m are of the order of

$$A_m = O((kr_0)^{2|m-\alpha|}), \tag{2.117a}$$

$$B_m = O((kr_0) e^{|m-\alpha| - |m|}). \tag{2.117b}$$

Now if the radius of the tube is diminished, $kr_0 \rightarrow 0$, while the amount of flux is kept constant, the coefficients

A_m become, according to Eq. (2.116a), vanishingly small, so that the wave function Eq. (2.113) converges in the field-free region toward the wave function Eq. (2.5) for scattering by a string carrying the same flux (Kretzschmar, 1965b). In particular, for sufficiently small values of kr_0 , the patterns of the probability current in the field-free region have bifurcation points for values of α that are not half-integers. For half-integer values of α , the current patterns are symmetric with respect to the incidence direction. Moreover, the circulation of the velocity field, Eq. (2.118), is equal to $-2\pi\hbar$ multiplied by the difference between α and the nearest integer. Thus, unlike the nonperiodic, weak-field solution of Eqs. (2.102) and (2.103), the wave function $\psi_{r_0,\alpha}$, Eq. (2.113), is periodic with respect to α in the field-free region, owing to the fact that a number of magnetic flux quanta, or fluxoids, equal to the nearest integer to α are trapped within the region of magnetic field. In general, one fluxoid is trapped when the circulation integral $\oint (M\mathbf{v} + q\mathbf{A}/c)ds$ is equal to $2\pi\hbar$ (London, 1961). The periodicity of $\psi_{r_0,\alpha}$ in the field-free region is due to the fact that, while at extremely small values of r , $r \ll kr_0^2$, the wave function Eq. (2.113) is dominated by the term $m=0$, the dominant term of $\psi_{r_0,\alpha}$ on the boundary $r=r_0$ of the flux region arises according to Eqs. (2.110b), (2.111), and (2.117b) from that value of m which coincides with the nearest integer to α , designated by N_α . It can be shown by applying an integral criterion (Whittaker and Watson, 1958) that the number of roots of the equation $\psi_{r_0,\alpha}=0$, contained within the contour $r=r_0$, is equal to N_α , each root accounting for one fluxoid. If the difference between α and its integer part $[\alpha]$ is less than $\frac{1}{2}$, there are $[\alpha]$ roots situated at a distance of the order of $r \sim kr_0^2$ from the center. If $\alpha - [\alpha] > \frac{1}{2}$, there are $[\alpha]$ roots at a distance of the order of $r \sim kr_0^2$, and one more root at $kr \sim (kr_0)^{2(\alpha - [\alpha])}$, $\theta = -\pi/2 - \pi(\alpha - [\alpha])$.

A persistent problem associated with the quantum effects of the fluxes was the origin of the kinetic momentum transported by the radial wave during scattering by a magnetic string. Peshkin, Talmi, and Tassie (1961), and subsequently Aharonov and Bohm (1961), pointed out that the conservation of kinetic momentum requires that the exchange of momentum occur in the region of the

magnetic string. The question of why the incident beam spreads, when the force is zero almost everywhere in the space, was more recently raised by Henneberger (1980,1981) and by Henneberger and Huguenin (1981), without, however, offering a satisfactory explanation. Since in the case of a string the exchange of kinetic momentum is the result of a divergent force acting over a vanishingly small area, analysis of the scattering by a string of flux does not provide an appropriate frame for answering the question. We shall consider further the problem of conservation of kinetic momentum during scattering by a magnetic flux uniformly distributed within a cylinder of radius r_0 . As discussed above, the scattering in the field-free region in the limit $kr_0 \rightarrow 0$ approaches the scattering by a string carrying the same amount of flux. We shall show that the momentum in the scattering wave is due to the magnetic force acting in the region of the flux.

The operator of the magnetic force has the components

$$\hat{F}_x = \frac{2\hbar^2\alpha}{Mr_0^2} \left[-i \frac{\partial}{\partial y} - \frac{\alpha x}{r_0^2} \right], \tag{2.118a}$$

$$\hat{F}_y = \frac{2\hbar^2\alpha}{Mr_0^2} \left[i \frac{\partial}{\partial x} - \frac{\alpha y}{r_0^2} \right], \tag{2.118b}$$

for $r < r_0$, and is equal to zero in the region $r > r_0$. For the present purpose the wave function, Eq. (2.113), can be approximated by retaining only the terms $m = [\alpha]$ and $m = [\alpha] + 1$,

$$\begin{aligned} \psi_{r_0,\alpha} \simeq & e^{-(i\pi/2)(\alpha - [\alpha])} B_{[\alpha]} \chi_{[\alpha]}^{(\alpha)}(kr) e^{i[\alpha]\theta} \\ & + e^{-(i\pi/2)(1 + [\alpha] - \alpha)} B_{[\alpha] + 1} \chi_{[\alpha] + 1}^{(\alpha)}(kr) \\ & \times e^{i([\alpha] + 1)\theta}, \end{aligned} \tag{2.119}$$

the influence of the other terms being noticeable only over an area of the order of $k^2 r_0^4$. The rate of transfer of kinetic momentum to the charged particle is, according to Eq. (1.89),

$$\text{Re} \int_0^{r_0} r dr \int_{-\pi}^{\pi} d\theta \psi_{r_0,\alpha}^* \hat{F}_x \psi_{r_0,\alpha}. \tag{2.120}$$

We first perform the integration over the angle θ , with the result

$$\begin{aligned} \text{Re} \int_{-\pi}^{\pi} \psi_{r_0,\alpha}^* \hat{F}_x \psi_{r_0,\alpha} d\theta = & \frac{2\pi\hbar^2 k\alpha}{Mr_0^2} B_{[\alpha]} B_{[\alpha] + 1} \sin\pi(\alpha - [\alpha]) \\ & \times \left[\chi_{[\alpha]}^{(\alpha)} \frac{d\chi_{[\alpha] + 1}^{(\alpha)}}{d(kr)} - \chi_{[\alpha] + 1}^{(\alpha)} \frac{d\chi_{[\alpha]}^{(\alpha)}}{d(kr)} + \left[\frac{2[\alpha] + 1}{kr} - \frac{2\alpha kr}{(kr_0)^2} \right] \chi_{[\alpha]}^{(\alpha)} \chi_{[\alpha] + 1}^{(\alpha)} \right], \end{aligned} \tag{2.121a}$$

$$\begin{aligned} \text{Re} \int_{-\pi}^{\pi} \psi_{r_0,\alpha}^* \hat{F}_y \psi_{r_0,\alpha} d\theta = & \frac{2\pi\hbar^2 k\alpha}{Mr_0^2} B_{[\alpha]} B_{[\alpha] + 1} \cos\pi(\alpha - [\alpha]) \\ & \times \left[\chi_{[\alpha]}^{(\alpha)} \frac{d\chi_{[\alpha] + 1}^{(\alpha)}}{d(kr)} - \chi_{[\alpha] + 1}^{(\alpha)} \frac{d\chi_{[\alpha]}^{(\alpha)}}{d(kr)} + \left[\frac{2[\alpha] + 1}{kr} - \frac{2\alpha kr}{(kr_0)^2} \right] \chi_{[\alpha]}^{(\alpha)} \chi_{[\alpha] + 1}^{(\alpha)} \right]. \end{aligned} \tag{2.121b}$$

The integration over r of the expression in Eqs. (2.121) can be performed with the aid of the transformation

$$\begin{aligned}
 &kr \left[\chi_{[\alpha]}^{(\alpha)} \frac{d\chi_{[\alpha]+1}^{(\alpha)}}{dkr} - \chi_{[\alpha]+1}^{(\alpha)} \frac{d\chi_{[\alpha]}^{(\alpha)}}{d(kr)} + \left[\frac{2[\alpha]+1}{kr} - \frac{2\alpha kr}{(kr_0)^2} \right] \chi_{[\alpha]}^{(\alpha)} \chi_{[\alpha]+1}^{(\alpha)} \right] \\
 &= \frac{(kr_0)^2}{2\alpha} \frac{\partial}{\partial(kr)} \left[kr \left[\frac{d\chi_{[\alpha]}^{(\alpha)}}{d(kr)} + \frac{\alpha kr}{(kr_0)^2} \chi_{[\alpha]}^{(\alpha)} - \frac{[\alpha]}{kr} \chi_{[\alpha]}^{(\alpha)} \right] \right. \\
 &\quad \left. \times \left[\frac{d\chi_{[\alpha]+1}^{(\alpha)}}{d(kr)} + \frac{[\alpha]+1}{kr} \chi_{[\alpha]+1}^{(\alpha)} - \frac{\alpha kr}{(kr_0)^2} \chi_{[\alpha]+1}^{(\alpha)} \right] + kr \chi_{[\alpha]}^{(\alpha)} \chi_{[\alpha]+1}^{(\alpha)} \right], \tag{2.122}
 \end{aligned}$$

valid for $r < r_0$. Equation (2.122) can be obtained by integrating Eq. (1.89) over θ , for a fixed kr . Then from Eqs. (2.111) and (2.112) in the limit $kr_0 \rightarrow 0$ we have

$$\begin{aligned}
 B_{[\alpha]} \left[\frac{d\chi_{[\alpha]}^{(\alpha)}}{d(kr)} + \frac{\alpha - [\alpha]}{kr_0} \chi_{[\alpha]}^{(\alpha)} \right] \Big|_{r=r_0} &= \frac{(kr_0)^{\alpha - [\alpha] - 1}}{2^{\alpha - [\alpha] - 1} \Gamma(\alpha - [\alpha])}, \tag{2.123a} \\
 B_{[\alpha]+1} \left[\frac{d\chi_{[\alpha]+1}^{(\alpha)}}{d(kr)} + \frac{1 + [\alpha] - \alpha}{kr_0} \chi_{[\alpha]+1}^{(\alpha)} \right] \Big|_{r=r_0} &= \frac{(kr_0)^{[\alpha] - \alpha}}{2^{[\alpha] - \alpha} \Gamma([\alpha] + 1 - \alpha)}. \tag{2.123b}
 \end{aligned}$$

Finally we obtain in the limit $kr_0 \rightarrow 0$ the expressions

$$\text{Re} \int_0^{r_0} r dr \int_{-\pi}^{\pi} d\theta \psi_{r_0, \alpha}^* \hat{F}_x \psi_{r_0, \alpha} = \frac{2\hbar^2 k}{M} \sin^2 \pi(\alpha - [\alpha]), \tag{2.124a}$$

$$\begin{aligned}
 \text{Re} \int_0^{r_0} r dr \int_{-\pi}^{\pi} d\theta \psi_{r_0, \alpha}^* \hat{F}_y \psi_{r_0, \alpha} &= \frac{2\hbar^2 k}{M} \sin \pi(\alpha - [\alpha]) \cos \pi(\alpha - [\alpha]), \tag{2.124b} \\
 &= \frac{2\hbar^2 k}{M} \sin \pi(\alpha - [\alpha]) \cos \pi(\alpha - [\alpha]),
 \end{aligned}$$

which coincide with Eqs. (2.34) if we take into account the fact that in those equations α was assumed to belong to the interval $0 - \frac{1}{2}$. Thus in complete analogy with classical mechanics, momentum scattering by a thin line of flux is due to the magnetic force acting on the incident particle. As will be discussed in the next section, the transfer of kinetic momentum to the charged particles is, however, a circumstantial property of the quantum effects of the fluxes.

Let us now consider briefly the commutation relations among components of the kinetic angular momentum operator,

$$\hat{\mathbf{L}} = \mathbf{r} \times \left[-i\hbar \nabla - \frac{q}{c} \mathbf{A} \right],$$

in the case of a cylindrical distribution of magnetic flux. It can be shown by direct calculation that the components of $\hat{\mathbf{L}}$ satisfy the relations

$$\begin{aligned}
 \hat{\Lambda}_y \hat{\Lambda}_z - \hat{\Lambda}_z \hat{\Lambda}_y &= i\hbar \hat{\Lambda}_x + \frac{iq\hbar}{c} x(xB_x + yB_y + zB_z), \\
 &\tag{2.125a}
 \end{aligned}$$

$$\begin{aligned}
 \hat{\Lambda}_z \hat{\Lambda}_x - \hat{\Lambda}_x \hat{\Lambda}_z &= i\hbar \hat{\Lambda}_y + \frac{iq\hbar}{c} y(xB_x + yB_y + zB_z), \\
 &\tag{2.125b}
 \end{aligned}$$

$$\begin{aligned}
 \hat{\Lambda}_x \hat{\Lambda}_y - \hat{\Lambda}_y \hat{\Lambda}_x &= i\hbar \hat{\Lambda}_z + \frac{iq\hbar}{c} z(xB_x + yB_y + zB_z), \\
 &\tag{2.125c}
 \end{aligned}$$

where $\mathbf{B} = \nabla \times \mathbf{A}$. We see that, in the field-free region, the relations between various components of the kinetic angular momentum are identical to the relations between components of the canonical momentum $\hat{\mathbf{L}} = \mathbf{r} \times (-i\hbar \nabla)$, while in the region of flux additional terms appear; these terms account for the fact that the spectra of $\hat{\Lambda}^2$ and $\hat{\Lambda}_z$ are different from the spectra of $\hat{\mathbf{L}}^2$ and \hat{L}_z .

F. Shielding effects

In order to appreciate the implications of the quantum effects of the fluxes, let us assume that the distribution of electromagnetic flux is shielded by reflecting barriers, which prevent the incident charged particles from interacting directly with the field strengths. We shall consider in this section an infinite magnetic string, surrounded by a perfectly reflecting cylinder of radius \tilde{R}_0 , having the axis coincident with the string, and shall see that for vanishing \tilde{R}_0 the scattering by this structure converges to the scattering by the bare string, discussed in Sec. II.A. The significance of this result is that the phase shift by $\alpha\theta$ in the asymptotic wave function, Eq. (2.13), is not the result of a direct action of the field strengths on the incident particles. Now in the case of scattering by a magnetic string surrounded by a perfectly reflecting cylinder, the space accessible to the incident particles is formally multiconnected, so that the eventual use of multivalued wave functions cannot be excluded *a priori*. In order to settle this question, we shall analyze the scattering by a tube of magnetic flux surrounded by a finite-height potential barrier, a situation free of ambiguities, and shall see that the idealized case is indeed obtained as the limit when the length of the potential barrier becomes very large.

The wave function for the scattering of a plane wave by an infinite magnetic string surrounded by a perfectly reflecting cylinder, as shown in Fig. 33, can be obtained by adding to the series in Eq. (2.5) suitable terms proportional to Hankel functions (Morse and Feshbach, 1953, p. 1376),

$$\psi_{\tilde{R}_0, \alpha}(r, \theta) = \sum_{m=-\infty}^{\infty} e^{-i(\pi/2)|m-\alpha|} \left[J_{|m-\alpha|}(kr) - \frac{J_{|m-\alpha|}(k\tilde{R}_0)}{H_{|m-\alpha|}^{(1)}(k\tilde{R}_0)} H_{|m-\alpha|}^{(1)}(kr) \right] e^{im\theta}, \quad r > \tilde{R}_0 \quad (2.126)$$

where the coefficients multiplying the Hankel functions have been chosen such that $\psi_{\tilde{R}_0, \alpha}(\tilde{R}_0, \theta) = 0$. Let us assume first that the radius of the cylinder is very small, $k\tilde{R}_0 \ll 1$. Since for $k\tilde{R}_0 \ll 1$ we have

$$\frac{J_{|m-\alpha|}(k\tilde{R}_0)}{H_{|m-\alpha|}^{(1)}(k\tilde{R}_0)} \simeq \frac{i\pi}{\Gamma(|m-\alpha|)\Gamma(|m-\alpha|+1)} \times \left[\frac{k\tilde{R}_0}{2} \right]^{2|m-\alpha|}, \quad (2.127)$$

while $J_{|m-\alpha|}(kr)$ and $H_{|m-\alpha|}^{(1)}(kr)$ are of the same order of magnitude in the asymptotic region $kr \gg 1$, the contribution to the total wave function of the wave scattered at the wall of the shielding cylinder becomes vanishingly small as the radius \tilde{R}_0 goes to zero. Thus the wave function $\psi_{\tilde{R}_0, \alpha}$ converges in this case with the wave function ψ_α , Eq. (2.5), representing scattering by a bare string (Aharonov *et al.*, 1984a). Since the shielded magnetic string is inaccessible to the incident particles, we conclude that the existence of quantum effects of the fluxes is independent of a direct action of the field strengths on the charged particles. In order to find out the effect of the shielding in the vicinity of the string, where $kr \ll 1$, we note that the ratio of the terms in the large parentheses appearing in Eq. (2.126) is given by

$$\frac{J_{|m-\alpha|}(k\tilde{R}_0)/H_{|m-\alpha|}^{(1)}(k\tilde{R}_0)}{J_{|m-\alpha|}(kr)/H_{|m-\alpha|}^{(1)}(kr)} \simeq \left[\frac{\tilde{R}_0}{r} \right]^{2|m-\alpha|}, \quad (2.128)$$

so that for fixed r and $\tilde{R}_0 \rightarrow 0$ the contribution of the shielding cylinder to the scattered wave can be neglected in this case, too. The convergence to zero of the ratio in Eq. (2.128) is not, however, uniform with respect to α . Thus, when an infinite magnetic string is shielded by barriers of very small transverse dimensions, the effects attributable to the shielding are negligible, except in cases when the amount of enclosed flux is close to an integer multiple of $2\pi\hbar c/q$. In these cases the shielding perturbs the probability distribution up to distances of the order of one wavelength from the magnetic string.

As can be seen from Eq. (2.13), the magnetic string shifts the phase of an incident plane wave by an amount proportional to the enclosed magnetic flux, and gives rise to a scattered wave whose amplitude is a periodic function of the flux. We have remarked in the preceding section that the change in kinetic momentum of the incident particles is not an effect specific to the enclosed fluxes; rather it follows the quantum diffraction of the phase-shifted components of the incident wave. If the radius \tilde{R}_0 of the shielding cylinder is large, $k\tilde{R}_0 \gg 1$, the diffraction effects are not dominant, as they were in the case of scattering by the bare string, and we therefore expect that in a first approximation the wave function $\psi_{\tilde{R}_0, \alpha}$ should be obtained from the flux-free wave function $\psi_{\tilde{R}_0, 0}$ through multiplication by the phase factor $\exp(i\alpha\theta)$. In order to show this, we shall use the asymptotic expressions of the functions J_ν and $H_\nu^{(1)} = J_\nu + iY_\nu$. When $\nu < k\tilde{R}_0$ is large and positive and $0 < \arccos(\nu/k\tilde{R}_0) < \pi/2$,

$$J_\nu(k\tilde{R}_0) \simeq \left[\frac{2}{\pi} \right]^{1/2} \frac{1}{(k^2\tilde{R}_0^2 - \nu^2)^{1/4}} \times \cos \left[(k^2\tilde{R}_0^2 - \nu^2)^{1/2} - \nu \arccos \frac{\nu}{k\tilde{R}_0} - \frac{\pi}{4} \right], \quad (2.129a)$$

$$Y_\nu(k\tilde{R}_0) \simeq \left[\frac{2}{\pi} \right]^{1/2} \frac{1}{(k^2\tilde{R}_0^2 - \nu^2)^{1/4}} \times \sin \left[(k^2\tilde{R}_0^2 - \nu^2)^{1/2} - \nu \arccos \frac{\nu}{k\tilde{R}_0} - \frac{\pi}{4} \right], \quad (2.129b)$$

and when $\nu > k\tilde{R}_0$ is large,

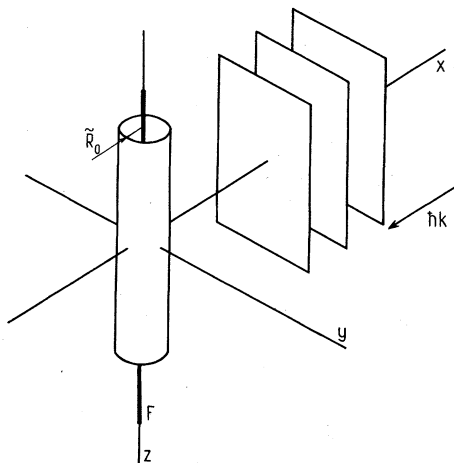


FIG. 33. Scattering of a plane wave by an infinite magnetic string, shielded by a reflecting cylinder of radius \tilde{R}_0 . For thin cylinders $k\tilde{R}_0 \ll 1$, scattering by the shielded string converges with scattering by the bare string. For large $k\tilde{R}_0$ the effect of the enclosed flux is mainly to shift by $qF\theta/\hbar c$ the phase of the wave function representing scattering by the shielding cylinder in the absence of flux.

$$J_\nu(k\tilde{R}_0) \simeq \frac{\exp\left\{(\nu^2 - k^2\tilde{R}_0^2)^{1/2} - \nu \ln \left[\frac{\nu}{k\tilde{R}_0} + \left(\frac{\nu^2}{k^2\tilde{R}_0^2} - 1 \right)^{1/2} \right] \right\}}{(2\pi)^{1/2}(\nu^2 - k^2\tilde{R}_0^2)^{1/4}}, \tag{2.130a}$$

$$Y_\nu(k\tilde{R}_0) \simeq - \left[\frac{2}{\pi} \right]^{1/2} \frac{\exp\left\{ \nu \ln \left[\frac{\nu}{k\tilde{R}_0} + \left(\frac{\nu^2}{k^2\tilde{R}_0^2} - 1 \right)^{1/2} \right] - (\nu^2 - k^2\tilde{R}_0^2)^{1/2} \right\}}{(\nu^2 - k^2\tilde{R}_0^2)^{1/4}} \tag{2.130b}$$

(Abramowitz and Stegun, 1965, pp. 365–366). With these functions we can approximate the ratio $J_\nu(k\tilde{R}_0)/H_\nu^{(1)}(k\tilde{R}_0)$ appearing in Eq. (2.126) as

$$\frac{J_\nu(k\tilde{R}_0)}{H_\nu^{(1)}(k\tilde{R}_0)} \simeq \begin{cases} \frac{1}{2} \left\{ 1 + \exp \left[-2i \left[(k^2\tilde{R}_0^2 - \nu^2)^{1/2} - \nu \arccos \frac{\nu}{k\tilde{R}_0} - \frac{\pi}{4} \right] \right] \right\}, & \nu < k\tilde{R}_0 \\ 0, & \nu > k\tilde{R}_0. \end{cases} \tag{2.131a}$$

$$\tag{2.131b}$$

Moreover, if we assume that $r \gg \tilde{R}_0$, then we can replace the Hankel function $H_{|m-\alpha|}^{(1)}(kr)$ by its asymptotic form for large arguments, Eq. (2.11). Then it can be shown that the principal contribution to the scattering wave arises from the exponential part of the coefficients in Eqs. (2.131) and is equal to

$$T_{\tilde{R}_0, \alpha} = - \frac{e^{ikr + i\pi/4}}{(2\pi kr)^{1/2}} \sum_{m \simeq -k\tilde{R}_0}^{k\tilde{R}_0} e^{i\Phi_m^{(\alpha)}}, \tag{2.132}$$

where the phase $\Phi_m^{(\alpha)}$ is given by

$$\Phi_m^{(\alpha)} = -\pi |m - \alpha| - 2[k^2\tilde{R}_0^2 - (m - \alpha)^2]^{1/2} + 2|m - \alpha| \arccos \frac{|m - \alpha|}{k\tilde{R}_0} + m\theta. \tag{2.133}$$

The sum $\sum \exp(i\Phi_m^{(\alpha)})$ can be evaluated in the limit $k\tilde{R}_0 \gg 1$ with the aid of the Poisson sum formula, Eqs. (1.71) and (1.72), by considering the Fourier transform of the general term of the series,

$$F_{\tilde{R}_0}(\xi) = \exp[i\alpha(\theta - \xi)] \int_{-\infty}^{\infty} d\nu \exp \left[-i\pi |\nu| - 2i(k^2\tilde{R}_0^2 - \nu^2)^{1/2} + 2i|\nu| \arccos \frac{|\nu|}{k\tilde{R}_0} + i\nu(\theta - \xi) \right], \tag{2.134}$$

where ξ is an integer multiple of 2π . The principal contribution to the integral, Eq. (2.134), arises from the region in ν space where the phase is stationary. It can be shown that such stationary points of the phase exist only for the value $\xi = 0$, when they are situated at $\nu_0 = k\tilde{R}_0 \sin(\theta/2)$. In the vicinity of this point the integrand in Eq. (2.134) is approximately equal to

$$-2k\tilde{R}_0 \cos(\theta/2) - \frac{1}{k\tilde{R}_0 \cos(\theta/2)} (\nu - \nu_0)^2.$$

After integrating Eq. (2.134) and using Eq. (1.72), we obtain for the scattered wave, Eq. (2.132),

$$T_{\tilde{R}_0, \alpha} = \left[\frac{k\tilde{R}_0}{2} \cos(\theta/2) \right]^{1/2} \frac{1}{(kr)^{1/2}} \times \exp[ikr - 2ik\tilde{R}_0 \cos(\theta/2) + i\alpha\theta - i\pi/4]. \tag{2.135}$$

Now as discussed in Sec. II.A, for $kr \gg 1$ we have

$$\sum_{m=-\infty}^{\infty} e^{-(i\pi/2)|m-\alpha|} J_{|m-\alpha|}(kr) e^{im\theta} \simeq e^{-ikr \cos\theta + i\alpha\theta}$$

so that wave function, Eq. (2.126), becomes for $kr > k\tilde{R}_0 \gg 1$

$$\psi_{\tilde{R}_0, \alpha} \simeq e^{i\alpha\theta} \psi_{\tilde{R}_0, 0} \tag{2.136}$$

where

$$\psi_{\tilde{R}_0, 0} = e^{-ikr \cos\theta} + \left[\frac{k\tilde{R}_0}{2} \cos(\theta/2) \right]^{1/2} \frac{1}{(kr)^{1/2}} \times \exp[ikr - 2ik\tilde{R}_0 \cos(\theta/2) - i\pi/4]. \tag{2.137}$$

The wave function $\psi_{\tilde{R}_0, 0}$ represents the scattering by a cylinder of radius \tilde{R}_0 in the absence of magnetic flux, and the scattered wave corresponds to classical elastic reflections of the particle from each portion of the half-

cylinder exposed to the incident wave (Morse and Feshbach, 1953, p. 1381). Neglected in Eqs. (2.136) and (2.137) are all the diffraction terms, whose amplitude is small when compared with $(k\tilde{R}_0)^{1/2}$. Thus in the quasi-classical approximation the magnetic flux enclosed within a cylinder of radius \tilde{R}_0 shifts the phase of the flux-free wave function, while leaving the distribution of kinetic momentum essentially unchanged.

A similar approach can be used to determine the wave function in the vicinity of the reflecting cylinder. For $k(r - \tilde{R}_0) \ll 1$ the expression of $\psi_{\tilde{R}_0, \alpha}$, Eq. (2.126), can be approximated by

$$\psi_{\tilde{R}_0, \alpha}(r, \theta) \simeq -\frac{2i(r - \tilde{R}_0)}{\pi\tilde{R}_0} \sum_{m=-\infty}^{\infty} \frac{1}{H_{|m-\alpha|}^{(1)}(k\tilde{R}_0)} \times e^{im\theta - (i\pi/2)|m-\alpha|}, \tag{2.138}$$

where we have used the fact that the Wronskian of the independent solutions J_ν and $H_\nu^{(1)}$ is

$$J_\nu(z)H_\nu^{(1)'}(z) - J_\nu'(z)H_\nu^{(1)}(z) = \frac{2i}{\pi z}. \tag{2.139}$$

Then substituting in Eq. (2.138) the asymptotic form of the Hankel function

$$\frac{1}{H_\nu^{(1)}(k\tilde{R}_0)} \simeq \begin{cases} \left[\frac{\pi}{2}\right]^{1/2} (k^2\tilde{R}_0^2 - \nu^2)^{1/4} \exp\left[-i(k^2\tilde{R}_0^2 - \nu^2)^{1/2} + i\nu \arccos \frac{\nu}{k\tilde{R}_0} + i\pi/4\right], & 0 < \nu < k\tilde{R}_0 \\ 0, & \nu > k\tilde{R}_0 \end{cases} \tag{2.140a}$$

$$\tag{2.140b}$$

where $0 < \arccos(\nu/k\tilde{R}_0) < \pi/2$, we obtain the wave function $\psi_{\tilde{R}_0, \alpha}$,

$$\psi_{\tilde{R}_0, \alpha} \simeq \left[\frac{2}{\pi}\right]^{1/2} \frac{r - \tilde{R}_0}{\tilde{R}_0} \sum_{m=-k\tilde{R}_0}^{k\tilde{R}_0} [k^2\tilde{R}_0^2 - (m - \alpha)^2]^{1/4} e^{i\Theta_m^{(\alpha)}}, \tag{2.141}$$

where the phase $\Theta_m^{(\alpha)}$ is given by

$$\Theta_m^{(\alpha)} = -[k^2\tilde{R}_0^2 - (m - \alpha)^2]^{1/2} + i|m - \alpha| \arccos \frac{|m - \alpha|}{k\tilde{R}_0} - \frac{\pi}{2}|m - \alpha| + m\theta. \tag{2.142}$$

As previously, the sum in Eq. (2.141) can be evaluated in the limit $k\tilde{R}_0 \gg 1$ with the aid of the Poisson formula, by considering the Fourier transform of the general term of the series,

$$\tilde{\mathcal{F}}_{\tilde{R}_0}(\xi) = e^{i\alpha(\theta - \xi)} \int_{-\infty}^{\infty} (k^2\tilde{R}_0^2 - \nu^2)^{1/4} \exp\left[-\frac{i\pi}{2}|\nu| - i(k^2\tilde{R}_0^2 - \nu^2)^{1/2} + i|\nu| \arccos \frac{|\nu|}{k\tilde{R}_0} + i\nu(\theta - \xi)\right] d\nu, \tag{2.143}$$

where ξ is an integer multiple of 2π . The phase of the integrand in Eq. (2.144) has a stationary point only for $\xi = 0$ and $-\pi/2 < \theta < \pi/2$, situated at $\tilde{\nu}_0 = k\tilde{R}_0 \sin\theta$. In the vicinity of this point the integrand in Eq. (2.144) is approximately equal to

$$(k\tilde{R}_0 \cos\theta)^{1/2} \exp\left[-ik\tilde{R}_0 \cos\theta - \frac{i}{2k\tilde{R}_0 \cos\theta}(\nu - \tilde{\nu}_0)^2\right].$$

After integrating Eq. (2.143) with respect to ν and using Eq. (1.72), we obtain the wave function $\psi_{\tilde{R}_0, \alpha}$,

$$\psi_{\tilde{R}_0, \alpha} \simeq \begin{cases} 2e^{-i\pi/4} k(r - \tilde{R}_0) \cos\theta e^{-ik\tilde{R}_0 \cos\theta + i\alpha\theta}, & -\pi/2 < \theta < \pi/2 \\ 0, & -\pi < \theta < -\pi/2, \pi/2 < \theta < \pi \end{cases} \tag{2.144a}$$

$$\tag{2.144b}$$

where $k(r - \tilde{R}_0) \ll 1$. It is apparent that, for $-\pi/2$

$< \theta < \pi/2$, the wave function is the superposition of the incident wave and of a wave reflected from each portion of the half-cylinder exposed to the incident wave, while the wave function is vanishing in the shadow of the cylinder, $-\pi < \theta < -\pi/2$ and $\pi/2 < \theta < \pi$.

The electromagnetic potentials φ, \mathbf{A} included in the Schrödinger equation are replaced in the hydrodynamical formulation of quantum mechanics by the field strengths \mathbf{E}, \mathbf{B} . As discussed in Sec. I.H, the Aharonov-Bohm effect appears in the hydrodynamical representation as a result of the penetration of the wave function into the region of the field strengths. However, if the region of the field strengths is shielded by perfectly reflecting barriers, the wave function is *exactly* zero in the shielded region. In this case the effects of the enclosed fluxes are incorporated into the theoretical description via boundary conditions, which must be fulfilled by the wave function at the frontier of the accessible region (Byers and Yang, 1961; Schulman, 1971; Strocchi and Wightman, 1974;

Inomata and Singh, 1978; Bohm and Hiley, 1979; Rothe, 1981). As pointed out by Merzbacher (1962), the correct boundary conditions and the corresponding wave functions can be obtained by a limiting process from more realistic models, which consider the physical space as singly connected. As an example of such a limiting process let us suppose that a magnetic flux $F=2\pi\hbar c\alpha/q$ uniformly distributed in a cylinder of radius r_0 is placed inside a cylindrical potential barrier of finite height \tilde{U} , having the same radius r_0 (Kretzschmar, 1965b). The Hamiltonian of a particle of charge q and mass M is then given by

$$H_{\tilde{U},\alpha}^{(r_0)} = -\frac{\hbar^2}{2M} \left[\frac{\partial^2}{\partial r^2} + \frac{1}{r} \frac{\partial}{\partial r} + \frac{1}{r^2} \left(\frac{\partial}{\partial \theta} - \frac{iq}{\hbar c} r A_\theta \right)^2 \right] + \tilde{U}(r), \tag{2.145}$$

where

$$\tilde{A}_m = -\frac{\frac{\kappa}{k} J_{|m-\alpha|}(kr_0) \chi_m^{(\alpha)'}(kr_0) - J'_{|m-\alpha|}(kr_0) \chi_m^{(\alpha)}(kr_0)}{\frac{\kappa}{k} H_{|m-\alpha|}^{(1)}(kr_0) \chi_m^{(\alpha)'}(kr_0) - H'_{|m-\alpha|}(kr_0) \chi_m^{(\alpha)}(kr_0)}, \tag{2.148a}$$

$$\tilde{B}_m = \frac{J_{|m-\alpha|}(kr_0) H_{|m-\alpha|}^{(1)'}(kr_0) - J'_{|m-\alpha|}(kr_0) H_{|m-\alpha|}^{(1)}(kr_0)}{\chi_m^{(\alpha)}(kr_0) H_{|m-\alpha|}^{(1)'}(kr_0) - \frac{\kappa}{k} \chi_m^{(\alpha)'}(kr_0) H_{|m-\alpha|}^{(1)}(kr_0)}. \tag{2.148b}$$

Now if we let the height of the potential barrier become very large for fixed r_0 , the asymptotic behavior of the functions $\chi_m^{(\alpha)}(kr_0)$, Eq. (2.111), results in the coefficients

$$\lim_{\tilde{U} \rightarrow \infty} \tilde{A}_m = -\frac{J_{|m-\alpha|}(kr_0)}{H_{|m-\alpha|}^{(1)}(kr_0)}, \tag{2.149a}$$

$$\lim_{\tilde{U} \rightarrow \infty} \tilde{B}_m = 0, \tag{2.149b}$$

which yield, when substituted in Eq. (2.147), just the expression of the eigenfunctions we have used in Eq. (2.126) to describe scattering by a perfectly reflecting cylinder.

We conclude from the analysis developed in this section that enclosed electromagnetic fluxes shift the phase of the wave function representing the incident charged particles, and moreover that flux-dependent phase shifts persist even when the overlap between the region accessible to the particles and the region of the field strengths is rendered arbitrarily small. The flux-dependent phase shifts produce in general observable changes in the patterns of the probability density and current, and as a secondary effect may result in a transfer of kinetic momentum to the incident particle, mediated by the forces associated with the scattering object. The existence of the quantum effects of the fluxes cannot be explained merely by taking into consideration the distribution of field strengths in the vicinity of the quasiclassical path of the incident particle, but rather requires a knowledge of the electromagnetic flux enclosed between pairs of such quasiclassical paths.

$$A_\theta^{(r_0)} = \frac{Fr}{2\pi r_0^2}, \quad \tilde{U}(r) = \tilde{U}, \quad r < r_0 \tag{2.146a}$$

$$A_\theta^{(r_0)} = \frac{F}{2\pi r}, \quad \tilde{U}(r) = 0, \quad r > r_0. \tag{2.146b}$$

If the energy of the particle is $\hbar^2 k^2/2M$, the eigenfunctions of the Hamiltonian (2.145) are

$$\tilde{\psi}_{r_0,m}^{(\alpha)}(r,\theta) = \begin{cases} [J_{|m-\alpha|}(kr) + \tilde{A}_m H_{|m-\alpha|}^{(1)}(kr)] e^{im\theta}, & r > r_0 \\ \tilde{B}_m \chi_m^{(\alpha)}(kr) e^{im\theta}, & r < r_0 \end{cases} \tag{2.147a}$$

where $\chi_m^{(\alpha)}$ is the function defined in Eq. (2.111), and

$$\kappa^2 = k^2 - \frac{2M\tilde{U}}{\hbar^2}.$$

The coefficients \tilde{A}_m and \tilde{B}_m can be determined from the continuity conditions at $r=r_0$ of $\tilde{\psi}_{r_0,m}^{(\alpha)}$ and $\partial\tilde{\psi}_{r_0,m}^{(\alpha)}/\partial r$ as

III. EXPERIMENTAL EVIDENCE

A. Observation of the quantum interference of electrons with an electrostatic biprism

As discussed in Sec. I, the position of the envelope of a quantum interference pattern is controlled by the field strengths acting on the incident particles, while the position of the fringes relative to the envelope of the pattern is determined by the amount of flux enclosed between the arms of the interference experiment. There are several types of experiments demonstrating the action of the enclosed electromagnetic fluxes, which can be distinguished according to the flux-carrying object and the method used for obtaining the interference pattern. The first experiments demonstrating the Aharonov-Bohm effect were based on the observation of flux-dependent shifts of the fringes produced with the electrostatic biprism of Möllenstedt and Düker (1956), which represents the quantum-mechanical analog of the Fresnel optical biprism. In a different arrangement, the electron interference pattern can be obtained with the aid of superconducting quantum interference devices, which were first applied to the investigation of quantum effects of the fluxes by Jaklevic *et al.* (1964a,1964b,1965). A third direction for experimental study is the quantization of the magnetic flux trapped in superconducting cylinders, ini-

tiated by Deaver and Fairbank (1961) and Doll and Näbauer (1961).

The first positive observation of quantum effects of the fluxes was reported by Chambers (1960), who used as a flux-carrying object a thin magnetized whisker. The results of Chambers were confirmed by Fowler, Marton, Simpson, and Suddeth (1961). Improved observations were then reported by Boersch, Hamisch, Grohmann, and Wohlleben (1961,1962), who used in their experiments filaments of ferromagnetic materials. The progressive shift of the fringes relative to the envelope of the pattern was demonstrated by Möllenstedt and Bayh (1962) and Bayh (1962), who produced magnetic flux with the aid of microscopic solenoids. All these experiments were based on the electrostatic biprism, and all placed the magnetic flux in the shadow of the biprism fiber. A clear separation between the region accessible to the electrons and the region of the field strengths was achieved in the experiments of Jaklevic *et al.* (1964b,1965) with superconducting quantum interference devices. They observed the modulation of the maximum supercurrent by the magnetic flux enclosed in a microscopic solenoid. Among the more recent experimental results concerning quantum effects of the fluxes are those of Wahl (1968,1970), and Lischke (1969,1970a,1970b), who studied quantization of the magnetic flux in superconducting tubes by use of electron interferometry modulated by the Aharonov-Bohm effect, and those of Henry and Deaver (1968,1970), who studied quantization for cylinders with a superconducting path passing several times around a single hole. A recent prominent study was that of Tonomura *et al.* (1982), who observed the effects on electron interference patterns of the magnetic flux enclosed in a microscopic toroidal magnet. All these experiments were performed with electrons. The same principles, however, were shown to apply for neutrons in the presence of a gravitational field by Colella, Overhauser, and Werner (1975).

In this section we shall analyze the electron interference patterns produced with the aid of the electrostatic biprism of Möllenstedt and Düker (1956). The electrostatic biprism consists of a thin metallized fiber held at a positive potential with respect to a pair of symmetric conductors grounded to the earth, as shown in Fig. 34. The electric field between the fiber and these conductors bends the paths of the electrons emerging from the source \mathcal{S} , thereby creating two virtual sources \mathcal{S}_1 and \mathcal{S}_2 . The effects of various distributions of electromagnetic fields can be analyzed by considering the phase difference in the observing plane between waves emerging from the virtual sources \mathcal{S}_1 and \mathcal{S}_2 , and these predictions can then be compared with the experimentally observed patterns.

In their experiments, Möllenstedt and Düker used a golden quartz fiber having a diameter of $2.5 \mu\text{m}$ and a length of 6 mm, while the grounded conductors shown in Fig. 34 were set at a distance of 2 mm from the fiber. They measured the distribution of potential of a model of the biprism enlarged 100 times, and found that in the working region of the biprism, which in real dimensions was about $15 \mu\text{m}$ from the fiber, the electric field E_f was

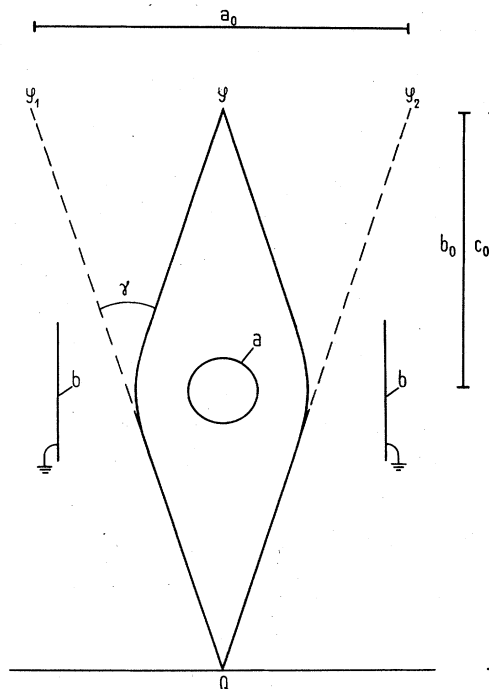


FIG. 34. Electrostatic biprism of Möllenstedt and Düker (1956). The metallized fiber a is kept at a positive potential with respect to the two grounded conductors b , thereby creating two virtual images \mathcal{S}_1 and \mathcal{S}_2 of the electron filament \mathcal{S} . The interference pattern is obtained as the superposition of the electron waves arriving in the observing plane from the directions of the virtual sources \mathcal{S}_1 and \mathcal{S}_2 . The bars represent the distance a_0 between the virtual sources \mathcal{S}_1 and \mathcal{S}_2 , and the distances b_0 and c_0 from the electron source \mathcal{S} to the center of the fiber and to the observing plane, respectively.

radial and inversely proportional to the distance r to the axis of the fiber,

$$E_f = \frac{AU_f}{r}, \quad (3.1)$$

where U_f is the potential of the fiber and A is a dimensionless constant equal to $A=0.14$. Since the potential of the metallized fiber is typically a few volts, while the kinetic energy of the incident electrons is several tens of keV, the paths of the electrons are deflected by a small angle γ , given by the ratio of the electron's incident momentum to the transverse momentum imparted by the electric field of the fiber. Thus it can be shown that the deflection angle for a particle of charge q and mass M is

$$\gamma = \frac{\pi A q U_f}{M v^2} (1 - v^2/c^2)^{1/2}; \quad (3.2)$$

the angular deviation is independent of the distance from the axis of the fiber to the path of the particle. This can be readily understood, since the $1/r$ dependence of the electric field of the fiber, Eq. (3.1), is compensated by the fact that the time spent by the particle in the vicinity of the fiber is proportional to r . This means that the paths

of the electrons, lying on one side of the fiber, are simply rotated by an angle γ , as shown in Fig. 35, so that the electron waves arrive in the observing plane along rays apparently emerging from the virtual image \mathcal{S}_1 of the source \mathcal{S} . On the other side of the fiber, the paths are rotated by the same angle γ but in the opposite sense, so that these components arrive in the observing plane apparently from the symmetric virtual source \mathcal{S}_2 . Möllenstedt and Düker checked experimentally both the path independence of the deflection angle γ and the proportionality of γ with the potential U_f of the fiber, and found good agreement with Eq. (3.2). In order to give some idea of the magnitude of the quantities involved in this problem, we note that for an incident electron energy of $Mv^2/2=20$ keV and a fiber potential $U_f=10$ V, the deflection angle γ is of the order of 10^{-4} rad.

From the position of the virtual sources we can determine the interference pattern. For small γ , the distance between the virtual sources \mathcal{S}_1 and \mathcal{S}_2 and the real source \mathcal{S} is equal to γb_0 , where, as shown in Fig. 34, b_0 is the distance from the source \mathcal{S} to the axis of the fiber. The distance between the two virtual images is thus $a_0=2\gamma b_0$, whence we can determine the spacing between consecutive fringes as $\lambda c_0/a_0$, where c_0 is the distance

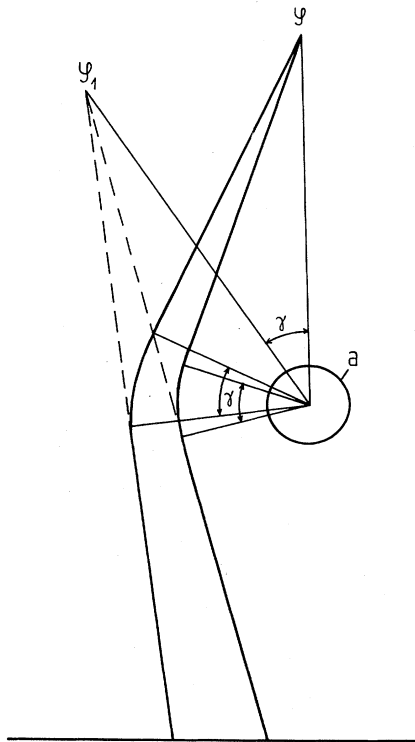


FIG. 35. Optics of the electrostatic biprism. The deflection angle γ , which is proportional to the potential of the fiber a , is independent of the distance from the axis of the fiber to the path of the electron. Consequently, the electron waves apparently arrive in the observing plane along straight lines emerging from the virtual images of the real source \mathcal{S} .

from the source to the observing plane, and λ the electron wavelength. The lengths b_0 and c_0 in the experiment of Möllenstedt and Düker were $b_0=3.95$ cm, $c_0=29.35$ cm, so that for a deflection angle of 10^{-4} rad and an acceleration voltage of 20 kV the interfringe was of the order of 3000 Å. Since the contributions arising from various parts of the source were incoherent, it was necessary, in order to observe an interference pattern, that the width of the source not exceed about 1000 Å. Such a narrow source was obtained by Möllenstedt and Düker (1956) by electron-optical demagnification with the aid of electrostatic cylindrical lenses. The diameter of the real electron source was about 50 μm , and after demagnification by a factor of 1000 they obtained a filament having a width of 500 Å and a length of a few millimeters, which was then used as the source \mathcal{S} for the biprism. The image formed in the observing plane was then magnified with the aid of two electrostatic lenses, as shown in Fig. 36.

The use of time-dependent solutions of the Schrödinger

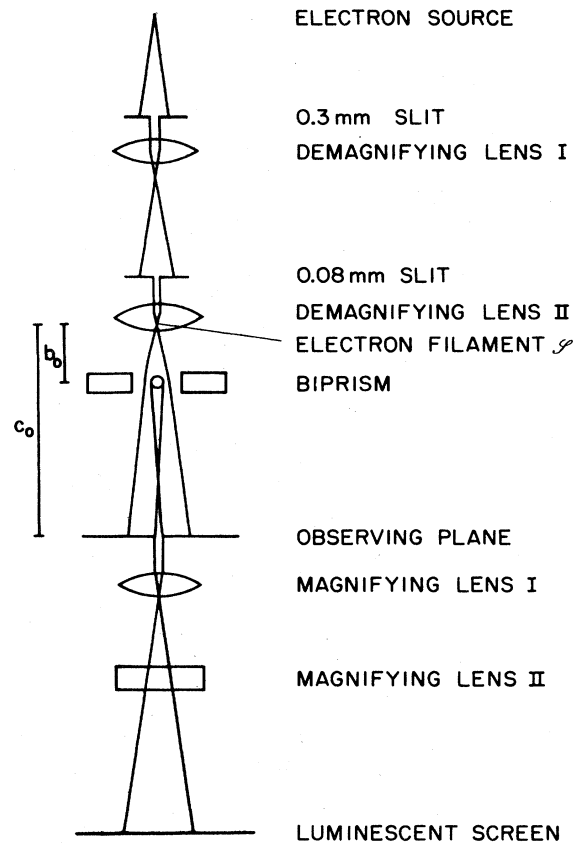


FIG. 36. Experimental arrangement used by Möllenstedt and Düker (1956) to observe the quantum interference of electrons. The diameter of the electron source was about 50 μm , and after successive demagnifications by a total factor of 1000 a filament was obtained having a width of 500 Å and a length of a few millimeters, which was used as the source \mathcal{S} for the biprism. The image obtained in the observing plane was then magnified with the aid of two electrostatic cylinder lenses.

equation in the analysis of the two-slit interference pattern developed in Sec. I was motivated by the transitory nature of the quantum effects of enclosed electric fluxes. Most experimental work on quantum effects of the fluxes refers, however, to the stationary magnetic case, for which we can also determine the probability distribution in the observing plane with the aid of Kirchhoff's formulation of the diffraction theory. In this approach it is assumed that the wave function on a surface Σ , lying in the vicinity of the object onto which the diffraction takes place, can be computed quasiclassically, while the further evolution of the state of the particle is given by a free-particle propagator. Since the wave function in the observing plane is the superposition of waves arriving from the directions of the two virtual sources, we shall first consider the contribution due to the source \mathcal{S}_2 . With the symbols used in Fig. 37, the wave function at point Q in the observing region is thus

$$\psi_2^{(0)}(Q) = \frac{ik}{2\pi} \int_0^\infty d\xi \int_{-\infty}^\infty d\eta \frac{e^{ikr_{QP}}}{r_{QP}} \cos(\mathbf{n}, \mathbf{r}_{QP}) \psi_2^{(0)}(P), \tag{3.3}$$

where \mathbf{n} is normal to the plane Σ , and

$$\psi_2^{(0)}(P) = \begin{cases} \frac{e^{ikr_{\mathcal{S}_2P}}}{r_{\mathcal{S}_2P}}, & \xi > 0 \\ 0, & \xi < 0. \end{cases} \tag{3.4a}$$

$$\tag{3.4b}$$

If the distance d from the observing point Q to the geometric shadow of the fiber shown in Fig. 37 is small compared to the distance \mathcal{S}_2Q , then the quantities r_{QP} and $r_{\mathcal{S}_2P}$ in the denominators of Eqs. (3.3) and (3.4) may be set constant, and $\cos(\mathbf{n}, \mathbf{r}_{QP}) \simeq 1$. Then the expression of the wave function in the observing region becomes

$$\psi_2^{(0)}(Q) \sim \exp \left[ik \left[D_s + D_q + \frac{z^2 + d^2}{2(D_s + D_q)} \right] \right] \times \int_{-w''}^\infty e^{iv^2} dv, \tag{3.5}$$

where

$$w'' = d \left[\frac{kD_s}{2(D_q + D_s)D_q} \right]^{1/2}. \tag{3.6}$$

Using the asymptotic expression of the complex Fresnel integral appearing in Eq. (3.5), we infer that in the region of the geometric shadow of the fiber, $d < 0$, the wave function is given by

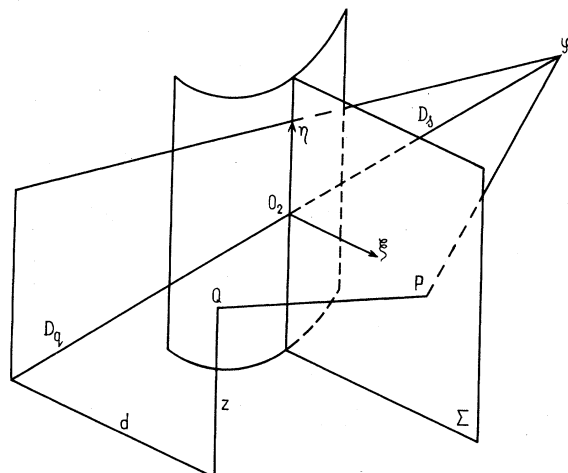


FIG. 37. The scattering of electrons by the edge of a cylindrical fiber according to Kirchhoff's theory of diffraction. In this approach it is assumed that the wave function in the plane Σ can be determined quasiclassically, and the probability distribution in the observing plane is further obtained with the aid of a free-particle propagator.

$$\psi_2^{(0)} \sim \exp \left[ik \left[D_s + D_q + \frac{z^2 + d^2}{2(D_s + D_q)} \right] \right] \times \left[-\frac{1}{2i|w''|} \right] e^{iw''^2}, \tag{3.7}$$

whereas in the illuminated region, $d > 0$, the wave function for large w'' becomes

$$\psi_2^{(0)} \sim \exp \left[ik \left[D_s + D_q + \frac{z^2 + d^2}{2(D_s + D_q)} \right] \right] \times \left[\pi^{1/2} e^{i\pi/4} + \frac{1}{2iw''} e^{iw''^2} \right]. \tag{3.8}$$

As mentioned previously, the wave function describing diffraction by a fiber is the superposition of contributions arriving in the observing plane from the directions of both virtual sources. Since the quantity $D_s + D_q + (z^2 + d^2)/2(D_s + D_q)$ is just the distance from the source point \mathcal{S}_2 to the observing point Q , the expression of $\psi_2^{(0)}(Q)$ in Eq. (3.5) corresponds to a spherical wave, modulated by the Fresnel integrals. Thus, for small deflection angles γ and with the notations of Fig. 38, the total wave function in the observing plane has the form

$$\psi^{(0)}(y, z) \sim \exp \left[ik \left[c_0 + \frac{z^2}{2c_0} + \frac{(y + b_0\gamma)^2}{2c_0} \right] \right] \int_{-w_1}^\infty e^{iv^2} dv + \exp \left[ik \left[c_0 + \frac{z^2}{2c_0} + \frac{(y - b_0\gamma)^2}{2c_0} \right] \right] \int_{-w_2}^\infty e^{iv^2} dv, \tag{3.9}$$

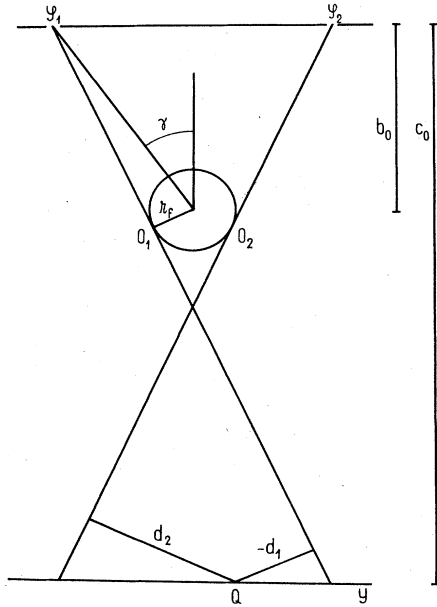


FIG. 38. Scattering of electrons by an electrostatic biprism, in Kirchhoff's approximation. The wave function in the observing region is the superposition of the waves arriving from the directions of the virtual sources \mathcal{S}_1 and \mathcal{S}_2 . The interference region is roughly delimited by the geometric shadow of the fiber, corresponding to the two virtual sources.

where

$$-w_1 = \left[y - (c_0 - b_0)\gamma + \frac{r_f c_0}{b_0} \right] \left[\frac{kb_0}{2c_0(c_0 - b_0)} \right]^{1/2}, \tag{3.10a}$$

$$w_2 = \left[y + (c_0 - b_0)\gamma - \frac{r_f c_0}{b_0} \right] \left[\frac{kb_0}{2c_0(c_0 - b_0)} \right]^{1/2}. \tag{3.10b}$$

The wave function, Eq. (3.9), yields the probability distribution in the observing plane for various potentials U_f via Eq. (3.2). The filamentary form of the electron source would be taken into consideration by an integration over the z variable of the square of the wave function, Eq. (3.9), but that does not alter the probability distribution in the y direction. Let us now compare the patterns observed by Möllenstedt and Düker (1956) at an electron acceleration voltage of 19.4 kV; these patterns are reproduced in Fig. 39, and have the predicted probability distribution given by Eq. (3.9). If the fiber is not too thin, and for relatively low potentials U_f , it can be shown, by replacing the Fresnel integrals in Eq. (3.9) with their asymptotic forms, that the interference pattern is dark in the central region, while its wings are characterized by two systems of Fresnel fringes, situated at

$$\pm y_N = \frac{r_f c_0}{b_0} - (c_0 - b_0)\gamma + \left[\frac{(c_0 - b_0)c_0\lambda}{b_0} \left(N - \frac{1}{4}\right) \right]^{1/2}, \tag{3.11}$$

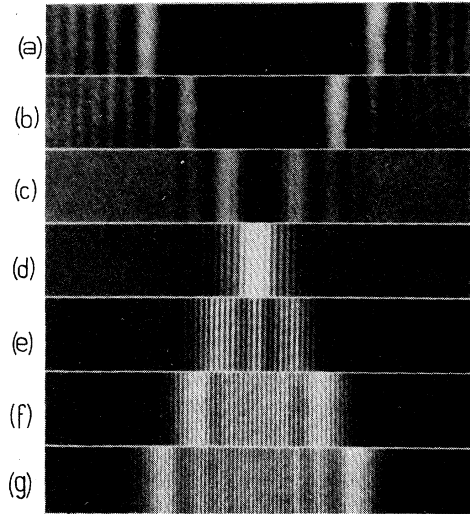


FIG. 39. Electron interference with the electrostatic biprism, for several values of the positive potential U_f of the biprism fiber, as observed by Möllenstedt and Düker (1956). (a) For $U_f=0$, the pattern corresponds to scattering by the biprism fiber and consists of two series of Fresnel fringes. (b) $U_f=1.5$ V and (c) $U_f=2.8$ V: The distance between the two Fresnel patterns is diminished. (d) $U_f=4.0$ V: The first maxima in each series are overlapping and give rise to equidistant Young fringes. (e) $U_f=5.0$ V, (f) $U_f=5.8$ V, and (g) $U_f=7.0$ V: The pattern of Young fringes is broadened and the distance between consecutive fringes diminished with increasing U_f .

where the maxima correspond to $N=1,3,5,\dots$, and the minima to $N=2,4,6,\dots$. For $U_f=0$, the deflection angle is $\gamma=0$, and the pattern simply corresponds to the scattering by the biprism fiber. The position of the Fresnel fringes predicted by Eq. (3.11) is in good agreement with the observed pattern, Fig. 39(a), when we substitute in Eq. (3.11) the values of the parameters $b_0=3.95$ cm, $c_0=29.3$ cm, $\lambda=0.087$ Å, $r_f=1.2$ μm. Now if the fiber is set at a positive potential, the separation between the two series of Fresnel fringes is gradually diminished, and since according to Eq. (3.2) the deflection angle for this experiment is given by $\gamma=1.1 \times 10^{-5} U_f$, with γ in rad and U_f in V, we expect that the first maxima in each series should coincide for a fiber potential of $U_f=4$ V, as actually observed in Fig. 39(d). For higher potentials U_f of the biprism fiber, the two illuminated wings are overlapping in the central part of the observing plane, and the pattern is dominated by equidistant Young fringes, the central fringe being light. The distance between consecutive fringes, which is determined by the phases of the exponential functions appearing in Eq. (3.9), is given in the observing plane by

$$\Delta = \frac{c_0\lambda}{2b_0\gamma}, \tag{3.12}$$

so that the central part of the pattern is broadened and the interfringe diminished with increasing U_f . Moreover, the intensity of the equidistant fringes is modulated by the oscillations of the Fresnel integrals in Eq. (3.9). This behavior is apparent in Figs. 39(e)–39(g), the observed distance between the fringes being in good agreement with Eq. (3.12).

While it is not surprising that we can predict with accuracy on the basis of quantum mechanics the probability distributions for various types of scatterings, it is quite remarkable that patterns characteristic of the interference between electromagnetic waves can be equally produced by particles with mass, and the experiments of Möllenstedt and Düker (1956) provide an impressive demonstration of this possibility.

B. Overall displacement of the biprism interference pattern by homogeneous magnetic fields

The location of the envelope of an interference pattern is determined by the strengths of the electric and magnetic fields acting directly on the charged particles. Consequently, in order to obtain positive evidence concerning the action of the electromagnetic fluxes, it is necessary to consider the dependence of the interference fringe position on the amount of flux enclosed between the arms of the experiment. Now the shadow of the biprism fiber is effective up to distances of the order of kr_f^2 , which in the arrangement of Möllenstedt and Düker (1956) would correspond to several tens of centimeters, so that the region just behind the fiber is practically inaccessible to the incident electrons. This means that we could study the quantum effects of the fluxes by altering the distribution of flux in the shadow of the biprism fiber. A simple way of doing that would be to apply a uniform magnetic field parallel to the axis of the fiber, as shown in Fig. 40, and to observe the position of the interference fringes as a function of the intensity of the applied field. While the magnetic force acting directly on the electrons will displace the envelope of the pattern in accordance with the classical laws, the presence of the magnetic flux in the region behind the fiber will cause a shift in the phase of the interfering components, thereby changing the position of the fringes in a characteristic way. In accordance with quantum mechanics, a distribution of uniform magnetic field will shift the interference pattern as a whole, i.e., in a first approximation, the position of the fringes relative to the envelope is independent of the intensity of the applied field. On the other hand, a distribution of magnetic field having the same intensity as the former in the accessible region but zero intensity in the shadow of the fiber, as shown in Fig. 41, will still produce the same displacement of the envelope, the position of the fringes relative to the envelope being, however, shifted by an amount proportional to the applied field. The effects of a uniform distribution of magnetic field on biprism interference patterns were studied by Chambers (1960), Boersch, Ham-

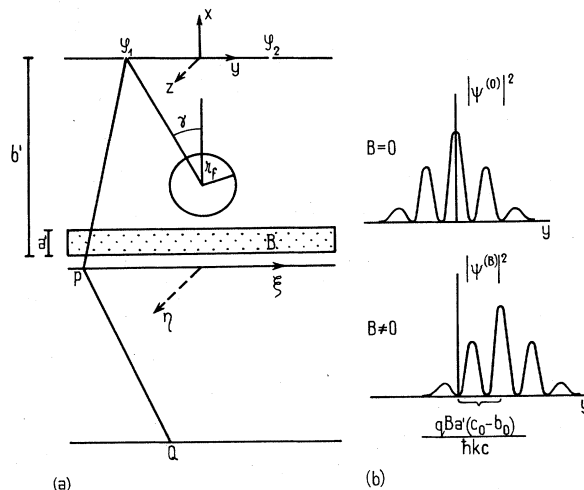


FIG. 40. (a) Biprism interference experiment in the presence of a uniform magnetic field and (b) overall displacement of the pattern due to the applied field. The envelope of the pattern is displaced by $qBa'(c_0 - b')/\hbar kc$, while the position of the fringes relative to the envelope remains unchanged.

isch, Grohmann, and Wohlleben (1961), and Bayh (1962), who observed an overall shift of the pattern, proportional to the intensity of the magnetic field. Their observations thus constitute some of the earliest evidence for the existence of an action of the inaccessible electromagnetic fluxes.

The effects on the biprism interference pattern of a magnetic field B parallel to the z axis, acting in the dotted region shown in Fig. 40, arise from the curvature of the

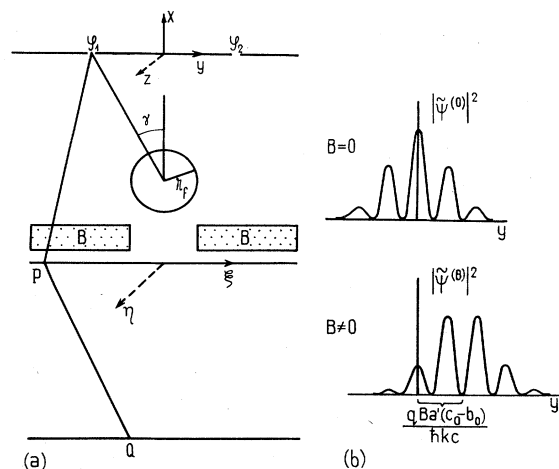


FIG. 41. (a) Thought experiment demonstrating the action of the inaccessible magnetic flux distribution in the shadow of the fiber, and (b) the corresponding interference pattern. While the envelope of the pattern is displaced by the same amount as in the case of the uniform magnetic field, the position of the fringes relative to the envelope is shifted by $qBa'r_f/\hbar kc$. The shift shown in (b) corresponds to $|q|Ba'r_f/\hbar kc = \frac{1}{2}$.

electron trajectories by the field, and from the phase shift due to the flux enclosed between the quasiclassical paths. We shall determine the probability distribution in the observing plane with the aid of Kirchhoff's theory of diffraction. Thus we consider the contribution of the virtual source \mathcal{S}_1 to the wave function in a plane Σ lying behind the fiber to be of the form

$$\psi_1^{(B)}(\xi, \eta) \sim e^{ikr_{\mathcal{S}_1 P} + iqBa'\xi/\hbar c}, \quad \xi < -r_f \tag{3.13a}$$

$$= 0, \quad \xi > -r_f, \tag{3.13b}$$

where we have assumed that $b' - b_0 \ll b_0$. The contribution of the virtual source \mathcal{S}_1 to the wave function in the observing plane is then obtained through the application of Eq. (3.3). Since the expression of the wave function at points Q lying in the central part of the observing plane is controlled by the oscillations of the exponential in Eq. (3.3), $\psi_1^{(B)}(Q)$ is proportional to

$$\psi_1^{(B)}(Q) \sim \int_{-\infty}^{-r_f} d\xi \int_{-\infty}^{\infty} d\eta \exp \left[ik(R_{\mathcal{S}_1 P} + R_{PQ}) + \frac{iqBa'}{\hbar c} \xi \right], \tag{3.14}$$

where

$$R_{\mathcal{S}_1 Q} \simeq b_0 + \frac{(\xi + b_0\gamma)^2 + \eta^2}{2b_0}, \tag{3.15a}$$

$$R_{QP} \simeq c_0 - b_0 + \frac{(y - \xi)^2 + (z - \eta)^2}{2(c_0 - b_0)}. \tag{3.15b}$$

The variables y and z in Eqs. (3.15) are the coordinates of the point Q in the observing plane, and the distances b_0 and c_0 have been defined in Fig. 38. The result of the integration (3.14) is

$$\psi_1^{(B)}(Q) \sim \exp \left[ik \frac{b_0\gamma}{c_0} y_B \right] \int_{-\bar{w}_1}^{\infty} e^{iv^2} dv, \tag{3.16}$$

where

$$-\bar{w}_1 = \left[y_B - (c_0 - b_0)\gamma + \frac{r_f c_0}{b_0} \right] \left[\frac{kb_0}{2c_0(c_0 - b_0)} \right]^{1/2}, \tag{3.17a}$$

and

$$y_B = y - \frac{qBa'}{\hbar kc} (c_0 - b_0). \tag{3.17b}$$

The contribution of the virtual source \mathcal{S}_2 in the plane Σ is

$$\psi_2^{(B)}(\xi, \eta) \sim e^{ikr_{\mathcal{S}_2 P} + iqBa'\xi/\hbar c}, \quad \xi > r_f \tag{3.18a}$$

$$= 0, \quad \xi < r_f, \tag{3.18b}$$

and it can be shown analogously that the component due to the virtual source \mathcal{S}_2 in the observing plane is given by

$$\psi_2^{(B)}(Q) \sim \exp \left[-ik \frac{b_0\gamma}{c_0} y_B \right] \int_{-\bar{w}_2}^{\infty} e^{iv^2} dv, \tag{3.19}$$

where

$$\bar{w}_2 = \left[y_B + (c_0 - b_0)\gamma - \frac{r_f c_0}{b_0} \right] \left[\frac{kb_0}{2c_0(c_0 - b_0)} \right]^{1/2}. \tag{3.20}$$

The total wave function in the observing plane is then

$$\psi^{(B)}(Q) = \psi_1^{(B)}(Q) + \psi_2^{(B)}(Q). \tag{3.21}$$

By comparing Eqs. (3.16)–(3.20) with the expressions corresponding to the field-free situation, Eqs. (3.9) and (3.10), we see that the application of a uniform field B displaces the whole interference pattern by $qBa'(c_0 - b_0)/\hbar kc$, a result previously obtained in Sec. I in the quasiclassical approximation. This action of the applied field is schematically represented in Fig. 40(b).

The term $qBa'\xi/\hbar c$ appearing in Eqs. (3.13) and (3.18) describes the kinetic momentum imparted to the incident electrons during their traversal of the strip of magnetic field. In Kirchhoff's approximation, the presence of the biprism fiber is taken into consideration by removing from the integration in Eq. (3.3) the portion of the plane Σ lying in the shadow of the fiber, while leaving the phase unchanged. Consequently the phases of the components $\psi_1^{(B)}(\xi, \eta)$ and $\psi_2^{(B)}(\xi, \eta)$, evaluated at $\xi = -r_f$ and $\xi = r_f$, respectively, differ by $2qBa'r_f/\hbar c$, and this shift is entirely due to the magnetic flux lying in the shadow of the fiber. Let us consider, for example, the effects of the distribution of magnetic field shown in Fig. 41(a); this field has the same intensity as the former in the accessible region and zero intensity in the shadow of the fiber. In this case the wave function in the plane Σ would be

$$\tilde{\psi}^{(B)}(\xi, \eta) = \begin{cases} e^{iqBa'r_f/\hbar c} \psi_1^{(B)}(\xi, \eta), & \xi < -r_f & (3.22a) \\ 0, & -r_f < \xi < r_f & (3.22b) \\ e^{-iqBa'r_f/\hbar c} \psi_2^{(B)}(\xi, \eta), & \xi > r_f. & (3.22c) \end{cases}$$

However, while the envelope of the pattern in the observing plane, corresponding to the form of the wave function, Eq. (3.22), will still be displaced by the same amount, $qBa'(c_0 - b_0)/\hbar kc$, this time the position of the fringes relative to the envelope will be shifted by $qBa'r_f/\pi\hbar c$ fringe widths. Thus the effects of a uniform magnetic field provide relevant information concerning the effects of the inaccessible magnetic flux distributed in the shadow of the biprism fiber.

The first experimental results concerning the quantum action of enclosed electromagnetic fluxes were reported by Chambers (1960), who produced interference fringes by an electrostatic biprism consisting of an aluminized quartz fiber. Among other experiments, Chambers examined the effect of the magnetic field produced by a pair of single Helmholtz coils 3 mm in diameter situated just behind the biprism, and observed that while fields up to 0.3 G were applied, sufficient to displace the pattern by up to 30 fringe widths, the appearance of the pattern was

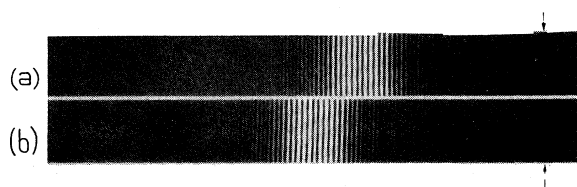


FIG. 42. Effect of a homogeneous magnetic field on the electron interference pattern, as observed by Bayh (1962): (a) interference pattern without magnetic field; (b) overall shift of the pattern by a distance proportional to the applied field. The arrows mark the location of the observing plane on the photographic plate.

completely unchanged. His observations were confirmed by Boersch, Hamisch, Grohmann, and Wohlleben (1961). The action of a homogeneous magnetic field was also investigated by Bayh (1962), who reported the patterns reproduced in Fig. 42. In Fig. 42(a) we see the system of equidistant fringes corresponding to a positive potential of the biprism fiber, the pattern being symmetric and having the central fringe light. The pattern shown in Fig. 42(b) was obtained in the presence of a magnetic field behind the fiber, produced with a pair of Helmholtz coils. We see that the interference pattern is displaced as a whole, while the position of the fringes relative to the envelope is unchanged, and in particular the central fringe remains light. Thus the observed overall displacement of the electron interference patterns by homogeneous magnetic fields constitute a first verification of the reality of the quantum effects of electromagnetic fluxes.

The action of field strengths on electron interference patterns was studied experimentally by Boersch, Hamisch, Wohlleben, and Grohmann (1960,1962), who used as a biprism antiparallel ferromagnetic domains, and also by Tonomura (1972). More details on the theoretical analysis of diffraction effects in electron microscopy can be found in the articles of Wohlleben (1967) and Cohen (1967).

C. Shift of the fringes relative to the envelope, produced by ferromagnetic filaments

The characteristic action of the electromagnetic fluxes is the shifting of the fringes relative to the envelope of the interference pattern, produced by distributions of flux which are completely enclosed in a region situated between the interfering components of the incident electron beam. Since the separation between the coherent electron waves is of the order of a few microns in most biprism experiments, the enclosed flux is often generated by thin filaments of ferromagnetic materials. Such experiments were carried out by Chambers (1960), Fowler, Marton, Simpson, and Suddeth (1961), and Boersch, Hamisch, Grohmann, and Wohlleben (1961,1962) for a cylindrical distribution of the enclosed flux, and more recently by

Tonomura *et al.* (1982) for a toroidal distribution of the flux. The predicted shifts of the fringes relative to the envelope of the pattern were observed in all these experiments, while the overlap between the incident electrons and the magnetic flux was insignificant.

The first positive observation of the action of an enclosed magnetic flux belongs to Chambers (1960), who produced the fringes with the aid of an electrostatic biprism consisting of an aluminized quartz fiber with a diameter of $1.5 \mu\text{m}$ flanked by two grounded metal plates. Moreover, unlike the experiment of Möllenstedt and Düker, Chambers's experiment had as its source a spot with a diameter of about 2000 \AA , and the distances b_0 and c_0 shown in Fig. 34 were $b_0 = 6.7 \text{ cm}$ and $c_0 = 20.1 \text{ cm}$. In order that the interference pattern not be blurred out by the finite source size, Chambers used very small biprism angles, of about $2 \times 10^{-5} \text{ rad}$, to obtain a fringe width in the observing plane of about 6000 \AA , for an incident electron energy of 20 keV . The magnetic flux was produced by an iron whisker, about $1 \mu\text{m}$ in diameter and 0.5 mm long, placed in the shadow of the fiber. Such whiskers are single magnetic domains (Kittel, 1946), and moreover they are found to taper with a slope of 10^{-3} rad (DeBlois, 1958), as schematically shown in Fig. 43. Consequently, the amount of enclosed magnetic flux is changing in the z direction of the axis of the whisker, which means that the relative phase of electron waves passing by the two sides of the whisker depends on the height z . As a result, the fringes will be tilted with respect to the envelope of the interference pattern, while the envelope it-

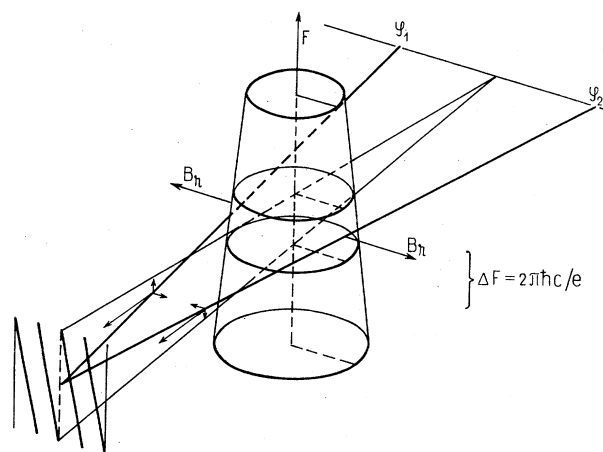


FIG. 43. Tilted fringes in the presence of magnetic flux enclosed by a tapering whisker. The whisker is a single magnetic domain of changing diameter, and as a result the interference fringes are tilted relative to the envelope by an angle proportional to the rate of change of the enclosed magnetic flux. While the tilt of the fringes can be attributed to the leakage of the radial field B_r , the total displacement of a fringe at a given section of the whisker is a measure of the magnetic flux enclosed at that section. The direction of the enclosed flux F shown in the drawing is opposite to the direction of the z axis, which points downward, and the charge of the incident electron is negative.

self will not be affected by the presence of the whisker. Since an iron whisker with a saturation field of 2×10^4 G and a diameter of $1 \mu\text{m}$ contains about 400 flux units, where one flux unit is $2\pi\hbar c/e = 4.1 \times 10^{-7}$ G cm², the flux content will change in the z direction at a rate of the order of 1 flux unit per micrometer. Moreover, since there is a pinhole magnification of $c_0/b_0 = 3$ between the biprism-fiber assembly and the observing plane, the change in the amount of flux enclosed in the whisker will produce a shift of 2π in the relative phase of the coherent components of the electron beam over a distance of $3 \mu\text{m}$ in the observing plane. Since the fringe width in the observing plane is $0.6 \mu\text{m}$, the predicted tilt of the fringes relative to the envelope is roughly 1 in 5. Precisely this was observed by Chambers, as can be appreciated from the patterns reproduced in Fig. 44. It is also apparent from Fig. 44(b) that the whisker taper is not uniform, but in this case becomes very small in the upper part of the figure.

The action of the magnetic flux enclosed in the tapering whisker can in fact be demonstrated by observing the fringes produced in the shadow of the whisker alone. The diffraction of one of the components of the incident beam in the shadow of the whisker is described by Eqs. (3.7) and (3.6), whence it can be inferred that the distance between these fringes is given by

$$\Delta_f = \frac{\lambda(c_0 - b_0)}{2r_f} \quad (3.23)$$

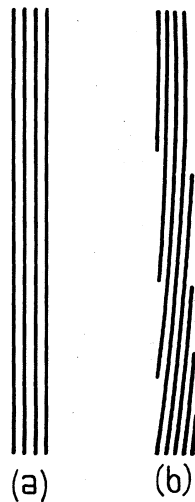


FIG. 44. Action of the magnetic flux of a tapering whisker on the biprism interference pattern, as observed by Chambers (1960): (a) fringe pattern due to biprism alone; (b) tilted fringes produced by a tapering whisker situated in the shadow of the biprism fiber. The tilt of the fringes relative to the envelope is proportional to the rate of change of the enclosed flux along the axis of the whisker, while the total displacement of a given fringe at a particular section is a measure of the magnetic flux enclosed at that section. The drawings reproduce the central part of the original patterns.

In the absence of magnetic flux the fringes are parallel to the envelope of the pattern, as can be appreciated from the pattern observed by Möllenstedt and Düker (1956), reproduced in Fig. 45(a). The electron wavelength was $\lambda = 0.087 \text{ \AA}$, the distance $c_0 - b_0 = 25.4$ cm, and the diameter of the fiber, set at zero potential, was $2r = 2.4 \mu\text{m}$. The observed distance between the fringes reportedly was 9200 \AA , in agreement with Eq. (3.23). The same type of fringes was studied by Chambers (1960) in connection with the problem of the quantum effects of the fluxes; Chambers replaced the fiber by a tapering whisker. As can be seen in Fig. 45(b), the fringes in the shadow of the whisker, which are due to the interference of the waves passing by both sides of the flux, are tilted relative to the envelope, while the Fresnel fringes corresponding to each of the coherent components are not affected by the enclosed flux. The parameter w'' defined in Eq. (3.6), which in the present case has the expression $w'' \simeq r_f [kb_0/2c_0(c_0 - b_0)]^{1/2}$, is of the order of $w'' \simeq 1$, so that the wave function, Eq. (3.5), cannot be approximated by the asymptotic form, Eq. (3.7). Consequently Eq. (3.23) is not applicable to the pattern in Fig. 45(b).

As pointed out by Fowler, Marton, Simpson, and Sudeth (1961), the study of biprism interference patterns provides a sensitive method for investigating the magnetic properties of very thin whiskers. Fowler *et al.* have produced fringes with the aid of an electrostatic biprism whose fiber was the tip of an iron whisker several millimeters in length. The source in their experiment was a spot with a diameter of $200\text{--}500 \text{ \AA}$, while the distances b_0 and c_0 were $b_0 = 5.2$ cm and $c_0 = 47.2$ cm, giving a magnification of about $c_0/b_0 \simeq 9$. The beam energy was $48\text{--}50$ keV. The interference pattern of a very slightly tapered whisker, observed by Fowler *et al.* (1961), is reproduced in Fig. 46. As can be appreciated from Fig. 46(a), the fringes are nearly parallel in the vicinity of the tip of the whisker, which means that the whisker is of nearly

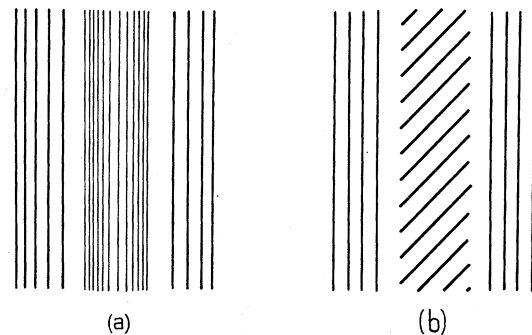


FIG. 45. Electron interference (a) in the shadow of a $2\text{-}\mu\text{m}$ fiber, observed by Möllenstedt and Düker (1956); (b) in the shadow of a tapering whisker, observed by Chambers (1960). The fringes in the shadow of the whisker, which are due to the interference of the components passing by both sides of the region of flux, are tilted relative to the envelope, while the Fresnel fringes, each corresponding to a coherent component, are not affected by the enclosed flux. The scales are different in the two drawings, which reproduce the original patterns.

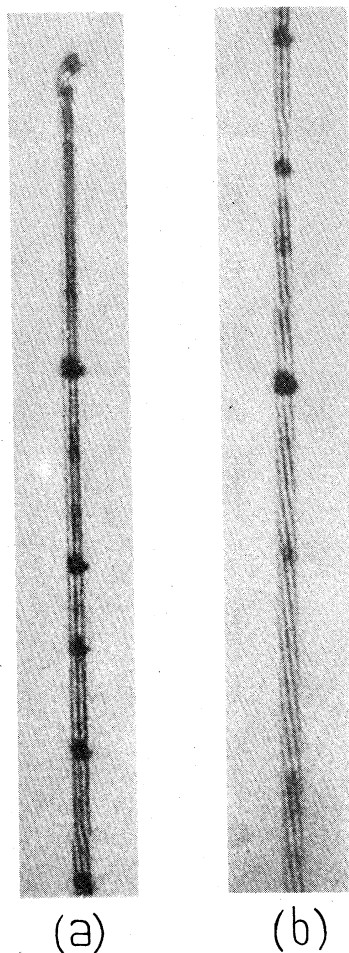


FIG. 46. Biprism interference pattern of a very slightly tapered whisker, observed by Fowler, Marton, Simpson, and Suddeth (1961): (a) tip of the whisker; (b) continuation of (a). The offset at the top of (b) is identical with that at the bottom of (a).

uniform diameter in the straight section at the end. At a point roughly $30 \mu\text{m}$ from the end, the fringes are offset slightly and assume a small tilt. The offset was attributed by Fowler *et al.* to the presence of a longitudinal field at the point of changing taper, which affects the envelope of the pattern. A little further along, the fringes are offset again and assume a greater tilt, as shown in Fig. 46(b). Fowler *et al.* also reported that when the whisker had its magnetization reversed by a strong external field, the direction of the fringe tilt was found to reverse, while the general details of the fringe pattern remained the same, with offsets and tilt occurring in the same points.

The tilt of the fringes relative to the envelope can be attributed to the radial leakage field of the tapering whisker. As pointed out by Pryce (1960), immediately outside a tapering whisker carrying a flux F , the leakage field is radial and given by $B_r = -(1/2\pi r)dF/dz$. This field exerts a force on the incident electrons and gives them a momentum component $p_z = \pm(e/2c)dF/dz$, the two signs corresponding to the different sides of the whisker, as

shown in Fig. 43. Consequently, the phase of the contributions arriving in the observing plane from the directions of the two virtual sources is

$$\pm \left[-\frac{e}{2c\hbar} \frac{dF}{dz} z + \frac{k\gamma b_0}{c_0} y \right], \quad (3.24)$$

so that the gradient in the z direction of the phase difference between these waves is given by $d(eF/\hbar c)/dz$. This is precisely the rate of change of the quantum phase difference $eF/\hbar c$, due to the enclosed flux F . However, as mentioned by Pryce (1960) and stressed by Aharonov and Bohm (1961), while the tilt or slope of the fringes is due to the leakage field of the whisker, the total displacement of a fringe at a given section of the whisker still depends on the flux enclosed at that section. We could determine the total displacement of the fringe by following the progressive buildup of the phase difference from the free end of the whisker, where it is zero, to any section where interference is being observed. Such a dependence on the leakage field at all sections of the whisker is, however, equivalent to a dependence on the amount of flux enclosed at a single section, and both viewpoints demonstrate that a knowledge of the field strengths acting directly on the incident electrons in the vicinity of a particular section of the whisker does not completely determine the resulting probability distribution in the observing plane.

The action of the magnetic flux was investigated in a different arrangement by Boersch, Hamisch, Grohmann, and Wohlleben (1961), and Boersch, Hamisch, and Grohmann (1962), who produced the flux by a thin layer of Permalloy deposited on the back of the biprism fiber. Boersch *et al.* observed the predicted flux-dependent shift of the fringes relative to the envelope, while the deviation due to the return magnetic field was about 10^{-9} rad, compared with several 10^{-5} rad for a fringe width. In the arrangement of Boersch, Hamisch, and Wohlleben (1962) shown in Fig. 47, the electron source, obtained by electron-microscopic demagnification, had a diameter of about 1200 \AA , and the energy of the electron beam was 40 keV. The dimensions of the layer of Permalloy were about 7 mm length, 5000 \AA width, and 200 \AA thickness, and since the source was a pointlike spot, every section of the interference pattern corresponded to a determined section of the layer. We have reproduced in Fig. 48 a sequence of patterns observed by Boersch, Hamisch, and Grohmann (1962), which demonstrate the action of the enclosed magnetic flux. In Fig. 48(a) we see a biprism interference pattern in the absence of the layer of Permalloy, the central fringe of the pattern being light. In Fig. 48(b) we see that the effect of the layer of Permalloy deposited in the shadow of the fiber is to interchange the light and dark fringes, while the envelope of the pattern is unaffected, which means that the enclosed flux was an odd multiple of $\pi\hbar c/e$. In the pattern shown in Fig. 48(c) the direction of the enclosed flux was reversed by an external magnetic field, and the identity of patterns in Figs. 48(b) and 48(c) demonstrates the periodicity with

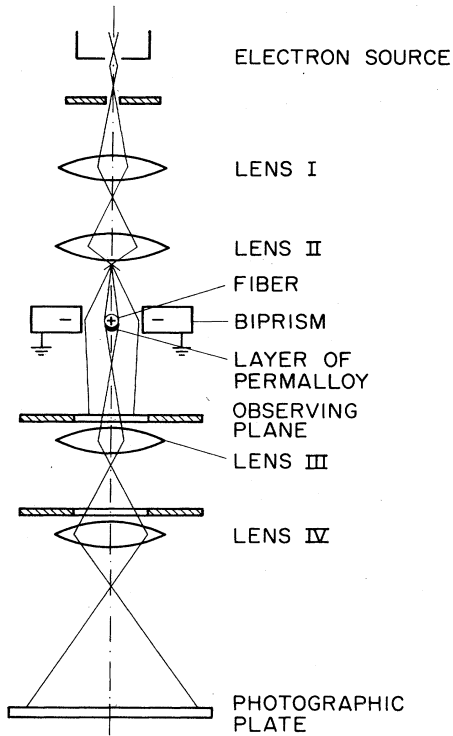


FIG. 47. Arrangement used by Boersch, Hamisch, and Grohmann (1962) to observe the quantum effects of the magnetic flux produced by a thin layer of Permalloy, deposited on the back of the biprism fiber.

$2\pi\hbar c/e$ of the effects of the enclosed fluxes. The observed interchange of light and dark fringes between Fig. 48(a) and Figs. 48(b) or 48(c) constitutes a clear demonstration of the reality of the quantum effects of enclosed fluxes.

From the analysis of flux-dependent interference patterns it is possible to determine the flux unit $2\pi\hbar c/e$. The value of the constant $2\pi\hbar c/e$, measured in connection with the quantum effects of the fluxes, was first reported by Möllenstedt and Bayh (1962), as will be discussed in the next section. In order to measure the constant $2\pi\hbar c/e$, Boersch, Hamisch, and Grohmann (1962) studied the effects on the electron interference pattern of magnetic fields in the transition region near the end of a thin layer of Permalloy deposited on the back of the fiber, as shown in Fig. 49(a). The patterns reproduced in Figs. 49(b) and 49(c) are the result of a quantum shift proportional to the enclosed magnetic flux, and of the Lorentz force acting in the vicinity of the end of the layer of Permalloy. The azimuthal component of the vector potential is given by

$$\tilde{A}_\theta = \frac{F}{4\pi r} \left[1 - \frac{z}{(z^2 + r^2)^{1/2}} \right], \quad (3.25)$$

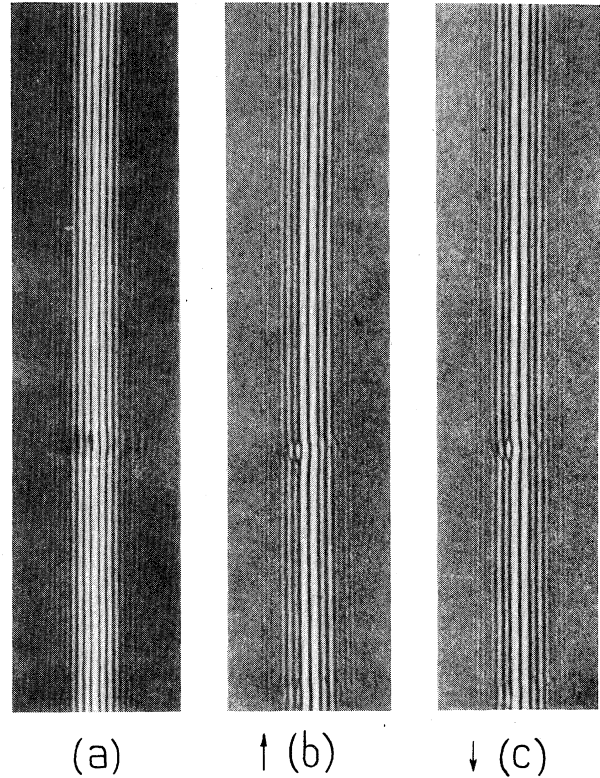


FIG. 48. Biprism patterns observed by Boersch, Hamisch, and Grohmann (1962), which demonstrate the quantum effects of the fluxes: (a) biprism interference pattern in the absence of the layer of Permalloy; (b) and (c), patterns in the presence of a layer of Permalloy deposited on the back of the biprism fiber. The arrows indicate the direction of the enclosed magnetic flux. The presence of the magnetic flux interchanges in this case the position of light and dark fringes between (a) and (b) or (c), an effect that is specific for the enclosed fluxes.

where z is the distance from the gold-Permalloy junction shown in Fig. 49(a), and r the distance to the axis of the filament of Permalloy, approximated as a string. The z component of the force is then

$$\frac{1}{r} \frac{\partial}{\partial r} (r\tilde{A}_\theta) = \frac{zF}{4\pi(z^2 + r^2)^{3/2}}, \quad (3.26)$$

so that the z component is zero in the plane of the junction and has opposite directions below and above that plane. Consequently, the Lorentz force displaces the envelope of the interference pattern in opposite directions, the envelope being unaffected in the plane $z=0$. Moreover, reversal of the magnetic field results in opposite displacements of the envelope, as is apparent from a comparison of patterns in Figs. 49(b) and 49(c). The magnetic flux enclosed in the Permalloy layer can be evaluated as the product of the saturation field and the area of the filament, which further divided by the fringe shift yields the flux unit. The flux-dependent phase shift can be determined from the connection of the fringes in the region of the gold-Permalloy junction. The experimental value ob-

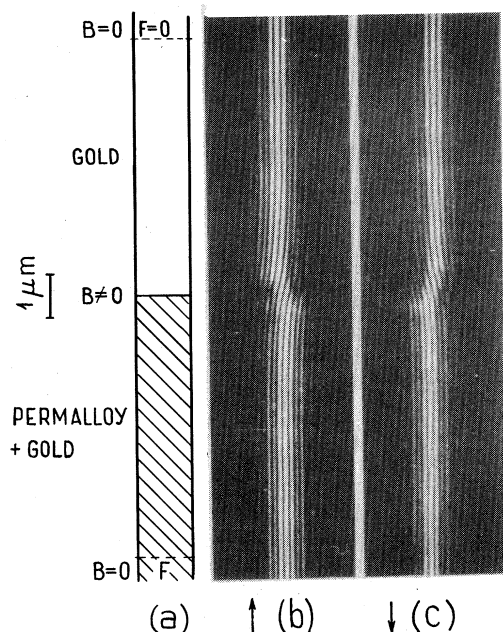


FIG. 49. (a) Diagram of the Permalloy-gold junction used by Boersch, Hamisch, and Grohmann (1962) in the experimental determination of the flux unit $2\pi\hbar c/e$; (b) and (c), fringe shifts in the biprism interference patterns, produced in the vicinity of the Permalloy-gold junction. The arrows indicate the directions of magnetization in the two cases. The displacement of the envelope seen in (b) and (c) is due to the longitudinal component of the magnetic field in the junction region, while the tilting of the fringes relative to the envelope is the effect of the magnetic flux enclosed between the interfering waves.

tained by Boersch, Hamisch, and Grohmann (1962) was $3.93 \times 10^{-7} \text{ G cm}^2$, with an error of 5%, in agreement with the theoretical value $F_0 = 4.13 \times 10^{-7} \text{ G cm}^2$.

The tilting of the fringes relative to the envelope, apparent in Figs. 49(b) and 49(c), is due to the radial component of the magnetic field in the transition region. The fact that the interference fringes are sharp even in the transition region demonstrates that the electrons arriving at a given section of the pattern are passing by a well-determined section of the fiber, so that, as discussed earlier in this section, the tilt of the fringes relative to the envelope also constitutes a verification of the reality of the quantum effects of the fluxes.

The quantum effects of a ferromagnetic layer evaporated on the biprism fiber have also been studied by Matteucci and Pozzi (1978). They observed the same inversion of contrast of the fringes produced by the enclosed flux, and reported that the magnetic field leakage was negligible.

Although the cylindrical distributions of ferromagnetic materials described above all yield a small longitudinal magnetic field acting on the incident electrons, the return field produces an overall displacement of the interference pattern, and not shifts of the fringes relative to the en-

velope. The magnitude of the deflection produced by the return fields is in fact negligible when compared with the fringe shift due to the enclosed flux. It is, however, interesting to consider the effects on the electron interference patterns of a toroidal distribution of magnetic flux, a case when there is no leakage field. Such an experiment was recently carried out by Tonomura *et al.* (1982), who made a small toroidal magnet of a thin film of Permalloy, the toroid width of a typical sample being 6400 \AA and the film thickness 400 \AA . This sample was illuminated by a collimated electron wave, while another collimated wave, coherent with the first, propagated externally to the toroid, as shown in Fig. 50. The two beams were then combined so as to interfere, and the hologram so obtained was then optically reconstructed on an enlarged scale (Gabor, 1949,1952).

The phase shift produced by the toroidal magnet in the phase of an illuminating electron wave is given by

$$\Delta\Phi_t = \begin{cases} 0, & \rho_2 < \rho \\ \frac{e(\rho_2 - \rho)F}{\hbar c(\rho_2 - \rho_1)}, & \rho_1 < \rho < \rho_2 \\ \frac{eF}{\hbar c}, & \rho < \rho_1 \end{cases} \quad (3.27a)$$

$$\Delta\Phi_t = \frac{e(\rho_2 - \rho)F}{\hbar c(\rho_2 - \rho_1)}, \quad \rho_1 < \rho < \rho_2 \quad (3.27b)$$

$$\Delta\Phi_t = \frac{eF}{\hbar c}, \quad \rho < \rho_1, \quad (3.27c)$$

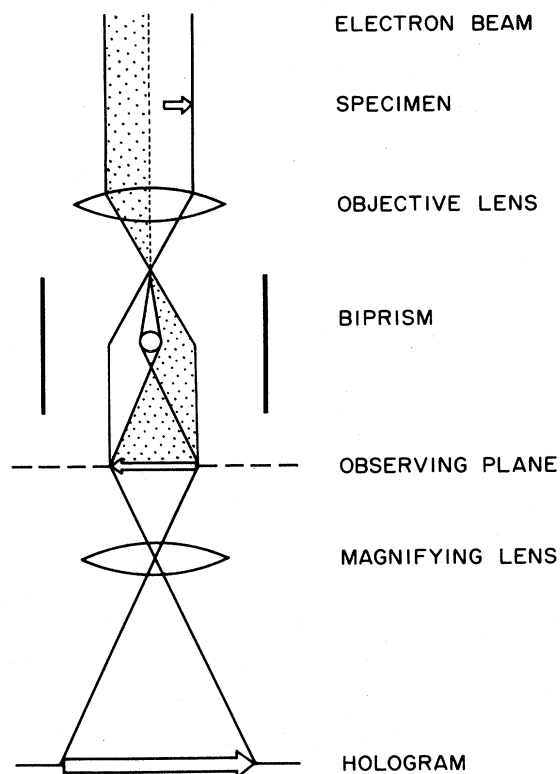


FIG. 50. Experimental arrangement used by Tonomura *et al.* (1982) to observe the quantum effects of the magnetic flux enclosed in a torus. The toroidal sample was illuminated by a collimated electron wave, while another collimated wave, coherent with the former, propagated externally to the toroid. The two beams were brought to interfere with the aid of an electrostatic biprism, and the hologram thus obtained was subsequently reconstructed on an enlarged scale.

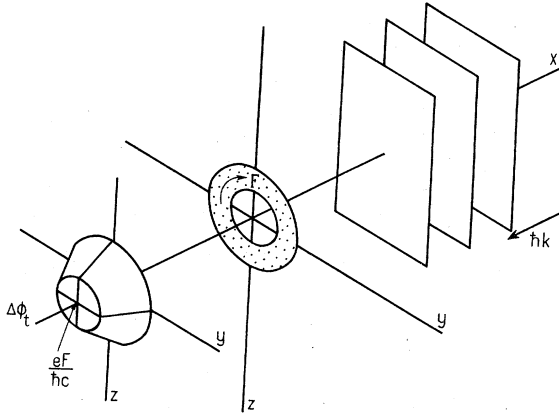


FIG. 51. Shift $\Delta\Phi_t$ produced by a toroidal magnet of flux F in the phase of the incident electron wave. The contours of constant phase are concentric circles in the plane perpendicular to the incidence direction, the phase being constant outside the shadow of the sample, while the total phase shift in the inner region is given by $qF/\hbar c$.

where ρ_1 and ρ_2 are, respectively, the minor and major radii of the ferromagnetic annulus, and F is the enclosed flux, as shown in Fig. 51. The term $eF/\hbar c(\rho_2 - \rho_1)$ is equal to the transverse azimuthal component in the y, z plane of the kinetic momentum acquired by the incident electron as it crosses the region of flux. According to Eq. (3.27), the contours of constant phase of the electron wave illuminating the magnetic sample are concentric circles in the plane perpendicular to the incident direction, where the phase is constant outside the shadow of the sample, and the total phase shift in the inner region is given by $eF/\hbar c$. Precisely this was observed by Tonomura *et al.* (1982), who obtained experimentally the contour map of the electron phase reproduced in Fig. 52. It is apparent from Fig. 52 that the phase in the inner region of the pattern is shifted by an odd multiple of π , while the shape of the magnetic sample appears as a clear image on the interferogram. As pointed out by Tonomura *et al.*, the part of the beam transmitted through the sample does not contribute to points outside the sample image, so that the phase of the beam reaching the inner region has indeed been shifted by the magnetic flux enclosed in the sample. The total phase shift between the inner and exterior regions is equal to 5.5 times 2π , according to the pattern shown in Fig. 52, in agreement with the theoretical value $eF/\hbar c$ obtained for a flux F corresponding to an enclosed magnetic field of 9500 G and a transverse area of $6400 \times 400 \text{ \AA}^2$.

The action of the magnetic flux enclosed in the toroidal sample can also be appreciated from the pattern reproduced in Fig. 53, obtained by the interference of the electron wave illuminating the sample with a coherent wave inclined at a certain angle β in the x, z plane. The in-

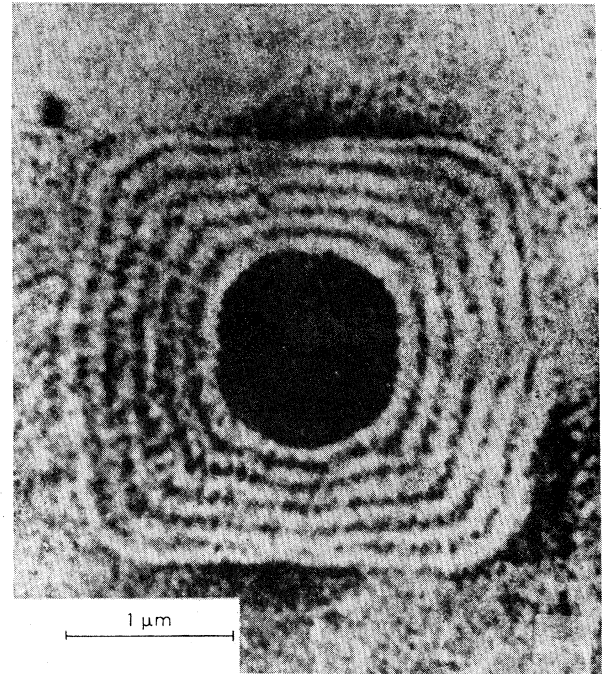


FIG. 52. Contours of constant phase of the electron wave illuminating a toroidal magnet, as observed by Tonomura *et al.* (1982). The phase in the inner region of the pattern is shifted by an odd multiple of π , while the shape of the magnetic sample is reproduced as a clear image on the interferogram. Since the sample does not contribute to points outside the sample image, the phase of the beam reaching the inner region was shifted by the enclosed magnetic flux.

terference fringes are the lines of constant phase difference δ_t , where according to Eq. (3.27) δ_t is given by

$$\delta_t = \begin{cases} k\beta\rho \cos\chi, & \rho_2 < \rho & (3.28a) \\ k\beta\rho \cos\chi - \frac{e(\rho_2 - \rho)F}{\hbar c(\rho_2 - \rho_1)}, & \rho_1 < \rho < \rho_2 & (3.28b) \\ k\beta\rho \cos\chi - \frac{eF}{\hbar c}, & \rho < \rho_1 & (3.28c) \end{cases}$$

and χ is the polar angle in the plane of the torus, relative to the z axis. Thus we expect to see a pattern of parallel fringes in the exterior region $\rho > \rho_2$, continued in the case of perfect radial symmetry by segments of conic cross sections with the focus at the center of the torus, abutting another system of parallel fringes in the inner region $\rho < \rho_1$; we would expect the inner system to be shifted with respect to the exterior fringes by $eF/2\pi\hbar c$ fringe widths. In the pattern observed by Tonomura *et al.* and reproduced in Fig. 53, we have $k\beta \lesssim eF/\hbar c(\rho_2 - \rho_1)$, so that the conic cross sections are ellipses. The distance between consecutive fringes is small at the bottom of the sample image, where the two wave vectors have the same direction, while the distance between fringes is comparatively large at the top of the pattern, where the com-

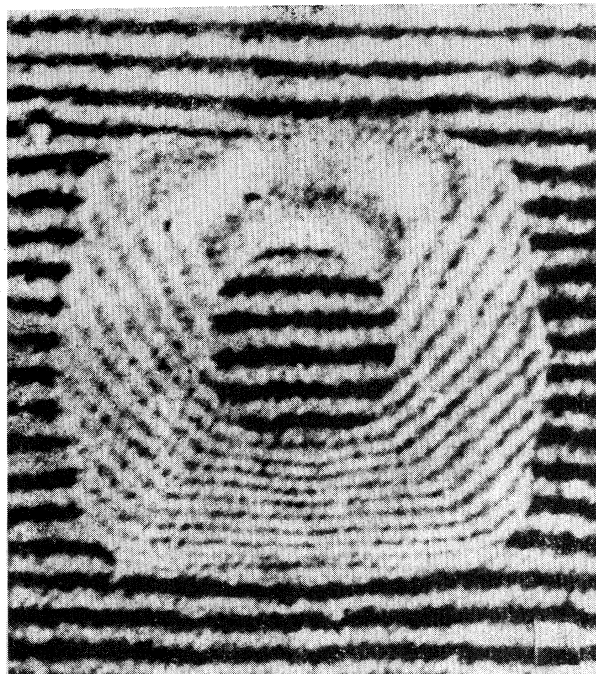


FIG. 53. Interference pattern obtained by the superposition of the wave illuminating the sample and of a coherent wave inclined at a certain angle relative to the former, as observed by Tonomura *et al.* (1982). The pattern consists of a system of parallel fringes in the exterior region, continued by segments of ellipses with the focus at the center of the toroidal sample, and terminated by another system of parallel fringes in the inner region, shifted with respect to the exterior ones by $qF/\hbar c$.

ponents of the wave vectors have opposite directions. Tonomura *et al.* (1982) have also studied the interference pattern of the toroidal sample at several incident electron energies, a parameter which markedly affects the penetrability of the electrons into the magnetic sample, but would not affect the flux-dependent phase difference. This was confirmed by Tonomura *et al.* at 80, 100, and 125 keV, a fact which proves that the quantum effects of the fluxes are independent of the degree of penetrability of the incident particles into the region of the field strengths.

D. Shift of the fringes relative to the envelope, produced by microscopic solenoids

Since in the interference experiments described in the preceding section the separation between the coherent electron beams was of the order of a few micrometers, an amount of enclosed magnetic flux comparable to the flux unit $F_0 = 2\pi\hbar c/e$ could be produced only by filaments of ferromagnetic materials, whose flux content was not subject to external control. On the other hand, the use of a microscopic solenoid as flux-carrying object requires a

larger separation between the coherent electron waves, of the order of a few tens of micrometers. In an experiment with a single electrostatic biprism, the fringes are observable provided that the fringe width $\lambda c_0/2b_0\gamma$, Eq. (3.12), exceeds the width d_e of the electron source. This condition imposes an upper limit on the diameter of the biprism fiber, of the order of $\lambda c_0/2d_e$. Assuming that $\lambda = 0.06 \text{ \AA}$, $d_e = 200 \text{ \AA}$, $c_0 = 50 \text{ cm}$, the diameter of the fiber, and thus the separation between the coherent beams, should be less than $70 \mu\text{m}$. However, with a fiber of such a large diameter it would also be necessary to use a large biprism angle γ , which in turn yields a small fringe width in the observing plane, so that the corresponding pattern would be difficult to observe.

As pointed out by Möllenstedt and Bayh (1961,1962) and by Bayh (1962), a relatively large separation between the coherent beams can be achieved without over-reducing the fringe system, by using three electrostatic biprisms instead of one, arranged as shown in Fig. 54. The separation of the beams is produced by the first fiber, held at a negative potential. The deflections due to the second biprism, held at a positive potential, render the directions of the two beams again convergent toward each other. However, the relative inclination of the beams is so large at this stage that the interference fringes cannot be observed. Therefore, a third biprism at a negative potential reduces the angular deflection of the beams until the in-

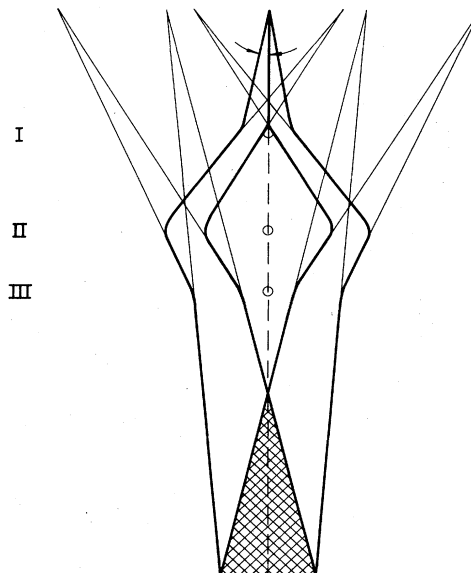


FIG. 54. Sequence of three electrostatic biprisms used by Möllenstedt and Bayh (1962) and by Bayh (1962) to produce a large separation between the coherent electron beams, without overreducing the fringe system. The fibers of the first and third biprisms are at negative potentials, while the fiber of the second biprism is at a positive potential. Since the deflection angle is independent of the distance from a ray to the fiber, the interference pattern in the observing plane is determined by the final position of the virtual sources.

interference fringes become observable. Since the deflection angle by each biprism is independent of the distance from a ray to the fiber, the interference pattern in the observing plane depends on the final position of the virtual source. The maximum separation between the two beams is obtained in the region above the fiber of the second biprism, the magnitude of the separation depending on the potential of the first biprism fiber and on the distance between biprisms I and II.

Möllenstedt and Bayh (1962) and Bayh (1962) used the system of three electrostatic biprisms to observe the effects on the electron interference pattern of a magnetic flux enclosed in a solenoid having a diameter of less than $20\ \mu\text{m}$, situated in the region above the second biprism fiber, as shown in Fig. 55. The electron source, obtained by electron-microscopic demagnification, was a filament having a width of about $100\ \text{\AA}$, and the distance from the filament to biprism I measured $24.5\ \text{cm}$. The diameter of the fiber of the first biprism was about $3\ \mu\text{m}$. The distance between biprisms I and II was $47\ \text{cm}$, while the distance between biprisms II and III was $5\ \text{cm}$, small enough so that the electron beams would not intersect the fiber of the third biprism. The observing plane was $25\ \text{cm}$ below biprism III, and the interference pattern formed in that

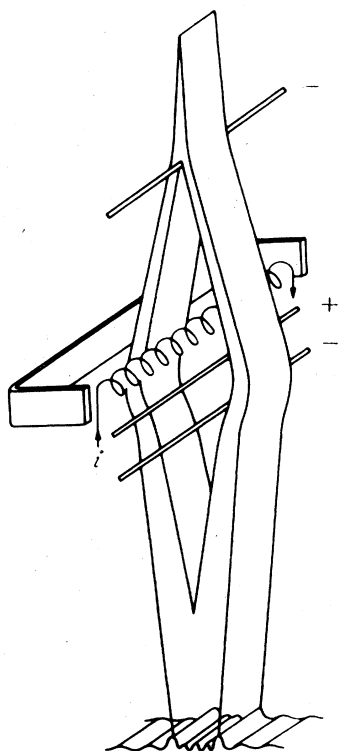


FIG. 55. Experimental arrangement used by Möllenstedt and Bayh (1962) and Bayh (1962) to observe the quantum effects of magnetic flux enclosed in a microscopic solenoid. The magnetic yoke serves to conduct the return magnetic flux enclosed in the solenoid.

plane was further magnified. The energy of the electron beam was $40\ \text{keV}$. A shield of highly permeable ferromagnetic material protected the interferometer against stray magnetic fields, which are particularly disturbing for a large separation of the beams. The enclosed magnetic flux was produced with the aid of a Wolfram coil whose diameter measured less than $20\ \mu\text{m}$ and whose length was more than $5\ \text{mm}$. The return magnetic flux of the coil was conducted through a highly permeable ferromagnetic yoke. Bayh (1962) calculated that, because the winding is not completely dense, the magnitude of the longitudinal magnetic component becomes as small as 5×10^{-3} of the magnetic field in the solenoid at a distance of $5\ \mu\text{m}$ from the surface of a typical solenoid used in the experiments. Moreover, Bayh (1962) checked that the magnetic field generated by the longitudinal component of the current flowing in the solenoid did not significantly affect the interference pattern. Now, according to Eq. (3.7), the probability density in a plane just above the second biprism, at a distance of $10\ \mu\text{m}$ toward the center from the geometric shadow of the first fiber, is 2×10^{-3} of the density observed in the illuminated part of the aforementioned plane. Since the separation between the beams is of the order of $50\text{--}60\ \mu\text{m}$ in the plane situated above the second fiber, the overlap between the incident electrons and the magnetic field was indeed fairly small in these experiments.

In order to record the effects on the interference pattern of the magnetic flux enclosed in the solenoid, a slit having a width of $0.5\ \text{mm}$ was placed in front of the photographic film, perpendicular to the direction of the fringes. The increase in current through the solenoid was then synchronized with the displacement of the film in the unperturbed direction of the fringes, thus yielding the pattern observed by Bayh (1962), which is reproduced in Fig. 56. As predicted theoretically, the fringes are shifted by an amount proportional to the enclosed flux, while the envelope of the pattern is not affected by the magnetic flux.

Now a changing magnetic flux gives rise to an electromotive force around the solenoid, which would affect the energy of the electron beam, the difference between the energy of the two coherent components being proportional to the rate of change of the magnetic flux,

$$\Delta \mathcal{E} = -\frac{e}{c} \frac{dF}{dt} \quad (3.29)$$

The relative phase of these components would be progressively shifted in time as

$$\exp \left[-\frac{i}{\hbar} \int \Delta \mathcal{E} dt \right] = \exp \left[\frac{ie}{\hbar c} \int dF \right], \quad (3.30)$$

which formally represents just the quantum action of the magnetic flux enclosed in the solenoid. The presence of the electromotive force in the case of a variable flux is the analog in time of the radial leakage field of a spatially

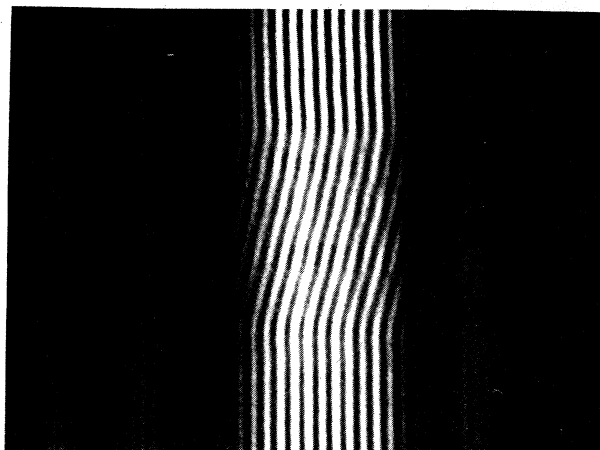


FIG. 56. Action of magnetic flux enclosed in a microscopic solenoid on a biprism interference pattern, as reported by Bayh (1962). At the bottom and at the top of the pattern, the magnetic flux is held constant. In the middle, the increase in magnetic flux is synchronous with the displacement of the photographic film; the flux produces a shift of about four fringes, while the envelope of the pattern remains unchanged.

changing flux of the tapering whisker mentioned in Sec. III.C. However, this situation demonstrates with even more clarity the limitations of the concept of force acting directly on a particle, when applied to the description of quantum interference processes. Indeed, the time integration appearing in Eq. (3.30) is meaningful only if the phase of each electron wave is preserved in the incidence region for the entire duration of the experiment. However, while the amplitudes for a given electron passing by opposite sides of the solenoid are coherent, the phases of distinct electrons emitted by different parts of the source or at different instants are *incoherent*. Since a given electron is represented by a wave train having a certain width, we can predict on the basis of the leaking electromotive force that the fringes will be tilted on a time scale. A pattern like that in Fig. 56 is obtained by the scattering of many independent electrons, and to each of these electrons the region in the vicinity of the solenoid appears to be identical as far as the fields acting directly on them are concerned. However, despite this identity conceived in terms of accessible field strengths, we find that the probability distribution in the observing plane is not the same for all the incident electrons, but rather the interference fringes observed at different instants of time are shifted by a distance proportional to the amount of enclosed flux. Since the traversal time of an electron from the source to the observing plane, of the order of 10^{-8} sec, is extremely small compared to the time necessary to obtain the interference pattern, the tilted fringes reproduced in Fig. 56 constitute in fact a sequence of patterns observed at successive values of the magnetic flux. The fairly small overlap between the incident electrons and the field strengths, in the experiments of Möllenstedt and Bayh (1962) and Bayh (1962) present a convincing demonstration of the

quantum action of the electromagnetic fluxes.

Möllenstedt and Bayh (1962) were the first to use the quantum effects of the fluxes for measuring the unit of magnetic flux $F_0 = 2\pi\hbar c/e$. They determined from the parameters of the microscopic solenoids and from the electric current the amount of magnetic flux that produced a phase shift by 2π in the interference pattern. The measured value of the flux unit was 4.07×10^{-7} G cm², with an error of 14%, in good agreement with the theoretical value $F_0 = 4.13 \times 10^{-7}$ G cm².

A similar experiment was later conducted by Schaal, Jönsson, and Krimmel (1966), who designed an electron interferometer that made possible the splitting of the two coherent beams up to 120 μ m. In this interferometer the second biprism of three was replaced by an electrostatic cylinder lens, the mechanical vibrations were minimized, and the magnetic fields were alternated. The magnetic field was produced by a solenoid having a diameter of 32 μ m; Schaal *et al.* observed shifts up to 20 fringe widths. The measured value of the flux unit was 4.15×10^{-7} G cm², with an error of 1.5%.

E. Flux-dependent effects observed with superconducting quantum interference devices

A property of many metals at very low temperatures is the coherence of the superconducting state on a macroscopic scale. As pointed out by Bardeen, Cooper, and Schrieffer (1957), superconductivity is due to an effective attractive interaction between electrons, which results from electron-phonon coupling. The consequence of the attractive interaction is the formation of pairs of electrons having opposite spins and momenta. Since the average distance between the electrons of a given pair is larger than the average distance between pairs, this gives correlations between electrons of opposite spin, extending over a large distance in real space. The possibility of observing macroscopic quantum interference effects in the superconducting state was pointed out by Josephson (1962), who predicted that a current will flow through a thin insulating barrier separating two superconductors, by means of quantum-mechanical tunneling of electron pairs, even if there is no voltage across the junction. Since the tunneling current is a periodic function of the phase difference across the junction, the current flowing through a pair of Josephson junctions coupled in parallel could then be controlled by the application of an external magnetic field. In this section we shall describe the experiments of Jaklevic, Lambe, Mercereau, and Silver (1964a, 1964b, 1965), who used such superconducting quantum interference devices to study the quantum effects of magnetic fluxes. They observed a flux-dependent modulation of the tunneling current through the junction pair, even when the magnetic flux was confined to a region not accessible to the superconductor, thereby confirming the reality of the quantum effects of enclosed fluxes.

We shall analyze the Josephson junction, shown schematically in Fig. 57, as a system of two quantum

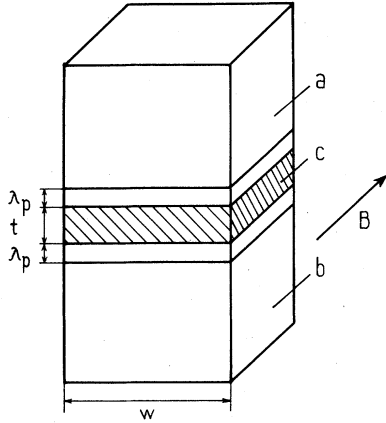


FIG. 57. Josephson junction of two superconductors a, b , separated by a thin insulating barrier c . A current flows through the junction, due to the quantum-mechanical tunneling of electron pairs, even if there is no voltage across the junction. In the presence of a uniform magnetic field B applied perpendicularly to the junction, the tunneling current depends on the magnetic flux enclosed by the effective cross-sectional area of the junction $(t + 2\lambda_p)w$, where λ_p is the penetration depth of the magnetic field into the superconductor.

states coupled together, an approach outlined by Feynman *et al.* (1965, Vol. III). Thus we let ψ_1 be the amplitude for finding an electron pair on one side of the barrier, and ψ_2 the amplitude for finding the pair on the other side; for simplicity, moreover, let us assume that the junction is symmetric. Then the amplitudes ψ_1 and ψ_2 are connected by the equations

$$i\hbar \frac{\partial \psi_1}{\partial t} = -\frac{qV}{2} \psi_1 + \mathcal{K} e^{(iq/\hbar c) \int_1^2 \mathbf{A} ds} \psi_2, \quad (3.31a)$$

$$i\hbar \frac{\partial \psi_2}{\partial t} = \mathcal{K} e^{-(iq/\hbar c) \int_1^2 \mathbf{A} ds} \psi_1 + \frac{qV}{2} \psi_2, \quad (3.31b)$$

where $q = -2e$ is the charge of the pair, \mathcal{K} is a characteristic of the junction, V is the potential difference across the junction, and \mathbf{A} is the vector potential in the region of the insulating barrier. Equations (3.31) can be analyzed in terms of the electron densities ρ_1^2, ρ_2^2 and the corresponding phases θ_1 and θ_2 by the substitutions

$$\psi_1 = \rho_1 e^{i\theta_1}, \quad (3.32a)$$

$$\psi_2 = \rho_2 e^{i\theta_2}. \quad (3.32b)$$

The resulting equations are

$$\frac{d}{dt}(\rho_1^2) = \frac{2}{\hbar} \mathcal{K} \rho_1 \rho_2 \sin \delta, \quad (3.33a)$$

$$\frac{d}{dt}(\rho_2^2) = -\frac{2}{\hbar} \mathcal{K} \rho_1 \rho_2 \sin \delta, \quad (3.33b)$$

and

$$\dot{\theta}_1 = \frac{\mathcal{K}}{\hbar} \frac{\rho_2}{\rho_1} \cos \delta + \frac{qV}{2\hbar}, \quad (3.34a)$$

$$\dot{\theta}_2 = \frac{\mathcal{K}}{\hbar} \frac{\rho_1}{\rho_2} \cos \delta - \frac{qV}{2\hbar}, \quad (3.34b)$$

where

$$\delta = \theta_2 - \theta_1 + \frac{q}{\hbar c} \int_1^2 \mathbf{A} ds. \quad (3.35)$$

Now Eqs. (3.33) describe how the pair density changes initially, and therefore they yield the current $J \sim \dot{\rho}_1$ that begins to flow across the junction,

$$J = J_0 \sin \delta. \quad (3.36)$$

On the other hand, from Eqs. (3.34) we see that for $\rho_1 = \rho_2$ we have

$$\dot{\theta}_2 - \dot{\theta}_1 = -\frac{qV}{\hbar}, \quad (3.37)$$

so that the quantity δ in Eq. (3.35) becomes

$$\delta = \delta_0 + \frac{q}{\hbar} \left[-\int V dt + \frac{1}{c} \int_1^2 \mathbf{A} ds \right]. \quad (3.38)$$

If the voltage V across the junction is constant and not equal to zero, the argument of the sine in Eq. (3.36) will oscillate rapidly, and the average current will be zero. On the other hand, if $V=0$, the tunneling current is given by

$$J = J_0 \sin \left[\delta_0 + \frac{q}{\hbar c} \int_1^2 \mathbf{A} ds \right], \quad (3.39)$$

so that we can get any current between J_0 and $-J_0$, depending on the difference δ_0 between the phases on the two sides of the barrier. The stationary superconducting tunneling effect described above was first observed experimentally by Anderson and Rowell (1963), while the tunneling current that would flow under certain resonance conditions when an oscillating voltage V is applied across the junction was observed by Shapiro (1963).

The effect on a Josephson junction of width w of an applied magnetic field B threading through the junction as shown in Fig. 57 can be computed by summing the current density, Eq. (3.39), over the entire area of the junction. The tunneling current thus obtained is given by

$$J = J_0 \frac{\sin(qF_j/2\hbar c)}{qF_j/2\hbar c} \sin \delta_0, \quad (3.40)$$

where $F_j = (2\lambda_p + t)wB$ is the magnetic flux enclosed by the effective cross-sectional area of the junction, and λ_p is the London penetration depth of the magnetic field into the superconductor. The maximum supercurrent is then

$$J_{\max} = J_0 \left| \frac{\sin(qF_j/2\hbar c)}{qF_j/2\hbar c} \right|, \quad (3.41)$$

a pattern characteristic of the diffraction of optical waves by a single slit. The modulation of the supercurrent by an applied magnetic force was observed experimentally by Rowell (1963).

As pointed out in a review by Anderson (1967), while the simple, one-slit pattern establishes the nature of the

superconducting interference phenomenon quite adequately, much more beautiful and useful experiments can be done with more complicated systems, in particular with the two-junction interferometer of Jaklevic, Lambe, Mercereau, and Silver (1964a,1964b,1965). The interferometer is a device consisting of two Josephson junctions coupled in parallel, as shown in Fig. 58. The current through the junction pair is the algebraic sum of the currents through each junction. As a result of the coherence of the superconducting state, it can be shown that the phase differences δ_1 and δ_2 across the two junctions are related by

$$\delta_2 - \delta_1 = \frac{q}{\hbar c} \int_{\Omega} \mathbf{A} \, ds, \quad (3.42)$$

where Ω is the loop crossing both junctions appearing in Fig. 58. Then if a magnetic field is applied normal to the plane of the junction pair, the maximum supercurrent through the double junction, obtained by summing the corresponding currents given by Eq. (3.40), has the form

$$J_{\max} = 2J_0 \left| \frac{\sin(qF_J/2\hbar c)}{qF_J/2\hbar c} \right| |\cos(qF_A/2\hbar c)|, \quad (3.43)$$

where F_A is the magnetic flux enclosed by the area of the junction pair. Thus, in addition to the single-slit diffraction pattern, there is a modulation whose periodicity in the maximum Josephson current is associated with a change by $2\pi\hbar c/q$ of the magnetic flux enclosed by the junction pair. On the other hand, if the region of applied magnetic field has no common points with the superconductor, the single-junction modulation disappears and the maximum supercurrent is modulated only by the enclosed magnetic flux,

$$J_{\max} = 2J_0 |\cos(qF_A/2\hbar c)|. \quad (3.44)$$

In their experiment, Jaklevic, Lambe, Mercereau, and Silver (1964a,1964b,1965) used tin-tin oxide-tin tunnel junctions separated by a plastic insulator, as shown in Fig. 59. The maximum Josephson supercurrent was obtained by the use of an ac averaging technique. First, Jaklevic *et al.* measured the maximum Josephson current as a function of the intensity of a uniform magnetic field applied to the long dimension of the substrate of the junction pair. The patterns obtained by Jaklevic *et al.*

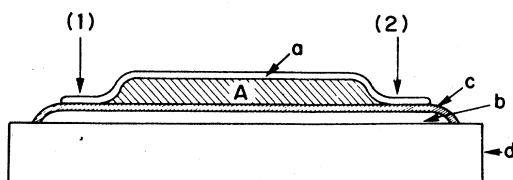


FIG. 58. Superconducting quantum interference device consisting of two Josephson junctions coupled in parallel, according to Jaklevic, Lambe, Mercereau, and Silver (1965). Junctions 1 and 2 are connected by superconductors *a* and *b*. These are separated by the thin oxide layer *c*, and form a loop enclosing the area *A*. The current flow is measured between *a* and *b*.

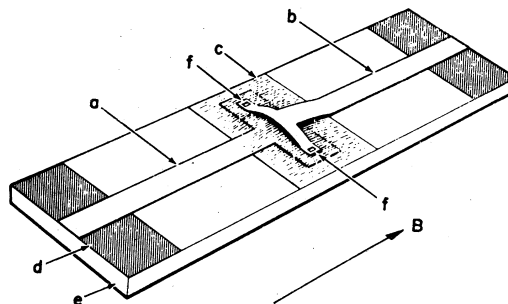


FIG. 59. Completed junction pair used by Jaklevic, Lambe, Mercereau, and Silver (1965) to demonstrate the macroscopic quantum interference in superconductors. A magnetic field *B* could be applied to the long dimension of the substrate *e*. The plastic insulator *c* is applied over the base tin film *a*, to mark out the junctions *f* and separate *a* from the second tin film *b*.

(1964a,1965) showed both the diffraction and the interference effects described by Eq. (3.43). In the case of the pattern reproduced in Fig. 60, the junction separation was $w=3$ mm and the junction width 0.5 mm, while the field periodicity was 16 mG. From the field spacing between interference peaks and the area *A* between the junctions, the flux period was determined to be 2.3×10^{-7} G cm², which in view of the reportedly large uncertainty in the area *A* is in reasonable agreement with the theoretical value $F_0/2=2.07 \times 10^{-7}$ G cm². This result also confirms the fact that the charge of an electron pair is indeed $|q|=2e$.

In order to demonstrate the action of an enclosed magnetic flux on the interference pattern, Jaklevic *et al.* (1964b,1965) constructed small solenoids by closely winding a fine insulated copper wire around a beryllium-copper core, with the core providing the return path. The tiny solenoid was introduced between the two junctions as shown in Fig. 61. Since the diameter of the solenoid was of the order of 100 μ m and its length about 1 cm, the field external to the solenoid at the superconductor was very small, reportedly less than 10^{-4} of the field needed to produce a shift by one fringe. The interference pattern due to the enclosed magnetic flux observed by Jaklevic *et al.* (1965) is reproduced in the lower part of Fig. 62, to-

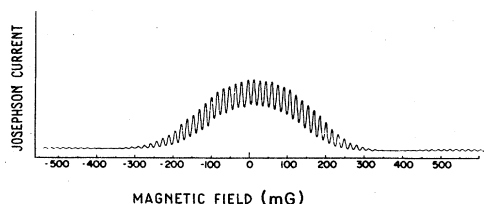


FIG. 60. Maximum Josephson current as a function of the intensity of an applied uniform magnetic field, as observed by Jaklevic, Lambe, Mercereau, and Silver (1965). The envelope of the pattern is determined by the single-junction diffraction effects, while the oscillations show the interference effects between the two junctions.

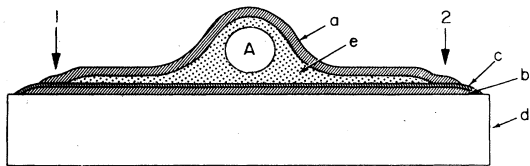


FIG. 61. Cross section of a Josephson junction pair used by Jaklevic *et al.* (1964b,1965) to demonstrate the action of an enclosed magnetic flux on superconducting quantum interference patterns. The thin oxide layer *c* separates the tin films *a* and *b*. Junctions 1 and 2 are connected in parallel by superconducting links enclosing the solenoid *A* embedded in a plastic insulator *e*. The current flow is measured between the films *a* and *b*.

gether with the pattern produced by a uniform magnetic field, shown in the upper part of the figure. As predicted by Eq. (3.44), the single-junction diffraction disappeared, and there remained only the modulation due to the enclosed magnetic flux. From the coil calibration and the measured field period Jaklevic *et al.* (1965) obtained a value for the flux unit of $F_0/2 = 2.1 \times 10^{-7} \text{ G cm}^2$, with an error of 5%. The agreement between measured and theoretical values of the flux unit consistently demonstrated that the static leakage field from the solenoid was indeed negligible. Moreover, to assure that the modulation of the interference pattern was not due to the electromotive force arising when the flux was changed, Jaklevic *et al.* (1965) also took interference data at fixed values of the flux, the flux being changed only when the interferometer was warmed to the normal state. The modulation of the maximum supercurrent was again observed, thus demonstrating unequivocally the reality of the quantum action of the enclosed fluxes.

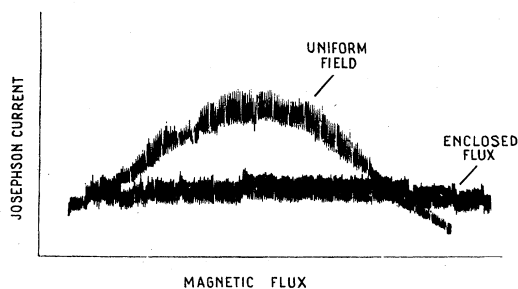


FIG. 62. Action of an enclosed magnetic flux on the maximum Josephson current for a junction pair (lower trace), compared with the action of a uniform magnetic field on the junction pair (upper trace), as observed by Jaklevic, Lambe, Mercereau, and Silver (1965). In the case of the enclosed flux the diffraction envelope disappears, and there remains only the periodic modulation with the amount of enclosed magnetic flux. The slight "beat" periodicity in both curves is reportedly due to a recorder defect.

F. Quantization of enclosed electromagnetic fluxes

If a block of superconducting material is introduced into a magnetic field, the electromotive forces generate currents in the surface of the block, so that the magnetic field cannot penetrate inside the superconductor. As shown by Meissner and Ochsenfeld (1933), the magnetic field vanishes inside the superconducting block even if the applied field is established while the block has a normal temperature, and is then cooled in the presence of the field. However, if a ring at normal temperature, Fig. 63(a), is cooled below the critical point in the presence of a magnetic field, the field is still expelled from the superconductor, but a certain amount of flux is now threading the inner section of the ring, as shown in Fig. 63(b). If the external field is removed, electromagnetic induction cancels the supercurrent in the outer surface of the ring, while the supercurrent in the inner surface remains unchanged, so that a certain amount of magnetic flux is now trapped by the ring, as shown in Fig. 63(c). The remark-

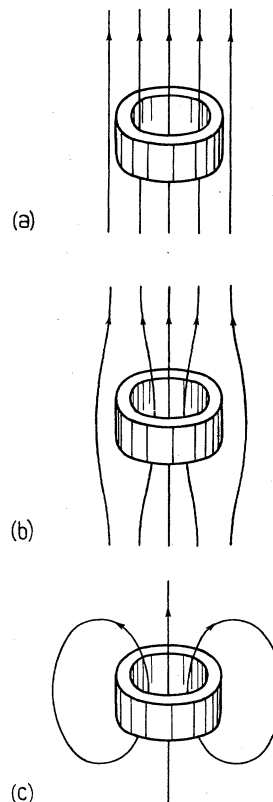


FIG. 63. Trapping of a magnetic flux by a superconducting ring, according to Feynman *et al.* (1965). (a) The ring, initially at normal temperature, is cooled below the critical point in the presence of an applied magnetic field. (b) The field is expelled from the superconductor, while a certain amount of flux is still threading through the inner section of the ring. (c) When the applied field is removed, electromagnetic induction produces the cancellation of the supercurrent in the outer surface of the ring, while the persistent supercurrent in the inner surface gives rise to the magnetic flux trapped by the ring.

able aspect of this process is that if the width of the ring is large compared to the penetration depth of the field into the superconductor, the amount of trapped flux is not arbitrary, but rather it is an integer multiple of $F_0/2 = \pi\hbar c/e$.

The quantization in multiples of $2\pi\hbar c/q$ of the magnetic flux trapped in a hollow superconductor in which the current is carried by particles of charge q was predicted by London (1948) on the basis of a phenomenological description emphasizing the coherent of the particles in the superconducting state. Thus if there exists an effective wave function ψ for particles of charge q and mass M which accounts for the superconducting state, the number density of such particles will be $\psi\psi^*$ and the current density

$$\mathcal{J} = \frac{iq\hbar}{2M}(\psi\nabla\psi^* - \psi^*\nabla\psi) - \frac{q^2}{Mc}\mathbf{A}\psi\psi^* \quad (3.45)$$

Now the phase of the wave function ψ must increase by an integer multiple of 2π with every rotation around the hole along a loop lying within the superconductor, as shown in Fig. 64. If we set $\psi = (\psi\psi^*)^{1/2}\exp(i\Phi/\hbar)$, we obtain from Eq. (3.45)

$$\nabla\Phi = \frac{M}{q}\frac{\mathcal{J}}{\psi\psi^*} + \frac{q}{c}\mathbf{A}, \quad (3.46)$$

so that as explained above the quantity

$$\mathcal{F} = \oint \left(\frac{Mc}{q^2}\frac{\mathcal{J}}{\psi\psi^*} + \mathbf{A} \right) ds \quad (3.47)$$

is an integer multiple of $2\pi\hbar c/q$,

$$\mathcal{F} = N\frac{2\pi\hbar c}{q}, \quad N = 0, \pm 1, \dots$$

London (1948) assumed that the charge q would be that of a single electron. However, Onsager (1961) pointed out that, due to the pairing of electrons in a superconductor, $q = -2e$, so that the fluxoid, Eq. (3.47), is quantized in integer multiples of $\pi\hbar c/e$,

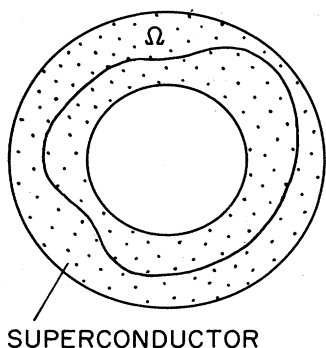


FIG. 64. Quantization of the fluxoid in a hollow superconductor. If the effective wave function ψ yields a number density $\psi\psi^*$ of particles in the superconducting state and a supercurrent \mathcal{J} , then due to the single valuedness of ψ the fluxoid $\mathcal{F} = \oint (Mc\mathcal{J}/q^2\psi\psi^* + \mathbf{A})ds$ is quantized in integer multiples of $2\pi\hbar c/q$, where $|q| = 2e$.

$$\mathcal{F} = N\frac{\pi\hbar c}{e}, \quad N = 0, \pm 1, \dots \quad (3.48)$$

A phenomenological theory of superconductivity, which incorporates the hypotheses leading to Eq. (3.48), was developed by Ginzburg and Landau (1950). It was later shown by Gor'kov (1959) that the Ginzburg-Landau theory can be seen as an extension of the microscopic theory of superconductivity of Bardeen, Cooper, and Schrieffer (1957) in the vicinity of the transition temperature, provided that q and M are twice the charge and mass of an electron. If the width of the ring is large compared to the penetration depth of the magnetic field into the superconductor, then it can be shown that the supercurrent inside the superconductor is zero, so that the expression of the fluxoid becomes $\mathcal{F} = \oint \mathbf{A} ds$. In this case, the magnetic flux trapped by the ring is necessarily an integer multiple of the flux unit $F_0/2 = \pi\hbar c/e$.

The fact that the magnetic flux trapped by a hollow superconducting cylinder is quantized in integer multiples of $\pi\hbar c/e$ was confirmed experimentally by Deaver and Fairbank (1961) and by Doll and Nábauer (1961,1962). Deaver and Fairbank used a tin cylinder, cooled through the superconducting transition in the presence of a known applied axial magnetic field. The net flux F in the cylinder was measured by moving the tin cylinder up and down one hundred times per sec and observing the electrical pickup in two small coils surrounding the ends of the cylinder. The quantization unit found experimentally was $F_0/2 = \pi\hbar c/e$, with an error of 20%. The dependence of the trapped flux on the intensity of the applied field observed by Deaver and Fairbank is reproduced in Fig. 65. Doll and Nábauer (1961,1962) measured the mechanical torque exerted by a magnetic field on a small superconducting lead tube with frozen-in magnetic flux, and also found quantization of the magnetic flux in integer multiples of $\pi\hbar c/e$. The dependence of the trapped flux on the intensity of the applied field observed by Doll and Nábauer is shown in Fig. 66.

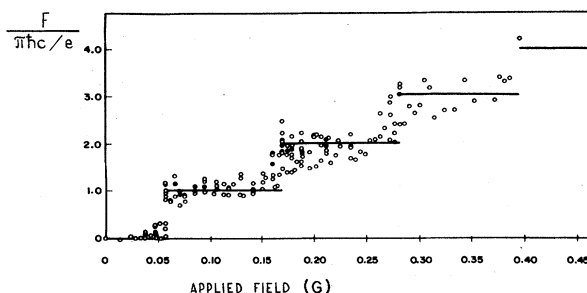


FIG. 65. Trapped flux in a superconducting hollow tin cylinder as a function of the magnetic field in which the cylinder was cooled below the superconducting transition temperature, as observed by Deaver and Fairbank (1961): \circ , individual data points; \bullet , average value of all data at a particular value of the field, including data that could not be plotted due to overlapping of points.

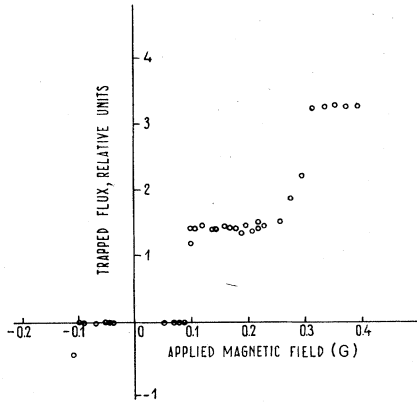


FIG. 66. Magnetic flux trapped in a superconducting lead tube as a function of the longitudinal magnetic field in which the tube was cooled below critical temperature, as observed by Doll and Näbauer (1961). The ordinate is proportional to the frozen-in flux.

In general, the penetration depth of the magnetic field into the superconducting ring is very small compared to the width of the ring and to its inner radius, so that the region of the superconductor and the region of enclosed flux have practically no common points. As emphasized by Peshkin (1981a), the fact that the stationary states of the superconductor are determined by the amount of inaccessible flux represents a bound-state analog of the Aharonov-Bohm scattering effect. Unlike the conventional electromagnetic effects, which depend on a finite overlap between probability density and field strengths, we have here another example of observable effects that are determined by the coherence of the phase across a region of vanishing overlap between charged particles and field strengths.

Recently it has been suggested that the electric flux might also be quantized in multiples of $\pi\hbar c/e$ (Post, 1982). As an example of quantization of the electric flux let us consider the case of a superconducting cylinder parallel to the z axis and moving in the x direction with a certain velocity v_0 , as shown in Fig. 15(b). If the longitudinal component of the magnetic field is B , there will exist inside the solenoid an electric field parallel to the y axis, $E = Bv_0/c$. The flux of this electric field through the loop in the y,t plane connecting the points Q, \mathcal{S} of Fig. 15(b) is given according to Eq. (1.78) by the integral over the area of the loop,

$$F_E = \int cE dy dt. \quad (3.49)$$

As explained at the end of Sec. I.F, the integration in the y,t plane can be transformed into an integration in the x,y plane by the substitution $dx = v_0 dt$. If the enclosed magnetic flux is quantized in multiples of $\pi\hbar c/e$, then the electric flux F_E , Eq. (3.49), will also be an integer multiple of $\pi\hbar c/e$. It should be pointed out that the electric flux defined in Eq. (3.49) is different from the conventional concept of electric flux as the integral of the nor-

mal component of the electric field over a surface in three-dimensional space.

Another macroscopic effect of enclosed fluxes occurs in the case of a charged particle whose motion is restricted to a ring encircling the region of magnetic flux. From the results derived in Sec. I.E, we infer that the ground-state energy of the charged particle is a periodic function of the amount of enclosed flux, as shown in Fig. 67. Since the kinetic energy of the pairs contributes to the free energy of the superconducting phase, the free energy will also be periodic in the flux (Byers and Yang, 1961; Brenig, 1961). Now the superconducting transition occurs at a temperature such that the free energies of the superconducting and normal phases should be equal. Since the free energy of the normal phase is essentially independent of the magnetic flux, it turns out that the transition temperature is a periodic function of the enclosed flux (Little and Parks, 1962; Parks and Little, 1964). The difference between the free energies of the normal and superconducting phases consists mainly in the ground-state kinetic energy of an electron pair, so that the change in the critical temperature ΔT_c produced by a flux F would be proportional to

$$\Delta T_c \sim \left[N - \frac{eF}{\pi\hbar c} \right]^2, \quad (3.50)$$

where N is an integer. In order to observe this effect, Little and Parks (1962) and Parks and Little (1964) measured the transition temperature of thin-walled superconducting hollow cylinders near the critical temperature as a function of the applied magnetic field in the axial direction. The magnetic field at the sample was varied sinusoidally, and the resulting variation in the resistance of the superconducting film was recorded, as shown in Fig. 68. From the observed oscillations in the resistance it was possible to determine the oscillations in the critical temperature. A periodic transition temperature with a period of $\pi\hbar c/e$ in the magnetic flux was observed in all samples. Hence Parks and Little (1964) determined the phase diagram for a thin cylindrical superconductor in an axial magnetic

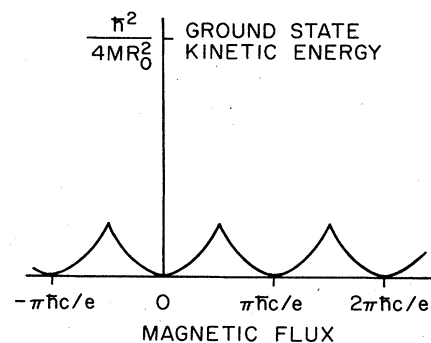


FIG. 67. Ground-state energy of an electron pair of charge $-2e$ and mass $2M$, whose motion is restricted to a ring enclosing a magnetic flux F . The energy is a periodic function of the enclosed magnetic flux, with periodicity $\pi\hbar c/e$.

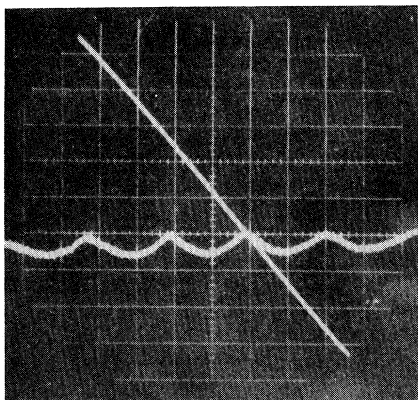


FIG. 68. Variation of the resistance of a hollow cylinder with applied magnetic field at its transition temperature, as observed by Parks and Little (1964). The upper trace is the magnetic field sweep.

field, represented schematically in Fig. 69. This phase diagram demonstrates that the flux-dependent shift of critical temperature occurs not only for those sinusoidal fields actually used in the experiments of Little and Parks, but also for any static magnetic fluxes enclosed in the hollow cylinder.

The periodicity of the quantum effects of the fluxes was also observed by Kwiram and Deaver (1964), who measured the flux change occurring in small, hollow tin cylinders cooled through the transition temperature in an applied magnetic field. The flux change occurring at the superconducting transition in an applied magnetic field was detected with a pickup coil wound closely around the cylinder. The observed period, Fig. 70, corresponds to a flux through the entire cross section of the cylinder of $2.0 \times 10^{-7} \text{ G cm}^2$. Although in the Kwiram-Deaver experiment there was field at the superconducting ring, Willis (1971) reportedly obtained identical results in subsequent experiments with long internal solenoids, when

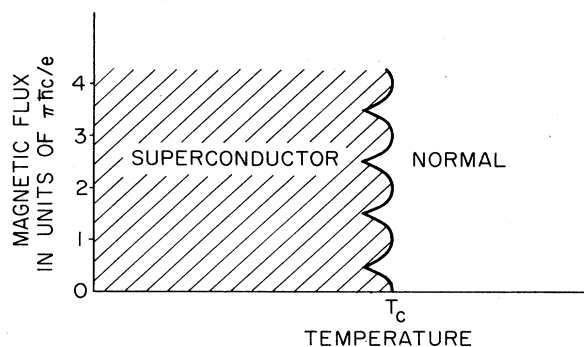


FIG. 69. Transition temperature of a thin hollow superconductor as a function of the enclosed magnetic flux, according to Parks and Little (1964). The oscillatory edge of the superconducting phase is a consequence of the periodicity of the kinetic energy of the electron pairs with the enclosed flux.

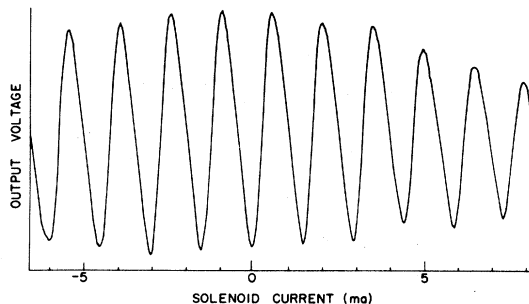


FIG. 70. Flux change occurring in a hollow tin cylinder cooled through the transition temperature in an applied magnetic field, as observed by Kwiram and Deaver (1964). The ring always chooses the available state of lowest energy, which is the one with trapped flux differing from the applied flux by no more than $\pi\hbar c/2e$.

there was no field at the ring (Deaver and Donaldson, 1982).

The magnetic flux trapped by superconducting hollow cylinders has also been studied with the aid of electron interferometers. Wahl (1968,1970) measured the amount of enclosed flux as a function of the magnetic field applied during cooling of the sample below the critical temperature, by observing the flux-dependent fringe shift in the interference pattern. The trapped flux had in most cases the values 0 , $2.19 \times 10^{-7} \text{ G cm}^2 \pm 6\%$, and $4.17 \times 10^{-7} \text{ G cm}^2 \pm 4\%$. Lischke (1969,1970a,1970b) and Boersch and Lischke (1970) also studied quantized magnetic flux in superconducting hollow cylinders with the aid of an electron interferometer. They observed the inversion of contrast shown in Figs. 71 and 72, corresponding to amounts of enclosed flux that are odd multiplets of $\pi\hbar c/e$, and the conservation of the pattern corresponding to flux changes by even multiples of $\pi\hbar c/e$, Figs. 72 and

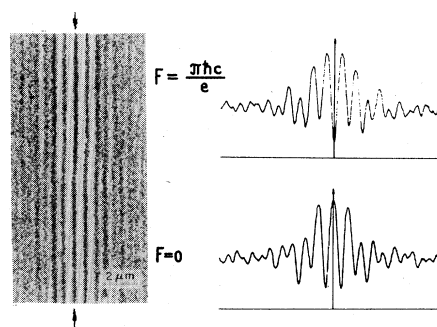


FIG. 71. Electron interferometer fringes and densitometer curves at the end of a superconducting hollow lead cylinder, as observed by Lischke (1969). At the bottom of the figure no flux is trapped and the phase shift is zero. At the upper part of the figure the trapped flux is $\pi\hbar c/e$ and the phase shift is π , resulting in the inversion of contrast of the fringes.

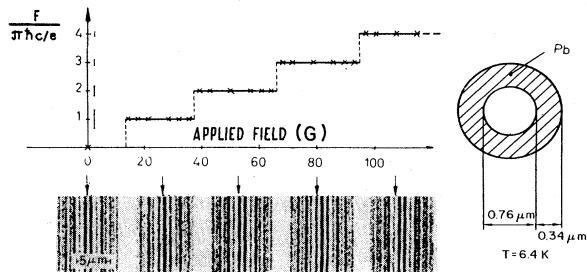


FIG. 72. Magnetic flux trapped in a hollow superconducting cylinder as a function of magnetic field applied during cooling of the sample, as observed by Boersch and Lischke (1970). Even multiples of $\pi\hbar c/e$ leave the pattern invariant, while odd multiples of $\pi\hbar c/e$ produce an inversion of contrast.

73. More recently, Möllenstedt, Schmidt, and Lichte (1982) also observed the phase shift between electron waves, due to a magnetic flux enclosed in a metallic cylinder.

As emphasized by Keller and Zumino (1961), what is always quantized in multiples of $\pi\hbar c/e$ is not the magnetic flux, but the fluxoid defined in Eq. (3.47). In fact, Bardeen (1961) has shown that in tubes of very small diameter and with wall thickness of the order of the penetration depth, the unit for quantization of the magnetic flux may depend on dimensions and temperature and be smaller than $\pi\hbar c/e$. The conservation of the fluxoid was investigated by Hunt and Mercereau (1965). In their experiments, a small amount of magnetic flux was trapped while a metallic ring was cooled below its critical temperature. The persistent current in the ring, which is proportional to the trapped flux, was then measured as a function of temperature, as the deflection angle of the ring suspended on a quartz torsion fiber in a small

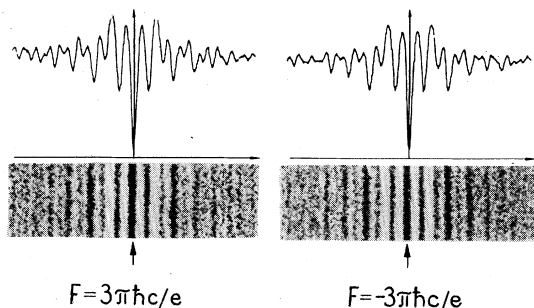


FIG. 73. Electron interference patterns produced by opposite magnetic fluxes trapped in a superconducting cylinder, as observed by Boersch and Lischke (1970). The pattern is invariant to flux changes by an even multiple of $\pi\hbar c/e$.

measuring magnetic field. As reported by Hunt and Mercereau (1964), very thin films of tin showed a decrease in the persistent current with increasing temperature and an increase in the current with decreasing temperature, which agrees with the dependence expected on the basis of the fluxoid conservation. In these experiments, the quantum numbers associated with the trapped flux and current were very large, of the order of 10^5-10^7 . However, when the trapped flux is of the order of $\pi\hbar c/e$, Lischke (1970b) reports some evidence suggesting that the magnetic flux would still be quantized in multiples of $\pi\hbar c/e$, even if the film thickness of the superconductor were smaller than the penetration depth.

The quantization of the fluxoid, Eq. (3.47), in multiples of $\pi\hbar c/e$ is analogous to the quantization in multiples of \hbar of the canonical angular momentum of a charged particle interacting with a distribution of applied electromagnetic fields, Eq. (1.120). The fact that the fluxoid coincides with the magnetic flux in the particular case of a hollow superconductor whose walls are thick compared to the penetration depth is a direct consequence of the fact that the current \mathcal{J} is zero inside the superconductor. However, the probability current Mv appearing in Eq. (1.120), which is the analog of the supercurrent \mathcal{J} in Eq. (3.47), is not in general zero, as can be appreciated for example by considering the problem of the rigid rotator discussed in Sec. I.E. Consequently, the requirement that the wave function be single valued does not imply quantization of the enclosed electromagnetic fluxes, as proposed by Costa de Beauregard (1972) and Costa de Beauregard and Viguereux (1974,1982).

Even in the case of the thick-wall, multiply connected superconductor, the effective wave function of the electron pairs depends not only on the magnetic flux but also on the number of times the inaccessible region is encircled (Schulman, 1971; Bernido and Inomata, 1980,1981; Berry, 1980; Gerry and Singh, 1982,1983). From the condition of single valuedness of the effective wave function, applied for example to the double-loop superconductor shown in Fig. 74, we infer that the magnetic flux trapped by this structure would be quantized in multiples of $\pi\hbar c/2e$, and in general the magnetic flux trapped by an N -turn superconducting loop would be a multiple of $\pi\hbar c/Ne$. The periodicity of $\pi\hbar c/2e$ of the magnetic flux trapped by a superconducting path passing twice around a single hole was observed experimentally by Henry and Deaver (1968,1970; Henry, 1970). Experimental work on the winding number dependence of the trapped magnetic flux was recently reviewed by Deaver and Donaldson (1982).

G. Quantum effects of electric fluxes

The electrostatic biprism described in Sec. III.A was applied to electron-interferometric measurement of the average inner potentials of the elements by Möllenstedt

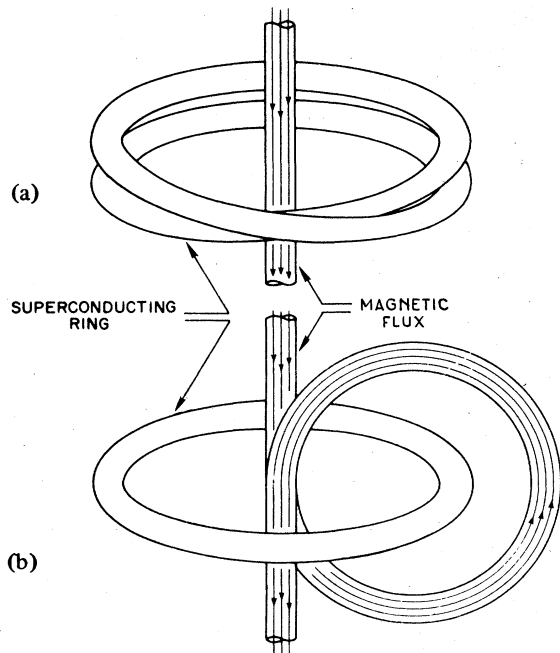


FIG. 74. Quantization of the magnetic flux for a superconducting path passing twice around a single hole [reproduced after Deaver and Donaldson (1982)]. As observed experimentally by Henry and Deaver (1968,1970), the magnetic flux trapped by the double superconducting loop is quantized in multiples of $\pi\hbar c/2e$.

and Keller (1957), and further by Langbein (1958), Fert and Faget (1958), Buhl (1959), and Keller (1961). The average inner potential U_0 is the constant term of the Fourier expansion of the scalar potential in the sample, and can be obtained as the integral of the potential U due to the atomic electrons and nuclear protons over the volume of the sample (Bethe, 1928). In a first approximation, the sample acts on the incident electrons of charge $-e$ as a potential well of depth $eU_0 > 0$. Then, if a thin layer of the substance under investigation is crossed by one of the coherent beams of a biprism interferometer, as shown in Fig. 75, the potential U_0 can be determined from the fringe shift produced in the interference pattern.

The thought experiment described in Sec. I.C demonstrating the quantum action of the electric flux was based on observation of the perturbation produced in the interference pattern by a transient charge distribution, sampled over very short intervals of time, which for a typical electron interference experiment are less than 10^{-10} sec. As will be shown further in this section, the action of the enclosed electric fluxes can, however, be demonstrated by a comparison involving interference patterns corresponding to stationary charge distributions, and we shall see that the shift of the fringes produced by a thin foil is due to the quantum action of the electric flux enclosed between the paths of the electrons from source to observing plane.

Let us first analyze the effect of the thin foil shown in Fig. 75 on the biprism interference pattern. According to

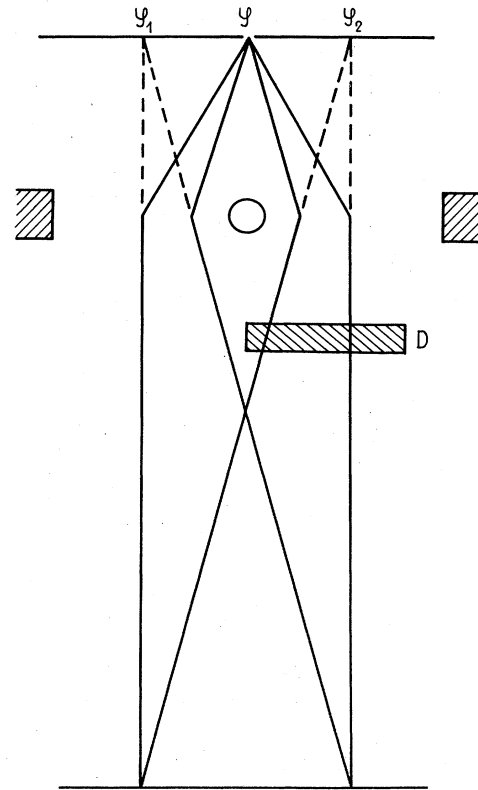


FIG. 75. Electron-interferometric measurements of the inner potential of a substance, according to Möllenstedt and Keller (1957). A thin layer of the substance under investigation is crossed by one of the coherent beams of the biprism interferometer. The inner potential is then determined from the fringe shift produced in the interference pattern.

the quasiclassical formalism developed in Sec. I, the amplitude for an electron emitted by the virtual source to arrive in the observing plane is proportional to $\exp(iS/\hbar)$, where S is the classical action, Eq. (1.12), for the stationary path under consideration. If the scalar potential is $U_0 > 0$ inside the foil and zero outside, there is an electric field acting normal to the surface of the foil, as shown in Fig. 76. When the electron crosses the foil, the y component of momentum is conserved, so that we have to consider only the changes in the x component of momentum. In the absence of the foil, the electron travels with a velocity $v < 0$ for a time $\tau_0 = -c_0/v$ from the source to the observing plane. We determine the trajectory of the electron crossing the foil and arriving in the observing plane after the same interval τ_0 as a correction to the unperturbed uniform motion. Thus the x component of the velocity inside the foil will be

$$v_{in} = -\frac{c_0}{\tau_0} - \frac{eU_0\tau_0}{Mc_0}, \tag{3.51}$$

while the velocity outside the sample is given by

$$v_{out} = -\frac{c_0}{\tau_0} + \frac{eU_0D\tau_0}{Mc_0^2}. \tag{3.52}$$

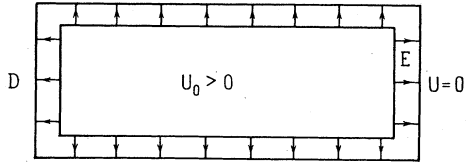


FIG. 76. Electric field acting normal to the surface of a thin foil of inner potential $U_0 > 0$, and thickness D .

The velocity slightly increases inside the foil and decreases outside with respect to the perturbed velocity, as can be appreciated from the x, t diagram of the motion shown in Fig. 77(a). The classical action of the problem is

$$S = \int (\frac{1}{2}Mv^2 + e\varphi)dt . \tag{3.53}$$

It can be shown by substituting in Eq. (3.53) the velocity, Eqs. (3.51) and (3.52), that the contribution to the action of the kinetic energy term is

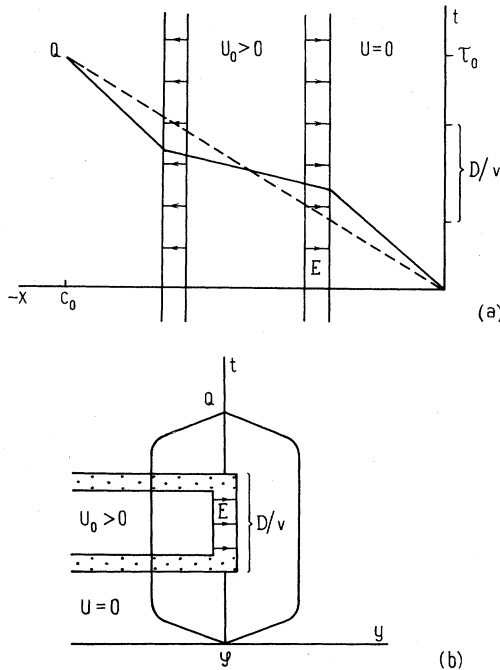


FIG. 77. Trajectory of an electron emitted by the source, which crosses a thin foil of thickness D and internal potential $U_0 > 0$, to arrive after a time interval τ_0 at the point Q in the observing plane: (a) the x, t projection of the path. The dashed line represents the unperturbed path. For fixed τ_0 the velocity of the particle increases inside the foil and decreases outside with respect to the unperturbed path, so that the contribution of the kinetic energy to the classical action is the same on both paths. (b) the y, t projection of the path. The phase of the wave component crossing the foil is shifted with respect to the unperturbed component by an amount proportional to the enclosed electric flux $\int cE_y dy dt$. In the region of the dotted horizontal strips, the electric field has an x component normal to the y, t plane, which does not contribute to the enclosed flux.

$$\int \frac{1}{2}Mv^2 dt = \frac{1}{2} \frac{Mc_0^2}{\tau_0} + \frac{eU_0\tau_0 D^2}{c_0^2} , \tag{3.54}$$

while the contribution of the potential becomes

$$\int e\varphi dt = \frac{eU_0 D \tau_0}{c_0} , \tag{3.55}$$

where D is the thickness of the foil. Since in a typical experiment we have $U_0 \simeq 10$ V, $\tau_0 \simeq 10^{-8}$ sec, $D/c_0 \simeq 10^{-8}$, the second term in Eq. (3.54) is negligible with respect to \hbar . Consequently, the phase shift with respect to the unperturbed trajectory is given by

$$\delta\Phi = \frac{eU_0\tau_0 D}{\hbar c_0} , \tag{3.56}$$

and is due to the electric flux enclosed between the stationary paths, as shown in Fig. 77(b).

In the experiment described above the electron has been acted upon by the x component of the electric field from the surface of the foil. In order to show that the phase shift in Eq. (3.56) is indeed due to the enclosed electric flux, let us suppose that when the electron is *inside* the sample we apply a potential $\varphi = -U_0$ of the type described in Sec. I.C, which does not give rise to supplementary electric fields acting upon the electron. This could be done, for example, by suppressing the surface charge distribution after the electron penetrated inside the foil, and reinstalling it before the electron left the foil, as represented in Fig. 78(a). In the new situation, the electron crossing the sample is acted upon by exactly the same fields as in the former case, but the potential in the foil is zero as long as the electron is crossing it. This means that the contribution given by Eq. (3.55) would vanish, and consequently the new total phase shift would be zero, as can be appreciated from Fig. 78(b). Thus the phase shift, Eq. (3.56), cannot be attributed to the presence of the x component of the electric field acting in the surface of the sample, and the observation of a shift of the interference fringes is sufficient to establish the reality of the quantum action of the enclosed electron flux.

Möllenstedt and Keller (1957) have actually used an asymmetric carbon foil with different thicknesses D_1, D_2 on the two sides of the biprism fiber. The only difference in the propagation of coherent electron waves arose from the increase by $(D_2 - D_1)/v$ in time spent by one of the beams in the region of the inner potential U_0 . According to Eq. (3.56), this should have resulted in a phase shift by $eU_0\tau_0(D_2 - D_1)/\hbar c_0$ of the relative phase of the interfering components. This phase shift would be proportional to the flux of the electric field, Eq. (1.78), through a space-time surface spanning the stationary paths connecting the electron source to the observing plane. The shift of the biprism interference fringes observed by Möllenstedt and Keller (1957) is shown in Fig. 79. Similar fringe shifts due to the core potential of various elements have been further observed by Langbein (1958) for carbon, Fert and Faget (1958) for carbon, Buhl (1959) for gold, silver, aluminum, and zinc sulfur, and Keller (1961)

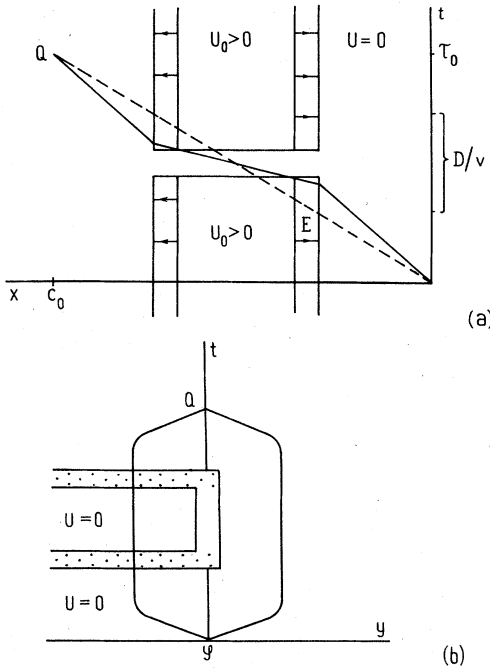


FIG. 78. Trajectory of an electron emitted by the source, which arrives at the point Q in the observing plane after a time interval τ_0 . It is assumed that after the electron penetrates inside the foil the surface charge distribution is suppressed, and later reinstated before the electron leaves the foil. Thus the scalar potential is zero when the electron is inside the foil. (a) The x, t projection of the path is not affected by the transient change of the charge distribution. (b) The y, t projection of the path, showing that the enclosed electric flux is equal to zero.

for carbon, aluminum, copper, silver, and gold. It is remarkable that although most of the work on the core potential of the elements was accomplished before the 1959 paper of Aharonov and Bohm, while the considerations of Ehrenberg and Siday (1949) were restricted to the quantum effects of magnetic fluxes, the observed fringe shifts

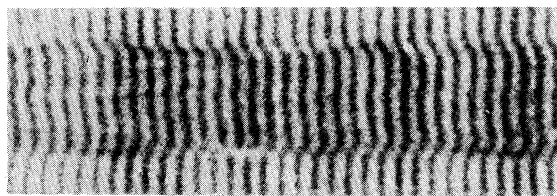


FIG. 79. Phase shift by π produced by a thin carbon foil, as observed by Möllenstedt and Keller (1957). The central horizontal part of the pattern corresponds to a strip of carbon foil having different thicknesses on the two sides of the biprism fiber, while the upper and lower parts of the pattern correspond to strips of carbon foil having the same thickness on both sides of the fiber. The resulting fringe shift demonstrates the quantum effects of electric fluxes.

discussed in this section provide an experimental proof of the quantum action of enclosed electric fluxes.

The contribution of the kinetic energy term, Eq. (3.54), to the classical action is essentially the same for the perturbed and unperturbed electron paths shown in Fig. 77(a); this fact represents a particular case of a more general situation. Thus let us consider the classical action for a particle of charge q and mass M , on a stationary path connecting the points \mathbf{r}_i, t_i and \mathbf{r}_f, t_f ,

$$S = \int_{t_i}^{t_f} \left[L_0 + \frac{q}{c} \mathbf{A} \cdot \mathbf{v} - q\varphi \right] dt, \quad (3.57)$$

where L_0 is the Lagrange function for the unperturbed motion, and φ, \mathbf{A} are the electromagnetic potentials describing the applied field distribution. For example, the unperturbed Lagrange function in a biprism experiment contains the kinetic energy term and the potential of the fiber, while φ and \mathbf{A} describe the electromagnetic fluxes. Let us denote by $\mathbf{r}_0(t)$ the unperturbed stationary paths, and by

$$\mathbf{r}(t) = \mathbf{r}_0(t) + \delta\mathbf{r}(t) \quad (3.58)$$

the perturbed stationary paths connecting the fixed points \mathbf{r}_i, t_i and \mathbf{r}_f, t_f . We determine the action on the perturbed path by substituting in Eq. (3.57) the formal expression of $\mathbf{r}(t)$, Eq. (3.58), and then developing L_0 in a series with respect to $\delta\mathbf{r}(t)$. Thus we have

$$L_0(\mathbf{r}, \dot{\mathbf{r}}) = L_0(\mathbf{r}_0, \dot{\mathbf{r}}_0) + \frac{\partial L_0}{\partial \mathbf{r}}(\mathbf{r}_0, \dot{\mathbf{r}}_0) \delta\mathbf{r} + \frac{\partial L_0}{\partial \dot{\mathbf{r}}} \delta\dot{\mathbf{r}} + \frac{1}{2} \left[\delta\mathbf{r} \frac{\partial}{\partial \mathbf{r}} + \delta\dot{\mathbf{r}} \frac{\partial}{\partial \dot{\mathbf{r}}} \right]^2 L_0(\mathbf{r}_0, \dot{\mathbf{r}}_0) + \dots \quad (3.59)$$

The contribution to the action of first-order terms in $\delta\dot{\mathbf{r}}$ can be transformed with the aid of an integration by parts into

$$\int_{t_i}^{t_f} \left[\frac{\partial L_0}{\partial \mathbf{r}_0} \delta\mathbf{r} + \frac{\partial L_0}{\partial \dot{\mathbf{r}}_0} \delta\dot{\mathbf{r}} \right] dt = \int_{t_i}^{t_f} \left[\frac{\partial L_0}{\partial \mathbf{r}_0} - \frac{d}{dt} \frac{\partial L_0}{\partial \dot{\mathbf{r}}_0} \right] \delta\mathbf{r} dt + \frac{\partial L_0}{\partial \dot{\mathbf{r}}_0} \delta\mathbf{r} \Big|_{t_i}^{t_f} \quad (3.60)$$

This contribution is equal to zero, because the Lagrange equations are fulfilled on the stationary path $\mathbf{r}_0(t)$, and moreover the end points are fixed so that $\delta\mathbf{r}(t_i) = 0$ and $\delta\mathbf{r}(t_f) = 0$. Now the path correction contains terms that are at least proportional to the applied fields. The contribution of the term L_0 to the action, obtained by integration along the perturbed path is equal to the contribution of L_0 obtained by integration along the unperturbed path, up to quadratic terms in the applied field. Since the area of the surface spanning the perturbed and unperturbed paths is of the order of $\delta\mathbf{r}$, the integral

$$\int_{t_i}^{t_f} (q \mathbf{A} \cdot \mathbf{v} / c - q\varphi) dt$$

also has the same value for perturbed and unperturbed paths, up to quadratic terms in the applied fields. We

conclude that the shift δS of the action of a particle moving on a stationary trajectory between the fixed points \mathbf{r}_i, t_i and \mathbf{r}_f, t_f , produced by the distribution of electromagnetic potentials $\varphi \mathbf{A}$, is equal, up to quadratic terms in the applied fields, to the integral of the potentials along the unperturbed stationary path connecting the points \mathbf{r}_i, t_i and \mathbf{r}_f, t_f ,

$$\delta S = \frac{q}{c} \int_{\mathbf{r}=\mathbf{r}_0(t)} (\mathbf{A} d\mathbf{r} - \varphi c dt). \quad (3.61)$$

In the case of a two-slit interference experiment, the point \mathbf{r}_i, t_i would correspond to the source of electrons and \mathbf{r}_f, t_f to a given point in the observing plane; moreover, there would be two stationary paths connecting \mathbf{r}_i, t_i and \mathbf{r}_f, t_f . Then the relative shift of the classical action corresponding to these paths would be given by the electromagnetic flux enclosed in the loop formed by the unperturbed stationary paths,

$$\delta S_1 - \delta S_2 = \frac{q}{c} \oint (c\varphi dt - \mathbf{A} d\mathbf{r}). \quad (3.62)$$

The field strengths acting in the region of the stationary paths and the electromagnetic flux enclosed between these paths are independent quantities, in the sense that we can alter the amount of enclosed flux while conserving the fields acting in the vicinity of the paths. Thus Eq. (3.62) means that any shift of the interference fringes observed at a fixed point in the observing plane, which depends linearly on the applied intensities, constitutes a manifestation of the quantum action of the electromagnetic flux enclosed between the stationary paths. The shifts produced by uniform field distributions, discussed in Sec. III.B, and the shifts produced by the inner potential of thin foils, discussed in the present section, are in this category, and another example will be considered in the next section.

A consequence of the fact that the relative phase shift observed at a fixed point in the observing plane is proportional to the enclosed flux is that an alternating flux which produces a shift of the order of π or larger will destroy the interference pattern. This fact was verified by Chambers (1960) and by Schaal, Jönsson, and Krimmel (1966). It is interesting to consider in this context the effect on the interference pattern of uniform distributions of electric or magnetic fields acting along the entire path of the particle from source to observing plane. In the case of the interference of particles of charge q coherently emitted by two virtual sources \mathcal{S}_1 and \mathcal{S}_2 , an electric field E applied as shown in Fig. 80(a) shifts the envelope of the pattern by $\delta_E = qEc_0^2/2Mv^2$. According to Eq. (3.62), the electric field will shift the relative phase at a point Q in the observing region with respect to the relative phase at Q in the absence of the field by $qEac_0/2\hbar v$. However, since the distance between consecutive fringes is $f_0 = 2\pi\hbar c_0/Mav$, the difference between relative phases at the points Q_0 and Q shown in Fig. 80(a) is equal to $2\pi\delta_E/f_0 = qEac_0/2\hbar v$. Thus the relative phase at the point Q in the presence of the electric field is equal to the relative phase at the point Q_0 in the absence of the field, i.e., the interference pattern is shifted by the uniform electric field as a whole.

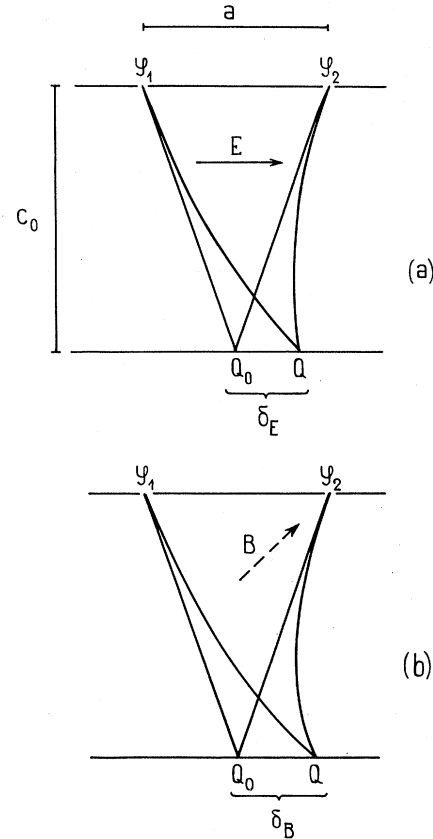


FIG. 80. (a) Action of a uniform electric field E , and (b) action of a uniform magnetic field B on a two-slit interference pattern. The shift of relative phase produced by the enclosed electromagnetic flux at the point Q is compensated for by the displacement of the observing point from Q_0 to Q , so that the position of the fringes relative to the envelope of the pattern is not affected by the applied fields.

A similar conclusion can be reached in the case of a uniform magnetic field B acting on the interfering particles along their entire path, as shown in Fig. 80(b). In this case the envelope is displaced by $\delta_B = qBc_0^2/2Mvc$. According to Eq. (3.62), the magnetic field will shift the relative phase of the two beams by $qBc_0a/2\hbar c$. In the same time, the difference between the relative phases at the points Q_0 and Q is $2\pi\delta_B/f_0 = qBc_0a/2\hbar c$. In this case, too, the relative phase at the point Q in the presence of the magnetic field is equal to the relative phase at the point Q_0 in the absence of the field, so that the position of the fringes with respect to the envelope is not affected by the applied magnetic field. The same conclusion was reached in Sec. I.B for electric and magnetic fields acting over regions having the form of strips crossed by the coherent beams.

The fact that the flux-dependent phase shift is compensated for by the displacement of the observing point was pointed out by Werner and Brill (1960). This compensating mechanism does not, however, lead to stability of the

interference pattern for alternative electromagnetic fluxes, as suggested by Werner and Brill (1960), but, on the contrary, the resulting overall displacement of the fringe system completely destroys the pattern for amplitudes of the enclosed flux larger than π . A detailed analysis of the problem of alternating fluxes, and its relevance for the electron interference experiment of Marton, Simpson, and Suddeth (1954), which reportedly was performed in the presence of stray 60-cycle magnetic fields, can be found in the review article by Greenberger and Overhauser (1979).

H. Effects of gravitational flux on the quantum interference of neutrons

Since the Hamiltonian of a particle of mass M moving in the Earth's gravitational field g is analogous to the Hamiltonian of a particle of charge q interacting with a uniform electric field E , the relative phase of two interfering beams could be shifted not only by the enclosed electric flux, but also by an enclosed gravitational flux. The possibility of an experimental test of gravitational effects in the quantum interference of neutrons was first suggested by Overhauser and Colella (1974), in the context of the successful construction of a neutron interferometer by Rauch, Treimer, and Bonse (1974). The predicted existence of a fringe shift due to the Earth's gravitational flux enclosed between two coherent neutron beams at different heights was experimentally confirmed by Colella, Overhauser, and Werner (1975) with the aid of an interferometer cut from a dislocation-free silicon crystal. The positive outcome of this experiment demonstrates that the concept of flux is relevant in the case of gravitational interaction, too.

The neutron interferometer used by Colella, Overhauser, and Werner (1975), shown schematically in Fig. 81, is analogous to the Mach interferometer for optical frequencies. An incident neutron beam is split by the first crystal slab into the transmitted and reflected beams AB and AC . These beams are further split by the second crystal slab, and the resulting components CD and BD are once more diffracted by the third slab, as shown in Fig. 81. In order to evaluate the effects of these successive splittings on the neutron beam, let us first consider the problem of a neutron beam incident on a cubic crystal, as shown in Fig. 82. If the scattering planes are perpendicular to the face of the crystal, the incident wave

$$\psi_n = e^{ik_\xi \xi + ik_\eta \eta} \tag{3.63}$$

is split inside the crystal into two standing waves along the y direction,

$$\psi_n = \psi_n^{(1)} + \psi_n^{(2)},$$

where

$$\psi_n^{(2)} = e^{ik_\xi \xi} \cos k_\eta \eta, \tag{3.64a}$$

and

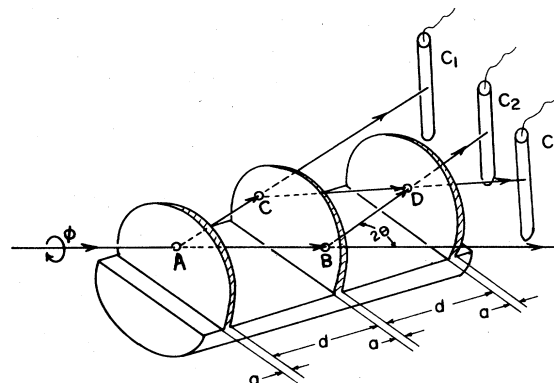


FIG. 81. Neutron interferometer cut from a dislocation-free silicon crystal, used by Colella, Overhauser, and Werner (1975) to observe the fringe shift due to the earth's gravitational flux enclosed between the coherent beams ABD and ACD . High-pressure ^3He detectors were used to monitor the beams C_1 , C_2 , and C_3 . The interferometer could be rotated by an angle Φ about the incident direction, thereby altering the amount of gravitational flux enclosed between the beams. The dimensions were $d=3.5$ cm and $a=2$ mm.

$$\psi_n^{(1)} = ie^{ik_\xi \xi} \sin k_\eta \eta. \tag{3.64b}$$

It can be shown that the wave number k_η is related to the lattice constant a_η by $|k_\eta| = \pi/a_\eta$, which represents the Bragg condition for getting a scattered wave. A justification of this relation, as well as a more detailed analysis of the propagation of neutrons through a thick crystal, can be found in the article of Greenberger and Overhauser (1979). The standing wave $\psi_n^{(2)}$ is centered at the atomic sites, where we have assumed that the atoms are located at $\eta = Na_\eta$, $N=0, \pm 1, \dots$, and as this wave is propagating in the ξ direction, it interacts relatively strongly with the crystal. On the other hand, the standing wave $\psi_n^{(1)}$ is centered between the atoms, and it can traverse the crystal relatively undisturbed. Consequently, when the beam reaches the opposite face of the crystal, it will have the form

$$\psi_n = \psi_n^{(1)} + be^{i\beta} \psi_n^{(2)}, \tag{3.65}$$

where the constants b and β depend on the substances and thickness of the crystal. In most experiments on neutron interference the absorption of neutrons can be neglected, so that we shall assume that $b=1$. Then the wave, Eq. (3.65), becomes

$$\psi_n = \frac{1}{2}(1 + e^{i\beta})e^{ik_\xi \xi + ik_\eta \eta} + \frac{1}{2}(1 - e^{i\beta})e^{ik_\xi \xi - ik_\eta \eta}. \tag{3.66}$$

The first term in Eq. (3.66) represents the transmitted wave, whose amplitude is proportional to $\cos(\beta/2)$, and the second term gives the reflected wave, whose amplitude is proportional to $\sin(\beta/2)$. The total intensity emerging

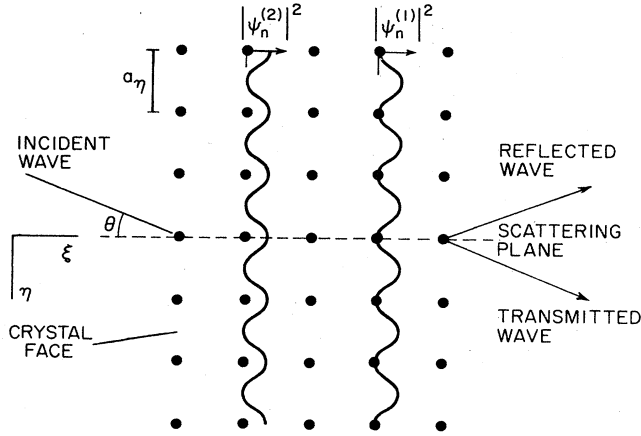


FIG. 82. Incident neutron beam scattered by a plane perpendicular to the crystal face. The incident wave is split inside the crystal into two standing waves in the y direction, ψ_1 , which is centered between the atoms, and ψ_2 , which is centered at the atomic sites. These waves are propagating inside the crystal in a direction normal to the face of the crystal. When these beams reach the opposite face of the crystal, they give rise to the transmitted and reflected waves.

from the crystal is equal to $\cos^2(\beta/2) + \sin^2(\beta/2) = 1$, the incident intensity.

Let us now consider the unperturbed interference of neutrons, in a region where the gravitational field is zero. The successive application of Eq. (3.66) for the first and second crystal slab shown in Fig. 81 yields the amplitudes of the beams CD and BD incident on the third slab as $-\sin^2(\beta/2)\exp(i\mu)$ and $-i\sin(\beta/2)\cos(\beta/2)\exp(i\nu)$, respectively. A further application of Eq. (3.66) finally yields the intensities of beams 2 and 3 as

$$I_2 = \sin^6 \frac{\beta}{2} + \sin^2 \frac{\beta}{2} \cos^4 \frac{\beta}{2} - \sin^3 \frac{\beta}{2} \cos \frac{\beta}{2} \sin \beta \cos(\mu - \nu), \quad (3.67a)$$

$$I_3 = 2 \sin^4 \frac{\beta}{2} \cos^2 \frac{\beta}{2} + \sin^3 \frac{\beta}{2} \cos \frac{\beta}{2} \sin \beta \cos(\mu - \nu). \quad (3.67b)$$

We see that the sum $I_2 + I_3$ is independent of the phase difference $\mu - \nu$, while $I_2 - I_3$ has the form

$$I_2 - I_3 = \sin^2 \frac{\beta}{2} \cos^2 \beta - \sin^2 \frac{\beta}{2} \sin^2 \beta \cos(\mu - \nu). \quad (3.68)$$

If the neutron interferometer is oriented in a gravitational field g which makes an angle Φ with the normal to the plane $ABCD$ (see Fig. 81), it can be shown that in a first-order approximation the relative phases of the beams arriving at the counters C_2 and C_3 are not affected by the *bending* of the paths, produced by the gravitational field (Overhauser and Colella, 1974). There will, however, be a

phase shift arising from the difference in the gravitational potential of the regions traversed by the upper and lower beams. This phase shift is given by the integral $(M/\hbar) \oint \varphi_g dt$ over the loop $ABCD$, where φ_g is the gravitational potential,

$$\varphi_g = -gr.$$

By taking into account the fact that the velocity of the neutrons inside the crystal is $v \cos \theta$ when their velocity in the free space is v , it can be shown that the gravitational phase shift δ_g is given by (Greenberger and Overhauser, 1979)

$$\delta_g = \frac{2Mg \sin \Phi d^2}{\hbar v} \tan \theta \left(1 + \frac{a}{d} \right). \quad (3.69)$$

If the interferometer is symmetric, then the phase difference in Eq. (3.68) is entirely of gravitational origin, $\mu - \nu = \delta_g$, and the expression of the intensity $I_2 - I_3$ becomes

$$I_2 - I_3 = \mathcal{A} - \mathcal{B} \cos \delta_g, \quad (3.70)$$

where $\mathcal{A} = \sin^2(\beta/2)\cos^2\beta$ and $\mathcal{B} = \sin^2(\beta/2)\sin^2\beta$. The gravitational phase difference δ_g can be altered by rotating the interferometer about the incidence direction by an angle Φ . In the experiment of Colella, Overhauser, and Werner (1975), the neutron wavelength was $\lambda = 1.44 \text{ \AA}$, the Bragg angle $\theta = 22.1^\circ$, the dimensions $a = 0.2 \text{ cm}$, and $d = 3.5 \text{ cm}$, so that a rotation of the interferometer by 180° would produce, according to Eqs. (3.69) and (3.70), a shift of about 19 fringes.

The existence of the gravitationally dependent fringe shift, Eq. (3.69), was confirmed by Colella, Overhauser, and Werner (1975), who measured the difference count $I_2 - I_3$ as a function of the interferometer rotation angle Φ , as shown in Fig. 83. In accordance with Eq. (3.70), the pattern of $I_2 - I_3$ has a minimum when the interference plane $ABCD$ is normal to the gravitational field. This experiment demonstrates that the enclosed gravitational flux does affect the relative phase of two coherent massive beams, the existence of the fringe shift being in principle independent of the presence of field strengths acting in the vicinity of the stationary paths.

An interference experiment testing the existence of an electromagnetic Aharonov-Bohm effect for neutrons was performed by Greenberger, Atwood, Arthur, Shull, and Schlenker (1981), and no measurable phase shift was found upon reversal of an enclosed magnetic flux. This confirms the fact that for a neutral particle there is no direct coupling to the electromagnetic flux.

Another possible source of enclosed flux is the Dirac string. However, Goddard and Olive (1978) have pointed out that as a result of Dirac's quantization condition, the magnetic flux gives rise to no observable Aharonov-Bohm effect. An exact solution of the Schrödinger equation in Aharonov-Bohm and Dirac monopole potentials has been reported by Roy and Singh (1983).

Conservation of isotopic spin suggests, although it does not require, the eventual existence of an isotopic spin

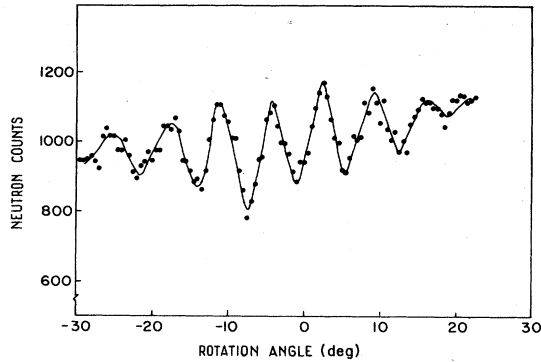


FIG. 83. Difference in neutron count $I_2 - I_3$ as a function of the interferometer rotation angle Φ , as observed by Colella, Greenberger, and Overhauser (1975). The intensities of the beams I_2 and I_3 are measured at fixed points in the observing region; the interference extremes observed at various interferometer rotation angles are due to modification of the gravitational flux enclosed by the stationary paths of the neutron interferometer.

gauge field. Wisnivesky and Aharonov (1967) and Wu and Yang (1975) have considered an interference experiment that would test the reality of this gauge field. However, the conditions necessary to perform the experiment are rather restrictive.

Finally, the existence of an Aharonov-Bohm effect for more general solutions of the gravitational field equations has been discussed by Wisnivesky and Aharonov (1967), Dowker (1967), Papini (1967), Krauss (1968), Anandan (1977,1979), and Ford and Vilenkin (1981).

IV. PHYSICAL SIGNIFICANCE

A. Concept of the nonintegrable phase factor in electromagnetism

The forces with which two charged particles interact are not in general equal and opposite, and therefore the momentum and energy of the individual particles are not conserved. Moreover, in a theory of electromagnetism based exclusively on the kinematical state of the charged particles, the interactions are distant in space and remote in time. A local, conservative picture of the electromagnetic effects, however, becomes possible if we ascribe a certain amount of momentum and energy to the electromagnetic field that fills the region of space between the charged particles. The properties of this electromagnetic continuum can be studied by observing its action on test charged particles. Its effects on a massive particle, with predominantly classical evolution, are determined by the force \mathbf{F} acting on the test particle. By separating out the velocity-dependent part of the force, we are able to characterize the electromagnetic field completely by the electric and magnetic field strengths \mathbf{E} and \mathbf{B} ,

$$\mathbf{F} = q\mathbf{E} + \frac{q}{c}\mathbf{v} \times \mathbf{B}. \quad (4.1)$$

The field strengths \mathbf{E} and \mathbf{B} are in turn generated by the distributions of charge and current throughout the space. Maxwell's equations for the electromagnetic field are often solved conveniently in terms of the electromagnetic potentials φ, \mathbf{A} ,

$$\mathbf{E} = -\nabla\varphi - \frac{1}{c}\frac{\partial\mathbf{A}}{\partial t}, \quad (4.2a)$$

$$\mathbf{B} = \nabla \times \mathbf{A}. \quad (4.2b)$$

While a distribution of potentials uniquely specifies the field strengths \mathbf{E}, \mathbf{B} , a given distribution of electromagnetic fields can be described by infinitely many choices of the potentials φ, \mathbf{A} , which differ by the derivatives of an arbitrary function of position and time,

$$\varphi' = \varphi - \frac{1}{c}\frac{\partial f}{\partial t}, \quad (4.3a)$$

$$\mathbf{A}' = \mathbf{A} + \nabla f. \quad (4.3b)$$

Due to the arbitrariness of the gauge function f , we must conclude that the potentials have no physical significance at the classical level of description of the interaction.

If the quantum-classical properties of the test particle are significant, the equations of motion based on the Lorentz force must be replaced by the Schrödinger equation for the wave function Ψ of the test particle,

$$i\hbar\frac{\partial\Psi}{\partial t} = -\frac{\hbar^2}{2M}\Delta\Psi + \frac{iq\hbar}{Mc}\mathbf{A}\nabla\Psi + \frac{iq\hbar}{2Mc}\text{div}\mathbf{A}\Psi + \frac{q^2}{2Mc^2}\mathbf{A}^2\Psi + q\varphi\Psi. \quad (4.4)$$

Since the electromagnetic potential enters explicitly in the Schrödinger equation (4.4), the possibility that the potentials possess a certain degree of physical relevance cannot be excluded *a priori*. However, it can be checked by a direct calculation that a change in the gauge of the potentials, Eqs. (4.3), is accompanied by a phase transformation of the wave function,

$$\Psi' = \Psi \exp\left[\frac{iqf}{\hbar c}\right], \quad (4.5)$$

which leaves invariant the probability distribution and the energy and momentum distributions of the particle. Since, even in quantum mechanics, energy and momentum effects depend on the direct action of the field strengths on the charged particle, it was thought that the primary quantities describing the electromagnetic continuum were still the electric and magnetic field strengths \mathbf{E} and \mathbf{B} , while no physical significance could be attributed to the electromagnetic potentials.

Electromagnetic effects with a classical analog are observable to the extent that there is a nonvanishing overlap between the probability distribution of the charged particle and the applied field strengths. The remarkable thing about the quantum effects described by Ehrenberg and Si-

day (1949) and by Aharonov and Bohm (1959) is that the effects of the electromagnetic fluxes remain observable even when the overlap between the probability distribution $\Psi\Psi^*$ and the field strengths \mathbf{E} and \mathbf{B} is rendered arbitrarily small. The reality of these effects means that a knowledge of the field strengths in regions where the probability $\Psi\Psi^*$ has finite values is not in general sufficient to determine completely the evolution of the quantum-mechanical state of a charged particle. While the phase of the wave function is finite, even in the region of the enclosed fluxes where the probability distribution eventually becomes very small, the concept of local action of the field strengths, as generally understood, refers to the overlap between the probability $\Psi\Psi^*$ and the field strengths, and not to the overlap between the phase of the wave function and the field strengths. Since the state of a charged particle can be influenced by electric and magnetic fluxes in regions where the particle never passed, we conclude that a picture of electromagnetism based on the *local* action of the field strengths is not possible in quantum mechanics.

The previous considerations raise the question of what constitutes an intrinsic and complete description of electromagnetism. The Aharonov-Bohm experiment shows that in a multiply connected region where the field strengths are zero, the observable electromagnetic effects depend periodically on the integral

$$\frac{q}{\hbar c} \oint (c\varphi dt - \mathbf{A} d\mathbf{r}) \quad (4.6)$$

around an unshrinkable loop. An examination of the Aharonov-Bohm experiment led Yang (1974) and Wu and Yang (1975) to the conclusion that the physically meaningful quantity characterizing the electromagnetic interaction in quantum mechanics is the phase factor

$$R = \exp \left[\frac{iq}{\hbar c} \oint (c\varphi dt - \mathbf{A} d\mathbf{r}) \right], \quad (4.7)$$

which can be taken as the basis of a description of electromagnetism. According to Eqs. (1.77) and (1.78), the integral $\oint (c\varphi dt - \mathbf{A} d\mathbf{r})$ is equal to the electromagnetic flux through the closed loop, so that the quantity R in Eq. (4.7) may be termed the reduced electromagnetic flux. In a simply connected region of space, specifying the reduced flux is equivalent to knowing the field strengths in that region. However, in a multiply connected space the specification of the nonintegrable phase factor, Eq. (4.7), for loops on the boundary of the accessible region is not sufficient to determine the distribution of electric and magnetic fields in the inaccessible region. The gauge-independent quantity R , Eq. (4.7), does not determine the electromagnetic potentials in the accessible region either. Thus the degree of detail provided in the accessible region by the nonintegrable phase factor is intermediate between that provided by the field strengths, which underdetermine the state of the electromagnetic continuum in that region, and that provided by the potentials, which overdescribe it.

As pointed out by Wu and Yang (1975), it is convenient to consider the concept of a phase factor for any path connecting two points P and Q ,

$$R_{PQ} = \exp \left[\frac{iq}{\hbar c} \int_P^Q (c\varphi dt - \mathbf{A} d\mathbf{r}) \right]. \quad (4.8)$$

The evolution of the state of a charged particle in terms of the phase factor, Eq. (4.8), is then described by the path-integral formalism discussed in Sec. I.A. The expression of the propagator, Eq. (1.13), can be readily transformed into

$$K(Q,P) \sim \int R_{QP} \exp \left[\frac{i}{\hbar} S_0(Q,P) \right] \mathcal{D}\mathbf{r}(\tau), \quad (4.9)$$

where R_{PQ} is the phase factor defined in Eq. (4.8), and

$$S_0(Q,P) = \int_P^Q \frac{1}{2} M \mathbf{v}^2 dt \quad (4.10)$$

is the unperturbed classical action between P and Q . The form of the propagator, Eq. (4.9), demonstrates that electromagnetic effects in quantum mechanics do indeed depend periodically on path integrals of the potentials. The nonintegrable phase factor also depends on the charge q of the particle and on the number of turns of a given path around the enclosed flux. Therefore the quantity R is not a pure field variable, but rather describes the dynamical interaction between the particle and the flux.

In the idealized case of a multiconnected space, where the separation between the accessible region and the enclosed fluxes is rigorous, the observable effects are periodic functions of the amount of enclosed flux. On the other hand, a certain degree of penetration of the particle into the region of the field strengths results in small corrections to the wave function, depending on the detailed field distribution in the shielded region. The essence of the quantum effects of enclosed fluxes is, however, the *persistence* of finite observable effects in the limit when direct contact between the incident particles and the field strengths becomes vanishingly small, a circumstance emphasized by Greenberger (1981).

B. Action of the nonintegrable phase factor on the parity of charged particles

A major consequence of the observation of quantum effects of the fluxes by Ehrenberg and Siday (1949) and Aharonov and Bohm (1959) is that we now realize that a knowledge of the field strengths in restricted regions of space is not sufficient to completely determine electromagnetic effects in quantum mechanics. An examination of the Aharonov-Bohm experiment led Wu and Yang (1975) to the conclusion that electromagnetism is the gauge-invariant manifestation of the nonintegrable phase factor

$$R = \exp \left[\frac{iq}{\hbar c} \int (c\varphi dt - \mathbf{A} d\mathbf{r}) \right].$$

While the field strengths do produce changes in the energy and momentum of the charged particles, such effects are primarily independent of the enclosed electromagnetic flux. In an attempt to identify the kinematical quantity whose average should be directly influenced by the enclosed flux, we consider in this section the gauge-independent, space-time property

$$I = \int \Psi^*(Q)\Psi(Q_+) \exp \left[\frac{iq}{\hbar c} \int_{Q_+}^Q \mathbf{A} \cdot d\mathbf{s} \right] d^3Q, \quad (4.11)$$

where the points $Q = (\mathbf{r}, t)$ and $Q_+ = (\mathbf{r}_+, t)$ are symmetric with respect to an arbitrary plane Π ; this generalizes the concept of parity of a square-integrable state Ψ with respect to the plane Π for the case of a nonvanishing distribution of electromagnetic fields. We show that the quantity I can be expressed as an average of the nonintegrable phase factor, Eq. (4.8), over all paths PQQ_+T connecting the points P, T in the incidence region, at the initial time t_0 , to the points Q, Q_+ in the region where I is being observed at the time t . In the case of scattering by an infinite magnetic string carrying the flux F , we find that the parity of a state that was symmetric in the incidence region becomes approximately $\cos(eF/\hbar c)$ in the observing region behind the string. The measurement of the parity of a free state is briefly discussed.

The fact that electromagnetic effects in quantum mechanics depend on path integrals of the potentials becomes apparent if we express the wave function at the time t in terms of the wave function at a previous time t_0 with the aid of a propagator K ,

$$\Psi(Q) = \int K(Q, P)\Psi(P)d^3P, \quad (4.12)$$

where P and Q denote the space and time coordinates, $P = (\mathbf{r}_0, t_0)$ and $Q = (\mathbf{r}, t)$. According to Eq. (4.9), the propagator $K(Q, P)$ is proportional to the exponential of the classical action multiplied by i/\hbar , summed over all paths $\mathbf{r}(\tau)$ connecting the points P and Q . The dominant contribution to the state arises from those paths for which the total classical action in the expression of the propagator is stationary. If for the situation under consideration there is a single stationary path connecting the points P and Q in the incidence and observing regions, respectively, then the final state is essentially determined by the field strengths. On the other hand, in cases where there are several stationary paths connecting the points P and Q , a knowledge of the field strengths in the vicinity of these paths becomes insufficient, and a description of the process of interaction must be supplemented by the specification of the nonintegrable phase factor R corresponding to the loops formed by pairs of such stationary paths.

Now in a field-free region of the space, the parity I_0 of a state Ψ with respect to a certain plane Π is the average value of the operator \hat{I}_0 defined as

$$\hat{I}_0\Psi(Q) = \Psi(Q_+),$$

where the points $Q = (\mathbf{r}, t)$ and $Q_+ = (\mathbf{r}_+, t)$ are symmetrical with respect to the plane Π . The parity

$$I_0 = \langle \Psi | \hat{I}_0 | \Psi \rangle, \quad (4.13)$$

which takes values in the range $-1-1$, can also be written as

$$I_0 = \int \rho(Q)\rho(Q_+) \exp \left[i \int_Q^{Q_+} \nabla\Phi \cdot d\mathbf{s} \right] d^3Q, \quad (4.14)$$

where the integration in the exponential is performed on the straight line connecting the points Q, Q_+ , and

$$\Psi(Q) = \rho(Q) \exp[i\Phi(Q)].$$

While Eq. (4.13) is applicable only in field-free regions of space, a gauge-invariant expression of the parity can be obtained by replacing $\nabla\Phi$ in Eq. (4.14) by the kinetic momentum

$$M\mathbf{v} = \hbar\nabla\Phi - \frac{q}{c}\mathbf{A}.$$

Thus, in the presence of an arbitrary distribution of electromagnetic fields, the parity of the state Ψ with respect to the plane Π is given by

$$I = \rho(Q)\rho(Q_+) \exp \left[\frac{i}{\hbar} \int_Q^{Q_+} M\mathbf{v} \cdot d\mathbf{s} \right] d^3Q,$$

which is equivalent to Eq. (4.11).

The parity of the state $\Psi(Q)$ can be obtained from the initial wave function and the electromagnetic field distribution by substituting in Eq. (4.11) the expression for the state $\Psi(Q)$, Eqs. (4.12) and (4.9),

$$I = \int R_{PQQ_+T} \exp \{ (i/\hbar) [S_0(Q_+, T) - S_0(Q, P)] \} \times \Psi^*(P)\Psi(T) \mathcal{D}_{\mathbf{r}_{PQ}}(\tau) \mathcal{D}_{\mathbf{r}_{TQ_+}}(\tau) d^3P d^3T d^3Q, \quad (4.15)$$

where R_{PQQ_+T} is the nonintegrable phase factor, Eq. (4.8), corresponding to the path PQQ_+T shown in Fig. 84, and P and T are points in the incidence region, at the time t_0 . The integrals are convergent provided that the state at the time t_0 is represented by a square-integrable wave function. If the spatial dimensions of the region of the field strengths are finite, and if the state at the time t_0 is assumed to be in a field-free region, then the potentials are vanishing in that region, and the integral appearing in the phase factor R , Eq. (4.14), can be completed by the path PT without changing its value. While any asymmetry in the electromagnetic fields would in principle modify the parity of the state of the particle onto which they are acting, the remarkable property of Eq. (4.15) is related to the form taken by the parity effects of the electromagnetic fields, namely that it represents an average of the nonintegrable phase factor, Eq. (4.7), over all paths connecting the field-free incidence region to the region where I is being observed. Thus Eq. (4.15) shows that the nonintegrable phase factor acts as a source of parity changes, analogously to the way in which the force is a source of momentum changes.

We have assumed thus far that the electromagnetic potentials are given functions of space and time. If the

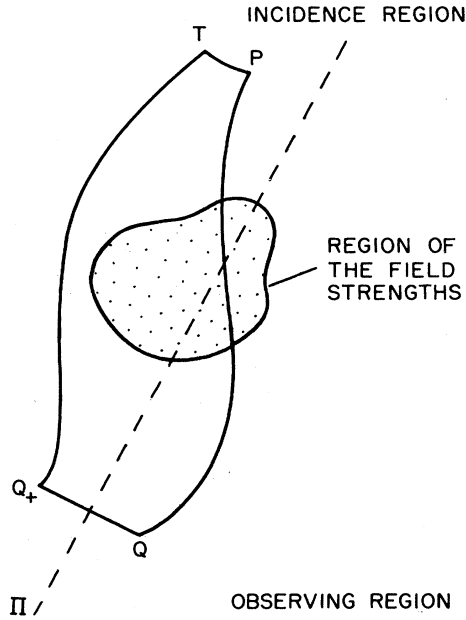


FIG. 84. Parity of the final state with respect to the plane Π , evaluated with the path-integral formalism. The parity of the final state is an average of the nonintegral phase factor R_{PQ_+TP} , for all positions of the points P, T in the field-free incidence region and Q in the observing region, where the positions of the points Q and Q_+ are symmetrical with respect to the plane Π .

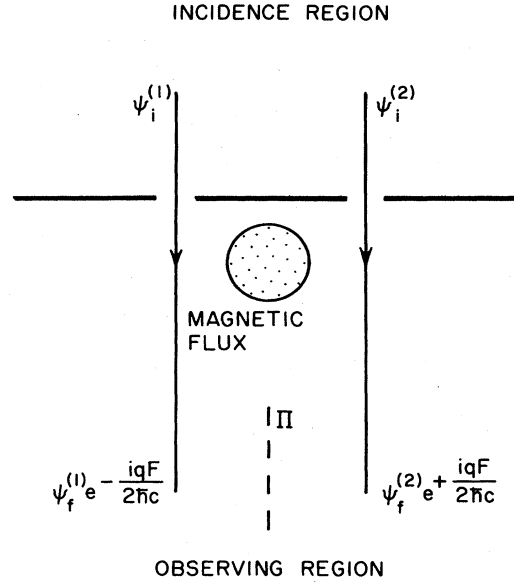


FIG. 85. Aharonov-Bohm scattering by a magnetic flux. In the absence of the flux the symmetric components $\psi_i^{(1)}$ and $\psi_i^{(2)}$ of the incident state evolve, respectively, into the final components $\psi_f^{(1)}$ and $\psi_f^{(2)}$. The presence of the magnetic flux F shifts the phases of these components by $\pm qF/2\hbar c$, thereby changing the parity of the state of the particle with respect to the plane Π by a factor of $\cos(qF/\hbar c)$.

sources of the electromagnetic fields were included in the analysis, then the parity of the whole system would be conserved during the interaction. This means that not only would the parity of the incident particle be affected by interaction with the enclosed fluxes, but the passage of the incident particle would also change the state of parity of the particles in the source. The parity of the state of the charged particles in a source of enclosed flux is in general zero, so that the conservation of the total parity in such cases bears no special significance.

As an example, let us consider Aharonov-Bohm scattering by an infinite magnetic string. In its conventional realization, Aharonov-Bohm scattering takes place in a two-slit interference experiment modified by the presence, in the inaccessible region between the slits, of a certain amount of magnetic flux, as shown in Fig. 85. In the absence of the flux the components $\psi_i^{(1)}$ and $\psi_i^{(2)}$ of the incident state

$$\psi_i = \psi_i^{(1)} + \psi_i^{(2)} \tag{4.16}$$

give rise, respectively, to the components $\psi_f^{(1)}$ and $\psi_f^{(2)}$ of the final state

$$\psi_f = \psi_f^{(1)} + \psi_f^{(2)}. \tag{4.17}$$

The presence of the magnetic flux F shifts the phase of the coherent components by $\pm qF/2\hbar c$, so that the expression of the flux-dependent state in the observing region becomes

$$\tilde{\psi}_f = \psi_f^{(1)} e^{-iqF/2\hbar c} + \psi_f^{(2)} e^{iqF/2\hbar c}. \tag{4.18}$$

The symmetry plane for the unperturbed scattering is perpendicular to the plane of the slits, and the intersection of these planes coincides with the z axis, situated midway between the two parallel slits. Let us choose as plane Π the symmetry plane defined above, and assume for simplicity that the components $\psi_i^{(1)}$ and $\psi_i^{(2)}$ are two wave packets, symmetric with respect to Π , and orthogonal because of their different localization. Then, since the unperturbed Hamiltonian commutes with the operator \hat{I}_0 for the aforementioned choice of plane Π , the parity I_0 is conserved during flux-free scattering by the two parallel slits,

$$\langle \psi_f | \hat{I}_0 \psi_f \rangle = \langle \psi_i | \hat{I}_0 \psi_i \rangle. \tag{4.19}$$

However, the parity will no longer be conserved in the presence of the magnetic flux, and it can be shown that the parity in the observing region has approximately the form

$$\langle \tilde{\psi}_f | \tilde{I}_0 \tilde{\psi}_f \rangle \cong \langle \psi_i | \hat{I}_0 \psi_i \rangle \cos(qF/\hbar c), \tag{4.20}$$

which, as discussed in Sec. II.B, is correct up to terms exponentially small in the square of the ratio of the separation between the coherent packets to their widths. Thus the parity of the final state, Eq. (4.18), is a periodic function of the amount of enclosed flux F , and in particular, a

flux of the $\pi\hbar c/q$ transforms an even state into an odd state, and conversely. It can be shown also that in the case of scattering of a plane wave by a magnetic string, the parity of the final state depends on the enclosed magnetic flux F in a manner similar to that in Eq. (4.20).

The parity of a free state can be measured, for example, with the setup shown in Fig. 86. The observed state is split in two coherent components, one of which is subject to an inversion produced by the cylindrical lens L . The beams are then recombined, and the resulting intensities are monitored by the counters C_1 and C_2 , situated at twice the focal distance from the lens L . By a suitable calibration of the beam splitters it can be arranged that the wave functions at the two counters C_1 and C_2 be, respectively, $\Psi + \hat{I}_0\Psi$, and $\Psi - \hat{I}_0\Psi$, so that the difference between the two signals is proportional to the parity of the state with respect to the plane Π ,

$$C_1 - C_2 \sim \langle \Psi | \hat{I}_0 \Psi \rangle .$$

If the observed state were the superposition of wave packets described in Eq. (4.18), the parity of that state would depend on the flux F , although the probability distribution of the state $\tilde{\psi}_f$ is practically independent of F .

The meaning of angular momentum for systems composed of magnetic sources and electric charges, as well as the nature of phases that affect the statistics of indistinguishable objects, was recently discussed by Goldhaber (1982). Goldhaber (1982) and Wilczek (1982b) have pointed out that such composites have unusual statistics, interpolating continuously between bosons and fermions. Silverman (1983) remarked that if a charged spinless boson orbiting a solenoid were to be observed behaving under rotations like a fermion, that would be equivalent to the quantization of the canonical angular momentum in integer multiples of \hbar .

While the average value of any observable quantity can

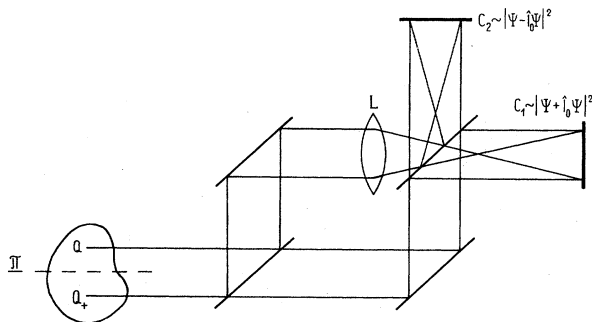


FIG. 86. Measurement of the parity I_0 of a free state. The observed state is split into two coherent components, one of which is subject to an inversion produced by the cylindrical lens L . The beams are then recombined and the resulting intensities are monitored by the counters C_1 and C_2 , situated at twice the focal distance from the lens L . It can be arranged that the wave functions in the region of the counters be $\Psi \pm \hat{I}_0\Psi$, so that the difference of the two signals is proportional to the parity of the state Ψ with respect to the plane Π , $C_1 - C_2 \sim \langle \Psi | \hat{I}_0 \Psi \rangle$.

in principle be expressed in terms of path integrals of the potentials, the average kinetic energy and momentum are not affected by enclosed fluxes if there is adequate shielding of the region of the field strengths. On the other hand, the changes of parity produced by enclosed fluxes remain observable even for an arbitrarily small overlap between the incident particles and the field strengths. It seems, then, appropriate to regard the parity of the state as the kinematical counterpart of the nonintegrable phase factor.

C. Nonlocal description of the quantum effects of the fluxes

The interpretation of quantum effects of the fluxes in terms of the global concept of the nonintegrable phase factor occupies an intermediate place between nonlocal theories, according to which the field strengths could act on distant charged particles, and theories that emphasize the local aspects of the electromagnetic interaction, trying to establish the physical significance of the potentials. We shall analyze in this section those theories which attribute the Aharonov-Bohm effect to a nonlocal action of the field strengths, and shall continue in the next section with a discussion of the possibility that electromagnetic potentials have an independent existence.

The suggestion that the quantum-mechanical motion of a charged particle in given electromagnetic fields can be regarded as the result of the nonlocal action of the field strengths was made by Noerdlinger (1962), who expressed the potentials φ, \mathbf{A} that intervene in the Schrödinger equation (4.4) in terms of the field strengths \mathbf{E}, \mathbf{B} . Thus, if we take the divergence of Eq. (4.2a) and the curl of Eq. (4.2b), and assume that the potentials fulfill the condition

$$\frac{1}{c} \frac{\partial \varphi}{\partial t} + \text{div} \mathbf{A} = 0 , \quad (4.21)$$

the relations between the field strengths and the potentials become

$$\Delta \varphi - \frac{1}{c^2} \frac{\partial^2 \varphi}{\partial t^2} = -\text{div} \mathbf{E} , \quad (4.22a)$$

$$\Delta \mathbf{A} - \frac{1}{c^2} \frac{\partial^2 \mathbf{A}}{\partial t^2} = -\text{curl} \mathbf{B} + \frac{1}{c} \frac{\partial \mathbf{E}}{\partial t} . \quad (4.22b)$$

A set of particular solutions of Eqs. (4.22) is

$$\varphi(\mathbf{r}, t) = \int \frac{\text{div} \mathbf{E} \left[\mathbf{r}', t - \frac{|\mathbf{r} - \mathbf{r}'|}{c} \right]}{4\pi |\mathbf{r} - \mathbf{r}'|} d^3 r' , \quad (4.23a)$$

$$\mathbf{A}(\mathbf{r}, t) = \int \frac{\left[\text{curl} \mathbf{B} - \frac{1}{c} \frac{\partial \mathbf{E}}{\partial t} \right] \left[\mathbf{r}', t - \frac{|\mathbf{r} - \mathbf{r}'|}{c} \right]}{4\pi |\mathbf{r} - \mathbf{r}'|} d^3 r' . \quad (4.23b)$$

Thus Eqs. (4.23) express the potentials in terms of the field strengths, although this may require consideration of

field strengths in regions where the particle never passed. An example of the application of Eqs. (4.23) was previously considered in Sec. II.D, Eq. (2.91).

An alternative representation was suggested by DeWitt (1962) and Belinfante (1962), who expressed the potentials as path-dependent integrals of the field strengths. These expressions can be obtained by submitting an arbitrary potential distribution φ, \mathbf{A} to a transformation, Eqs. (4.3), generated by the gauge function

$$f_D = \int_{\infty}^{r,t} (c\varphi dt - \mathbf{A} d\mathbf{r}), \quad (4.24)$$

where the integration path connects the field-free region at spatial infinity to the point where the potentials are being evaluated. The partial derivative of the gauge function f_D comprises a term equal and opposite to the corresponding component of the potential at the point \mathbf{r}, t and a term related to the flux through neighboring integration paths, as shown in Fig. 87. Assuming that the integration paths in Eq. (4.24) are defined by the functions z^μ of the end point \mathbf{r}, t and of the parameter ξ ,

$$z^\mu = z^\mu(\mathbf{r}, t; \xi), \quad (4.25)$$

so that

$$z^\mu(\mathbf{r}, t; \xi=0) = x^\mu \quad (4.26)$$

and

$$\lim_{\xi \rightarrow -\infty} z^\mu(\mathbf{r}, t; \xi) = r_\infty, \quad (4.27)$$

the gauge-transformed expression of the potentials becomes

$$A'_\mu = \int_{-\infty}^0 F_{\nu\sigma}(z) \frac{\partial z^\nu}{\partial \xi} \frac{\partial z^\sigma}{\partial x^\mu} d\xi. \quad (4.28)$$

This form of the potentials, reported by DeWitt (1962), provides an interpretation of the Aharonov-Bohm effect in terms of the field strengths, acting, however, nonlocally on the charged particle. The expression of the potentials by Eq. (4.28) is still dependent upon the choice of integration paths $z^\mu(\mathbf{r}, t; \xi)$. It can in fact be shown that a different set of paths $\tilde{z}^\mu(\mathbf{r}, t; \xi)$ in Eq. (4.28) would produce another distribution of potentials. These new potentials can be obtained from the old potentials by a transformation, Eqs. (4.3), whose gauge function is given by the electromagnetic flux enclosed between paths belonging to the two families, as shown in Fig. 87.

The gauge transformation generated by the function f_D , Eq. (4.24), can be applied in the case of idealized field distributions like an infinite magnetic string or a toroidal string. The resulting potential distributions are, however, singular, and due attention must be given to the convergence of the line integrals involved in the transformation. Formulations of the quantum-mechanical interaction of charged particles emphasizing the use of field strengths in connection with the Aharonov-Bohm effect have been also discussed by Mandelstam (1962), Strocchi and Wightman (1974), Vainshtein and Sokolov (1975), Menikoff and Sharp (1977), Goldin, Menikoff, and Sharp (1981), and Cloizeaux (1983). There is, however, no

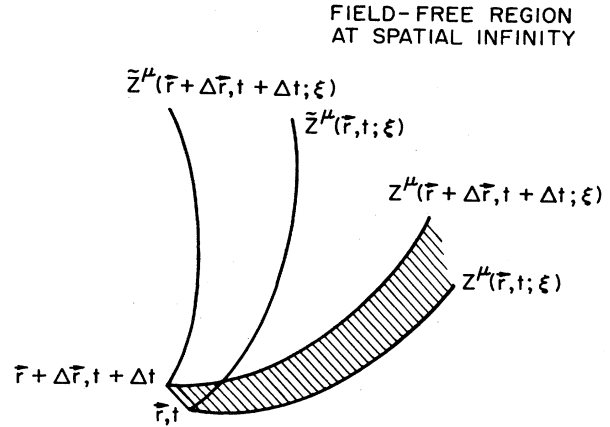


FIG. 87. Integration paths in DeWitt's expression of the electromagnetic potentials in terms of the field strengths [Eq. (4.28)]; this expression involves the electromagnetic flux enclosed between neighboring paths $z^\mu(\mathbf{r}, t; \xi)$ and $z^\mu(\mathbf{r} + \Delta\mathbf{r}, t + \Delta t; \xi)$, where ξ describes the paths parametrically from the field-free region at spatial infinity to the point \mathbf{r}, t . A different set of paths $\tilde{z}^\mu(\mathbf{r}, t; \xi)$ arriving at the same point \mathbf{r}, t would produce another distribution of potentials, related to the former by a gauge function equal to the flux enclosed between the two paths.

unique representation of the electromagnetic interaction through field strengths, for such theories are still subject to gauge transformations generated by arbitrary functions f of $\mathbf{E}(\mathbf{r}, t)$ and $\mathbf{B}(\mathbf{r}, t)$.

Recently Roy (1980) and Roy and Singh (1984) demonstrated that the quantum effects of a finite-length string can be consistently described by considering the changes in the probability distribution of the incident state, produced by interaction with the return magnetic field of the string. The work of Roy (1980) emphasized the possibility of field-strength representations of the quantum effects of the fluxes, in contradistinction to the description based on gauge-dependent electromagnetic potentials originally suggested by Aharonov and Bohm (1959). As an example of this approach, we show below that the canonical angular momentum of the eigenstates of a charged particle interacting with a finite-length string is quantized in integer multiples of \hbar . This quantization of angular momentum, which was briefly discussed at the end of Sec. II.C, is equivalent to the existence of quantum effects of the magnetic flux enclosed in the string.

We shall further analyze the changes in the phase of the wave function of a particle of charge q and mass M , produced by the action of the return magnetic field of a string of length L_0 and carrying the flux F . The phase changes will be determined by considering the pattern of the velocity field, \mathbf{v} , Eq. (1.112), which according to Eqs. (1.110) and (1.111) is governed in the classical limit by classical equations of motion and boundary conditions. The eigenfunctions of a *free* particle having energy

$\hbar^2 k^2/2M$ and angular momentum $\hbar m$ about the z axis are given by $J_m(kr)\exp(im\theta)$, where r and θ are the polar coordinates in the plane of motion, and J_m the Bessel function of order m . At large distances, where $r \gg |m|/k$, this state is the superposition of two radial waves

$$\psi_m^\pm = \frac{1}{[2\pi kr]^{1/2}} \exp \left[\pm i \left[kr - m \frac{\pi}{2} - \frac{\pi}{4} \right] + im\theta \right], \quad (4.29)$$

whose velocity fields \mathbf{v}_\pm have a radial component $\pm \hbar k/M$ and an azimuthal component $\hbar m/Mr$. Thus the velocity patterns of the free states, Eq. (4.29), consist of the straight lines Γ_0 shown in Fig. 88. Let us now consider the effects on the pattern of the velocity field \mathbf{v} of a magnetic flux F enclosed in a string of length L_0 , oriented along the z axis and having its center at the origin of the coordinates. We approximate the solution in the presence of a magnetic flux by Eq. (4.29), which is the solution for zero flux. This results in a change Δv_\perp of the velocity field, produced by the z component of the magnetic strength $B_z(r,z)$ such that the field is normal to the unperturbed direction of \mathbf{v} and has the magnitude

$$\Delta v_\perp(r,z) = \frac{q}{Mc} \int_r^\infty B_z(r,z) dr, \quad (4.30)$$

where quadratic terms in B_z have been neglected. The lines of the velocity field are correspondingly displaced, and it can be shown that the distance between any pair of paths Γ_0 and Γ_F , converging in the absence and in the presence, respectively, of the magnetic flux to the same asymptotic limit, is given by

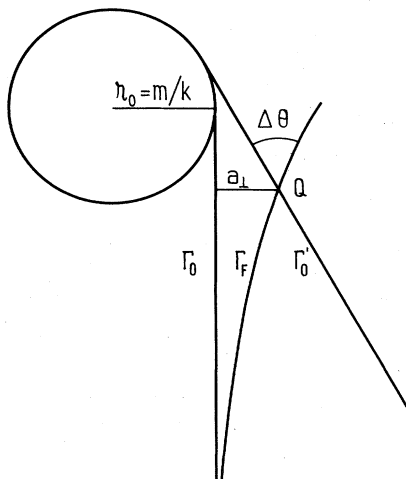


FIG. 88. Action of the return flux of a finite-length magnetic string F on the phase of the eigenfunctions with cylindrical symmetry of a charged particle of energy $\hbar^2 k^2/2M$ and angular momentum $\hbar m$ about the string. In the absence of the flux, the probability current flows along straight lines Γ_0 and Γ_0' . The return magnetic field of the string shifts the current line Γ_0 into the line Γ_F . For very large lengths of magnetic string, the resulting variation of the kinetic angular momentum converges to the finite value $-qF/2\pi\hbar c$.

$$a_\perp(r,z) = \int_r^\infty \frac{M}{\hbar k} \Delta v_\perp(r,z) dr. \quad (4.31)$$

As a result of the displacement described in Eqs. (4.30) and (4.31), the paths Γ_0' and Γ_F shown in Fig. 88, which intersect the same point Q in the absence and in the presence, respectively, of the magnetic flux, are inclined one with respect to the other by the angle

$$\Delta\theta(r,z) = \frac{a_\perp(r,z)}{r} + \frac{M\Delta v_\perp(r,z)}{\hbar k}, \quad (4.32)$$

an approximation valid for $|\Delta\theta| \ll 1$ and $r \gg |m|/k$. Substituting in Eq. (4.32) the expressions of Δv_\perp [Eq. (4.30)] and of a_\perp [Eq. (4.31)] yields, after an integration by parts,

$$\Delta\theta(r,z) = \frac{q}{\hbar k c r} \int_r^\infty r B_z(r,z) dr. \quad (4.33)$$

Since the magnitude of \mathbf{v} is conserved during interaction with the magnetic field, the change in the azimuthal component of the velocity field is given by

$$\Delta v_\theta = \frac{\hbar k \Delta\theta}{M},$$

so that the variation $\hbar\Delta\lambda$ of the kinetic angular momentum of the particle is

$$\Delta\lambda = kr\Delta\theta. \quad (4.34)$$

Substituting above the expression of $\Delta\theta(r,z)$, Eq. (4.33), yields

$$\Delta\lambda = \frac{q}{\hbar c} \int_r^\infty r B_z(r,z) dr, \quad (4.35)$$

in agreement with the previous result, Eq. (2.74). As discussed at the end of Sec. II.C, the variation in the kinetic angular momentum is compensated for by the change in the vector potential, Eq. (2.75), so that the canonical angular momentum

$$\lambda(r,z) + \frac{q}{\hbar c} r A_\theta(r,z) = m \quad (4.36)$$

is a constant independent of r and z . Since at very large distances, $r \gg L_0$, the angular momentum is quantized in integer multiples of \hbar , from Eq. (4.36) the canonical angular momentum turns out to be an integer multiple of \hbar throughout the space.

In order to appreciate the kinematical effects of the return magnetic field of a finite-length string, let us evaluate the variations Δv_\perp , a_\perp , and $\Delta\lambda$ in the median plane $z=0$, where the field strength is

$$B_z(r,0) = -\frac{F}{2\pi} \frac{L_0/2}{(r^2 + L_0^2/4)^{3/2}}. \quad (4.37)$$

Equations (4.30), (4.31), and (4.34) yield

$$\Delta v_\perp = -\frac{qF}{\pi M L_0 c} \left[1 - \frac{r}{(r^2 + L_0^2/4)^{1/2}} \right], \quad (4.38a)$$

$$a_{\perp} = -\frac{qF}{2\pi\hbar ck} \frac{L_0/2}{r + (r^2 + L_0^2/4)^{1/2}}, \quad (4.38b)$$

and

$$\Delta\lambda = -\frac{qF}{2\pi\hbar c} \frac{L_0/2}{(r^2 + L_0^2/4)^{1/2}}. \quad (4.38c)$$

It is apparent from Eqs. (4.38) that the change Δv_{\perp} of the velocity field becomes vanishingly small for large L_0 . On the other hand, the displacement a_{\perp} of the lines, and the variation $\Delta\lambda$ of the kinetic angular momentum converge for large L_0 to the finite limits $a_{\perp} = -qF/2\pi\hbar ck$ and $\Delta\lambda = -qF/2\pi\hbar c$, and in this respect a finite-length string, though very long, is quite different from an infinite magnetic string, with no return fields.

In the preceding analysis we assumed that the radial distance was large compared to the particle wavelength, $r \gg |m|/k$. At small distances, $r \lesssim |m|/k$, the incoming and outgoing waves, Eq. (4.29), are described by Hankel functions, which are singular at the origin. Consequently, the radial component of the quantum-mechanical velocity field becomes vanishingly small as the lines of current approach the origin on spiralled paths.

The nonlocal character of the representation of the Aharonov-Bohm effect based on the action of the field strengths on the phase of the wave function becomes apparent when we consider the distribution of the probability density of the particle. Thus the presence of a return field implies quantization of the canonical angular momentum of the eigenstates in integer multiples of \hbar . Now a suitable superposition of states, Eq. (4.29) can describe a wave packet whose evolution is restricted, for example, to the region in the vicinity of the center of the string, where return fields are negligible. As discussed in Sec. II.B, the phase of the packet will, however, be shifted by an amount proportional to the magnetic flux of the string. This means that the flux-dependent phase shift is attributed to the presence of the return magnetic field in a region where the particle does not move.

Throughout this work it has been assumed that electromagnetic fluxes are given functions of position and time. However, Aharonov and Bohm (1961) included in their treatment the sources of flux by means of a many-body Schrödinger equation. They showed that the results are precisely the same as those given by specified field distributions, in the limit of large mechanical inertia of the particles in the source. Peshkin, Talmi, and Tassie (1961) reached a similar conclusion by considering a mechanical model of the source of magnetic field, in the form of a long charged cylinder having a moment of inertia \mathcal{I}_0 . They found that, in the limit of large \mathcal{I}_0 , the introduction force vanishes, and the interaction can be described by electromagnetic distribution specified as functions of position and time. The problem of the forces exerted by freely moving charges upon one another was discussed in detail by Breitenberger (1968), with the aid of Darwin's expression of the Lagrange function for two charged particles. The possibility that lag forces were exerted on the passing particle in response to the perturba-

tion of motion of the particles in the source was reviewed by Boyer (1973a,1973b). Boyer points out that, although energy calculations provide a suggestion of a lag effect, there is no realistic account of the electromagnetic force that would have to act on the passing particle.

In a completely different approach, Liebowitz (1965,1966) asserted that there is an additional term besides the Lorentz force acting on a charged particle, given by the gradient of an interaction energy between the magnetic field of the incident particle and the magnetic field of the particles in the source. However, Hraskó (1966) pointed out that a similar term is already included in the field part of the conventional Lagrange function, so that from a heuristic viewpoint its repetition in the interaction part of the Lagrange function would be unlikely. Moreover, Kasper (1966,1967) argues that, because of the skin effect, the magnetic field of the incident particle cannot always penetrate into the region of the sources of the electromagnetic flux, a conclusion with which Liebowitz (1967) disagrees. The validity of Liebowitz's theory was tested experimentally by Lischke (1970b), who placed the source of an enclosed magnetic flux in a superconducting shield, so that the magnetic field of the incident particle could not penetrate into the region of the enclosed flux. The quantum effects of the enclosed magnetic flux were still observed, thus proving that the existence of Liebowitz's force is unlikely.

D. Possibility of local observation of the electromagnetic potentials

The characterization of a physical process as local or nonlocal is to a certain extent arbitrary. For example, the interactions are local in classical electromagnetism when regarded as being mediated by the field strengths, but become nonlocal if the field strengths are expressed as retarded integrals depending on the charge distribution. Similarly, the action of the field strengths in the Aharonov-Bohm effect is nonlocal when viewed in terms of the probability density of the incident charged particles, but the same effect can also be described as the local action of the field strengths on the phase of the wave function of the charged particles. What is beyond any doubt is the fact that before the discovery of the Aharonov-Bohm effect it was believed that electromagnetic effects on a charged particle confined to a certain region of space were entirely determined by the distribution of field strengths in the accessible region, whether the motion of the particle was described classically or quantum mechanically. Now, however, Ehrenberg and Siday (1949) and Aharonov and Bohm (1959) have demonstrated that the distribution of electromagnetic flux in the *inaccessible* region can produce observable changes in the probability pattern of the charged particle, even when the overlap between the probability density and the field strengths is vanishingly small. Therefore, whatever may

be the description of the quantum effects of the fluxes, it remains true that a knowledge of the field strengths in the region of space accessible to the charged particle is not in general sufficient to account for all the electromagnetic effects that may actually occur in that region. These electromagnetic effects may be completely and consistently described by specification of the nonintegrable phase factor R , Eq. (4.7), correspondingly to all the loops at the boundary of the region under consideration.

The global interpretation of quantum effects of the fluxes in terms of the nonintegrable phase factor, which requires specification of the electromagnetic variables inside and on the boundary of the region accessible to the charged particle, occupies an intermediate place between the nonlocal theories discussed in the preceding section and the local approaches presented further in this section, which seek to give a physical significance to the electromagnetic potentials. The principal question as to the observability of the potentials is based on their gauge arbitrariness, Eqs. (4.3) and (4.6). Since the nonintegrable phase factor, Eq. (4.7), is invariant to regular gauge changes which conserve the field distribution throughout the space, the existence of quantum effects of the fluxes is not sufficient to demonstrate the reality of the electromagnetic potentials. On the other hand, the field concept was introduced just in order to localize the description of the electromagnetic interaction, so that the adoption of nonlocal, or even intermediate, global representations of electromagnetism would partly remove the justification for the use of field variables. The importance of having a coherent and clear conception of the quantum effects of the fluxes was stressed by Aharonov and Bohm (1961, 1962, 1963), who suggested that a further interpretation of the potentials is needed in quantum mechanics.

In an attempt to attribute a local significance to the electromagnetic potentials, Trammel (1964) discussed the action and reaction forces between two charged particles and suggested that the vector potential could be related to the canonical momentum of the charged particles. A similar observation was reported by Costa de Beauregard (1966a, 1966b), who pointed out that the conservation of momentum and energy in electromagnetism can be expressed conveniently with the aid of the vector potential in a *particular* gauge. Moreover, Boyer (1973a) considered the interaction between a charged particle and a solenoid, and found that the field energy and momentum can be expressed in terms of the vector potential of the solenoid at the position of the moving particle. More recently, Konopinski (1978) suggested that the vector potential describes the field momentum available for exchange with kinetic momenta of charged matter, and Fowles (1980) pointed out that the vector potential could be related to the momentum of the electromagnetic field of the moving charges. In order to appreciate these considerations quantitatively, let us analyze the interaction of two particles of charges q_1 and q_2 and masses M_1 and M_2 . The Lagrange function of the system of the two particles can be obtained by considering the Lagrange function of one of the particles

$$L_1 = -M_1 c^2 \left[1 - \frac{v_1^2}{c^2} \right]^{1/2} - q_1 \varphi_2(\mathbf{r}_1, t) + \frac{q_1}{c} \mathbf{v}_1 \cdot \mathbf{A}_2(\mathbf{r}_1, t) \quad (4.39)$$

in the presence of the potentials due to the other particle,

$$\varphi_2(\mathbf{r}_1) = \frac{q_2}{R_{12}} \quad (4.40a)$$

$$\mathbf{A}_2(\mathbf{r}_1) = \frac{q_2}{2c} \left[\frac{\mathbf{v}_2}{R_{12}} + \frac{(\mathbf{v}_1 \mathbf{R}_{12}) \mathbf{R}_{12}}{R_{12}^3} \right], \quad (4.40b)$$

where \mathbf{v}_1 and \mathbf{v}_2 are the velocities of the particles and $\mathbf{R}_{12} = \mathbf{r}_1 - \mathbf{r}_2$ the distance between them (see, for example, Landau and Lifshitz, 1951). If radiation effects are neglected, the total Lagrange function of the system is given by

$$L_{12} = \frac{1}{2} M_1 v_1^2 + \frac{M_1 v_1^4}{8c^2} + \frac{1}{2} M_2 v_2^2 + \frac{M_2 v_2^4}{8c^2} - \frac{q_1 q_2}{R_{12}} + \frac{q_1 q_2}{2c^2 R_{12}} \left[\mathbf{v}_1 \mathbf{v}_2 + \frac{(\mathbf{v}_1 \mathbf{R}_{12})(\mathbf{v}_2 \mathbf{R}_{12})}{R_{12}^2} \right]. \quad (4.41)$$

The total canonical momentum becomes

$$\begin{aligned} \frac{\partial L_{12}}{\partial \mathbf{v}_1} + \frac{\partial L_{12}}{\partial \mathbf{v}_2} = & M_1 \left[1 + \frac{v_1^2}{2c^2} \right] \mathbf{v}_1 + M_2 \left[1 + \frac{v_2^2}{2c^2} \right] \mathbf{v}_2 \\ & + \frac{q_1 q_2}{2c^2 R_{12}} \left[\mathbf{v}_1 + \frac{\mathbf{R}_{12}(\mathbf{v}_1 \mathbf{R}_{12})}{R_{12}^2} \right] \\ & + \frac{q_1 q_2}{2c^2 R_{12}} \left[\mathbf{v}_2 + \frac{\mathbf{R}_{12}(\mathbf{v}_2 \mathbf{R}_{12})}{R_{12}^2} \right]. \end{aligned} \quad (4.42)$$

Now the rate of change of the canonical momentum can be expressed with the aid of the Lagrange equations as

$$\frac{d}{dt} \left[\frac{\partial L_{12}}{\partial \mathbf{v}_1} + \frac{\partial L_{12}}{\partial \mathbf{v}_2} \right] = \frac{\partial L_{12}}{\partial \mathbf{r}_1} + \frac{\partial L_{12}}{\partial \mathbf{r}_2}. \quad (4.43)$$

However, since the Lagrange function, Eq. (4.41), depends only on the relative distance $\mathbf{R}_{12} = \mathbf{r}_1 - \mathbf{r}_2$, we have

$$\frac{\partial L_{12}}{\partial \mathbf{r}_1} + \frac{\partial L_{12}}{\partial \mathbf{r}_2} = 0, \quad (4.44)$$

so that the total canonical momentum is conserved (Darwin, 1920; for a review of the problem see Breitenberger, 1968). If we compare the expression of the canonical momentum, Eq. (4.42), with the potential, Eq. (4.40b), we see that the canonical momentum can be written as

$$\begin{aligned} \frac{\partial L_{12}}{\partial \mathbf{v}_1} + \frac{\partial L_{12}}{\partial \mathbf{v}_2} = & M_1 \left[1 + \frac{v_1^2}{2c^2} \right] \mathbf{v}_1 + \frac{q_1}{c} \mathbf{A}_2(\mathbf{r}_1) \\ & + M_2 \left[1 + \frac{v_2^2}{2c^2} \right] \mathbf{v}_2 + \frac{q_2}{c} \mathbf{A}_1(\mathbf{r}_2), \end{aligned} \quad (4.45)$$

where $\mathbf{A}_1(\mathbf{r}_2)$ is obtained from Eq. (4.40b) by a permutation of the indices. Since, on the other hand, the sum of the kinetic momentum of the two particles and of the momentum of the electromagnetic field is also conserved, the terms in Eq. (4.45) proportional to the vector potential represent the momentum of the field. However, the latter is obtained from the cross product $\mathbf{E} \times \mathbf{B}$, so that the identification can hold only in a particular gauge. It is this analogy that suggests, but does not require, the possibility of a local significance of the vector potential.

It is worthwhile to point out that the potentials of a moving charge are connected by

$$\mathbf{A} = \frac{\mathbf{v}}{c} \varphi, \quad (4.46)$$

where \mathbf{v} is the retarded velocity. According to Eq. (4.46), we could regard the vector potential \mathbf{A} as the current of the scalar density φ . However, while Eq. (4.46) holds when the potentials fulfill the Lorentz condition $\partial\varphi/c\partial t + \text{div} \mathbf{A} = 0$, the potentials, Eqs. (4.40), are expressed in a different gauge. This example shows that arguments concerning the local reality of the potentials must be regarded with caution.

Wisnivesky and Aharonov (1967) and Aharonov, Pendleton, and Peterson (1969) apparently considered the quantum effects of the fluxes as a manifestation of the nonlocality of the electromagnetic interaction; later Aharonov and Carmi (1973, 1974), Harris and Semon (1980), and Semon (1982) discussed the possibility of attributing a local kinematical significance to the electromagnetic potentials, analogous to the mechanical potentials that appear in noninertial frames of reference. The observable effects depend, however, on loop integrals of the potentials in the noninertial frame, and therefore do not uniquely determine the local value of the potentials.

From a different viewpoint, Philippidis, Bohm, and Kaye (1982) have emphasized the importance of the concept of the electromagnetic vector potential in quantum-potential representations of quantum mechanics. In this approach it is assumed that the particles move classically along paths identical to the lines of the conventional probability current, as a result of the action of a force which would depend on the wave function of the particle. These arguments concerning the significance of the vector potential are heuristic in nature, and the observable effects still depend on loop integrals of the potentials.

An apparent dependence on the gauge of the potentials can be seen in conventional perturbation theory, which yields the transition amplitudes between the eigenstates $\psi_n^{(0)}$ of an unperturbed Hamiltonian \hat{H}_0 ,

$$\hat{H}_0 = \frac{\hat{\mathbf{p}}^2}{2M} + U, \quad (4.47a)$$

$$\hat{H}_0 \psi_n^{(0)} = E_n^{(0)} \psi_n^{(0)}, \quad (4.47b)$$

produced by a potential-dependent perturbation \hat{V} in the Schrödinger equation

$$i\hbar \frac{\partial \Psi}{\partial t} = (\hat{H}_0 + \hat{V}) \Psi, \quad (4.48)$$

where $\hat{\mathbf{p}} = -i\hbar \nabla$ and U is a static potential energy. If the perturbation \hat{V} describes the interaction of a charged particle with a distribution of potentials φ, \mathbf{A} , a change of gauge of the potentials, Eq. (4.3), will introduce a phase factor $\exp(iqf/\hbar c)$ in the solution of Eq. (4.48), while the eigenstates, Eqs. (4.47), remain unaffected. It was, however, shown that as far as resonant interactions are concerned, the transition probabilities are unaffected by the choice of gauge (Goldman, 1977a; Haller and Sohn, 1979; Aharonov and Au, 1979; Olariu, Popescu, and Collins, 1979). In order to obtain a manifest gauge invariance of the perturbation theory, Yang (1976) suggested that the basis states ψ_n be chosen as the eigenfunctions of a basis-defining operator

$$\hat{H}_B = \frac{1}{2M} \left[\hat{\mathbf{p}} - \frac{q}{c} \mathbf{A} \right]^2 + U, \quad (4.49a)$$

$$\hat{H}_B \psi_n = E_n(t) \psi_n. \quad (4.49b)$$

With such a definition, both the basis states ψ_n and the time-dependent solution Ψ would be multiplied by the phase factor $\exp(iqf/\hbar c)$ as the result of a gauge change, so that the transition amplitudes would become manifestly gauge invariant. Kobe, Wen, and Yang (1982) and Yang (1982, 1983) supported this choice of a basis-defining operator on the grounds that radiation-counting devices measure radiation energy fluxes, whose flow is governed by an energy conservation law involving \hat{H}_B . It must, however, be stressed that in principle it is not necessary for the initial and final states of a problem to be the eigenstates of a certain operator, the only requirement being that the wave functions representing the same states i, f in different gauges be related by

$$\psi'_{i,f} = \psi_{i,f} \exp \left[\frac{iqf}{\hbar c} \right]. \quad (4.50)$$

The requirement stated by Eq. (4.50) is automatically fulfilled when the initial and final states are eigenstates of a gauge-invariant operator, but this operator may represent not only the sum of kinetic and static potential energy, as \hat{H}_B does, but also the kinetic energy alone, or the kinetic momentum, or the kinetic angular momentum, or any other measurable quantity whatsoever (Aharonov and Au, 1983; Epstein, 1983; Au, 1983).

As an example of a situation when the eigenstates of \hat{H}_B are not useful as wave functions for the initial and final states, let us consider a charged particle interacting with an applied electromagnetic field that varies adiabatically in time. The quasistationary states of the problem have the form

$$\Psi_n(t) = \psi_n(t) e^{-i(i/\hbar) \tilde{\mathcal{E}}_n(t)t}, \quad (4.51)$$

where $\tilde{\psi}_n$ are the eigenfunctions of the complete Hamiltonian $\hat{H} = \hat{H}_B + q\varphi$ (Landau and Lifshitz, 1977, p. 194)

$$\hat{H}\tilde{\psi}_n = \tilde{\mathcal{E}}_n(t)\tilde{\psi}_n, \tag{4.52a}$$

$$\hat{H} = \frac{1}{2M} \left[\hat{\mathbf{p}} - \frac{q}{c} \mathbf{A} \right]^2 + U + q\varphi. \tag{4.52b}$$

Let us assume that the potential energy $U = M\omega^2 x^2/2$ corresponds to a one-dimensional charged harmonic oscillator of frequency ω , which interacts with a uniform electric field whose intensity $E(t)$ is varying adiabatically in time. The eigenfunctions of the complete Hamiltonian \hat{H} , Eq. (4.52), can be expressed as the conventional Hermitian polynomials, centered, however, on $x_0(t) = qE(t)/M\omega^2$. In the same time, the energy eigenvalues of the full Hamiltonian \hat{H} will be shifted by $q^2 E^2(t)/2M\omega^2$. In accordance with Ehrenfest's principle, this corresponds to the work $\int qE dx_0$ done by the applied field on the particle. By contrast, the eigenstates of the operator \hat{H}_B , Eq. (4.49), are *unaffected* by the applied field. It is interesting that a perturbation that appears to be adiabatic in a certain gauge is not necessarily adiabatic in all gauges. For example, the uniform field $E(t)$ can be represented by the potentials $\varphi = -E(t)x$, $\mathbf{A} = 0$, and if $E(t)$ is adiabatic, $|\Delta E/\Delta t| \ll |E(T)|/t$, then $\varphi(t)$ will also be adiabatic. The same electric field $E(t)$ can be represented by the potentials $\varphi = 0$, $A_x = -c \int_0^t E(\tau) d\tau$, $A_y = 0$, $A_z = 0$, which are no longer adiabatic. Therefore, in this case the quasistationary states of the problem are related to the eigenfunctions of the full Hamiltonian including the potentials in the gauge $\varphi = -E(t)x$, $\mathbf{A} = 0$. There are other problems where the differences between \hat{H}_0 , \hat{H}_B , or \hat{H} as basis-defining operators are not important. It can be shown, for example, that the transition probabilities between eigenstates of operators of the type in Eq. (4.49a) are identical at resonance to the transition probabilities between eigenstates of the unperturbed Hamiltonian, Eq. (4.47a) (Olariu, Popescu, and Collins, 1979).

E. Multivalued representations

The electromagnetic potentials generated by a distribution of enclosed electromagnetic fluxes can be obtained in a field-free region of space by differentiation of a scalar function f_0 according to (Byers and Yang, 1961)

$$\varphi = -\frac{1}{c} \frac{\partial f_0}{\partial t}, \tag{4.53a}$$

$$\mathbf{A} = \nabla f_0. \tag{4.53b}$$

This means that if Ψ_0 is a local solution of the Schrödinger equation in the field-free region for vanishing potentials, then

$$\Psi_{\varphi, \mathbf{A}} = \Psi_{(\varphi, \mathbf{A})=0} \exp(iqf_0/\hbar c) \tag{4.54}$$

will be a local solution of the Schrödinger equation including the potentials φ, \mathbf{A} . However, the phase factor $\exp(iqf_0/\hbar c)$ is in general multivalued in the region accessible to the incident particle, so that the functions appearing in Eq. (4.54) must be rendered single valued by cuts.

In this section we show that wave functions obtained with the aid of multivalued gauge transformations which eliminate the potentials from the field-free region can be used in the description of two-slit scattering of charged particles in the presence of an infinite magnetic string, provided that certain cuts are appropriately placed in the domain of definition of the wave functions. These cuts render the components of the total wave function single valued, though discontinuous, and approximate the behavior of the actual states in regions of rapid phase variation.

Let us assume that in the absence of magnetic flux the incident wave packet is split into two coherent components $\psi_0^{(1)}$ and $\psi_0^{(2)}$, each passing through one of the slits to arrive in the observing plane with the total amplitude

$$\psi_0 = \psi_0^{(1)} + \psi_0^{(2)}. \tag{4.55}$$

If the enclosed flux F is generated by a magnetic string coinciding with the z axis, the vector potential of the string can be expressed as

$$\mathbf{A} = \frac{F}{2\pi} \nabla \theta, \tag{4.56}$$

where θ is the polar angle in the x, y plane. The states in the presence of the magnetic string are single-valued solutions of the Schrödinger equation including the vector potential, Eq. (4.56). According to Eq. (4.54), these solutions are connected to the solutions in the field-free region of the Schrödinger equation including the potential $\mathbf{A} = 0$ by

$$\psi_{\mathbf{A}} = \psi_{\mathbf{A}=0} \exp(iqF\theta/2\pi\hbar c). \tag{4.57}$$

This suggests that the wave functions representing the coherent packets could be obtained through multiplication

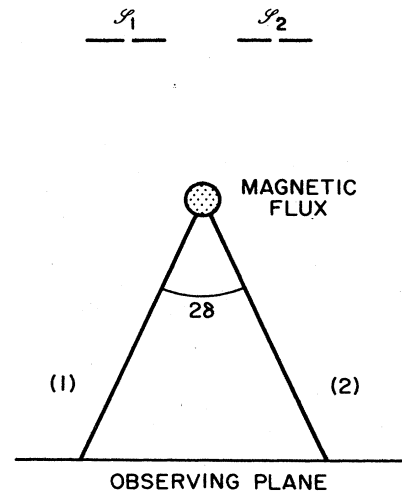


FIG. 89. Representation of two-slit scattering of a charged particle in the presence of a magnetic string, with the aid of multivalued functions. These functions are rendered single valued through the cuts shown in the figure by the heavy lines. The cuts approximate the continuous, single-valued states in regions of rapid phase variation.

by the phase factor $\exp(iqF\theta/2\pi\hbar c)$. However, for noninteger $qF/2\pi\hbar c$ the phase factor is multivalued, so that the solutions $\psi_{A=0}^{(1)}$ and $\psi_{A=0}^{(2)}$ which would represent the packets must be rendered uniform by cuts. Since these cuts are in general distinct for the two coherent states, we shall choose the origin of the polar angle θ such that the bisector of the angle determined by the cuts coincides with line $|\theta| = \pi$, as shown in Fig. 89. If we assume further that, except for the region in the vicinity of the cuts, the states $\psi_{A=0}^{(1)}$ and $\psi_{A=0}^{(2)}$ are essentially the same as the unperturbed states $\psi_0^{(1)}$ and $\psi_0^{(2)}$, and restrict the angle θ to the interval $-\pi < \theta < \pi$, the expressions of the amplitudes $\psi_F^{(1)}$ and $\psi_F^{(2)}$ for arrival in the observing plane through each of the slits are

$$\psi_F^{(1)} = \begin{cases} \psi_0^{(1)} e^{iqF\theta/2\pi\hbar c}, & -\pi \leq \theta < \pi - \delta \\ \psi_0^{(1)} e^{iqF(\theta - 2\pi)/2\pi\hbar c}, & \pi - \delta < \theta \leq \pi \end{cases} \quad (4.58)$$

and

$$\psi_F^{(2)} = \begin{cases} \psi_0^{(2)} e^{iqF\theta/2\pi\hbar c}, & -(\pi - \delta) < \theta \leq \pi \\ \psi_0^{(2)} e^{iqF(\theta + 2\pi)/2\pi\hbar c}, & -\pi \leq \theta < -(\pi - \delta), \end{cases} \quad (4.59)$$

where 2δ is the angle between the cuts. Thus the cut operates upon the wave function like a $qF/\hbar c$ phase shifter (Wegener, 1960). The total amplitude ψ_F for arrival in the observing plane is the superposition of the states given by Eqs. (4.58) and (4.59), and is

$$\psi_F = \begin{cases} (\psi_0^{(1)} + \psi_0^{(2)}) e^{iqF\theta/2\pi\hbar c}, & -(\pi - \delta) < \theta < \pi - \delta \\ \left[\psi_0^{(1)} e^{-iqF/2\hbar c} + \psi_0^{(2)} e^{iqF/2\hbar c} \right] e^{iqF(\theta - \pi)/2\pi\hbar c}, & \pi - \delta < \theta \leq \pi \\ \left[\psi_0^{(1)} e^{iqF/2\hbar c} + \psi_0^{(2)} e^{-iqF/2\hbar c} \right] e^{iqF(\theta + \pi)/2\pi\hbar c}, & -\pi \leq \theta < -(\pi - \delta). \end{cases} \quad (4.60a)$$

$$\psi_F = \begin{cases} \left[\psi_0^{(1)} e^{-iqF/2\hbar c} + \psi_0^{(2)} e^{iqF/2\hbar c} \right] e^{iqF(\theta - \pi)/2\pi\hbar c}, & \pi - \delta < \theta \leq \pi \end{cases} \quad (4.60b)$$

$$\psi_F = \begin{cases} \left[\psi_0^{(1)} e^{iqF/2\hbar c} + \psi_0^{(2)} e^{-iqF/2\hbar c} \right] e^{iqF(\theta + \pi)/2\pi\hbar c}, & -\pi \leq \theta < -(\pi - \delta). \end{cases} \quad (4.60c)$$

This analysis is essentially equivalent to the original demonstration by Aharonov and Bohm (1959) of the existence of the quantum effects of enclosed magnetic fluxes. It is apparent from Eq. (4.60a) that the magnetic string does not affect the coherence of the components of the total wave function in the incidence region. On the other hand, according to Eqs. (4.60b) and (4.60c), the relative phase of the components passing by opposite sides of the string is shifted by $qF/\hbar c$, which generally results in flux-dependent changes in the probability pattern, observable throughout the region between the two cuts.

It is interesting to compare the analysis from this section with the propagator technique developed in Secs. I and II. If we use Eq. (1.6) to compute the wave function in the observing plane, the principal contribution will arise from the regions in the vicinity of the slits, or from the regions in the vicinity of the virtual images of the electron source in actual experiments. The propagator of a charged particle in the presence of a magnetic string, Eq. (2.43), is a periodic function of the difference between coordinates of the observing point θ and of the source point θ' , although the propagator undergoes a rapid but continuous variation across the surface $|\theta - \theta'| = \pi$. Equation (2.48) approximates the propagator well, unless $|\theta - \theta'|$ is close to π , when the phase of the approximate form is discontinuous by $qF/\hbar c$. Then if we use this approximate expression in the calculation, we must observe the condition that $|\theta - \theta'| < \pi$, under which Eq. (2.48) is valid. The condition $|\theta - \theta'| < \pi$ determines two distinct regions corresponding to the different angular positions of the slits, across which the phases of the coherent components are varying by $qF/\hbar c$, and this fact is reflected by the cuts appearing in the wave-function equations (4.60).

The gauge transformation approach can also be used to

describe scattering by a pair of magnetic strings carrying opposite fluxes, considered in Sec. II.D. The vector potential of this magnetic distribution is

$$\mathbf{A} = \frac{F}{2\pi} \nabla(\theta_1 - \theta_2), \quad (4.61)$$

where θ_1 and θ_2 represent the polar angles about each of the strings. Then an approximate form of the flux-dependent wave function is given by

$$\psi_F = \psi_0 e^{iqF(\theta_1 - \theta_2)/2\pi\hbar c}, \quad (4.62)$$

where ψ_0 is the unperturbed wave function. From the results reported in Sec. II.D, it is apparent that the cut which renders the phase factor single valued in Eq. (4.62) would be the surface spanning the strings, shown in cross section by the dotted line in Fig. 29. It must be emphasized that, in the vicinity of the cut, the effects of the enclosed fluxes are not mere phase shifts, but involve observable changes in the probability pattern.

Let us now consider a distribution of enclosed electromagnetic fields that is complementary to a field-free region, and let us moreover assume that the whole space is in principle accessible to a charged particle, although the probability for the particle to be found in the region of the field strengths may be very small. If the distribution of the field strengths is represented *throughout* the space by the potentials φ, \mathbf{A} , the potentials in the field-free region can be expressed in the form of Eqs. (4.53). The function f_0 appearing in Eqs. (4.53) is not single valued, but it increases by

$$\Delta f_0 = \oint (c\varphi dt - \mathbf{A} \cdot d\mathbf{r})$$

with every rotation around the region of enclosed flux.

The potentials φ, \mathbf{A} from the field-free region can be eliminated by a gauge transformation generated by the function $-f_0$, and the solutions of the Schrödinger equation in the two gauges are connected in the field-free region by

$$\Psi_{(\varphi, \mathbf{A})=0} = \Psi_{\varphi, \mathbf{A}} e^{-iqf_0/\hbar c} \quad (4.63)$$

The Schrödinger equation in the gauge $\varphi=0, \mathbf{A}=0$ formally coincides with that of a free particle. However, the gauge transformation generated by the singular function $-f_0$ changes the distribution of field strengths (Ingraham, 1972; Zeilinger, 1979; Bohm and Hiley, 1979; Mignaco and Novaes, 1979; Bawin and Burnel, 1980; Rowe, 1980). This modification can be compensated for by imposing periodic boundary conditions on the wave function $\Psi_{\varphi, \mathbf{A}}$ such that the reduced electromagnetic flux remaining in the equation and the reduced flux hidden in the periodic boundary conditions add up to the reduced electromagnetic flux of the real electromagnetic distribution (Byers and Yang, 1961; Kretschmar, 1965a; Breitenecker and Grumm, 1980; Rothe, 1981; Wilczek, 1982a, 1982b; Jackiw and Redlich, 1983). Thus it is the solution $\Psi_{\varphi, \mathbf{A}}$, corresponding to the regular potential distribution, which has the property of single valuedness (Buchdahl, 1962; Merzbacher, 1962; Pandres, 1962; Riess, 1973; Mignaco and Novaes, 1979), while the phase factor $\exp(ief_0/\hbar c)$ and $\Psi_{(\varphi, \mathbf{A})=0}$ are in general multivalued. For example, the vector potential $A_r=0, A=F/2\pi r, r>R_0$ of an infinite solenoid of radius R_0 , carrying the magnetic flux F , could be eliminated in the field-free region by a gauge transformation generated by the function $-f_0 = -F\theta/2\pi$. This transformation, however, introduces into the field distribution a fictitious magnetic string along the z axis, carrying the flux $-F$, equal and opposite to the total flux in the solenoid. If we now consider the scattering of a plane wave by an infinite magnetic string discussed in Sec. II.A, we see that the regular solution $\Psi_{\varphi, \mathbf{A}}$ in Eq. (4.63) would correspond to the continuous, single-valued wave function $\psi_\alpha(r, \theta)$, Eq. (2.5), while the phase factor in Eq. (4.63) would be the multivalued function $\exp(-ieF\theta/2\pi\hbar c)$. If we multiply the asymptotic expression of $\psi_\alpha(r, \theta)$, Eq. (2.13), by this multivalued phase factor, we see that the state designated in Eq. (4.63) by $\Psi_{(\varphi, \mathbf{A})=0}$ approaches the unperturbed incident wave $\exp(-ikx)$. This justifies the premise that led us to the expression of the total wave function in the observing region, Eqs. (4.60). On the other hand, there are essential differences between the gauge-transformed state $\Psi_{(\varphi, \mathbf{A})=0}$ and the true unperturbed state $\Psi_{F=0} = \exp(-ikx)$ corresponding to a situation when the enclosed flux was zero. These differences appear in the case of scattering by an infinite magnetic string in the vicinity of the half-plane $|\theta| = \pi$. The states designated by the index $\mathbf{A}=0$ in the development leading to Eqs. (4.60), which were rendered single valued by cuts, are thus approximations of states of the type of $\Psi_{(\varphi, \mathbf{A})=0}$ in Eq. (4.63), and *not* of the true unperturbed state $\Psi_{F=0}$.

By imposing an unnecessary requirement of single valuedness on the phase factor appearing in the singular

transformation, Eq. (4.63), Costa de Beauregard (1972) inferred that a perfectly enclosed magnetic flux would be quantized in integer multiples of $2\pi\hbar c/e$. Later, by allowing double-valued phase factors in the transformation, Eq. (4.63), which would be consistent with a representation of the electrons by the Dirac equation, Costa de Beauregard and Vigoureux (1974, 1982) predicted the quantization of the enclosed magnetic flux in multiples of $\pi\hbar c/e$. However, as emphasized by Keller and Zumino (1961), the quantity that is always quantized is the holoid, Eq. (1.120) or Eq. (3.47), and not the electromagnetic flux itself. As discussed in Sec. III.F, Bardeen (1961) has in fact shown that in superconducting tubes of very small diameter, with wall thickness of the order of the penetration depth, the unit of quantization of the magnetic flux may depend on dimensions and temperature and be smaller than $\pi\hbar c/e$. Thus, in general, the magnetic flux is not quantized in multiples of $\pi\hbar c/e$, even if completely trapped in a certain region of space.

In the accessible region, the probability distribution is invariant to the multivalued gauge transformation, Eq. (4.63), provided that the boundary conditions and the representation of the operators is consistent with the chosen gauge of the potentials. If the entire space is in principle accessible to the charged particles, and the electromagnetic field is specified by regular potential distributions, the boundary condition is that the wave functions be single valued when the operators for the canonical momentum have the conventional representation $\hat{\mathbf{p}} = -i\hbar\nabla$. In this case the property of single valuedness is a consequence of the commutation of the components of the canonical momentum, which ensures that $\nabla \times \nabla \Psi = 0$ at every point in space. If the space is formally multiconnected, so that there are certain regions that are inaccessible to the charged particles, the eventual use of multivalued wave functions cannot be excluded *a priori*. If we apply the condition of single valuedness of the wave function in the gauge where the potentials are vanishing in the accessible region, then all the effects of the enclosed fluxes will be transformed away by the multivalued phase factor in Eq. (4.63). With such an approach, the wave function would be multivalued in the regular gauge φ, \mathbf{A} , while the probability distribution would remain identical to that of a free particle in the absence of any flux. This possibility was already mentioned by Aharonov and Bohm (1961), who stressed, however, that the requirement of single valuedness must be applied to $\Psi_{\varphi, \mathbf{A}}$ and not to $\Psi_{(\varphi, \mathbf{A})=0}$.

More recently, Bocchieri and Loinger (1978, 1979, 1984) and Bocchieri, Loinger, and Siragusa (1979) suggested that quantum effects of the fluxes do not exist, basing their analysis on an improper use of multivalued wave functions in a representation where the potentials are regular and the canonical momentum has the form $\hat{\mathbf{p}} = -i\hbar\nabla$. Later they attempted to relate their conclusion of the nonexistence of the Aharonov-Bohm effect to formulations of quantum electrodynamics involving solely the field strengths \mathbf{E} and \mathbf{B} (Bocchieri and Loinger, 1980, 1981a, 1981b; Bocchieri, Loinger, and Siragusa, 1980). Throughout these works, Bocchieri, Loinger, and

Siragusa took the position that the experimental evidence concerning the reality of the quantum effects of the fluxes would be inconclusive, their assertion being, however, hard to reconcile with the multitude of positive experimental results discussed in Sec. III.

The theoretical viewpoint of Bocchieri, Loinger, and Siragusa can best be illustrated by the problem of the rigid rotator in the presence of a magnetic string, discussed in Sec. I.E. Thus, in the regular or Stokesian representation, the vector potential of the string is

$$A_\theta = \frac{F}{2\pi R_0}, \quad A_r = 0, \quad (4.64)$$

and the Schrödinger equation has the form

$$\frac{1}{2MR_0^2} \left[-i\hbar \frac{\partial}{\partial \theta} - \frac{qF}{2\pi c} \right]^2 \psi_A = E_{R_0 m}^{(F)} \psi_A, \quad (4.65)$$

where $\hat{p}_\theta = -i\hbar \partial/\partial \theta$ is the operator of the canonical angular momentum and $-i\hbar \partial/\partial \theta - qF/2\pi c$ is the operator of the kinetic angular momentum. The solutions of Eq. (4.65) have the form

$$\psi_A(\theta) \sim e^{im\theta}, \quad (4.66)$$

and the condition of single valuedness

$$\psi_A(\theta + 2\pi) = \psi_A(\theta) \quad (4.67)$$

renders the eigenvalues m of the canonical angular momentum integer numbers. The corresponding energy eigenvalue is then

$$E_{R_0 m}^{(F)} = \frac{\hbar^2}{2MR_0^2} \left[m - \frac{qF}{2\pi\hbar c} \right]^2, \quad (4.68)$$

and it depends on the amount of enclosed flux. As discussed at the beginning of this section, the potential acting on the charged particle can be eliminated by a gauge transformation generated by the function $-F\theta/2\pi$. The gauge-transformed potential is

$$A'_\theta = 0, \quad A'_r = 0, \quad (4.69)$$

and the Schrödinger equation has the form

$$\frac{1}{2MR_0^2} \frac{\partial^2 \psi_{A=0}}{\partial \theta^2} = E_{R_0 m}^{(F)} \psi_{A=0}. \quad (4.70)$$

The operator of the canonical angular momentum in the new gauge is

$$e^{-iqF\theta/2\pi\hbar c} \left[-i\hbar \frac{\partial}{\partial \theta} \right] e^{iqF\theta/2\pi\hbar c} = -i\hbar \frac{\partial}{\partial \theta} + \frac{qF}{2\pi c}, \quad (4.71)$$

while the operator of the kinetic angular momentum becomes (Kretzschmar, 1965a)

$$e^{-iqF\theta/2\pi\hbar c} \left[-i\hbar \frac{\partial}{\partial \theta} - \frac{qF}{2\pi c} \right] e^{iqF\theta/2\pi\hbar c} = -i\hbar \frac{\partial}{\partial \theta}. \quad (4.72)$$

The periodic boundary condition is (Rothe, 1981)

$$\psi_{A=0}(\theta + 2\pi) = e^{-iqF/\hbar c} \psi_{A=0}(\theta), \quad (4.73)$$

so that the eigenfunctions of Eq. (4.70) are

$$\psi_{A=0} = e^{i(m - qF/2\pi\hbar c)\theta}, \quad m = 0, \pm 1. \quad (4.74)$$

According to Eq. (4.71) the canonical momentum is again m , an integer, while the energy eigenvalues $E_{R_0 m}^{(F)}$ are equally given by Eq. (4.68). Now according to Bocchieri, Loinger, and Siragusa (1980) and Bocchieri and Loinger (1980), the eigenfunctions of Eq. (4.65) would be

$$\psi_{A=0}^{\text{BLS}} = e^{i(m - qF/2\pi\hbar c)\theta}, \quad m = 0, \pm 1, \dots, \quad (4.75)$$

a set of multivalued functions, while the operators would preserve their conventional expressions, in particular, the canonical angular momentum would be $-i\hbar \partial/\partial \theta$ and the kinetic angular momentum $-i\hbar \partial/\partial \theta - qF/2\pi c$. Thus the canonical angular momentum would have noninteger eigenvalues $m - qF/2\pi\hbar c$, while the kinetic angular momentum would be m , an integer. The energy eigenvalues defined by Eq. (4.65) would then be $E^{\text{BLS}} = \hbar^2 m^2 / 2MR_0^2$, a spectrum that is independent of the enclosed flux.

The suggestion of Bocchieri, Loinger, and Siragusa that the Schrödinger equation (4.65) should be solved for the regular potential distribution, Eq. (4.64), and the conventional representation $\hat{p} = -i\hbar \nabla$ of the canonical momentum in terms of multivalued functions has been criticized in the literature, as has their assertion that the experimental evidence on quantum effects of the fluxes is inconclusive (Klein, 1979, 1981; Mackinnon, 1979; Greenberger, 1981; Lipkin, 1981; Peshkin, 1981a, 1981b; Boersch *et al.*, 1981; Lipkin and Peshkin, 1982; Asorey, 1982; Ruijsenaars, 1983; Aharonov, Au, Lerner, and Liang, 1984b). In a paper dealing with the recent experiments of Tonomura *et al.* (1982) on toroidal magnets, Bocchieri, Loinger, and Siragusa (1982) attribute the observed fringe shifts to the penetration of the electron wave into the region of the magnetic field, which would thus act directly on the *phase* of the wave function. Such a viewpoint is, however, in marked contrast with their earlier statements denying the existence of any observable effects of enclosed fluxes.

Merzbacher (1962) has pointed out that physical space is always simply connected, so that the wave functions cannot be other than single valued. The wave functions in idealized situations involving multiconnected spaces, like the scattering by magnetic strings, can be obtained as limiting forms of more realistic situations where the space is simply connected and the wave functions are unambiguously single valued. Such an approach was pursued in Secs. II.E and II.F, and the results obtained there fully confirmed the reality of the quantum effects of enclosed fluxes.

As discussed in Sec. I.H, the single valuedness of the wave functions entails the quantization of the circulation of the velocity field, Eq. (1.120). A consequence of Eq. (1.120) is that if in two situations the field strength distributions are different, then it is not in general possible to

prepare two states having identical velocity fields. If the identity of incident states is decided, however, in terms of the probability density ρ^2 and the probability current $\mathbf{j}=\rho^2\mathbf{v}$, then it is possible to arrange that the differences between the two states be arbitrarily small, by making the probability ρ^2 vanishingly small in the region of the field strengths. It is worthwhile to remark that the number of fluxoid trapped, according to Eq. (1.120), in a certain loop is changing when a zero of the wave function crosses the loop under consideration.

CONCLUSIONS

The remarkable nature of the quantum effects of the fluxes lies in their persistence as observable actions of electromagnetic fields on the probability distribution of charged particles, even when the overlap between particles and field strengths is rendered arbitrarily small. The reality of these effects means that a knowledge of the field strengths in a region accessible to a charged particle is not in general sufficient to uniquely specify the evolution of the state of the particle in that region.

The observable action of enclosed electromagnetic fluxes demonstrates the conceptual limitations of any theory of electromagnetic phenomena based solely on the local action of the field strengths. This situation is in a sense analogous to the nondependence of the fringe pattern on the orientation of the interferometer in the Michelson's experiment, which demonstrated the limitations of traditional notions of space and time. While the invariance of the interference pattern in Michelson's experiment heralded the new conception of space and time introduced by the theory of relativity, it remains to be seen whether the quantum effects of the fluxes, too, precede a major change in our conception of electromagnetism.

REFERENCES

- Abramowitz, M., and I. Stegun, Eds., 1965, *Handbook of Mathematical Functions* (Dover, New York).
- Aharonov, Y., and C. K. Au, 1979, *Phys. Rev. D* **20**, 1553.
- Aharonov, Y., and C. K. Au, 1983, *Phys. Lett. A* **95**, 412.
- Aharonov, Y., C. K. Au, E. C. Lerner, and J. Q. Liang, 1984a, *Phys. Rev. D* **29**, 2396.
- Aharonov, Y., C. K. Au, E. C. Lerner, and J. Q. Liang, 1984b, *Lett. Nuovo Cimento* **39**, 145.
- Aharonov, Y., and D. Bohm, 1959, *Phys. Rev.* **115**, 485.
- Aharonov, Y., and D. Bohm, 1961, *Phys. Rev.* **123**, 1511.
- Aharonov, Y., and D. Bohm, 1962, *Phys. Rev.* **125**, 2192.
- Aharonov, Y., and D. Bohm, 1963, *Phys. Rev.* **130**, 1625.
- Aharonov, Y., and G. Carmi, 1973, *Found. Phys.* **3**, 493.
- Aharonov, Y., and G. Carmi, 1974, *Found. Phys.* **4**, 75.
- Aharonov, Y., H. Pendleton, and A. Peterson, 1969, *Int. J. Theor. Phys.* **2**, 213.
- Aharonov, Y., and M. Vardi, 1979, *Phys. Rev. D* **20**, 3213.
- Anandan, J., 1977, *Phys. Rev. D* **15**, 1448.
- Anandan, J., 1979, *Nuovo Cimento A* **53**, 221.
- Anderson, P. W., 1967, *Prog. Low Temp. Phys.* **5**, 1.
- Anderson, P. W., and J. M. Rowell, 1963, *Phys. Rev. Lett.* **10**, 230.
- Asorey, M., 1982, *Lett. Math. Phys.* **6**, 429.
- Au, C. K., 1983, *Phys. Lett. A* **98**, 245.
- Bardeen, John, 1961, *Phys. Rev. Lett.* **7**, 162.
- Bardeen, John, L. N. Cooper, and J. B. Schrieffer, 1957, *Phys. Rev.* **108**, 1175.
- Bardeen, John, and J. R. Schrieffer, 1961, *Prog. Low Temp. Phys.* **3**, 170.
- Bawin, M., and A. Burnel, 1980, *Lett. Nuovo Cimento* **27**, 4.
- Bayh, W., 1962, *Z. Phys.* **169**, 492.
- Baym, G., 1969, *Lectures on Quantum Mechanics* (Benjamin, New York), pp. 68–79.
- Belinfante, F. J., 1962, *Phys. Rev.* **128**, 2832.
- Bernido, C., and A. Inomata, 1980, *Phys. Lett. A* **77**, 394.
- Bernido, C., and A. Inomata, 1981, *J. Math. Phys.* **22**, 715.
- Berry, M. V., 1980, *Eur. J. Phys.* **1**, 240.
- Berry, M. V., R. G. Chambers, M. D. Large, C. Upstill, and J. C. Walmsley, 1980, *Eur. J. Phys.* **1**, 154.
- Bethe, H., 1928, *Ann. Phys. (Leipzig)* **87**, 55.
- Bocchieri, P., and A. Loinger, 1978, *Nuovo Cimento A* **47**, 475.
- Bocchieri, P., and A. Loinger, 1979, *Lett. Nuovo Cimento* **25**, 476.
- Bocchieri, P., and A. Loinger, 1980, *Nuovo Cimento A* **59**, 121.
- Bocchieri, P., and A. Loinger, 1981a, *Lett. Nuovo Cimento* **30**, 449.
- Bocchieri, P., and A. Loinger, 1981b, *Nuovo Cimento A* **66**, 164.
- Bocchieri, P., and A. Loinger, 1982, *Lett. Nuovo Cimento* **35**, 469.
- Bocchieri, P., and A. Loinger, 1984, *Lett. Nuovo Cimento* **39**, 148.
- Bocchieri, P., A. Loinger, and G. Siragusa, 1979, *Nuovo Cimento A* **51**, 1.
- Bocchieri, P., A. Loinger, and G. Siragusa, 1980, *Nuovo Cimento A* **56**, 55.
- Bocchieri, P., A. Loinger, and G. Siragusa, 1982, *Lett. Nuovo Cimento* **35**, 370.
- Boersch, H., K. Grohmann, H. Hamisch, B. Lischke, and D. Wohlleben, 1981, *Lett. Nuovo Cimento* **30**, 257.
- Boersch, H., H. Hamisch, and K. Grohmann, 1962, *Z. Phys.* **169**, 263.
- Boersch, H., H. Hamisch, D. Wohlleben, and K. Grohmann, 1960, *Z. Phys.* **159**, 397.
- Boersch, H., H. Hamisch, K. Grohmann, and D. Wohlleben, 1961, *Z. Phys.* **165**, 79.
- Boersch, H., H. Hamisch, K. Grohmann, and D. Wohlleben, 1962, *Z. Phys.* **167**, 72.
- Boersch, H., and B. Lischke, 1970, *Z. Phys.* **237**, 449.
- Bohm, D., and B. J. Hiley, 1979, *Nuovo Cimento A* **52**, 295.
- Bohm, D., and C. Philippidis, 1971, *Acta Phys. Acad. Sci. Hung.* **30**, 221.
- Bohr, N., 1913, *Philos. Mag.* **26**, 1, 476, 857.
- Bohr, N., 1928, *Nature* **121**, 580.
- Boyer, T. H., 1972a, *Am. J. Phys.* **40**, 56.
- Boyer, T. H., 1972b, *Am. J. Phys.* **40**, 1708.
- Boyer, T. H., 1973a, *Phys. Rev. D* **8**, 1667.
- Boyer, T. H., 1973b, *Phys. Rev. D* **8**, 1679.
- Breitenberger, E., 1968, *Am. J. Phys.* **36**, 505.
- Breitenecker, M., and H.-R. Grumm, 1980, *Nuovo Cimento A* **55**, 453.
- Brenig, W., 1961, *Phys. Rev. Lett.* **7**, 337.
- Buchdahl, H. A., 1962, *Am. J. Phys.* **30**, 829.
- Buhl, R., 1959, *Z. Phys.* **155**, 395.

- Byers, N., and C. N. Yang, 1961, *Phys. Rev. Lett.* **7**, 46.
- Casati, G., and I. Guarneri, 1979, *Phys. Rev. Lett.* **42**, 1579.
- Caser, S., 1982, *Phys. Lett. A* **92**, 13.
- Chambers, R. G., 1960, *Phys. Rev. Lett.* **5**, 3.
- Cohen, M. S., 1967, *J. Appl. Phys.* **38**, 4966.
- Colella, R., A. W. Overhauser, and S. A. Werner, 1975, *Phys. Rev. Lett.* **34**, 1472.
- Corinaldesi, E., and F. Rafeli, 1978, *Am. J. Phys.* **46**, 1185.
- Costa de Beauregard, O., 1966a, *C. R. Acad. Sci. Ser. B* **263**, 1007.
- Costa de Beauregard, O., 1966b, *C. R. Acad. Sci. Ser. B* **263**, 1047.
- Costa de Beauregard, O., 1972, *Phys. Lett. A* **41**, 299.
- Costa de Beauregard, O., and J. M. Vigoureux, 1974, *Phys. Rev. D* **9**, 1626.
- Costa de Beauregard, O., and J. M. Vigoureux, 1982, *Lett. Nuovo Cimento* **33**, 79.
- Danos, M., 1982, *Am. J. Phys.* **50**, 64.
- Darwin, C. G., 1920, *Philos. Mag.* **30**, 537.
- Deaver, B. S., and G. B. Donaldson, 1982, *Phys. Lett. A* **89**, 178.
- Deaver, B. S., and W. M. Fairbank, 1961, *Phys. Rev. Lett.* **7**, 43.
- DeBlois, R. W., 1958, *J. Appl. Phys.* **29**, 459.
- des Cloizeaux, J., 1983, *J. Phys. (Paris)* **44**, 885.
- DeWitt, B. S., 1962, *Phys. Rev.* **125**, 2189.
- Doll, R., and M. Näbauer, 1961, *Phys. Rev. Lett.* **7**, 51.
- Doll, R., and M. Näbauer, 1962, *Z. Phys.* **169**, 526.
- Dowker, J. S., 1967, *Nuovo Cimento B* **52**, 129.
- Ehrenberg, W., and R. E. Siday, 1949, *Proc. Phys. Soc. London Sect. B* **62**, 8.
- Ehrenfest, P., 1916, *Verslagen K. Ned. Akad. Amsterdam* **25**, 412; abridged English translation available in B. L. van der Waerden, Ed., *Sources of Quantum Mechanics* (North-Holland, Amsterdam, 1967).
- Ehrenfest, P., 1927, *Z. Phys.* **45**, 455.
- Epstein, S. T., 1983, *Phys. Lett. A* **97**, 29.
- Erlichson, H., 1970, *Am. J. Phys.* **38**, 162.
- Erlichson, H., 1972, *Am. J. Phys.* **40**, 1707.
- Feinberg, E. L., 1962, *Usp. Fiz. Nauk* **78**, 53 [*Sov. Phys.—Usp.* **5**, 753 (1963)].
- Fert, Ch., and J. Faget, 1958, cited in M. Keller, *Z. Phys.* **164**, 274 (1961).
- Feynman, R. P., 1948, *Rev. Mod. Phys.* **20**, 367.
- Feynman, R. P., and A. R. Hibbs, 1965, *Quantum Mechanics and Path Integrals* (McGraw-Hill, New York).
- Feynman, R. P., R. B. Leighton, and M. Sands, 1965, *The Feynman Lectures on Physics* (Addison-Wesley, Reading, Mass.), Vol. II, pp. 15-7–15-14; Vol. III, Sec. 21.
- Ford, L. H., and A. Vilenkin, 1981, *J. Phys. A* **14**, 2353.
- Fowler, H. A., L. Marton, J. Arol Simpson, and J. A. Suddeth, 1961, *J. Appl. Phys.* **32**, 1153.
- Fowles, G. R., 1980, *Am. J. Phys.* **48**, 779.
- Franz, W., 1939, *Verh. Dtsch. Phys. Ges., Nr. 2*, p. 65.
- Franz, W., 1940, *Phys. Ber.* **21**, 686.
- Franz, W., 1965, *Z. Phys.* **184**, 85.
- Frolov, P., and V. D. Skarzhinsky, 1983, *Nuovo Cimento B* **76**, 35.
- Furry, W. H., and N. F. Ramsey, 1960, *Phys. Rev.* **118**, 623.
- Gabor, D., 1949, *Proc. R. Soc. London* **197**, 454.
- Gabor, D., 1951, *Proc. Phys. Soc. London Sect. B* **64**, 449.
- Gerry, C., and V. A. Singh, 1979, *Phys. Rev. D* **20**, 2550.
- Gerry, C. C., and V. A. Singh, 1982, *Phys. Lett. A* **92**, 11.
- Gerry, C., and V. A. Singh, 1983, *Nuovo Cimento B* **73**, 161.
- Ginzburg, V. L., and L. D. Landau, 1950, *Zh. Eksp. Teor. Fiz.* **20**, 1064.
- Goddard, P., and D. Olive, 1978, *Rep. Prog. Phys.* **41**, 1357.
- Goldhaber, A. S., 1982, *Phys. Rev. Lett.* **49**, 905.
- Goldin, G. A., R. Menikoff, and D. H. Sharp, 1981, *J. Math. Phys.* **22**, 1664.
- Goldman, T., 1977, *Phys. Rev. D* **15**, 1063.
- Gor'kov, L. P., 1959, *Zh. Eksp. Teor. Fiz.* **36**, 1918 [*Sov. Phys.—JETP* **9**, 1364 (1959)].
- Greenberger, D. M., 1981, *Phys. Rev. D* **23**, 1460.
- Greenberger, D. M., D. K. Atwood, J. Arthur, C. G. Shull, and M. Schlenker, 1981, *Phys. Rev. Lett.* **47**, 751.
- Greenberger, D. M., and A. W. Overhauser, 1979, *Rev. Mod. Phys.* **51**, 43.
- Grumm, H.-R., 1981, *Acta Phys. Austriaca* **53**, 113.
- Guillod, F., and P. Huguenin, 1984, *Helv. Phys. Acta* **57**, 86.
- Haller, K., and R. B. Sohn, 1979, *Phys. Rev. A* **20**, 1541.
- Harris, J. H., and M. D. Semon, 1980, *Found. Phys.* **10**, 151.
- Henneberger, W. C., 1980, *Phys. Rev. A* **22**, 1383.
- Henneberger, W. C., 1981, *J. Math. Phys.* **22**, 116.
- Henneberger, W. C., and P. Huguenin, 1981, *Helv. Phys. Acta* **54**, 444.
- Henry, H. L., 1970, Ph.D. thesis (University of Virginia).
- Henry, H. L., and B. S. Deaver, 1968, *Bull. Am. Phys. Soc.* **13**, 1691.
- Henry, H. L., and B. S. Deaver, 1970, *Bull. Am. Phys. Soc.* **15**, 1353.
- Hraskó, P., 1966, *Nuovo Cimento B* **44**, 452.
- Huguenin, P., 1981, *Eur. J. Phys.* **2**, 165.
- Hunt, T. K., and J. E. Mercereau, 1964, *Phys. Rev.* **135**, 944A.
- Ingraham, R. L., 1972, *Am. J. Phys.* **40**, 1449.
- Inomata, A., and V. A. Singh, 1978, *J. Math. Phys.* **19**, 2318.
- Jackiw, R., and A. N. Redlich, 1983, *Phys. Rev. Lett.* **50**, 555.
- Jaklevic, R. C., J. Lambe, J. E. Mercereau, and A. H. Silver, 1965, *Phys. Rev.* **140**, 1628A.
- Jaklevic, R. C., J. J. Lambe, A. H. Silver, and J. E. Mercereau, 1964a, *Phys. Rev. Lett.* **12**, 159.
- Jaklevic, R. C., J. J. Lambe, A. H. Silver, and J. E. Mercereau, 1964b, *Phys. Rev. Lett.* **12**, 274.
- Jammer, M., 1966, *The Conceptual Development of Quantum Mechanics* (McGraw-Hill, New York).
- Jánossy, L., 1970, *Acta Phys. Acad. Sci. Hung.* **29**, 419.
- Jánossy, L., 1974, *Found. Phys.* **4**, 445.
- Josephson, B. D., 1962, *Phys. Lett.* **1**, 251.
- Kasper, E., 1966, *Z. Phys.* **196**, 415.
- Kasper, E., 1967, *Z. Phys.* **207**, 24.
- Kawamura, K., Y. Zempo, and Y. Irie, 1982, *Prog. Theor. Phys.* **67**, 1263.
- Keller, J. B., and B. Zumino, 1961, *Phys. Rev. Lett.* **7**, 164.
- Keller, M., 1961, *Z. Phys.* **164**, 274.
- Kittel, C., 1946, *Phys. Rev.* **70**, 965.
- Klein, U., 1979, *Lett. Nuovo Cimento* **25**, 33.
- Klein, U., 1981, *Phys. Rev. D* **23**, 1463.
- Kobe, D. H., 1979, *Ann. Phys. (N.Y.)* **123**, 381.
- Kobe, D. H., 1982, *J. Phys. A* **15**, L543.
- Kobe, D. H., E. C.-T. Wen, and K.-H. Yang, 1982, *Phys. Rev. D* **26**, 1927.
- Konopinski, E. J., 1978, *Am. J. Phys.* **46**, 499.
- Krauss, K., 1968, *Ann. Phys. (N.Y.)* **50**, 102.
- Kretzschmar, M., 1965a, *Z. Phys.* **185**, 73.
- Kretzschmar, M., 1965b, *Z. Phys.* **185**, 84.
- Kretzschmar, M., 1965c, *Z. Phys.* **185**, 97.
- Kwiram, A. L., and B. S. Deaver, 1964, *Phys. Rev. Lett.* **13**, 189.

- Landau, L., 1930, *Z. Phys.* **64**, 629.
- Landau, L., and E. Lifschitz, 1951, *The Classical Theory of Fields* (Addison-Wesley, Reading, Mass.).
- Landau, L., and E. Lifschitz, 1960, *Mechanics* (Pergamon, New York), pp. 154–156.
- Landau, L., and E. Lifshitz, 1977, *Quantum Mechanics* (Pergamon, New York).
- Langbein, W., 1958, *Naturwissenschaften* **45**, 510.
- Lenz, F., 1962, *Naturwissenschaften* **49**, 82.
- Lewis, R. R., 1983, *Phys. Rev. A* **28**, 1228.
- Liebowitz, B., 1965, *Nuovo Cimento* **38**, 932.
- Liebowitz, B., 1966, *Nuovo Cimento B* **46**, 125.
- Liebowitz, B., 1967, *Z. Phys.* **207**, 20.
- Lipkin, H. J., 1981, *Phys. Rev. D* **23**, 1466.
- Lipkin, H. J., and M. Peshkin, 1982, *Phys. Lett. B* **118**, 385.
- Lischke, B., 1969, *Phys. Rev. Lett.* **22**, 1366.
- Lischke, B., 1970a, *Z. Phys.* **237**, 469.
- Lischke, B., 1970b, *Z. Phys.* **239**, 360.
- Little, W. A., and R. D. Parks, 1962, *Phys. Rev. Lett.* **9**, 9.
- London, F., 1948, *Phys. Rev.* **74**, 562.
- London, F., 1961, *Superfluids* (Dover, New York), p. 152.
- Lyuboshits, V. L., and Ya. A. Smorodinski, 1978, *Zh. Eksp. Teor. Fiz.* **75**, 40.
- Mackinnon, L., 1979, *Lett. Nuovo Cimento* **26**, 397.
- Madelung, E., 1926, *Z. Phys.* **40**, 322.
- Mandelstam, S., 1962, *Ann. Phys. (N.Y.)* **19**, 1.
- Marcuse, D., 1970, *Engineering Quantum Electronics* (Harcourt, Brace & World, New York), pp. 55–57.
- Martin, C., 1976, *Lett. Math. Phys.* **1**, 155.
- Marton, L., J. Arol Simpson, and J. A. Suddeth, 1954, *Rev. Sci. Instrum.* **25**, 1099.
- Matteucci, G., and G. Pozzi, 1978, *Am. J. Phys.* **46**, 619.
- Meissner, W., and R. Ochsenfeld, 1933, *Naturwissenschaften* **21**, 787.
- Menikoff, R., and D. H. Sharp, 1977, *J. Math. Phys.* **18**, 471.
- Merzbacher, E., 1962, *Am. J. Phys.* **30**, 237.
- Mignaco, J. A., and C. A. Novaes, 1979, *Lett. Nuovo Cimento* **26**, 453.
- Mitler, H. E., 1961, *Phys. Rev.* **124**, 940.
- Möllenstedt, G., and W. Bayh, 1961, *Naturwissenschaften* **48**, 400.
- Möllenstedt, G., and W. Bayh, 1962, *Naturwissenschaften* **49**, 81.
- Möllenstedt, G., and H. Düker, 1956, *Z. Phys.* **145**, 377.
- Möllenstedt, G., and M. Keller, 1957, *Z. Phys.* **148**, 34.
- Möllenstedt, G., H. Schmidt, and H. Lichte, 1982, communication to the 10th International Congress on Electron Microscopy (Hamburg).
- Morse, P. M., and H. Feshbach, 1953, *Methods of Theoretical Physics* (McGraw-Hill, New York).
- Noerdlinger, P. D., 1962, *Nuovo Cimento* **23**, 158.
- Olariu, S., and I. Iovitzu Popescu, 1983, *Phys. Rev. D* **27**, 383.
- Olariu, S., I. Iovitzu Popescu, and C. B. Collins, 1979, *Phys. Rev. D* **20**, 3095.
- Onsager, L., 1961, *Phys. Rev. Lett.* **7**, 50.
- Overhauser, A. W., and R. Colella, 1974, *Phys. Rev. Lett.* **33**, 1237.
- Pandres, D., 1962, *J. Math. Phys.* **3**, 305.
- Panofsky, W. K. H., and M. Phillips, 1962, *Classical Electricity and Magnetism* (Addison-Wesley, Reading, Mass.), pp. 43–44.
- Papini, G., 1967, *Nuovo Cimento B* **52**, 136.
- Parks, R. D., and W. A. Little, 1964, *Phys. Rev.* **133**, 97A.
- Pauli, W., 1933, in *Handbuch der Physik*, 2nd ed., edited by H. Geiger and K. Scheel (Springer, Berlin), Vol. 24.
- Peshkin, M., 1981a, *Phys. Rev. A* **23**, 360.
- Peshkin, M., 1981b, *Phys. Rep.* **80**, 375.
- Peshkin, M., I. Talmi, and L. J. Tassie, 1961, *Ann. Phys. (N.Y.)* **12**, 426.
- Philippidis, C., D. Bohm, and R. D. Kaye, 1982, *Nuovo Cimento B* **71**, 75.
- Philippidis, C., C. Dewdney, and B. J. Hiley, 1979, *Nuovo Cimento B* **52**, 15.
- Post, E. J., 1982, *Phys. Lett. A* **92**, 224.
- Pryce, M. H. L., 1960, quoted in R. G. Chambers, *Phys. Rev. Lett.* **5**, 3 (1960).
- Purcell, K. M., and W. C. Henneberger, 1978, *Am. J. Phys.* **46**, 1255.
- Rauch, H., W. Treimer, and U. Bonse, 1974, *Phys. Lett. A* **47**, 369.
- Riess, J., 1973, *Helv. Phys. Acta* **45**, 1066.
- Rothe, H. J., 1981, *Nuovo Cimento A* **62**, 54.
- Rowe, E. G. P., 1980, *Nuovo Cimento A* **56**, 16.
- Rowell, J. M., 1963, *Phys. Rev. Lett.* **11**, 200.
- Roy, S. M., 1980, *Phys. Rev. Lett.* **44**, 111.
- Roy, S. M., and V. Singh, 1983, *Phys. Rev. Lett.* **51**, 2069.
- Roy, S. M., and V. Singh, 1984, *Nuovo Cimento A* **79**, 391.
- Ruijsenaars, S. N. M., 1983, *Ann. Phys. (N.Y.)* **146**, 1.
- Sakurai, J. J., 1967, *Advanced Quantum Mechanics* (Addison-Wesley, Reading, Mass.), pp. 15–18.
- Schaal, G., C. Jönsson, and E. F. Krimmel, 1966/1967, *Optik (Stuttgart)* **24**, 529.
- Schulman, L. S., 1971, *J. Math. Phys.* **12**, 304.
- Semon, M. D., 1982, *Found. Phys.* **12**, 49.
- Shapiro, S., 1963, *Phys. Rev. Lett.* **11**, 80.
- Silverman, M. P., 1983, *Phys. Rev. Lett.* **51**, 1927.
- Sommerfeld, A., 1916, *Ann. Phys. (Leipzig)* **51**, 1, 125.
- Strocchi, F., and A. S. Wightman, 1974, *J. Math. Phys.* **15**, 2189.
- Takabayasi, T., 1983, *Prog. Theor. Phys.* **69**, 1323.
- Tassie, L. J., and M. Peshkin, 1961, *Ann. Phys. (N.Y.)* **16**, 177.
- Todorov, N. S., 1974, *Phys. Lett. A* **46**, 375.
- Tomonaga, S. I., 1966, *Quantum Mechanics* (North-Holland, Amsterdam).
- Tonomura, A., 1972, *Jpn. J. Appl. Phys.* **11**, 493.
- Tonomura, A., T. Matsuda, J. Endo, T. Arii, and K. Mihama, 1980, *Phys. Rev. Lett.* **44**, 1430.
- Tonomura, A., T. Matsuda, R. Suzuki, A. Fukuhara, N. Osakabe, H. Umezaki, J. Endo, K. Shinagawa, Y. Sugita, and H. Fujiwara, 1982, *Phys. Rev. Lett.* **48**, 1443.
- Trammel, G. T., 1964, *Phys. Rev.* **134**, 1183B.
- Vainshtein, A. I., and V. V. Sokolov, 1975, *Yad. Fiz.* **22**, 618 [Sov. J. Nucl. Phys. **22**, 319 (1976)].
- von Westenholz, C., 1973, *Ann. Inst. Henri Poincaré A* **18**, 353.
- Wahl, H., 1968/1969, *Optik* **28**, 417.
- Wahl, H., 1970, *Optik* **30**, 508, 577.
- Wegener, H., 1960, *Z. Phys.* **159**, 243.
- Weisskopf, V. F., 1961, in *Lectures in Theoretical Physics*, edited by W. E. Brittin, B. W. Downs, and J. Downs (Interscience, New York), Vol. III, p. 54.
- Werner, F. G., and D. R. Brill, 1960, *Phys. Rev. Lett.* **4**, 344.
- Whittaker, E. T., and G. N. Watson, 1958, *A Course of Modern Analysis*, 4th ed. (Cambridge University, Cambridge), p. 119.
- Wigner, E. P., 1959, quoted in F. G. Werner and D. R. Brill, *Phys. Rev. Lett.* **4**, 344 (1960).
- Wilczek, F., 1982a, *Phys. Rev. Lett.* **48**, 1144.
- Wilczek, F., 1982b, *Phys. Rev. Lett.* **49**, 957.
- Willis, W. D., 1971, M. S. thesis (University of Virginia); cited by B. S. Deaver and G. B. Donaldson, *Phys. Lett. A* **89**, 178

- (1982).
- Wisnivesky, D., and Y. Aharonov, 1967, *Ann. Phys. (N.Y.)* **45**, 479.
- Wódkiewicz, K., 1984, *Phys. Rev. A* **29**, 1527.
- Wohlleben, D., 1967, *J. Appl. Phys.* **38**, 3341.
- Woodilla, J., and H. Schwartz, 1971, *Am. J. Phys.* **39**, 111.
- Wu, T. T., and C. N. Yang, 1975, *Phys. Rev. D* **12**, 3845.
- Yang, C. N., 1974, *Phys. Rev. Lett.* **33**, 445.
- Yang, K.-H., 1976, *Ann. Phys. (N.Y.)* **101**, 62.
- Yang, K.-H., 1982, *Phys. Lett. A* **92**, 71.
- Yang, K.-H., 1983, *Phys. Lett. A* **94**, 259.
- Zeilinger, A., 1979, *Lett. Nuovo Cimento* **25**, 333.

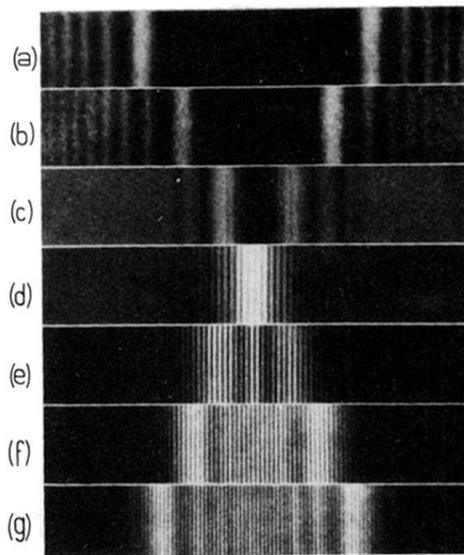


FIG. 39. Electron interference with the electrostatic biprism, for several values of the positive potential U_f of the biprism fiber, as observed by Möllenstedt and Düker (1956). (a) For $U_f=0$, the pattern corresponds to scattering by the biprism fiber and consists of two series of Fresnel fringes. (b) $U_f=1.5$ V and (c) $U_f=2.8$ V: The distance between the two Fresnel patterns is diminished. (d) $U_f=4.0$ V: The first maxima in each series are overlapping and give rise to equidistant Young fringes. (e) $U_f=5.0$ V, (f) $U_f=5.8$ V, and (g) $U_f=7.0$ V: The pattern of Young fringes is broadened and the distance between consecutive fringes diminished with increasing U_f .

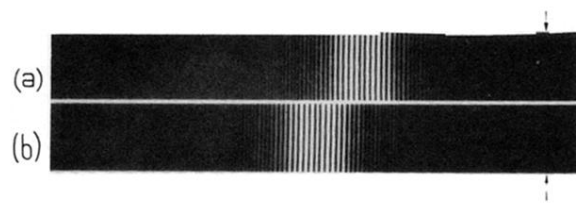


FIG. 42. Effect of a homogeneous magnetic field on the electron interference pattern, as observed by Bayh (1962): (a) interference pattern without magnetic field; (b) overall shift of the pattern by a distance proportional to the applied field. The arrows mark the location of the observing plane on the photographic plate.

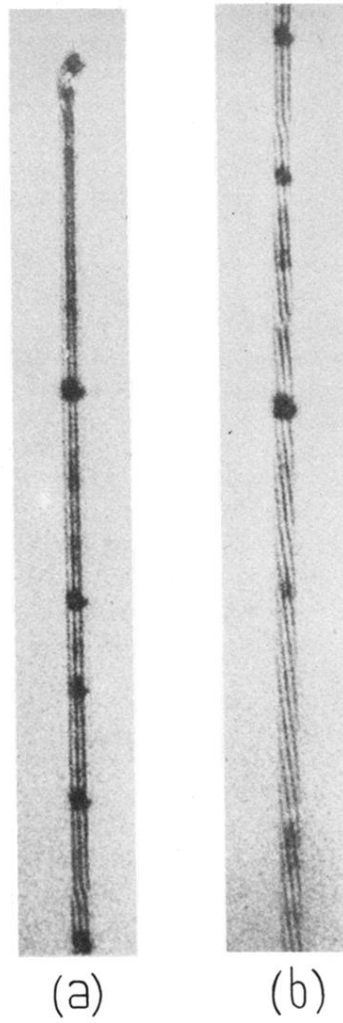


FIG. 46. Biprism interference pattern of a very slightly tapered whisker, observed by Fowler, Marton, Simpson, and Suddeth (1961): (a) tip of the whisker; (b) continuation of (a). The offset at the top of (b) is identical with that at the bottom of (a).

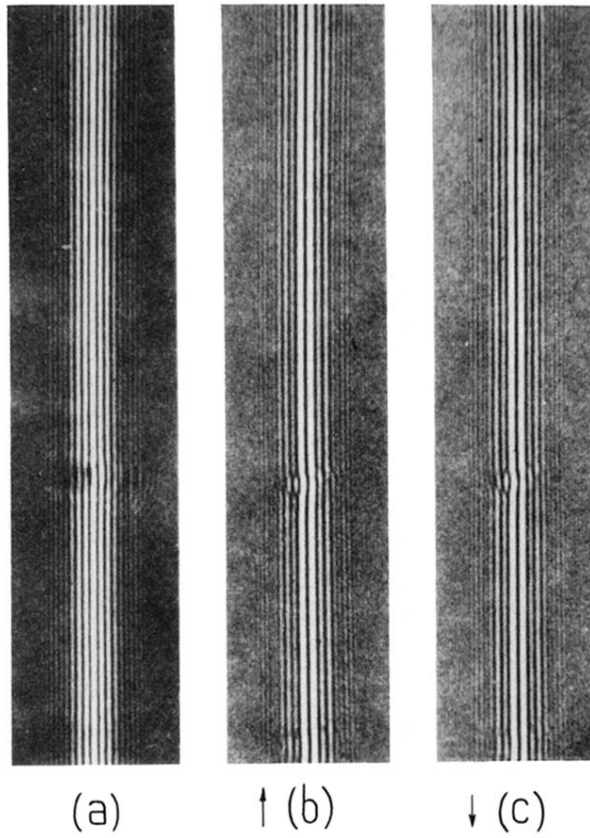


FIG. 48. Biprism patterns observed by Boersch, Hamisch, and Grohmann (1962), which demonstrate the quantum effects of the fluxes: (a) biprism interference pattern in the absence of the layer of Permalloy; (b) and (c), patterns in the presence of a layer of Permalloy deposited on the back of the biprism fiber. The arrows indicate the direction of the enclosed magnetic flux. The presence of the magnetic flux interchanges in this case the position of light and dark fringes between (a) and (b) or (c), an effect that is specific for the enclosed fluxes.

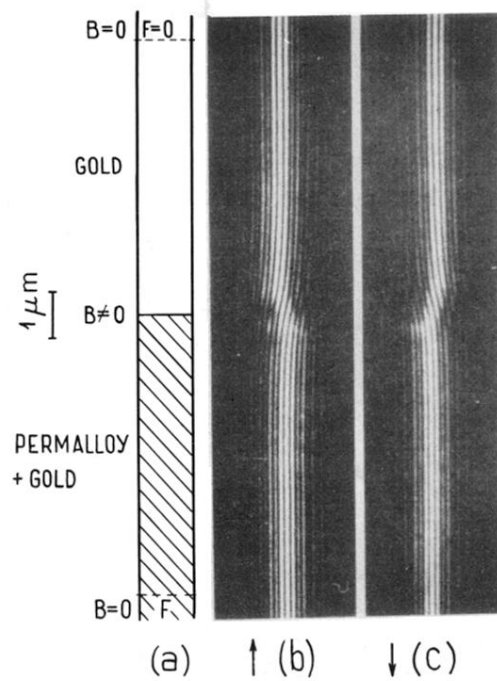


FIG. 49. (a) Diagram of the Permalloy-gold junction used by Boersch, Hamisch, and Grohmann (1962) in the experimental determination of the flux unit $2\pi\hbar c/e$; (b) and (c), fringe shifts in the biprism interference patterns, produced in the vicinity of the Permalloy-gold junction. The arrows indicate the directions of magnetization in the two cases. The displacement of the envelope seen in (b) and (c) is due to the longitudinal component of the magnetic field in the junction region, while the tilting of the fringes relative to the envelope is the effect of the magnetic flux enclosed between the interfering waves.

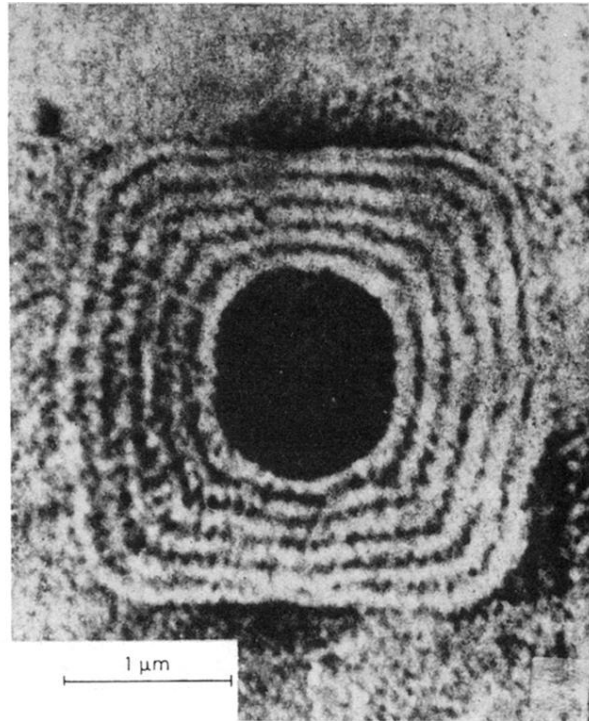


FIG. 52. Contours of constant phase of the electron wave illuminating a toroidal magnet, as observed by Tonomura *et al.* (1982). The phase in the inner region of the pattern is shifted by an odd multiple of π , while the shape of the magnetic sample is reproduced as a clear image on the interferogram. Since the sample does not contribute to points outside the sample image, the phase of the beam reaching the inner region was shifted by the *enclosed* magnetic flux.

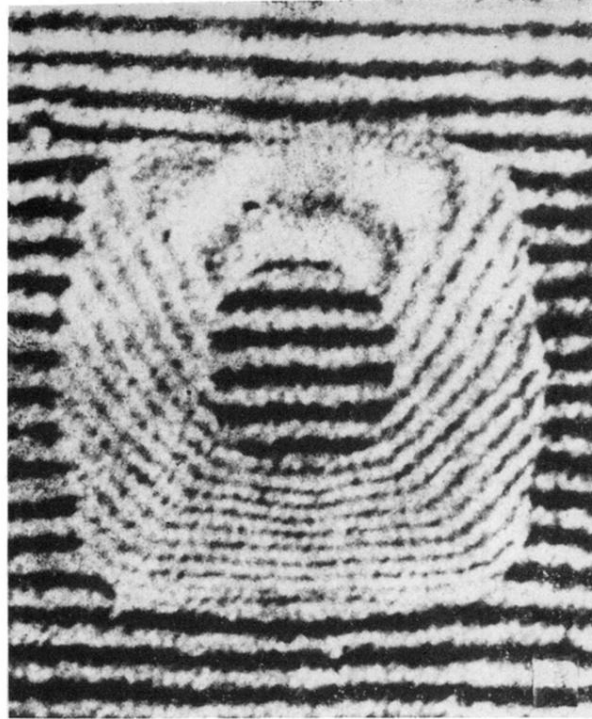


FIG. 53. Interference pattern obtained by the superposition of the wave illuminating the sample and of a coherent wave inclined at a certain angle relative to the former, as observed by Tonomura *et al.* (1982). The pattern consists of a system of parallel fringes in the exterior region, continued by segments of ellipses with the focus at the center of the toroidal sample, and terminated by another system of parallel fringes in the inner region, shifted with respect to the exterior ones by $qF/\hbar c$.

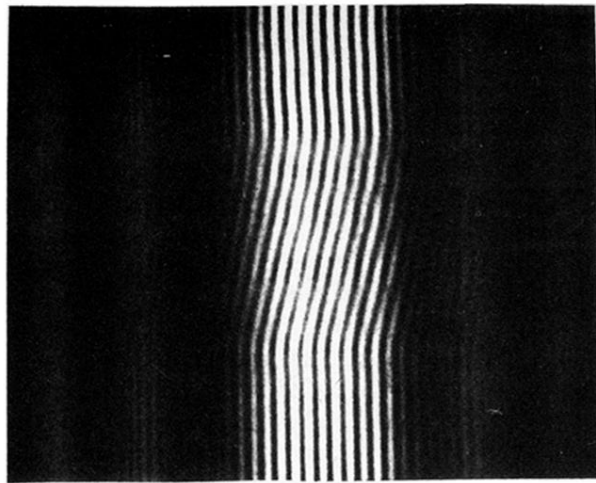


FIG. 56. Action of magnetic flux enclosed in a microscopic solenoid on a biprism interference pattern, as reported by Bayh (1962). At the bottom and at the top of the pattern, the magnetic flux is held constant. In the middle, the increase in magnetic flux is synchronous with the displacement of the photographic film; the flux produces a shift of about four fringes, while the envelope of the pattern remains unchanged.

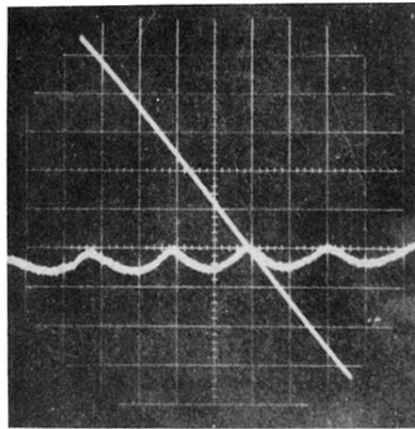


FIG. 68. Variation of the resistance of a hollow cylinder with applied magnetic field at its transition temperature, as observed by Parks and Little (1964). The upper trace is the magnetic field sweep.

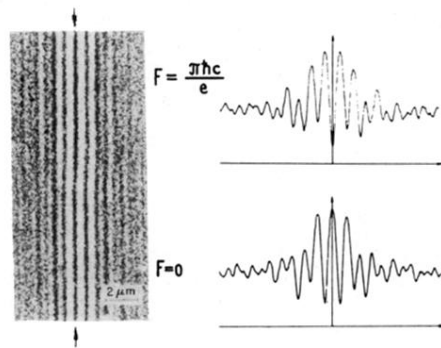


FIG. 71. Electron interferometer fringes and densitometer curves at the end of a superconducting hollow lead cylinder, as observed by Lischke (1969). At the bottom of the figure no flux is trapped and the phase shift is zero. At the upper part of the figure the trapped flux is $\pi \hbar c / e$ and the phase shift is π , resulting in the inversion of contrast of the fringes.

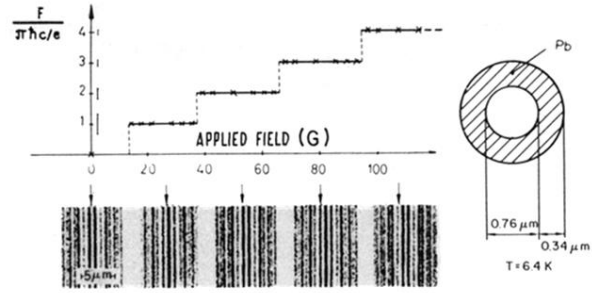


FIG. 72. Magnetic flux trapped in a hollow superconducting cylinder as a function of magnetic field applied during cooling of the sample, as observed by Boersch and Lischke (1970). Even multiples of $\pi\hbar c/e$ leave the pattern invariant, while odd multiples of $\pi\hbar c/e$ produce an inversion of contrast.

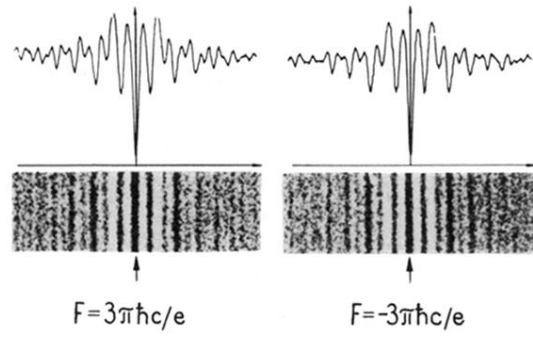


FIG. 73. Electron interference patterns produced by opposite magnetic fluxes trapped in a superconducting cylinder, as observed by Boersch and Lischke (1970). The pattern is invariant to flux changes by an even multiple of $\pi\hbar c/e$.

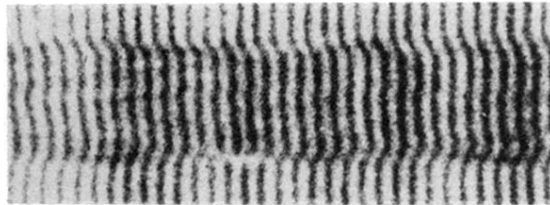


FIG. 79. Phase shift by π produced by a thin carbon foil, as observed by Möllenstedt and Keller (1957). The central horizontal part of the pattern corresponds to a strip of carbon foil having different thicknesses on the two sides of the biprism fiber, while the upper and lower parts of the pattern correspond to strips of carbon foil having the same thickness on both sides of the fiber. The resulting fringe shift demonstrates the quantum effects of electric fluxes.